

PDR

Accession No. _____

DRAFT

INTERIM REPORT

SAND82-1557

CALCULATIONS OF RADIONUCLIDE RELEASES FROM
HYPOTHETICAL NUCLEAR WASTE REPOSITORIES
IN BASALT, BEDDED SALT AND TUFF:
AN EVALUATION OF COMPLIANCE
WITH
EPA DRAFT STANDARD 40CFR191
AND DRAFT REGULATION 10CFR60

R. E. Pepping
M. S. Y. Chu
M. D. Siegel

July 1982

Sandia National Laboratories
Fuel Cycle Risk Analysis Division
Albuquerque, New Mexico 87185

Prepared for
Division of Waste Management
Office of Nuclear Material Safety and Safeguards
U.S. Nuclear Regulatory Commission
Washington, D.C. 20555
Under Memorandum of Understanding DOE 40-550-75
NRC FIN No. A1165

8211020686 820731
PDR RES
8211020686 PDR

DRAFT

NOTICE

This report was prepared as an account of work sponsored by an agency of the United States Government. Neither the United States Government nor any agency thereof, or any of their employees, makes any warranty, expressed or implied, or assumes any legal liability or responsibility for any third party's use, or the results of such use, of any information, apparatus, product or process disclosed in this report, or represents that its use by such third party would not infringe privately owned rights.

EXECUTIVE SUMMARY

The Environmental Protection Agency (EPA) has drafted a standard, 40CFR191, for the geologic disposal of radioactive wastes. The standard regulates the total integrated discharge of radionuclides from a geologic repository for 10,000 years. The standard is conceptually simple; it is a probabilistic statement with a well-defined method of consequence calculation. In deriving the standard, the EPA used simplified analyses of geologic repositories in several candidate media to show that these performance objectives were not unduly restrictive.

The Nuclear Regulatory Commission (NRC) is responsible for enforcing the EPA Standard and is currently developing appropriate Federal regulations (10CFR60). The Department of Energy (DOE) is involved in selecting actual sites for geologic repositories and will submit applications to NRC for approval of construction. NRC is expected to evaluate these applications and perform compliance assessment with the EPA Standard. Sandia National Laboratories (SNL) is funded by NRC to provide information and insight useful in preparing for this compliance assessment task. The objectives of this work include the following:

- . Demonstration of the use of existing methodology developed at Sandia in the assessment of compliance of hypothetical repositories with the draft EPA Standard, 40CFR191.
- . Identification of ambiguities within the draft EPA Standard which need to be clarified before a final assessment of compliance can be made.
- . Assessment of the achievability of the draft EPA Standard.
- . Identification of areas of importance that merit further investigation by the NRC.

This work consists of simplified repository analyses in the following geologic media: basalt, bedded salt and tuff. The conceptual models of the repository sites are consistent with our understanding of the characteristics of the sites currently being investigated by the DOE. We have supplemented these data from specific sites with information from similar geological formations and environments. It must be stressed that we have not attempted to model any specific real site. Therefore, the results of this work must not be interpreted as a definitive statement on any specific site or formation.

A large amount of uncertainty in the results is introduced by the paucity of experimental and field geochemical and hydrological data that is relevant to the design of a waste repository. In

addition, it was impossible to provide exact mathematical descriptions of fluid flow and radionuclide migration due to the complexity of these systems and time constraints. We have attempted to place conservative and reasonable bounds on the numerical ranges of variables for which the data are sparse. These ranges should have produced overestimates of the calculated potential radionuclide discharge.

The major objective of these analyses was to calculate potential radionuclide releases from hypothetical repositories. During our analyses we applied several new techniques in the performance assessment methodology. These assumptions and mathematical approximations are discussed in the appendices which are included with each report. We have developed a method to estimate radionuclide retardation in fractured media within joints that are filled with secondary minerals and in the presence of matrix diffusion. We have calculated possible values for the vertical and horizontal hydraulic gradients induced by the thermal buoyancy produced by the waste heat in the repository. We have also estimated the probabilities of single and multiple intrusions by drilling into a bedded salt waste repository.

The main conclusions derived from this work are as follows:

1. Two possible interpretations of the draft EPA Standard have been presented which should be further studied and clarified by the EPA.
2. Analyses performed with different source models show that the compliance assessment is very sensitive to assumptions about the rate of radionuclide release from the repository.
3. Large radionuclide releases could result from drilling into a HLW repository in bedded salt when waste canisters are directly breached or when a brine pocket below the engineered facility is punctured.
4. Discharge of radionuclides with low retardation such as ^{99}Tc and ^{14}C could result in violations of the draft EPA Standard in the three geological environments considered in this study.
5. Sorption of radionuclides by zeolitized tuff may be a sufficient barrier to migration of actinides even in the absence of solubility limits.
6. All the scenarios analyzed that lead to significant radionuclide discharges involve either human intrusion or some disruption process. Further study of the probabilities of such events would yield valuable insights about the safety of repository sites.p

SAND82-0689

TECHNICAL ASSISTANCE FOR REGULATORY DEVELOPMENT:
A SIMPLIFIED REPOSITORY ANALYSIS IN A HYPOTHETICAL
BASALT FORMATION

R. E. Pepping
M. S. Chu
M. D. Siegel

Sandia National Laboratories
Fuel Cycle Risk Analysis Division
Albuquerque, NM 87185

Fin No. A-1165. Task 3

ABSTRACT

An analysis of a hypothetical nuclear waste repository in a basalt formation has been performed to demonstrate the application of existing analysis tools to the assessment of compliance of the repository with the draft EPA Standard, 40CFR191 (draft). The tools have been developed by Sandia National Laboratories for use by NRC in such analyses. The hypothetical site is based on descriptive and quantitative data for a candidate basalt repository in the early stages of site characterization. The effects of uncertainty in input data on the assessment of compliance have been demonstrated. Other sources of uncertainty resulting from interpretation of the standard and its probabilistic nature are discussed. The results of the calculations presented indicate that compliance with the draft standard may be achieved if ambiguities are resolved and assumptions are justified. A familiarity with the existing analysis tools developed by Sandia is useful, but not essential.

TABLE OF CONTENTS

	<u>Page</u>
1. Introduction	1
2. The Reference Basalt Site	3
3. Waste and Repository Description	7
3.1 Waste	7
3.2 Subsurface facility	7
4. Geochemistry	9
4.1 Retardation Factors	9
4.2 Solubility	12
4.3 Matrix Diffusion	12
5. Groundwater Transport Model	16
6. Scenarios Analyzed	18
6.1 Scenario I -- Routine Release	19
6.2 Scenario II -- Fractures in Dense Basalt ..	23
6.3 Scenario III -- Borehole	25
7. The Draft EPA Standard, 40CFR191	34
7.1 Interpretations of the Draft Standard	34
7.2 Implementations of Different Interpretations	37
7.3 Estimation of Probabilities of Scenarios ..	39
8. Results of Analyses	41
9. Conclusions	58

	<u>Page</u>
Appendix A -- Retardation	A-1
Appendix B -- Redox Conditions in the Reference Repository and Appropriate Values of K_d	B-1
Appendix C -- An Approximate Treatment of Matrix Diffusion as a Retardation Mechanism .	C-1
Appendix D -- Calculation of Thermal Buoyancy Gradient	D-1
Appendix E -- The Mixing Cell Source Model	E-1
Appendix F -- Rationale for the Selection of Scenarios Analyzed in Basalt	F-1
References	R-1

FIGURES

1.	General Geologic Features of the Site	4
2.	Stratigraphic Cross-Section of Hypothetical Repository in Basalt	5
3.	Routine Release Scenario (Scenario I)	22
4.	Fractured Dense Basalt Scenario (Scenario II) ...	24
5.	Borehole Scenario (Scenario III)	29
6.	Scenario I only CCDF - 1st 10,000 Years	42
7.	Scenario I only CCDF - 2nd 10,000 Years	42
8.	Scenario I only CCDF - 3rd 10,000 Years	43
9.	Scenario I only CCDF - 4th 10,000 Years	43
10.	Scenario I only CCDF - 5th 10,000 Years	44
11.	Scenario II only CCDF - 1st 10,000 Years	44
12.	Scenario II only CCDF - 2nd 10,000 Years	45
13.	Scenario II only CCDF - 3rd 10,000 Years	45
14.	Scenario II only CCDF - 4th 10,000 Years	46
15.	Scenario II only CCDF - 5th 10,000 Years	46
16.	Scenario III only CCDF - 1st 10,000 Years	47
17.	Scenario III only CCDF - 2nd 10,000 Years	47
18.	Scenario III only CCDF - 3rd 10,000 Years	48
19.	Scenario III only CCDF - 4th 10,000 Years	48
20.	Scenario III only CCDF - 5th 10,000 Years	49
21.	All Scenario CCDF - 1st 10,000 Years	49
22.	All Scenario CCDF - 2nd 10,000 Years	50
23.	All Scenario CCDF - 3rd 10,000 Years	50

24.	All Scenario CCDF - 4th 10,000 Years	51
25.	All Scenario CCDF - 5th 10,000 Years	51
26.	Scenario III (leach limited) only CCDF - 1st 10,000 Years	53
27.	Scenario III (leach limited) only CCDF - 2nd 10,000 Years	53
28.	Scenario III (leach limited) only CCDF - 3rd 10,000 Years	54
29.	Scenario III (leach limited) only CCDF - 4th 10,000 Years	54
30.	Scenario III (leach limited) only CCDF - 5th 10,000 Years	55
31.	All Scenario CCDF (leach limited III) - 1st 10,000 Years	55
32.	All Scenario CCDF (leach limited III) - 2nd 10,000 Years	56
33.	All Scenario CCDF (leach limited III) - 3rd 10,000 Years	56
34.	All Scenario CCDF (leach limited III) - 4th 10,000 Years	57
35.	All Scenario CCDF (leach limited III) - 5th 10,000 Years	57
B-1	K_d Data	B-3
D-1	Water Column Assumed for Thermal Buoyancy Calculation	D-1
D-2	Isotherm Used in Calculating Thermal Buoyancy ..	D-3
E-1	Implementation of the Mixing Cell Source Model for NWFT/DVM	E-4
E-2	Effects of Mixing Cell Assumption on Integrated Discharge Relative to the Leach-Limited Source Model	E-5

TABLES

1.	Reference Hydraulic Properties	6
2.	Inventory of Reference Repository	8
3.	Geochemical Environment of Stratigraphic Layers in Basalt Repository	13
4.	K_d Ranges	14
5.	Ranges of Solubilities of Selected Elements Used for Basalt Reference Repository Conditions	15
6.	Additional Data Ranges and Distributions	21
7.	Scenario II: EPA Ratios of Radionuclides Discharged into I-M	27
8.	Scenario III: EPA Ratios of Radionuclides	31
9.	Scenario III: EPA Ratios Summed Over All Radionuclides	32
10.	Mean Values of Contributions to the EPA Sum (100 Vectors) for Scenario III with Leach-Limited Source	33
11.	Cumulative Releases to the Accessible Environment for 10,000 Years After Disposal	35
C-1	Scenario II Discharges with Matrix Retardation	C-9
C-2	Summary of Effects of Diffusion Into Rock Matrix on TID	C-10
C-3	Vector #15 Data Used to Estimate Retardation Due to Diffusion into the Rock Matrix	C-11
C-4	Vector #24 Data Used to Estimate Retardation Due to Diffusion into the Rock Matrix	C-12
C-5	Vector #62 Data Used to Estimate Retardation Due to Diffusion into the Rock Matrix	C-13
D-1	Hydraulic Gradient Produced by Thermal Effects	D-2

1. Introduction

The EPA is expected to issue its draft standard on the geologic disposal of radioactive wastes, 40CFR191, in the near future. A 180 day period is expected for public comment on the standard. Other government agencies, such as the NRC, are also expected to comment on the standard. Sandia is funded by the NRC to provide information and insight useful in preparing these comments. The objective of this effort is to perform calculations similar to those performed by EPA in developing their standard. We have calculated integrated discharges of radionuclides in plausible scenarios. A number of media have been proposed as candidate hosts for nuclear waste repositories: bedded salt, domed salt, basalt, tuff and granite. This report documents analyses of a repository in basalt.

The reference basalt repository is hypothetical. The characteristics of the reference basalt site in this study were chosen to be consistent with our current understanding of the proposed candidate repository site in order to determine the realism of the assumed EPA repositories. Chapter 2 describes the reference site in this study. First, the general characteristics of the site and surrounding region are described; then, the stratigraphy and lithology of the reference site are presented.

Chapter 3 describes the reference repository and the radioactive wastes stored. This includes the waste inventory, the waste form, the waste canisters and leaching behavior.

Chapter 4 presents the geochemical parameters used in the analysis. The geochemical environment of each subsurface layer has been described. Special emphasis has been placed on the calculation of retardation factors of radionuclides in basalt. We assumed that the transport of radionuclides in basalt takes place almost exclusively in partially filled fractures. Retardation factors were calculated using distribution coefficients for radionuclides in secondary minerals in the fractures.

Chapter 5 describes the groundwater transport model used in these analyses. The flow is represented by a quasi-two-dimensional Darcian model. Sandia's distributed velocity method (DVM)¹ was used to calculate radionuclide transport.

Chapter 6 describes the scenarios analyzed by Sandia in calculating the integrated releases of radionuclides for times up to 50,000 years. A base case routine release scenario and two disruptive scenarios were analyzed.

Chapter 7 describes the draft EPA Standard and identifies points requiring clarification in the Standard. Chapter 8 presents results of numerical calculations and compares them to the requirements of the EPA Standard.

It would be misleading to assume that the results of these model calculations can provide a detailed description of the performance of a real repository. A large amount of uncertainty in the results is introduced by the paucity of experimental and field geochemical and hydrological data that is relevant to the design of a waste repository in basalt formations. In addition, it was impossible to provide exact mathematical descriptions of fluid flow and radionuclide migration due to the complexity of this system and time and budgetary constraints. However, with better in-situ measurements or site characterization, and additional resources, the realism and accuracy of these calculations could be greatly improved.

It should be noted that the results presented here represent a first pass at the analyses that real repositories will require. The motivation for performing a demonstration analysis at this time is twofold. First, we gain experience in identifying necessary assumptions, areas of sparse data or weak models, and potential problems with implementing the draft standard. Secondly, the numerical values indicate the likelihood that the hypothetical repository complies with the draft standard. It therefore indicates the importance of validating assumptions and improving data for any real candidate repository that is similar.

Appendices A through F describe several assumptions and mathematical approximations that we have developed in order to estimate radionuclide discharge from the repository. Appendix A outlines and derives a new method for approximation of the retardation factor for radionuclide migration in fractured media. Appendix B describes our conception of the geochemical environments along possible nuclide migration paths and discusses the uncertainty related to choices of relevant values of radionuclide distribution coefficient (K_d). In Appendix C, a method

to approximate the radionuclide retardation caused by matrix diffusion is discussed. In Appendix D, vertical hydraulic gradients induced by thermal effects are calculated. Appendix E describes an optional source model, the mixing cell, used in some of the analyses. Appendix F discusses the rationale for scenario selection.

2. The Reference Basalt Site

The reference basalt repository is located in the center of a drainage basin within a region of flood basalts. This reference site is shown schematically in Figure 1. Mountains along the northern, northwestern and southwestern edges of the site are zones of recharge to the groundwater system. A major river, River C, flows through the site from the northwest to the southeast. The deeper groundwater near the repository site discharges to the upper unconfined aquifers west of mountain M1.

This region is underlain by a sequence of basaltic lava flows. The sequence of flows contains sedimentary beds of regional extent. Overlying the volcanic rocks is an unconfined aquifer consisting of alluvial sand and gravel. The geologic cross-section at the Reference Site (A-A' cut) is shown schematically in Figure 2. The repository is located in the middle of a dense basalt formation. Overlying this horizon is a sequence of four layers of alternating interflows and dense basalts. Above these four layers lies a water-bearing interbed (Layer I-V) consisting mainly of sandstone and clay. Above interbed I-V is a basalt formation consisting of three members with distinct chemical signatures. This basalt formation is overlain by a major confined aquifer system (Layer I-M) predominantly composed of tuffaceous siltstone and sandstone. Above aquifer I-M lies a basalt formation (J) which, in turn, is overlain by an unconfined aquifer (UA).

Ranges of horizontal and vertical hydraulic conductivity (K_v) and effective porosity for each layer are presented in Table 1. A normal distribution was assigned to each range of porosity to be consistent with a real basalt site. The sample population for K_v that was used in this work was determined by the following method. First, values of K_v were sampled from a lognormal distribution. The sampled values were then subtracted from $K_v(\max)$. The resulting sample population is skewed toward the high end of the range. For this system this procedure produces more conservative estimates of discharge than those of the standard lognormal distribution. A 70 percent rank correlation

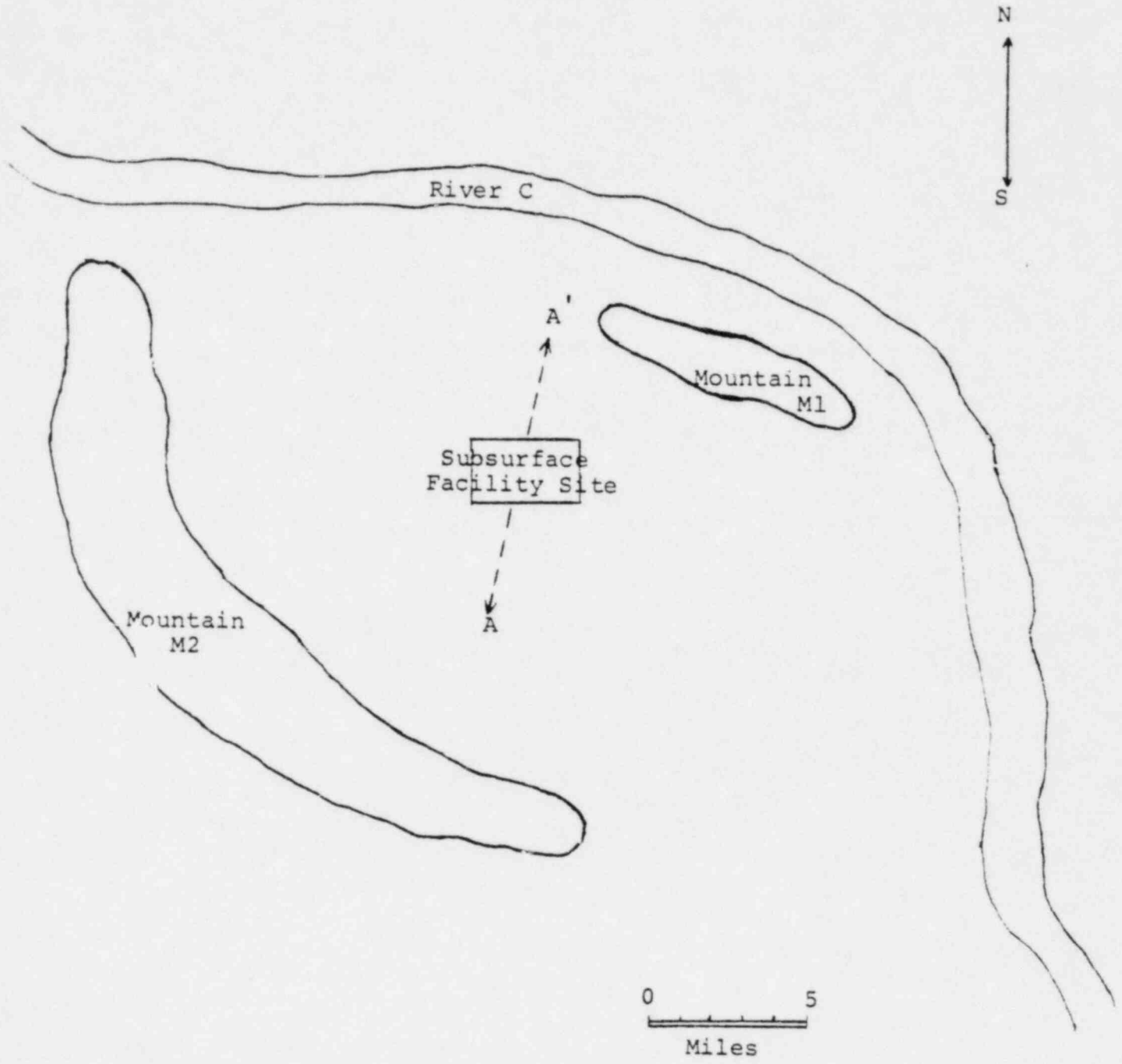


Figure 1. General Geologic Features of the Reference Site

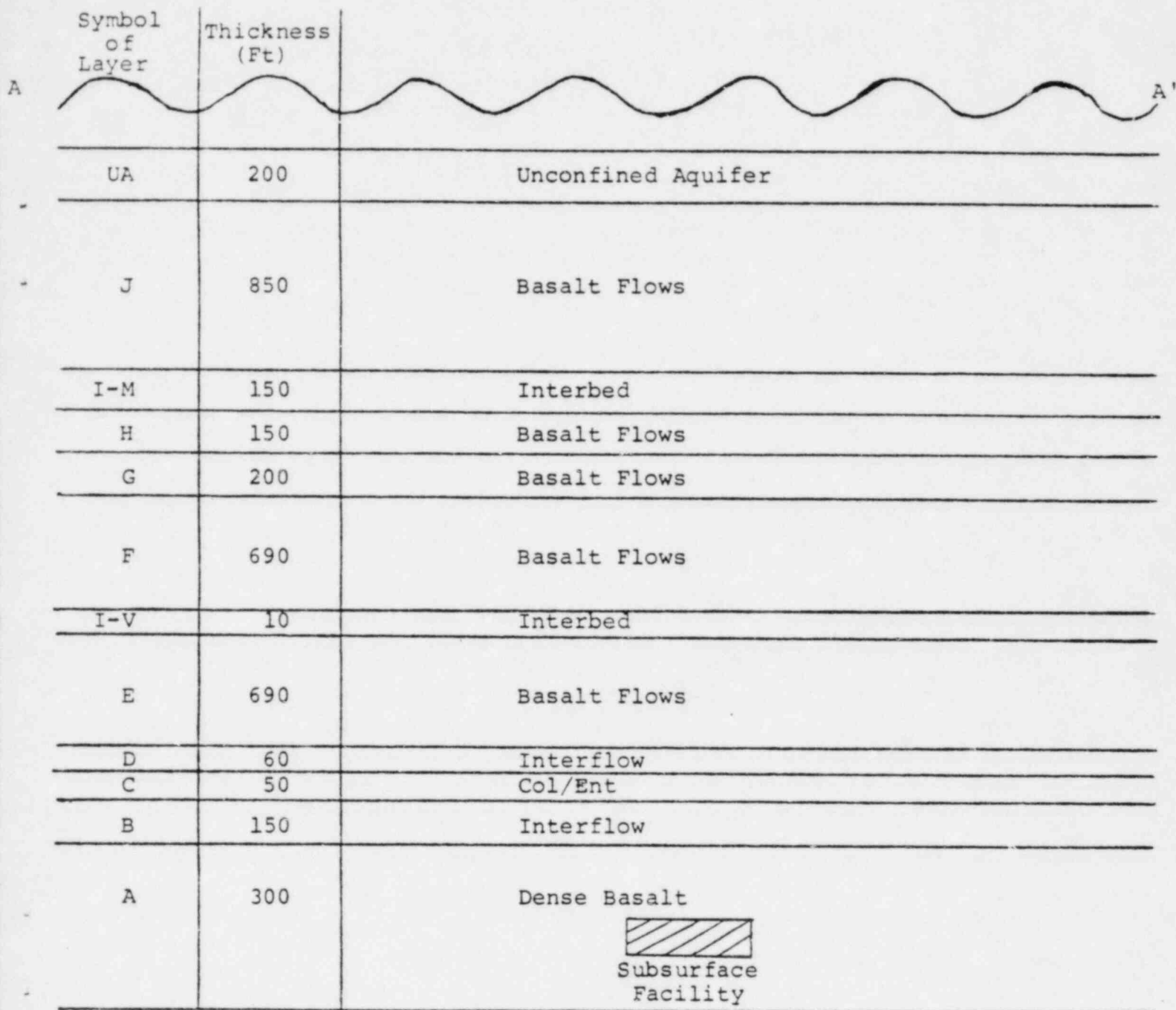


Figure 2. Stratigraphic Cross-Section of Hypothetical Repository in Basalt

Table 1
Reference Hydraulic Properties

<u>Layer</u>	<u>Horizontal Hydraulic Conductivity (ft/d)</u>	<u>Vertical Hydraulic Conductivity (ft/d)</u>	<u>Effective Porosity</u>
A	$(10^{-8} - 10^{-5})$	$(10^{-7} - 10^{-4})$	$(10^{-3} - 0.025)$
B	$(10^{-3} - 10^{-1})$	$(10^{-3} - 10^{-1})$	$(10^{-2} - 0.12)$
C	$(10^{-8} - 10^{-3})$	$(10^{-7} - 10^{-2})$	$(10^{-3} - 0.025)$
D	$(10^{-3} - 10^{-1})$	$(10^{-3} - 10^{-1})$	$(10^{-2} - 0.12)$
E	$(10^{-8} - 10^{-3})$	$(10^{-7} - 10^{-2})$	$(10^{-3} - 0.12)$
I-V	$(10^{-1} - 10)$	$(10^{-2} - 1)$	$(0.1 - 0.2)$
F	$(10^{-6} - 10^{-2})$	$(10^{-6} - 10^{-2})$	$(10^{-3} - 0.12)$
G	$(10^{-4} - 10)$	$(10^{-4} - 10)$	$(10^{-3} - 0.12)$
H	$(10^{-4} - 10^2)$	$(10^{-4} - 10^2)$	$(10^{-3} - 0.12)$
I-M	$(1 - 150)$	$(10^{-1} - 15)$	$(0.1 - 0.2)$
J	$(10^{-4} - 2000)$	$(10^{-4} - 2000)$	$(10^{-3} - 0.12)$
UA	$(1 - 10^4)$		$(0.1 - 0.3)$

is assumed to exist between porosity and hydraulic conductivity. This minimizes the occurrence of physically unreasonable combinations of these variables.

The horizontal hydraulic gradients in I-Y, I-M, and UA are assumed to have a range of 10^{-4} to 10^{-2} . The vertical gradient is assumed to be upward and small in magnitude.

3. Waste and Repository Description

3.1 Waste

The inventory (Table 2) assumed in this work is equal to half the projected accumulation of 10-year-old spent fuel in the United States by the year 2010. This would contain a total of 103,250 BWR and 60,500 PWR assemblies; a total of 46,800 metric tons of heavy metal (MTHM). The criteria for selection of key radionuclides are described in detail in Reference 2. In addition to these criteria, all radionuclides specified in the Release Limit Table of the EPA Standard are included in this inventory list.

All canisters containing the wastes are assumed to have a life of 1,000 years after emplacement. At year 1,000, all canisters fail simultaneously and radionuclide release begins. Radionuclide release is assumed to be determined by a constant rate of breakdown of the waste form. The waste matrix is assumed to dissolve at an annual rate of 10^{-4} to 10^{-7} of the original mass. Radionuclides are assumed to be uniformly distributed throughout the matrix so that their release rate is directly proportional to the matrix dissolution rate.

3.2 Subsurface Facility

The reference subsurface facility is a mined facility at a depth of 3,000 feet below the surface. A description of the facility is summarized in the following table.

Areal dimensions -- 9,840 feet x 7,870 feet

Number of storage rooms -- 120

Storage room dimensions -- length = 3,560 feet

Table 2

Inventory of Reference Repository
(Spent fuel from 46,800 MTHM)

<u>Radionuclide</u>	<u>Half Life</u>	<u>Curies</u>
Pu240	6.76E3	2.1E7
U236	2.39E7	1.0E4
Th232	1.41E10	1.7E-5
Ra228	6.7	4.7E-6
Cm245	8.27E3	8.4E3
Pu241	14.6	3.2E9
Am241	433.	7.5E7
Np237	2.14E6	1.5E4
U233	1.62E5	1.8
Th229	7300.	1.3E-3
Cm246	4710.	1.6E3
Pu242	3.79E5	7.5E4
U238	4.51E9	1.5E4
Pu238	89.	9.4E7
U234	2.47E5	3.5E3
Th230	8.E4	0.19
Ra226	1600.	3.5E-4
Pb210	21.	3.3E-5
Am243	7650.	6.6E5
Pu239	2.44E4	1.4E7
U235	7.1E8	7.5E2
Pa231	3.25E4	0.25
Ac227	21.6	5.2E-2
Tc99	2.14E5	6.1E5
I129	1.6E7	1.5E3
Sn126	1.0E5	2.2E4
Sr90	28.9	2.4E9
C14	5730.	3.5E4
Cs135	2.0E6	1.3E4
Cs137	30.	3.5E9

width = 100 feet

height = 40 feet

Porosity of backfilled region -- 18 percent

4. Geochemistry

4.1 Retardation Factors

One of the most important barriers to the movement of dissolved radionuclides in ground water is retardation due to the interaction between radionuclides and the geologic medium. The retardation factor is defined as the ratio of the velocity of the fluid to the velocity of the retarded radionuclide. A radionuclide with a retardation factor of 10 would travel at one-tenth the velocity of the ground water. A general expression for the retardation factor is given by:³

$$R = 1 + K_d \rho \psi (1 - \emptyset_{eff}) / \emptyset_{eff} \quad (4.1)$$

where

ψ = utilization factor

K_d = distribution coefficient of radionuclide
in cm^3/g

ρ = particle density of rock in g/cm^3

\emptyset_{eff} = effective porosity of rock matrix

The utilization factor (ψ) is the fractional volume of the rock matrix that interacts with the fluid. For flow in porous media, ψ approaches unity. In fractured media such as basalt, groundwater travels almost exclusively in fractures. Most of the bulk rock matrix does not interact with the fluid; under these conditions, ψ may be much less than unity. It will be shown that a simpler expression than Equation (4.1) can be used to calculate the retardation factor if we make certain assumptions about ψ .

In the reference site, nearly all of the fractures in the basalts are assumed to be lined with secondary mineralization. We have assumed that the groundwater comes in contact only with the secondary minerals. Therefore the volume of the rock matrix that interacts with the fluid is equal to the volume of the secondary mineralization. The utilization factor can be calculated as

$$\psi = \frac{\text{volume of secondary mineralization}}{\text{total rock volume}}$$

The volume of secondary mineralization is equal to a fraction or multiple (f) of the volume of open space remaining in the fractures (fracture porosity). For a unit volume of rock matrix, the utilization factor can be calculated as

$$\psi = \frac{f \cdot \text{fracture porosity}}{1 - \text{total porosity}}$$

If we assume

$$\phi_{\text{total}} \sim \phi_{\text{eff}} \sim \phi_{\text{fracture}}$$

then

$$\psi = f \phi_{\text{eff}} / (1 - \phi_{\text{eff}}) \quad (4.2)$$

Therefore Equation (4.1) becomes

$$R = 1 + f K_d \rho \quad (4.3)$$

In our calculations, we have assumed that the original fractures have been on the average one-half filled with secondary minerals. Therefore, $f = 1$ and

$$R = 1 + K_d \rho \quad (4.4)$$

In this study Equation (4.4) rather than the more general Equation (4.1) has been used to calculate R. Note that the values of K_d and ρ_s for the secondary minerals must be used in the equation. A more detailed derivation of Equation (4.3) is given in Appendix A.

The distribution coefficient K_d for radionuclides in rock-water systems is defined as

$$K_d = \frac{\text{mass on solid phase per unit mass of solid}}{\text{mass in solution per unit volume of solution}}$$

Calculations of radionuclide discharge from a repository are sensitive to values of K_d .⁴ The magnitude of K_d is influenced by many factors including solution composition, pH, Eh and temperature. Laboratory measurements of K_d have been made under a variety of physico-chemical conditions. The geochemical environment along postulated ground water flow paths must be characterized in order to choose the K_d values that were obtained under the most relevant laboratory conditions.

The geochemical environment that was postulated for each stratigraphic layer shown in Figure 2 is described in Table 3. Equation (4.1) with a utilization factor of unity was used to calculate the retardation factors for layers which are assumed to be porous. Equation (4.4) was used for layers in which ground water flows predominantly through fractures. The redox potential along the flow path and the nature of the minerals which interact with the fluid are also described in Table 3.

Table 4 shows the ranges and distributions of K_d used in this study. For basalt and secondary minerals it was assumed that data ranges obtained from experimental measurements mark the 95 percent confidence level interval. From these limits, new ranges for the 99.9 percent confidence level were generated and are shown in Table 4. The last column of the table shows the ranges of K_d in sandstone/siltstone for use in the unconfined aquifer layer. Appendix B contains a description of the data set from which the K_d values were selected and a discussion of the Eh-pH conditions in each stratum.

4.2 Solubility

The determination of solubilities of radionuclides in ground water associated with a repository in basalt requires a detailed knowledge of the aqueous geochemistry of these radionuclides. Until detailed calculations can be made, the solubility ranges employed to characterize the bedded salt reference site environment⁵ have been used in this study (Table 5). The upper limits of these ranges are probably above the real upper limits for groundwater in this study. The solubilities of these elements in waters from the basalt repository would be lower than those in the salt brines due to the lower ionic strength and higher pH of the water in the basalt.

4.3 Matrix Diffusion

In our calculations, we have assumed that the radionuclide retardation caused by diffusion into the basalt matrix is negligible. This assumption leads to conservative (high) estimates of integrated discharge. It will be shown later that for several calculations this conservative estimate resulted in apparent violation of the draft EPA Standard.⁷ In Appendix C, a method to approximate the retardation due to matrix diffusion is outlined. It is shown that the retardation calculated in this manner has the potential to reduce all discharges to levels below the EPA standard.

Table 3
 Geochemical Environment of Stratigraphic
 Layers in Basalt Repository

<u>Layer</u>	<u>Type of Medium</u>	<u>Redox Conditions</u>	<u>Mineralogy</u>
A	Fractured	Reducing	Secondary minerals
B	Fractured	Reducing	Secondary minerals
C	Fractured	Reducing	Secondary minerals
D	Fractured	Reducing	Secondary minerals
E	Fractured	Reducing	Secondary minerals
I-V	Porous	Oxidizing	Secondary minerals
F	Fractured	Reducing	Secondary minerals
G	Fractured	Reducing	Secondary minerals
H	Fractured	Reducing	Secondary minerals
I-M	Porous	Oxidizing	Secondary minerals
J	Fractured	Reducing	Secondary minerals
UA	Porous	Oxidizing	Sandstone/silt

Density of secondary minerals = 2.3 g/cm³

Density of rock in layer I-V and I-M = 3.3 g/cm³

Table 4
 K_d Ranges (cm^3/g)

Element	Reducing SM*	Oxidizing SM*	Reducing Basalt	Oxidizing Sandstone/Siltstone
Cm, Am	(25., 2.0E6)	(25., 2.0E6)	(33., 300.)	(1.0E-2, 1.0E5)
Pu	(45., 5.2E3)	(37., 1.5E4)	(0.35, 4.24E4)	(1.0E-2, 1.0E4)
Np	(1.5, 2.8E4)	(4.0, 430.)	(1.7, 1.56E3)	(1.0E-2, 50.)
U	(4.0, 1.3E3)	(2.4, 1.5E4)	(34., 57.)	(1.0E-2, 1.0E4)
Th	(25., 2.0E6)	(25., 2.0E6)	(33., 300.)	(1.0E-2, 1.0E4)
Pa	(25., 2.0E6)	(25., 2.0E6)	(33., 300.)	(1.0E-2, 1.0E4)
Ac	(25., 2.0E6)	(25., 2.0E6)	(33., 300.)	(1.0E-2, 1.0E4)
Pb	(17., 5.8E3)	(17., 5.8E3)	(68., 320.)	(1.0E-2, 1.0E4)
Ra	(17., 5.8E3)	(17., 5.8E3)	(68., 320.)	(1.0E-2, 500.)
Sn	(17., 5.8E3)	(17., 5.8E3)	(68., 320.)	(1.0E-2, 500.)
Tc	(0.2, 750.)	(0.6, 10.0)	(0.2, 4.16E4)	(1.0E-2, 1.0E3)
I	(0.7, 6.0)	(0.7, 6.0)	0	(1.0E-2, 100.)
Sr	(0.8, 1.38E3)	(185., 590.)	(67., 600.)	(1.0E-2, 500.)
Cs	(97., 1.3E6)	(97., 1.3E6)	(51., 2.0E3)	(1.0E-2, 1.0E4)
C	0.	0.	0.	0.

Distribution of K_d : Lognormal

*SM = Secondary Minerals

Table 5

Ranges of Solubilities of Selected Elements
Used for Basalt Reference Repository Conditions*

<u>Element</u>	<u>Log₁₀ Mass Fraction (g/g)</u>
Tc	Low
I	No Limit
Sn	-10 \pm 2
Cs	No Limit
Ra	-8 \pm 1
Th	-7.1 \pm 0.6
U	-4.7 \pm 1
Np	-15.6 \pm 3
Pu	-9.6 \pm 2
Am	No Limit
Cm	No Limit
Pb	-7.5 \pm 1
Pa	-5 \pm 0.6

*Data are from Muller, et al., 1981,⁵ for bedded salt repository. Values are mean \pm 1 as calculated from the thermochemical data.

5. Groundwater Transport Model

In the calculations of radionuclide transport it is assumed that groundwater flows upward from the vicinity of the repository to an aquifer, whereupon it moves horizontally toward the biosphere. This flow is modelled as being quasi-two-dimensional and described by Darcy's Law:

$$q = Q/A = KI \quad (5.1)$$

where Q is the volumetric flow rate through an area A , normal to the flow direction, I is the hydraulic gradient, K is the hydraulic conductivity, and q is the Darcy velocity. When the flow passes through a series of layers with different hydraulic properties, an "effective" hydraulic conductivity may be calculated by

$$K = \frac{\sum_i L_i}{\sum_i \frac{L_i}{K_i}} \quad (5.2)$$

with

L_i = thickness of layer i

K_i = hydraulic conductivity of layer i

The total groundwater travel time is given by

$$\text{Time} = \sum_{i=1} \frac{L_i}{V_i} \quad (5.3)$$

where V_i is the interstitial groundwater velocity in layer i and is equal to q/θ_i , with θ_i being the effective porosity of layer i .

When a radionuclide (RN) is transported by groundwater, the radionuclide travel time (T_{RN}) is increased by its retardation factor. This is given by

$$T_{RN} = \sum_i \frac{L_i \cdot R_i^{RN}}{V_i} \quad (5.4)$$

where R_i^{RN} is the retardation factor of radionuclide RN in layer i .

The Distributed Velocity Method (DVM) has been developed by Sandia¹ to simulate long chains of radionuclides transported by groundwater. In this study we calculated the average velocity of radionuclides using Equation (5.4). Then the DVM code was used to calculate the discharges of radionuclides.

The fission and activation product radionuclides Tc99, I129, Sn126, Sr90, C14, Cs135, and Cs137 were also considered in this work.

Table 6 shows the data ranges and distributions for some additional variables used in the calculations of these scenarios.

Two source model descriptions were used in this analysis. In the first source model assumes the solid matrix containing the waste radionuclides, e.g., spent fuel elements or borosilicate glass, breaks down at a constant rate. This is the so called "leach limited source model". Radionuclide release then occurs at a rate determined by the inventory in each differential mass increment that is released. For simplicity, radionuclides are assumed to be homogeneously distributed throughout the solid matrix. The leach-limited source model is most easily compared with the requirements of 10CFR60. Simply stated, 10CFR60 requires that release rates not exceed a specified rate of 10^{-5} /year. The release rate is equal to the reciprocal of the leach period.

The second source model assumes that the backfilled regions can be modeled as a mixing cell. The waste matrix still is assumed to decompose at a constant rate. However, the radionuclides are assumed to instantaneously mix with water in the mixing cell. Radionuclide release from the backfilled regions is sensitive to the radionuclide concentration in the mixing cell. This model is discussed further in Appendix E.

NWFT/DVM allows user-selection of the source model. It also has an algorithm for automated source model selection. In the scenarios to be described, only Scenario III had the necessary conditions to select the mixing cell model. For comparison, this scenario was also analyzed with the leach-limited source model imposed.

6.1 Scenario I -- Routine Release

In this scenario, it was assumed that groundwater migrates into the repository and saturates the pore volume of the repository. When the waste canisters fail at 1,000 years, this column of water having the cross-sectional area of the repository slowly transports leached and dissolved radionuclides vertically through the basalt layers to the aquifer system I-M and then horizontally through the aquifer to a discharge point 1 mile down gradient. In our base case and in the other

scenarios, it was assumed that there existed little or no natural vertical gradient. A temperature field in the vicinity of the repository due to the heat generated from the decaying wastes produces an upward hydraulic gradient due to thermal buoyancy for the groundwater. For our base case, we estimated that this thermal buoyancy effect generated a hydraulic gradient ranging from 5×10^{-3} to 3×10^{-2} . This gradient is assumed to be constant along a vertical column which has the hydraulic conductivity given by Equation 5.2. The derivation of this calculation is presented in more detail in Appendix D. It was also assumed that the upward flow of groundwater into aquifer I-M does not alter the natural hydraulic gradient in the I-M. Figure 3 schematically shows the transport route in this scenario.

Integrated discharges for each vector were calculated at a distance of 1 mile down gradient in aquifer I-M. The results of these calculations are as follows. The integrated discharges for each actinide radionuclide were all zero for all vectors. For the fission products radionuclides, there were some small discharges but they were all below the EPA release limits.

In this scenario, all 100 vectors resulted in a leach limited source as determined by the automatic source selection algorithm of NWFT/DVM.

Table 6

Additional Data Ranges and Distributions

	<u>Range</u>	<u>Distribution</u>
Leach Period (year)	$10^4 - 10^7$	Log Uniform
Horizontal gradient in aquifer	$10^{-4} - 10^{-2}$	Uniform
Conductivity of borehole	0.05 - 50	Log Uniform
Porosity of borehole	0.05 - 0.5	Normal
Vertical upward gradient in Scenarios I and II	$5 \times 10^{-3} - 3 \times 10^{-2}$	Uniform
Vertical upward gradient in Scenario III	$3 \times 10^{-3} - 2 \times 10^{-2}$	Uniform
Dispersivity (ft)	50	

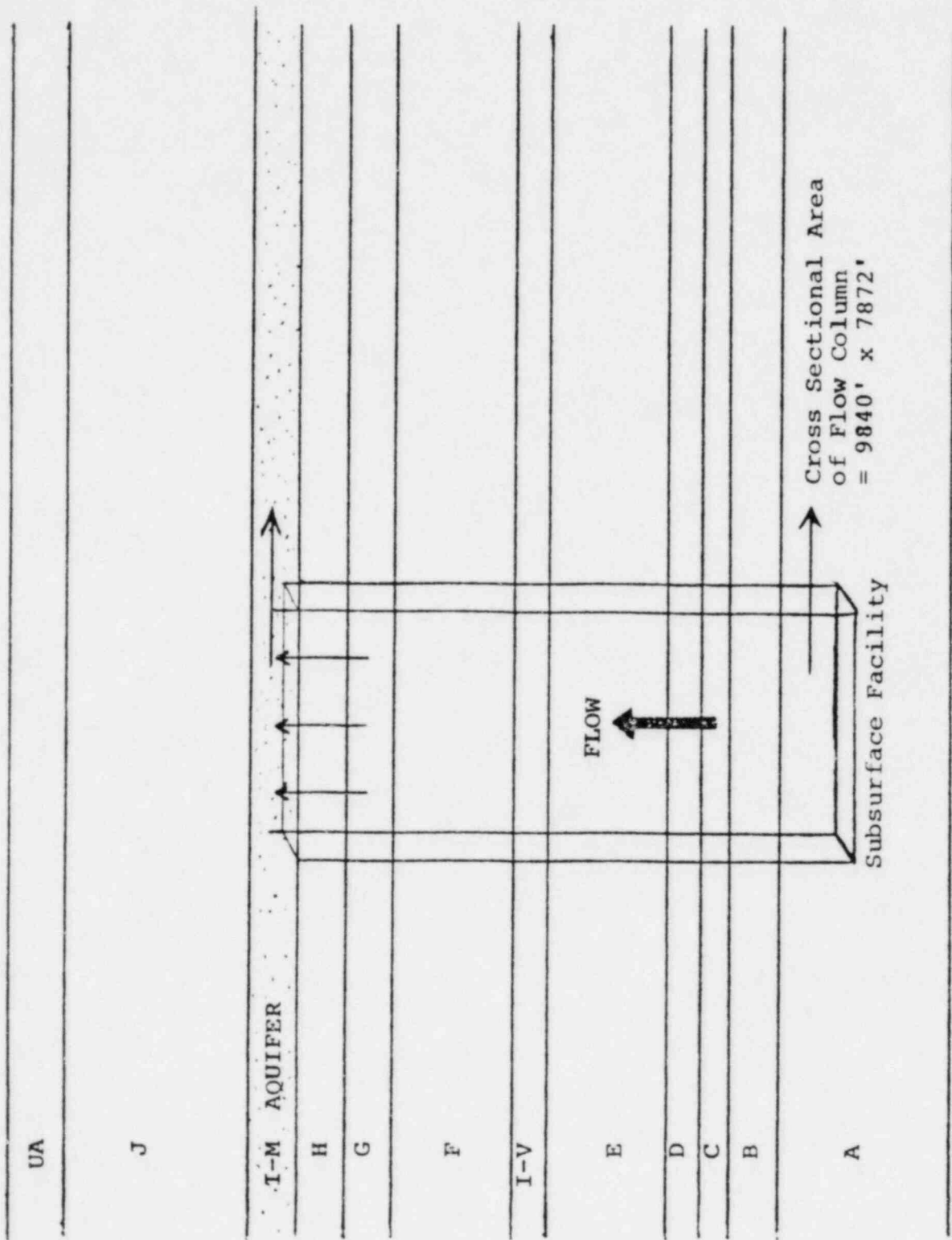


Figure 3. Routine Release Scenario

6.2 Scenario II -- Fractures in Dense Basalt

This scenario is based on the assumption that the hydrologic properties of the dense basalt unit (Layer A) containing the subsurface facility have been altered. Specifically, this scenario assumes that the hydraulic conductivity and porosity have been increased due to the production of fractures in the rock strata. The generation of these new fractures could be caused by one or more of several processes: thermal stress from waste heat, mechanical stress from the construction of the repository, or the occurrence of an earthquake swarm. The increased conductivity and porosity enhance the upward migration of radionuclides released from the subsurface facility.

In the calculations of radionuclide releases the following assumptions were made (Figure 4):

1. The fractured zone is located above the subsurface facility in the dense basalt unit (Layer A).
2. The fractures in the dense basalt layer occur immediately after closure of the subsurface facility.
3. The fractured zone has the same cross-sectional area as that of the subsurface facility, i.e., 9840' x 7872', and it extends upward through all of Layer A.
4. The hydraulic conductivity of the fractured zone is arbitrarily increased by two orders of magnitude and the porosity is increased by a factor of four. That is,

$$K_{\text{fractured basalt}} = 100 \cdot K_{\text{dense basalt}}$$
$$\phi_{\text{fractured basalt}} = 4 \cdot \phi_{\text{dense basalt}}$$

5. The vertical hydraulic gradient is the same as that used in Scenario I, i.e., 5×10^{-3} to 3×10^{-2} .

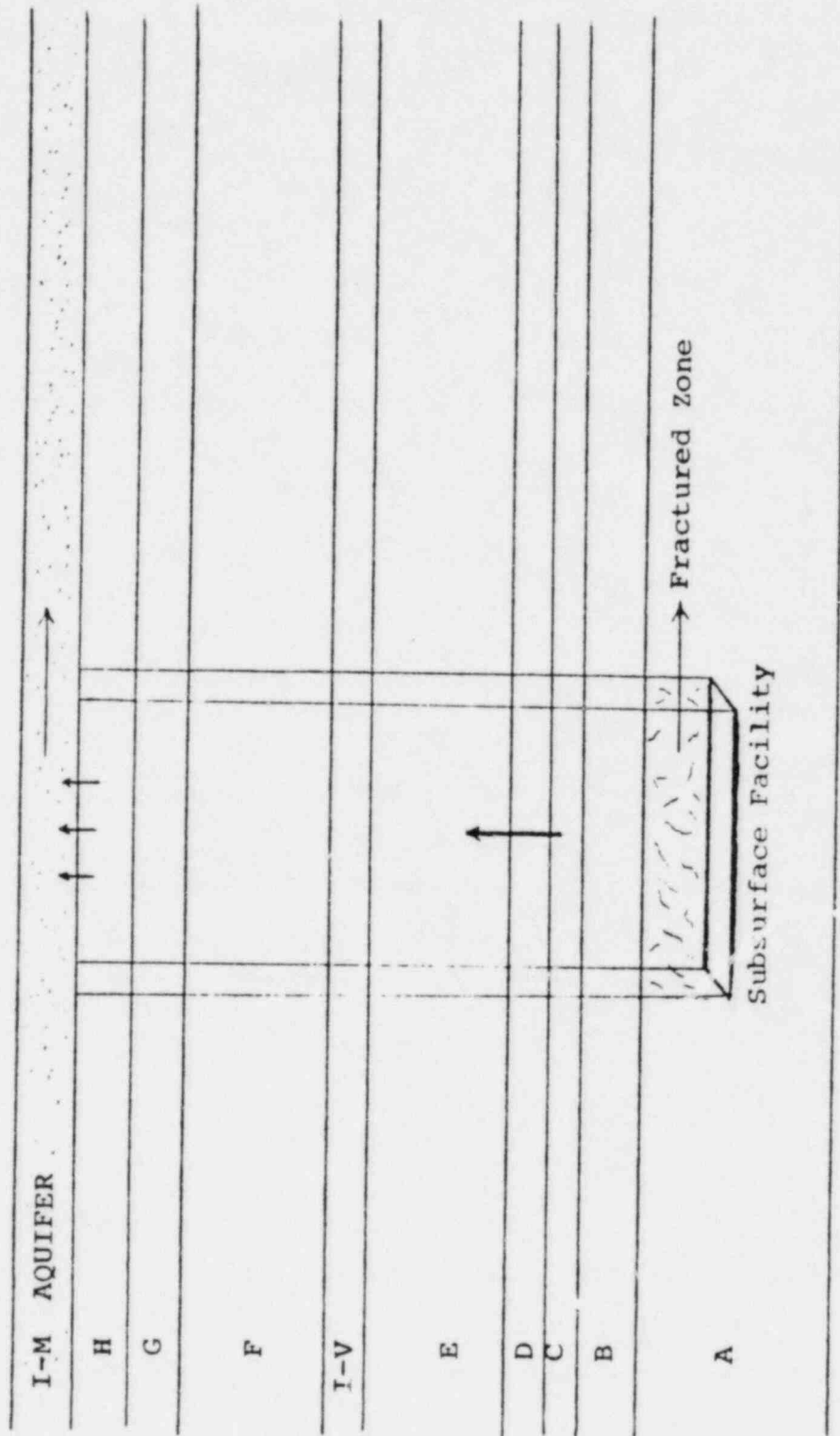


Figure 4. Fractured Dense Basalt Scenario

The same 100 vectors as those used in the routine-release scenario were used in the calculations of integrated discharges of radionuclides in this scenario. Two calculations were performed. First, discharges were calculated for releases into aquifer I-M directly above the repository. Table 7 lists the radionuclides and the vectors that showed violation of the draft EPA Standard. Second, numbers in parentheses in Table 7 show results of calculations when discharge location was moved 1 mile down gradient in aquifer I-M.

Table 7 shows that few of the sampled input vectors violate the draft EPA Standard. In these calculations, however, the retardation due to matrix diffusion was ignored. A method for estimating the magnitude of this effect is described in Appendix C. When the retardation due to matrix diffusion is calculated by this method, it is possible that no vectors violate the draft EPA Standard.

For readers familiar with the technical criteria of 10CFR60, it is worth mentioning that of all the "violating" vectors listed in Table 7, all except one (vector #24) have leach rates greater than 10^{-5} /year. Also, all vectors except two (#4 and #71) have groundwater travel time from the repository to the discharge location greater than 1,000 years.

For Scenario II all 100 vectors used the leach-limited source model as determined by the automatic source selection algorithm of NWFT/DVM.

6.3 Scenario III -- Borehole

This scenario assumes that there exists a borehole or a zone of high conductivity that connects the repository to the unconfined upper aquifer (Layer UA). This zone is of very small areal extent (Figure 5). The high conductivity zone could be related to one of the following:

- borehole
- degraded shaft seal
- disturbed rock zone around a borehole or shaft.

This last mode can occur during relaxation of emplacement stresses or as a result of earthquake.

The following assumptions were used in the calculations of this scenario:

1. Cross-sectional area of this disruptive zone is 2 square feet.
2. Hydraulic conductivity of this zone has a range of 0.05 ft/day to 50 ft/day. A lognormal distribution is assigned to this range.

Table 7

Scenario II
 EPA Ratios* of Radionuclides Discharge into I-M

0-10,000 years:

<u>Vector #</u>	<u>14C</u>
5	1.28 (1.34)**†
71	1.14 (1.15)†
77	1.19 (1.22)†

10,000-20,000 years:

<u>Vector #</u>	<u>99Tc</u>
13	2.73 (0.)
62	3.43 (1.18)
65	2.11 (1.68)

20,000-30,000 years:

<u>Vector #</u>	<u>99Tc</u>
5	1.79 (1.29)
13	2.62 (0.)
25	1.97 (1.08)
62	2.09 (3.43)
65	2.10 (2.00)
87	1.95 (2.04)

30,000-40,000 years:

<u>Vector #</u>	<u>99Tc</u>	<u>234U</u>	<u>236U</u>	<u>238U</u>
5	3.21 (4.21)			
15	1.49 (1.27)			
20	2.14 (2.27)			
24		3.29 (0.55)	1.29 (0.19)	1.45 (0.25)
25	3.16 (4.09)			
62	0.002 (1.42)			
65	1.00 (1.99)			
87	2.25 (2.22)			

Table 7 (Continued)

40,000-50,000 years:

<u>Vector #</u>	<u>99Tc</u>	<u>234U</u>	<u>236U</u>	<u>238U</u>
4	1.26 (1.22)			
10	1.05 (0.88)	2.79 (0.)	1.05 (0.)	1.25 (0.)
15	2.28 (2.54)			
20	2.38 (2.88)			
24		4.42 (3.61)	2.04 (1.43)	2.01 (1.61)
87	1.29 (1.42)			

*EPA Ratio is the ratio of integrated discharge of radionuclide (over 10,000 years) to the allowed EPA Release Limit.

**Numbers in parentheses represent the results of calculations when discharge location is at a distance 1 mile down gradient in aquifer I-M.

†The small increase is the result of numerical dispersion.

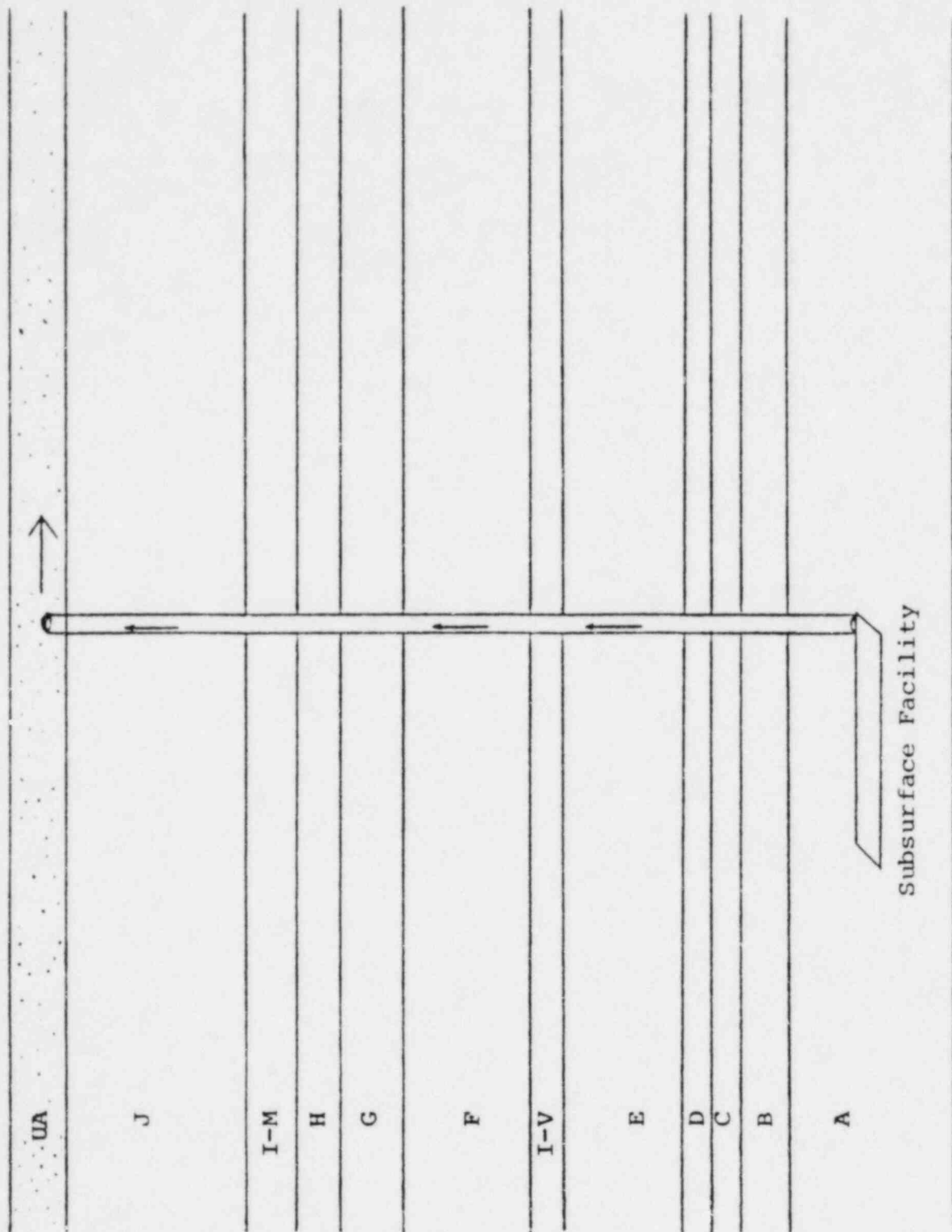


Figure 5. Borehole Scenario

3. Porosity of this zone has a range of 0.05 to 0.5. A normal distribution is assigned to this range.
4. The hydraulic gradient in UA is unperturbed due to the smallness of this zone.
5. The same head difference typical of thermal buoyancy as calculated in Appendix C is assumed here. However, due to the extra 1,000 foot path length between I-M and UA, the vertical upward gradient between the repository and aquifer UA is reduced to the range 3×10^{-3} - 2×10^{-2} .
6. Layer UA is composed mainly of sandstone/siltstone and is characterized by an oxidizing environment.
7. The redox potential in the small disruptive zone is reducing and the rock type is fresh basalt.
8. The discharge location is 1 mile down gradient in aquifer UA.
9. The entire radionuclide inventory in the repository is available for leaching and transport.

Integrated discharges of each radionuclide were calculated for each vector and divided by the EPA Release Limit to produce the "EPA Ratio". Table 8 shows those radionuclides and vectors that produce EPA Ratios of magnitude exceeding one. For each vector the EPA Ratios were then summed over all radionuclides and the results are shown in Table 9.

In the analysis of Scenario III, all 100 vectors chose the mixing cell source model as determined by the automatic source selection algorithm of NWFT/DVM. For comparison this scenario was also analyzed with the leach-limited source model imposed. With this source model, too many vectors gave large discharges to list each violating vector as in Tables 8 and 9. In Table 10 we show the mean values for the 100 vectors for each radionuclide that had significant discharge. From this table the main radionuclides appear to be ^{243}Am , ^{240}Pu , ^{239}Pu , and ^{234}U .

Table 8
 Scenario III
 EPA Ratios of Radionuclides

²⁴³Am:

<u>Vector #</u>	<u>10⁴-2x10⁴ years</u>	<u>2x10⁴-3x10⁴ years</u>	<u>3x10⁴-4x10⁴ years</u>
13		1.30	1.15
36	2.34	1.93	

Table 9

Scenario III
EPA Ratios Summed Over all Radionuclides

<u>Vector #</u>	<u>10⁴-2x10⁴ years</u>	<u>2x10⁴-3x10⁴ years</u>	<u>3x10⁴-4x10⁴ years</u>	<u>4x10⁴-5x10⁴ years</u>
13		1.4	1.20	
36	2.49	2.25	1.73	1.55

Table 10

Mean Values of Contributions to the EPA Sum (100 Vectors)
for Scenario III With Leach-Limited Source

Radionuclide	10,000 year period				
	1	2	3	4	5
240 Pu	8.56	9.75	3.23	1.87	.69
236 U	.12	.34	.46	.64	.56
245 Cm	.01	.02	.02	.01	.01
241 Am	.05	.02	.02	.01	.01
237 Np	.31	.78	.97	.81	.99
233 U	.01	.07	.13	.25	.31
229 Th	.01	.08	.21	.49	.78
242 Pu	.06	.14	.12	.18	.16
238 U	.15	.35	.49	.66	.54
234 U	.34	.82	1.15	1.52	1.22
230 Th	.01	.05	.10	.22	.30
226 Ra	.02	.20	.48	.91	1.24
210 Pb	0.	.03	.06	.13	.19
243 Am	1.35	3.83	2.60	1.84	1.16
239 Pu	9.02	17.95	12.38	13.91	10.19
235 U	.01	.02	.03	.04	.04
231 Pa	0.	0.	.01	.01	.02
227 Ac	0.	.01	.03	.05	.08
99 Tc	.05	.07	.06	.06	.06
126 Sn	0.	.04	.06	.04	.03
14 C	.13	.04	.01	0.	0.

7. The Draft EPA Standard, 40CFR191

The Environmental Protection Agency (EPA) has issued a draft of its proposed generally applicable standard for the protection of public health from the geologic disposal of radioactive wastes.⁷ The standard is expressed in terms of the total integrated discharge of the radionuclides comprising the wastes to the accessible environment. In Table 11 is given a list of radionuclides expected in radioactive waste and the corresponding EPA release limits.⁷ Since events and processes leading to radionuclide release will generally result in the release of mixtures of radionuclides, a sum rule is imposed on mixtures of radionuclide discharges:

$$\text{EPA Sum} \quad \sum_i \frac{Q_i}{\text{EPA}_i} \quad \left\{ \begin{array}{l} \leq 1. \text{ for reasonably foreseeable} \\ \text{releases} \\ \leq 10. \text{ for very unlikely releases} \end{array} \right.$$

where Q_i is the integrated discharge over 10,000 years of radionuclide i and EPA_i is the release limit of radionuclide i in the draft standard. Q_i is scaled for the amount of waste in the geologic repository according to the assumed 1000 metric tons of heavy metal (MTHM).

In the draft EPA Standard, a "reasonably foreseeable" release is defined as any release expected to occur with a probability of greater than 0.01 in the 10,000 year period addressed by the standard. A "very unlikely release" is defined as any release expected to occur with a probability of less than 0.01 but greater than 0.0001 in the 10,000 year period addressed by the standard. Any release with a probability of occurrence of less than 0.0001 in the 10,000 year period need not be considered in analyses.⁸

7.1 Interpretations of the Draft Standard

In attempting to assess compliance with the draft standard, three points of confusion have arisen which should be clarified by the EPA in the final issue of the standard:

Table 11

Cumulative Releases to the Accessible
Environment for 10,000 Years After Disposal⁷

<u>Radionuclide</u>	<u>Release Limit Curies Per 1000 MTHM)</u>
Americium-241	10
Americium-243	4
Carbon-14	200
Cesium-135	2000
Cesium-137	500
Iodine-129	500
Neptunium-237	20
Plutonium-238	400
Plutonium-239	100
Plutonium-240	100
Plutonium-242	100
Radium-226	3
Strontium-90	80
Technetium-99	2000
Tin-126	80
Any other alpha-emitting radionuclide	10
Any other radionuclide which does not emit alpha particles	500

1. Compliance with the draft standard cannot be guaranteed with 100 percent confidence. There are inherent uncertainties in calculations required to assess compliance resulting from uncertainty in input data, numerical dispersion on computer models, and uncertainty as to how well models represent the physical system, to name a few. It will be shown in later sections that a fraction of the input vectors may lead to violations of the standard due to uncertainty in the input data. Clarification from EPA may be necessary as to how uncertainty in compliance assessment should be treated.
2. The categories in Table 10 denoting "any alpha" and "any non-alpha" decaying radionuclides are vague. Many of the radionuclides in nuclear wastes decay in more than one way. For the analyses to be presented, we have interpreted these categories as meaning the dominant decay mode.
3. The standard uses, but does not define, the word "release". The interpretation of this word affects the manner in which compliance is assessed. We offer two interpretations below.

Interpretation 1: The word "release" defines a unique event or scenario leading to radionuclide release. The draft EPA Standard is applied independently to each scenario.

Interpretation 2: A "release" involves all events or processes that may result in discharges to the environment during the regulatory period. The magnitude of the discharge is given by its corresponding EPA Sum. The standard could be rephrased as saying, for example, "Values of EPA Sum greater than 1 shall occur with a probability of less than 0.01 in 10,000 years." Estimation of the probability of exceeding a given value of EPA Sum includes contributions from all scenarios.

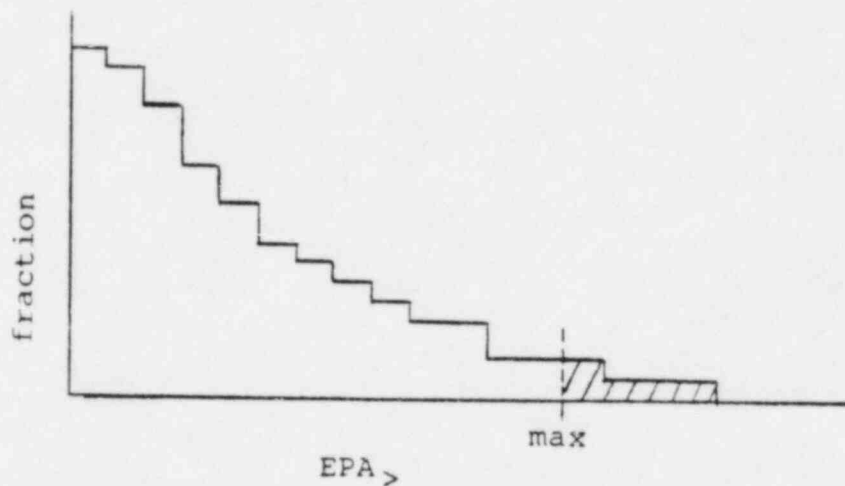
We have performed analyses based on both interpretations.

7.2 Implementations of Different Interpretations

Interpretation 1

The probability assigned to the scenario indicates whether values of the EPA Sum will be compared to 1 or 10. Different values of the EPA Sum result from different combinations of input data chosen by the sampling procedure.⁶ Thus, there is sampling error in the assessment of compliance.

The results of calculations are presented in a Complimentary Cumulative Distribution Function (CCDF) as suggested by EPA.⁸ Such a CCDF is illustrated in the following diagram,



For N input vectors the plotted curve specifies the fraction of those vectors producing a value of the EPA Sum greater than some value denoted by $EPA_{>}$. In this example, the shaded area indicated that a fraction of the vectors violate the standard.

Interpretation 2

According to this interpretation, the analyst is presumed to have the same set of scenarios and probabilities as in Interpretation 1. Each scenario is again analyzed to estimate the EPA Sum as in Interpretation 1.

However, with this interpretation, compliance is estimated by constructing a CCDF from all scenarios. The construction of this CCDF is aided by first constructing a plot of probability versus the EPA Sum for all scenarios. An important point should be made regarding the probabilities used in the construction of the CCDF. The probability used is that of the scenario's occurrence and the particular combination of the input data used in the calculation of the EPA Sum.

Construction of the CCDF then includes contributions from all scenarios analyzed expected to produce an EPA Sum greater than a given value, $EPA_{>}$. The probability, $p_{>}$, associated with $EPA_{>}$ is given by

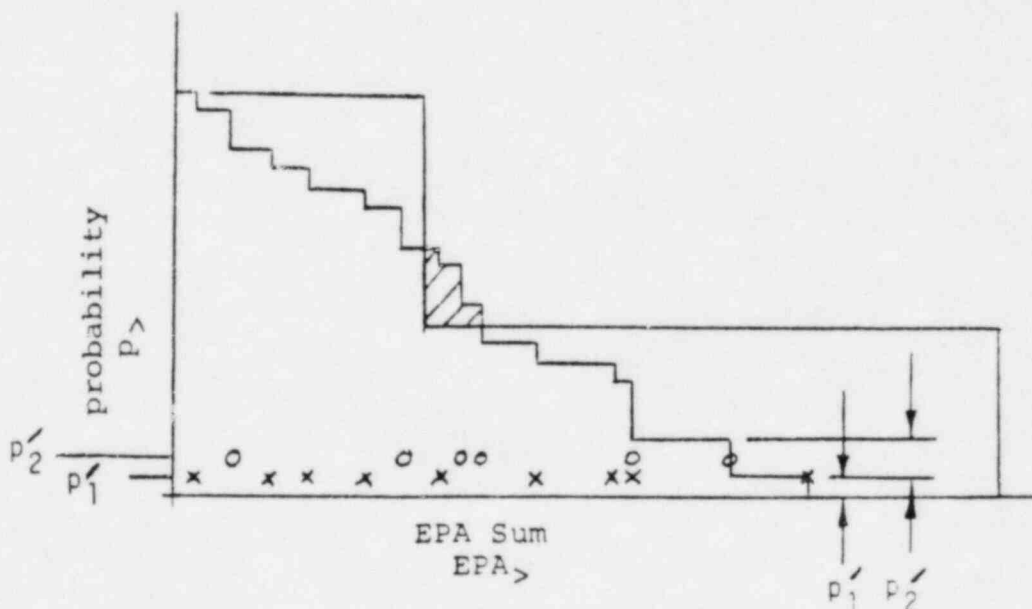
$$p_{>} = \sum_s p_s \cdot p_c (EPA \text{ SUM} > EPA_{>} | s)$$

$$= \sum_s \frac{p_s}{N} \cdot (\text{Number of vectors with } EPA \text{ Sum} > EPA_{>} \text{ for scenario, } s.)$$

where p_s is the probability of scenario s and p_c is the conditional probability of the state of the repository, given scenario s . The last step, substitution for p_c , follows from the fact that the LHS method selects N input vectors with equal probability. For simplicity, we write

$$p_s' = \frac{p_s}{N}$$

Construction of the CCDF is illustrated in the following diagram for the case of two scenarios where, for clarity, the CCDF is superimposed on the probability versus EPA Sum plot,



Compliance with the draft EPA Standard is then determined by comparison of the constructed CCDF with an envelope defined by the standard and illustrated in the diagram. The shaded area in the diagram defines the part of the constructed CCDF outside of the EPA limit and indicates non-compliance with the standard.

7.3 Estimation of Probabilities of Scenarios

Although the methods developed at Sandia may be used with ranges and distributions for p_s , the scenario probability, we have used fixed values in this analysis. The site we have assumed for this analysis has not been characterized sufficiently well to allow estimation of the probabilities. Since the draft EPA Standard requires this information and since it may introduce further uncertainty into estimates of compliance, it is appropriate in this work to discuss the likely sources of the probabilities.

- Option 1. Of the scenarios to be analyzed, the analyst may have reason to believe that the processes involved are stochastic in nature. In such a case, methods may exist to estimate this probability with the final uncertainty in the estimate resulting from uncertainty in input data and the accuracy of models used to perform the estimate. At least one attempt has been made to address faulting in this manner with input data describing existing fault density and stress states required.⁹
- Option 2. Historical data may be available that may be extrapolated into the future to estimate probabilities of some scenarios. An example of use of such data is the estimation of exploratory drilling for petroleum resources. In the reference site analysis of a hypothetical nuclear waste repository in bedded salt, drilling records for similar sites were used to estimate the probability of future exploratory drilling into the repository.⁴

Option 3. In the absence of historical records and detailed understanding of the processes involved, expert judgement may be used to estimate scenario probabilities (the Delphi Method).

The Delphi Method is implicit in both Option 1 and Option 2 since unquantifiable judgements must be made as to the applicability of data and models.

8. Results of Demonstration Analyses

For this demonstration, three basic scenarios and several variations on them have been analyzed in detail. A detailed analysis of scenario probabilities has not been performed due to constraints on the allowed effort and the fact that site characterization is in its early stages. The three scenarios analyzed are assumed to form a complete set of mutually exclusive scenarios describing the repository over the 0-10,000 year interval.

$$\sum_s p_s = 1$$

The three scenarios analyzed have been discussed previously. We assume the following probabilities:

<u>Scenario, s</u>	<u>Description</u>	<u>P_s</u>
1	The undisturbed site	0.33
2	The large areal extent, high conductivity zone, e.g., fractures	0.01
3	The small areal extent, high conductivity zone, e.g., a borehole	0.66

Calculations have been performed for the three scenarios to estimate values of the EPA Sum during each 10,000 year interval from zero to 50,000 years post-closure. Thus, for Interpretation 1, five CCDF's have been constructed for each of the three scenarios. For Interpretation 2, five CCDF's have been calculated. CCDF's based on Interpretation 1 appear in Figure 6 through 20. CCDF's based on Interpretation 2 appear in Figures 21 through 25.

In Figures 6 through 25 the automatic source selection algorithm of NWFT/DVM has been used. For Scenarios I and II, the algorithm selected leach-limited sources for all 100 vectors. For Scenario III the algorithm selected the mixing cell source model for all 100 vectors. For comparison, Scenario III was also evaluated with the leach limited

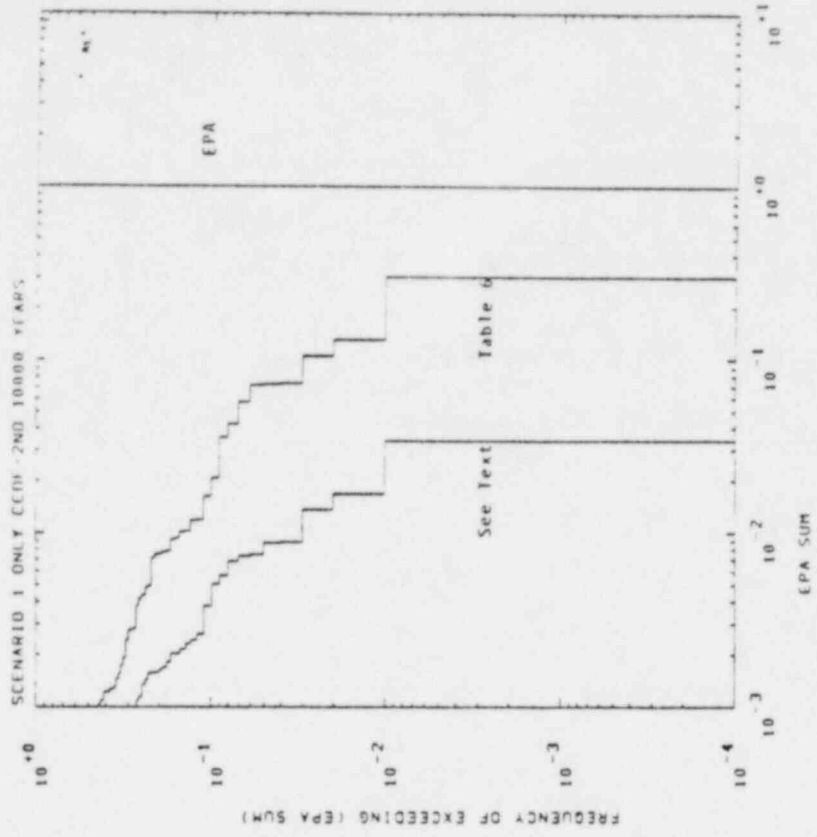


Figure 7

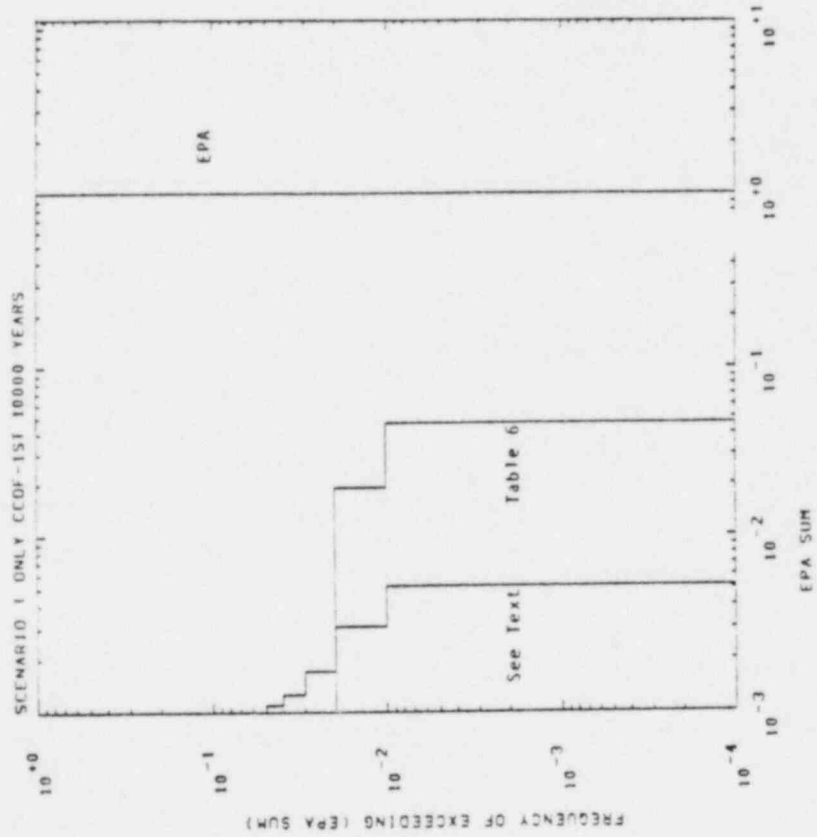


Figure 6

SCENARIO 1 ONLY CCDF-3RD 10000 YEARS

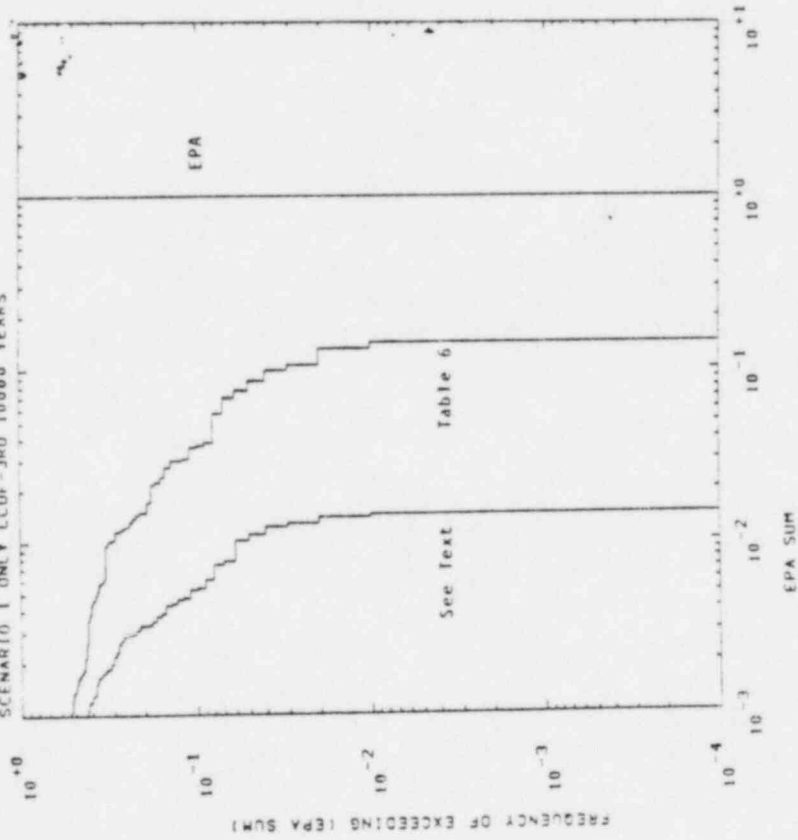


Figure 8

SCENARIO 1 ONLY CCDF-4TH 10000 YEARS

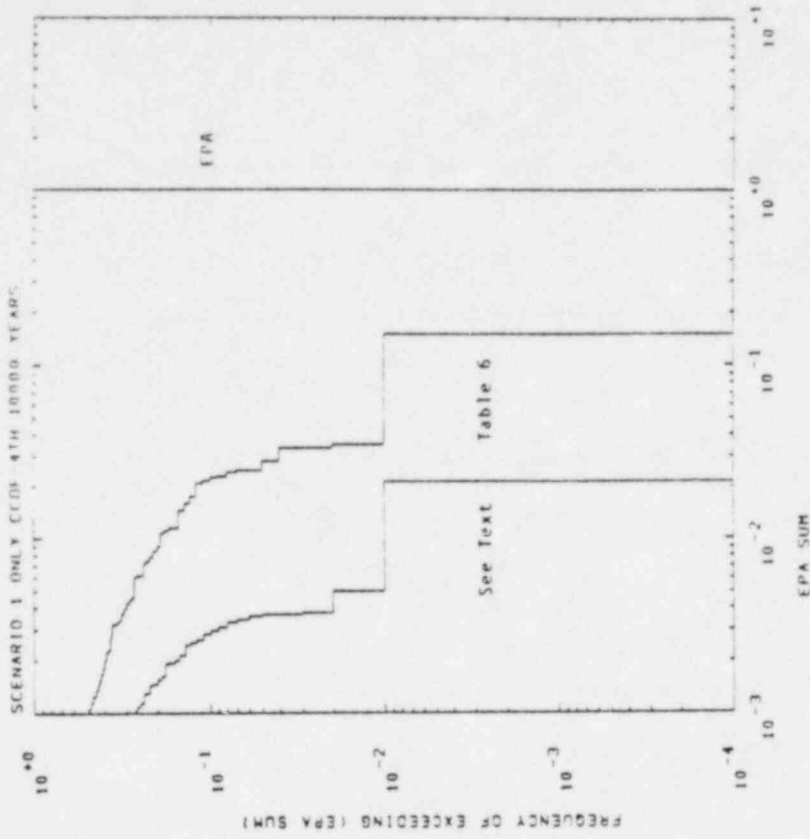


Figure 9

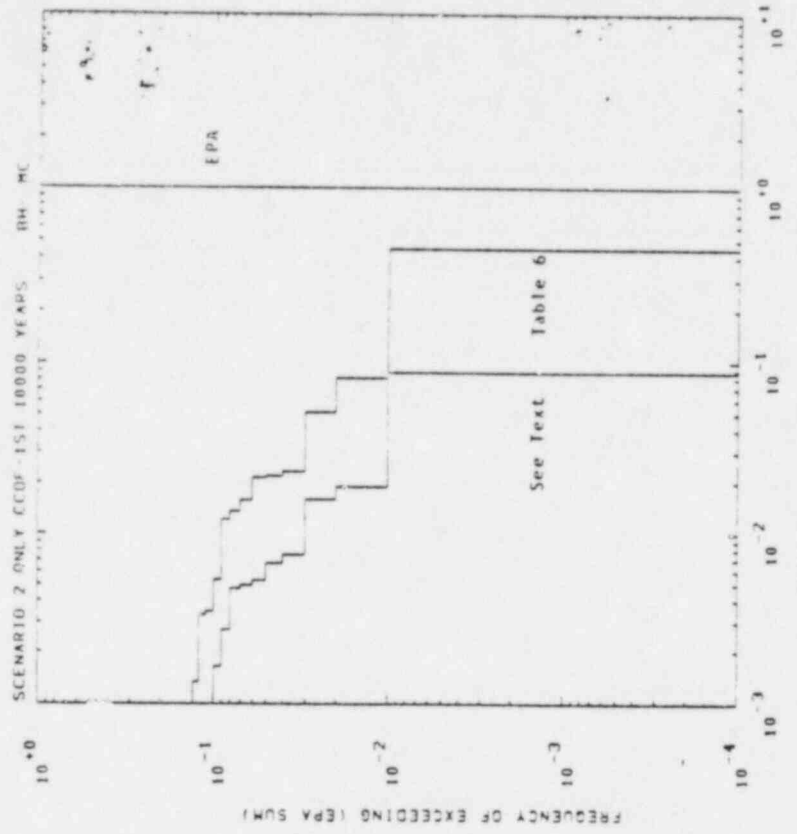


Figure 10

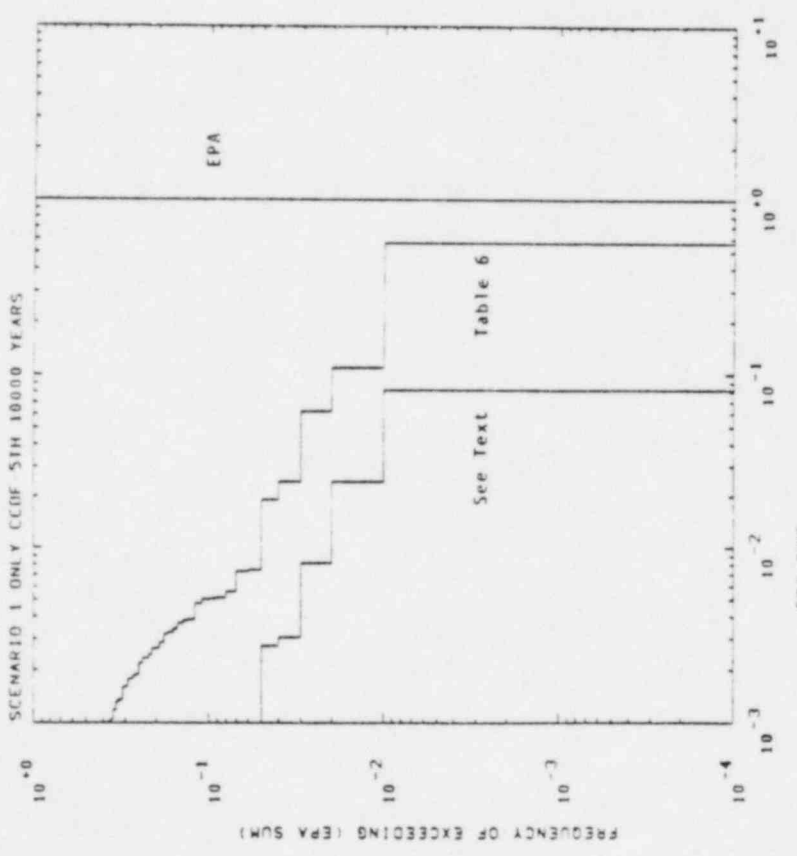


Figure 11

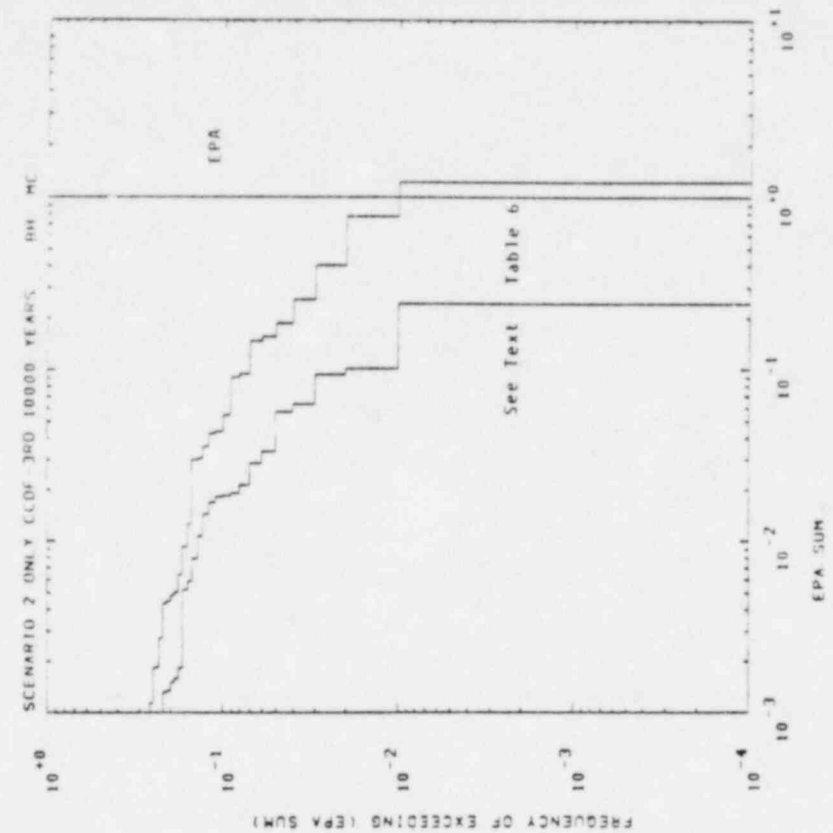


Figure 12

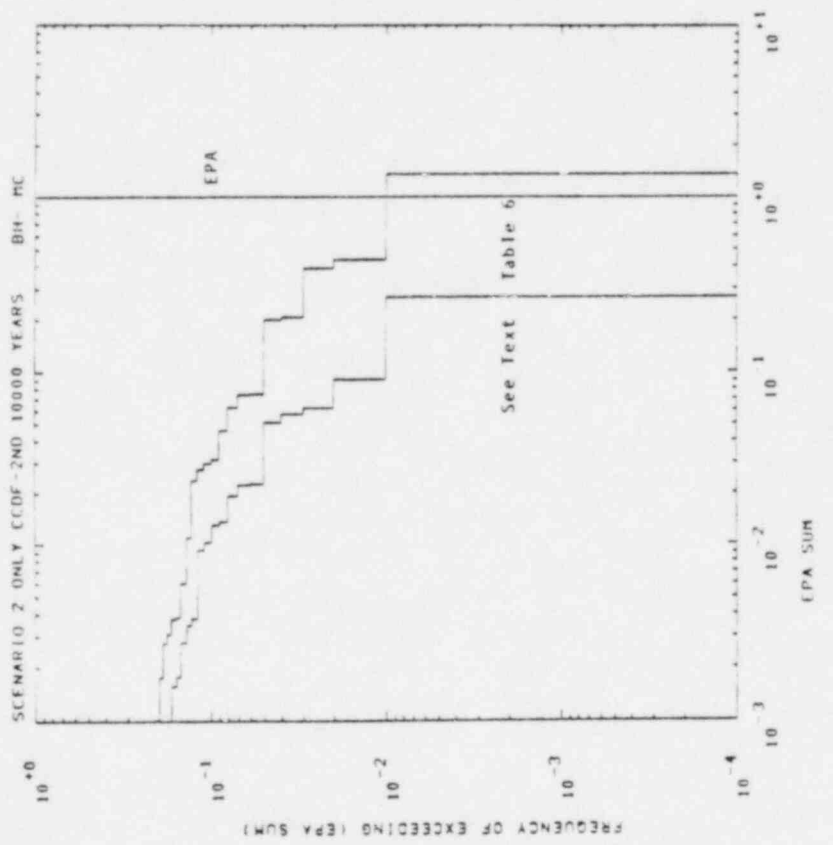


Figure 13

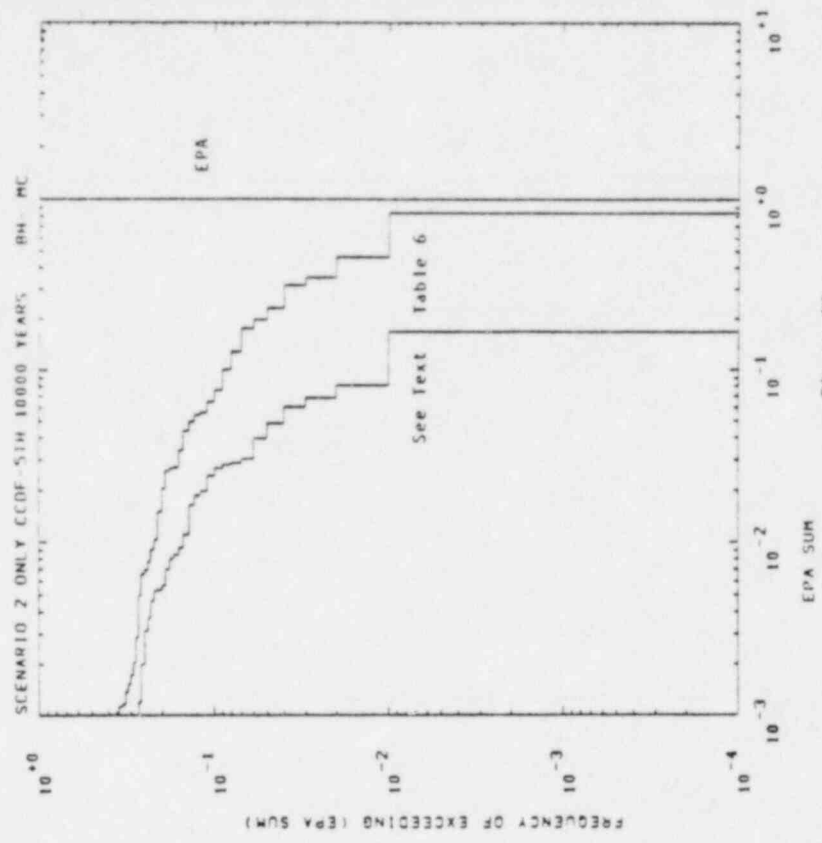


Figure 14

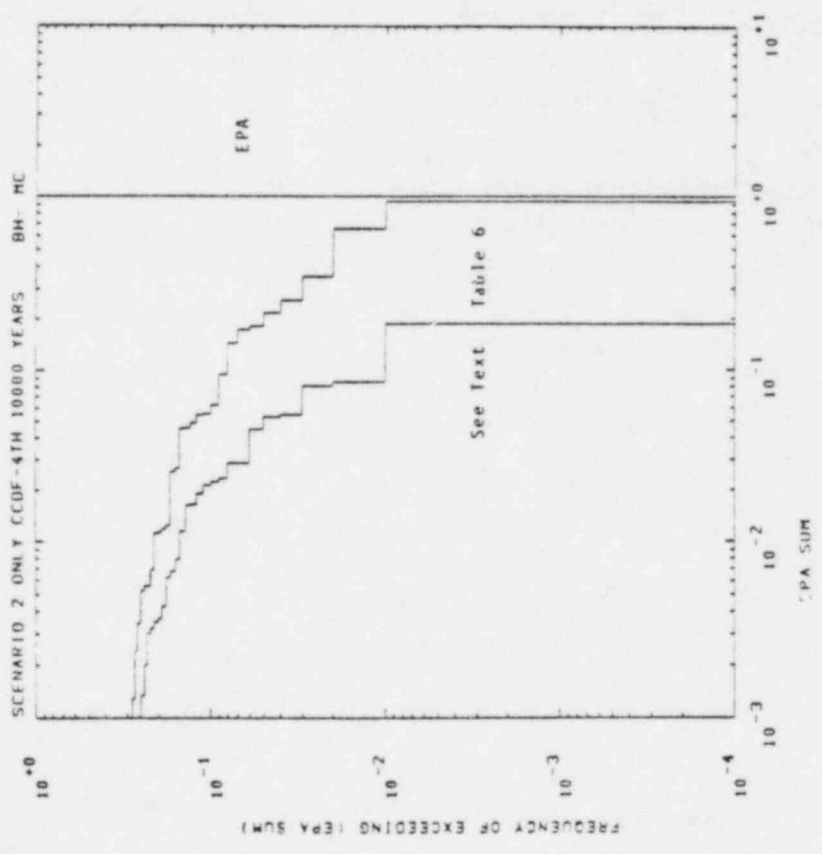


Figure 15

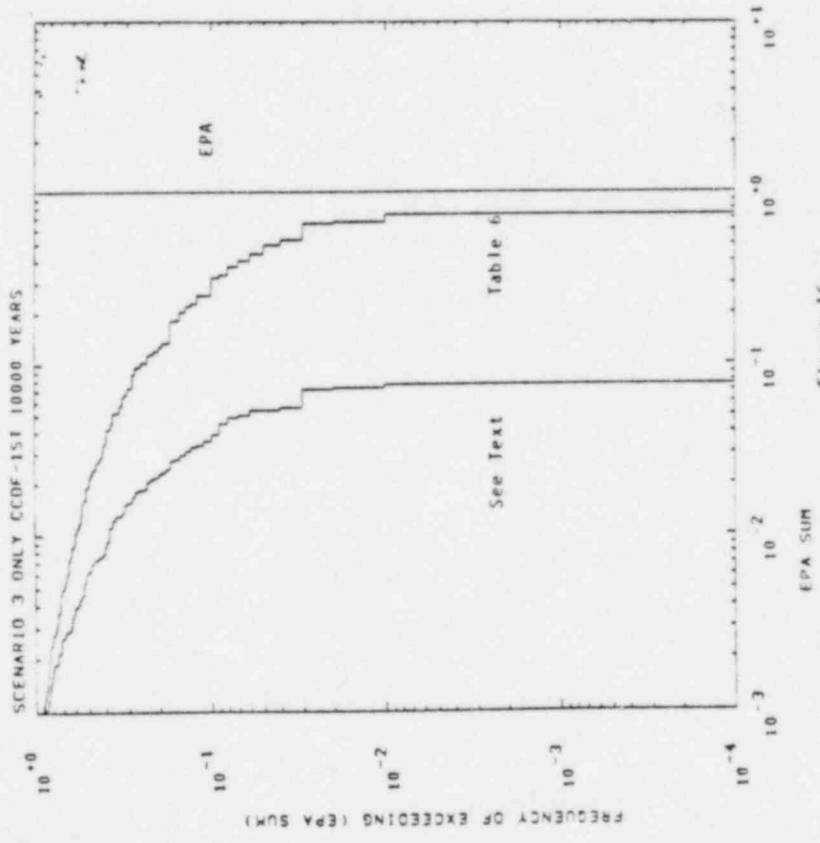


Figure 16

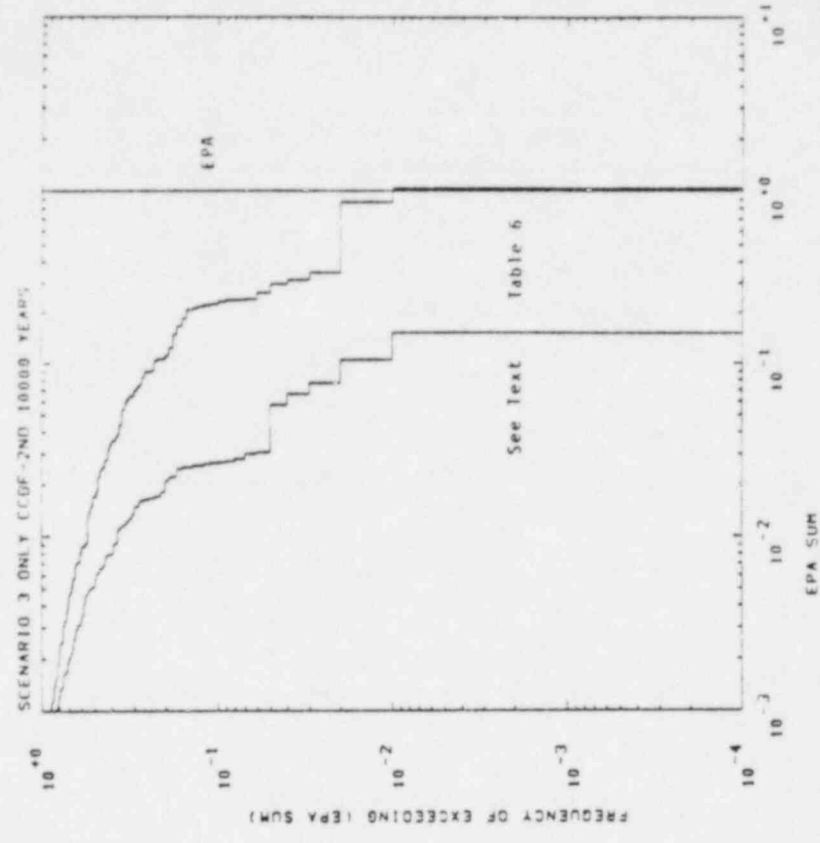


Figure 17

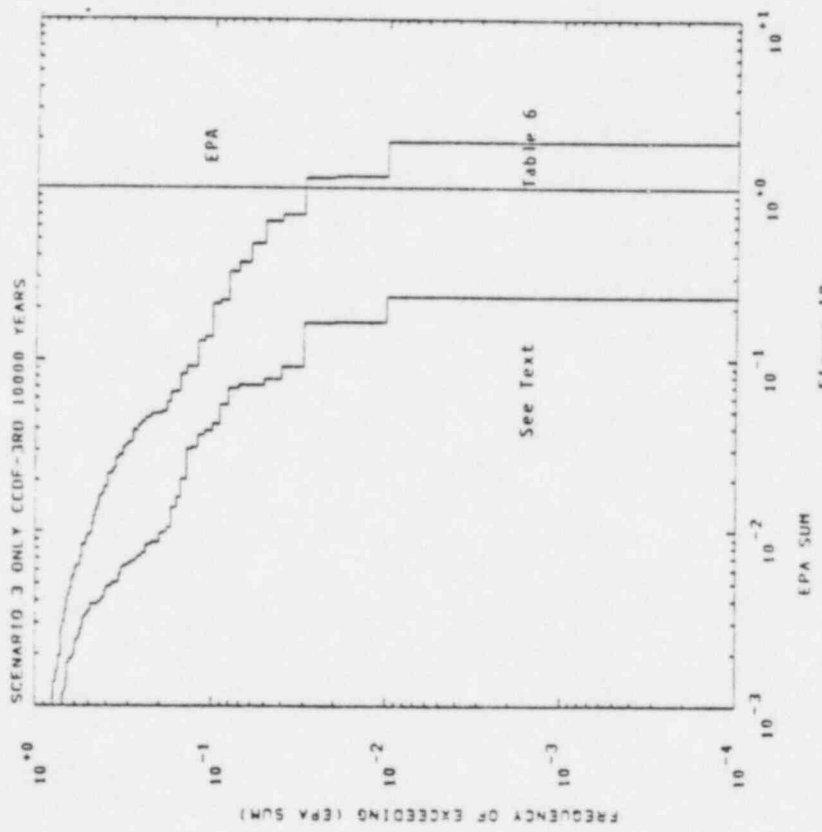


Figure 18

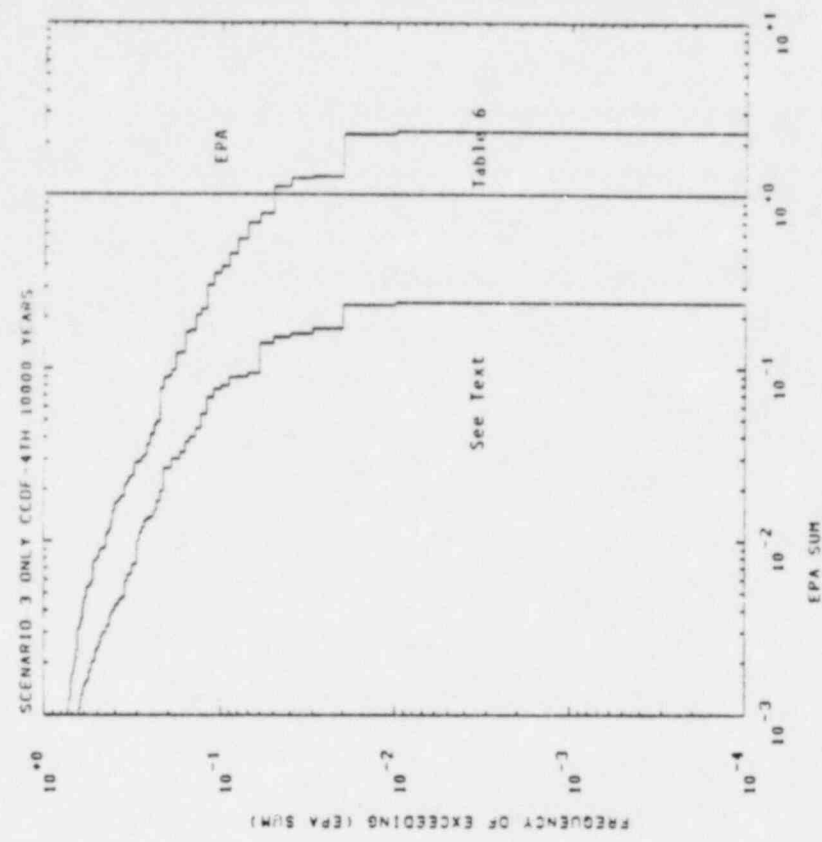


Figure 19

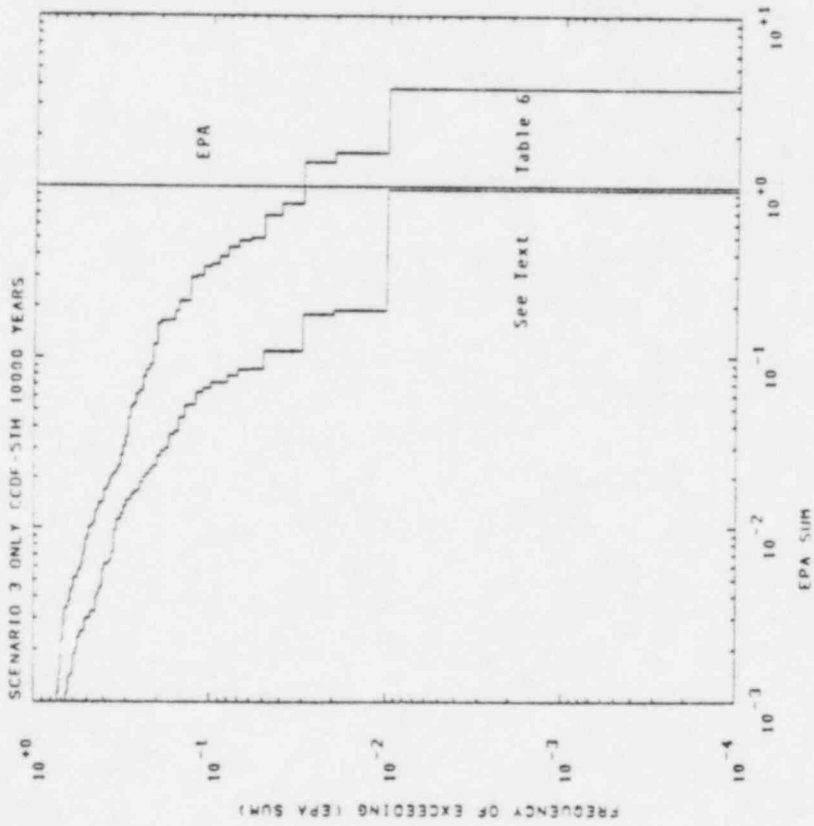


Figure 20

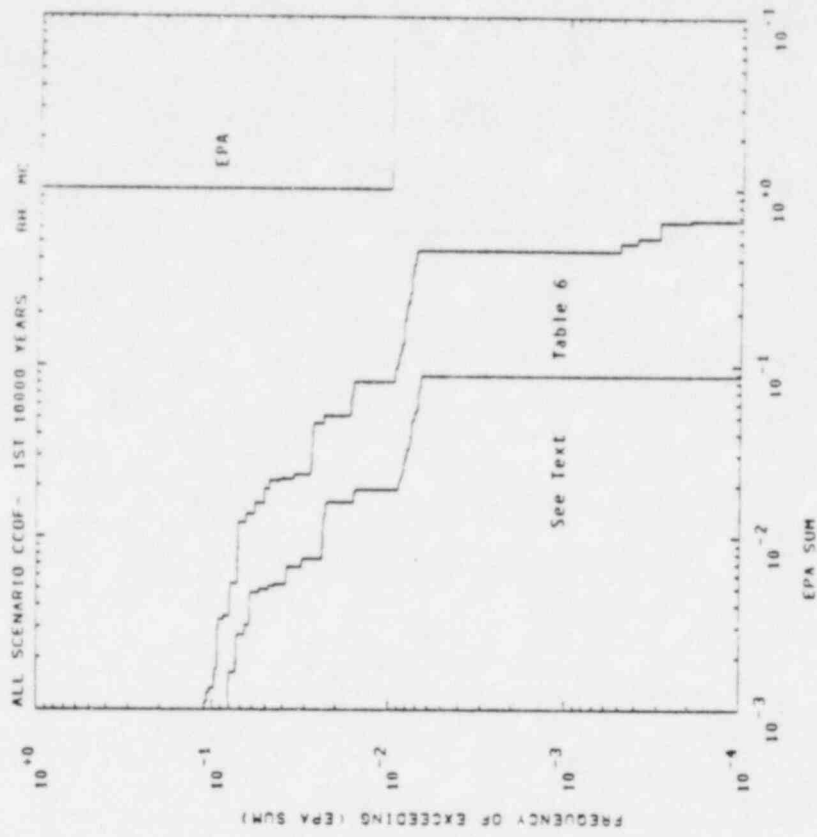


Figure 21

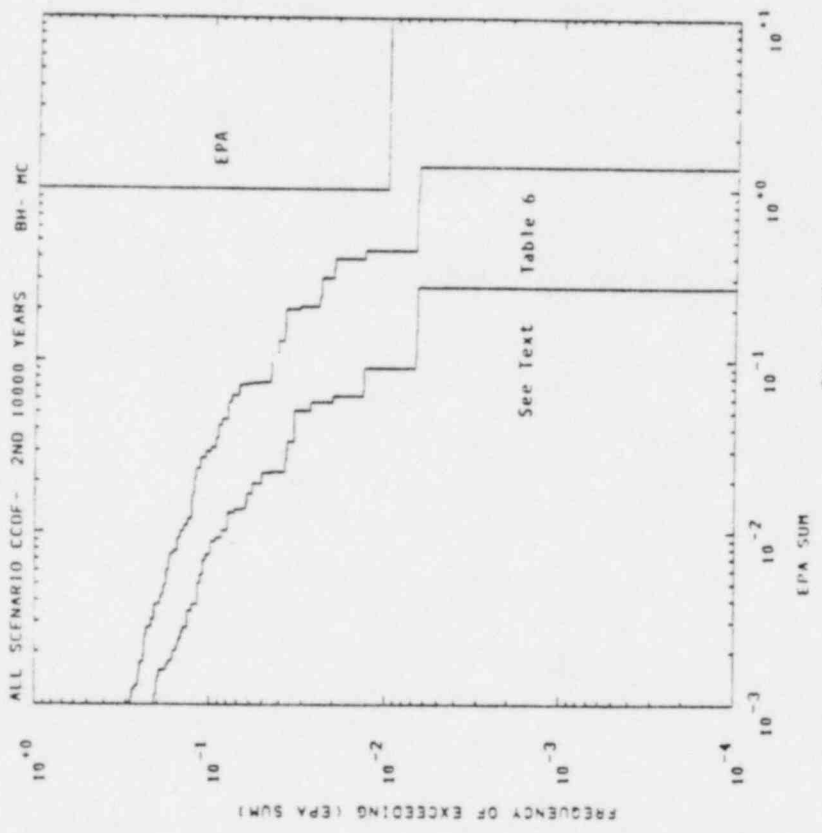


Figure 22

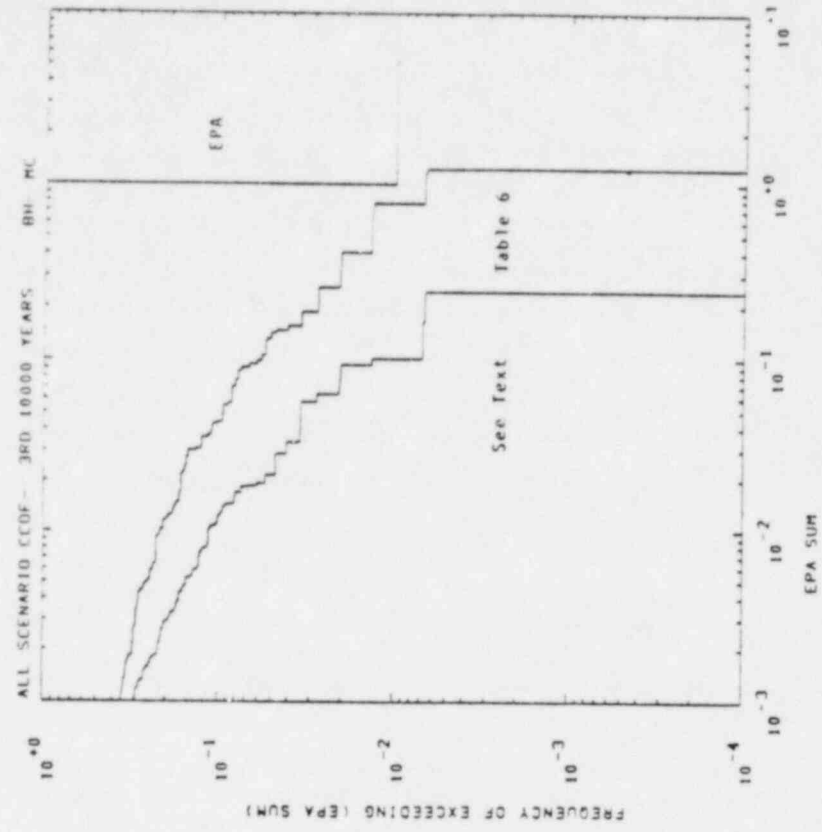


Figure 23

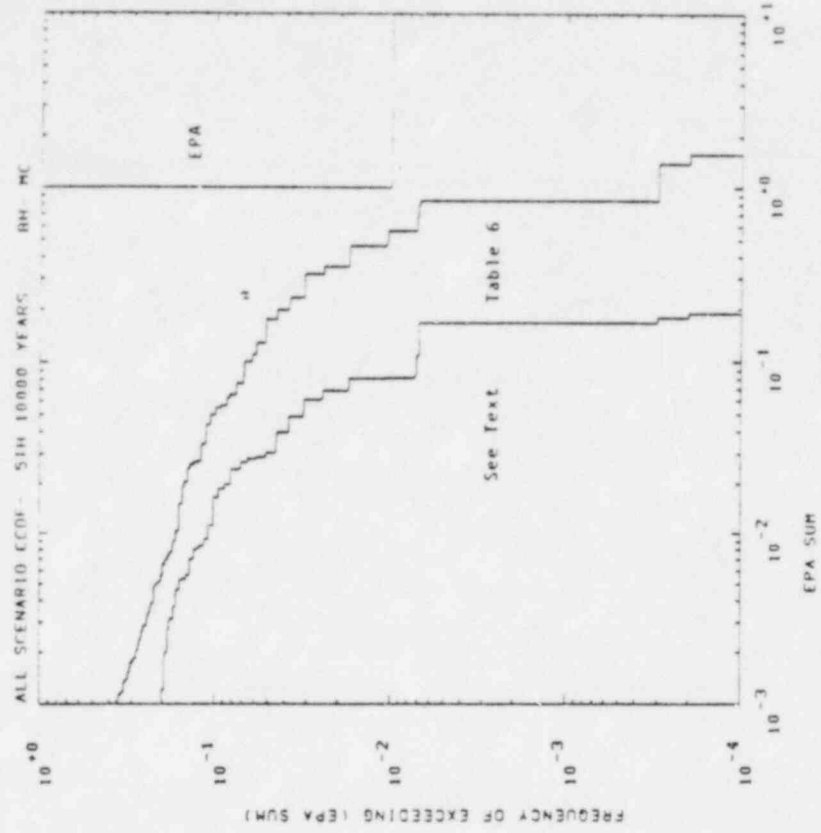


Figure 24

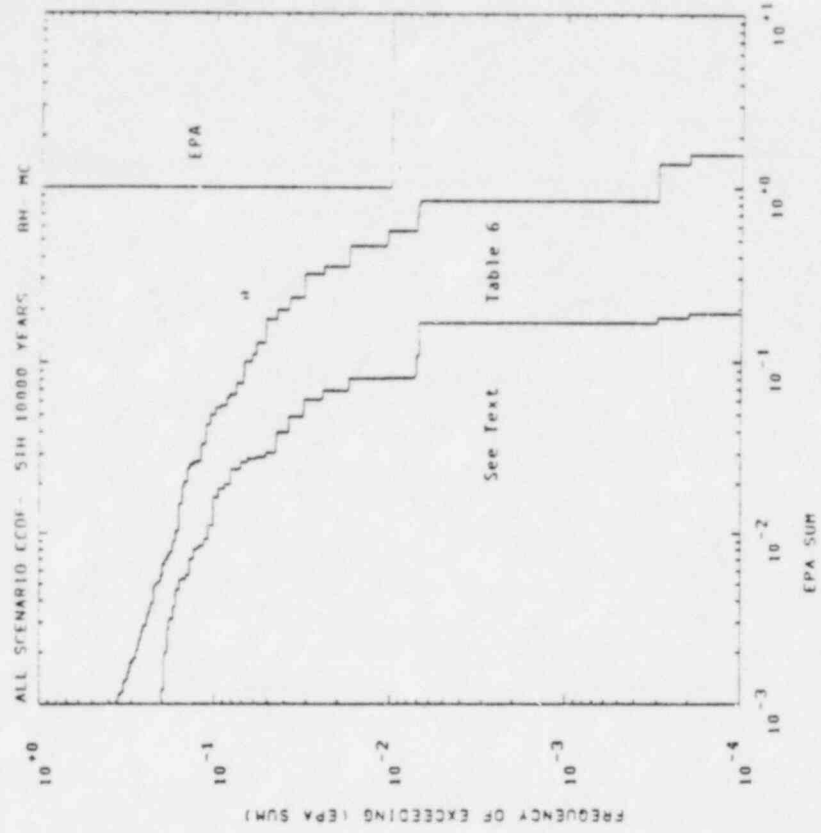


Figure 25

source model imposed. These results are shown in Figures 26 through 35.

Note that the draft EPA Standard addresses only the first 10,000 year interval. We have extended the analysis to 50,000 years by assuming that the standard applies to each 10,000 year interval. In each figure, two curves appear. The data used in Table 6 were used to generate one CCDF. The lower CCDF was constructed to provide a semi-quantitative indication of the results of imposing the 10CFR60 requirement of an annual fractional release rate of 10^{-5} /year. Using data in Table 6, the leach rate (the reciprocal of the leach period) may be as great as 10^{-4} /year. The input vectors producing the largest values of the EPA Sum were examined to determine the dominant radionuclides. These vectors are dominated by contributions to the EPA Sum by ^{99}Tc and ^{14}C . For the vectors producing the largest EPA Sum values, these radionuclides are released at a leach limited rate, rather than a solubility limited rate. A simple multiplicative factor may be applied to the computed EPA Sum to estimate the value corresponding to a different release rate. To construct the lower curve, the multiplicative factor has been chosen to estimate releases as if the sampled range of leach rates was 10^{-5} to 10^{-7} /year. This procedure is only applicable to leach limited radionuclides. Similar corrections for the other technical criteria of 10CFR60 have not been attempted.

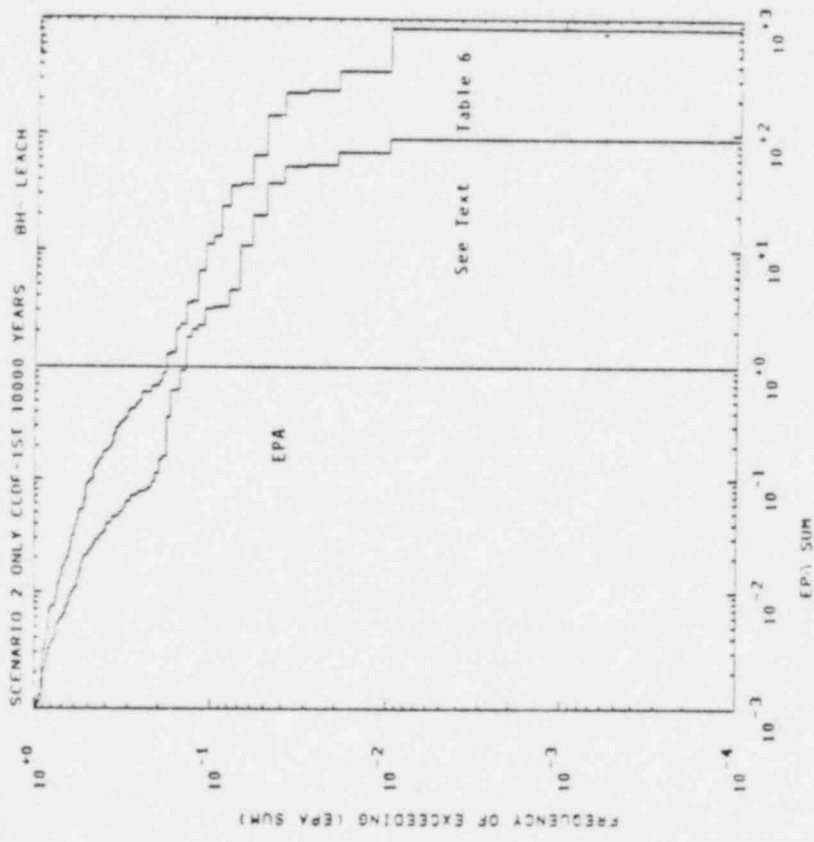


Figure 26

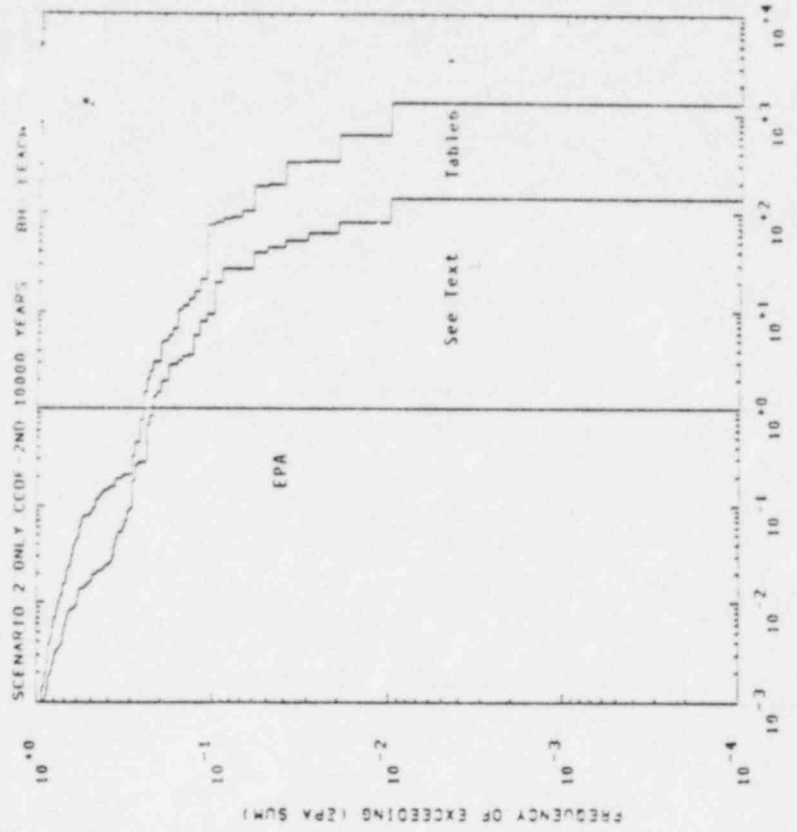


Figure 27

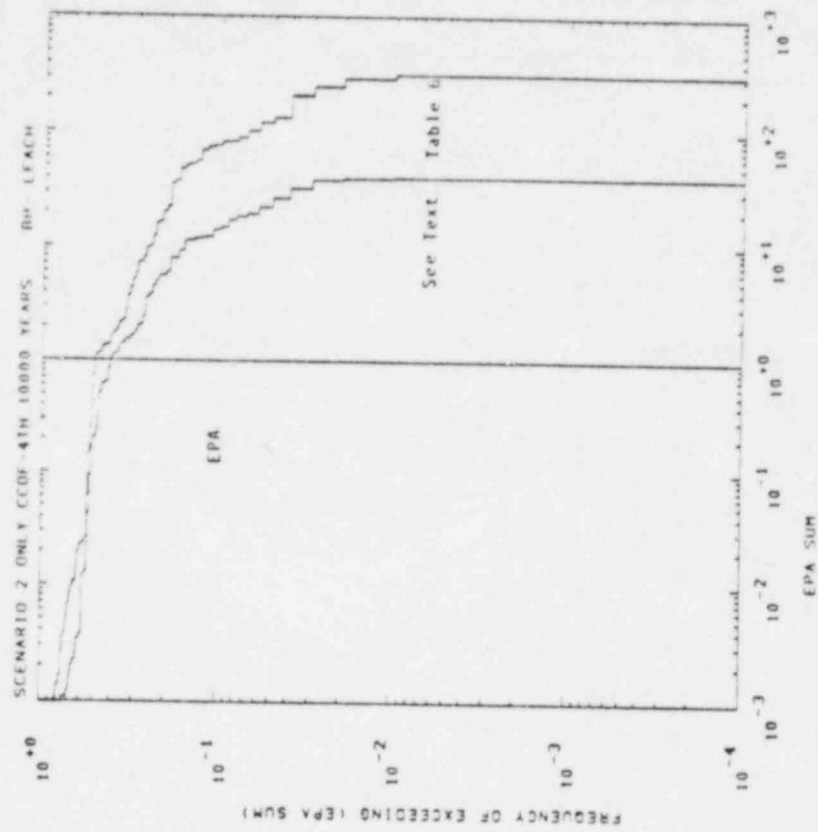


Figure 28

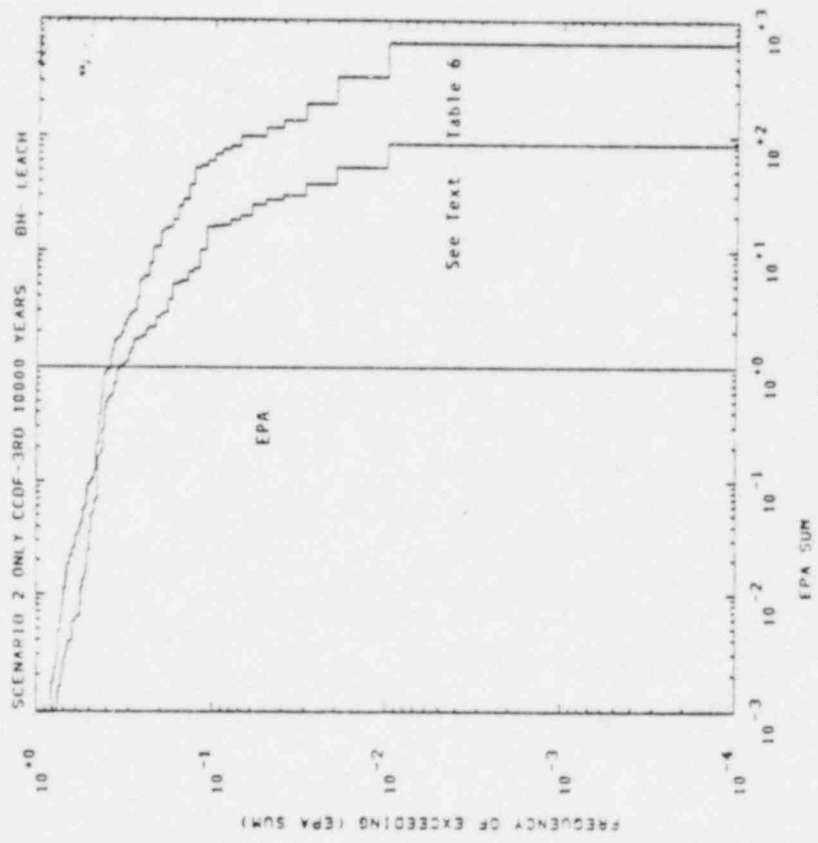


Figure 29

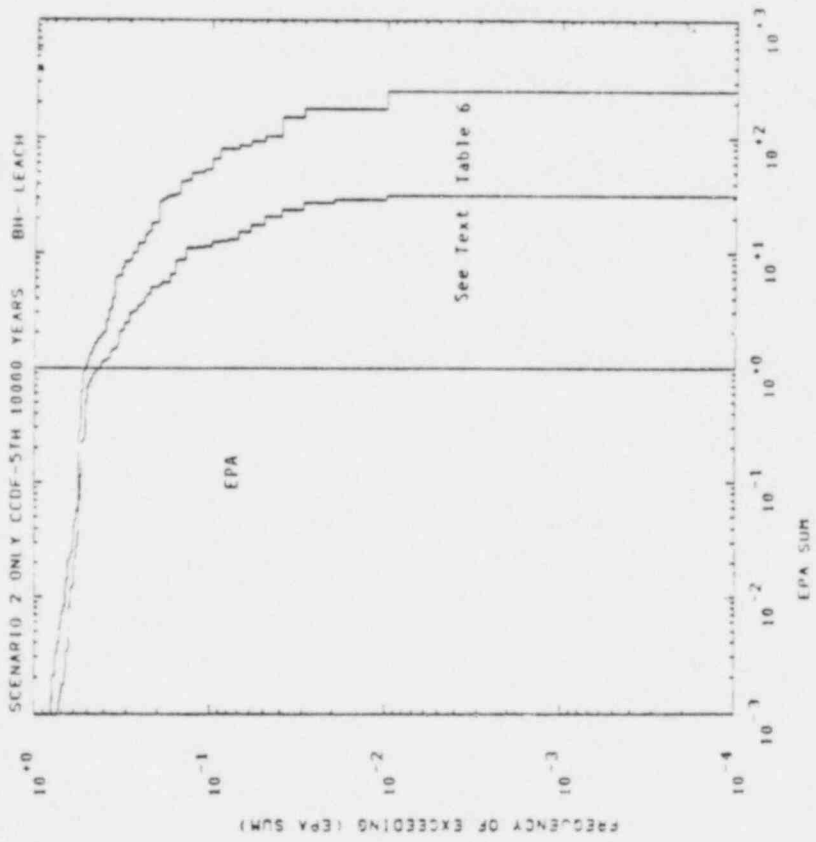


Figure 30

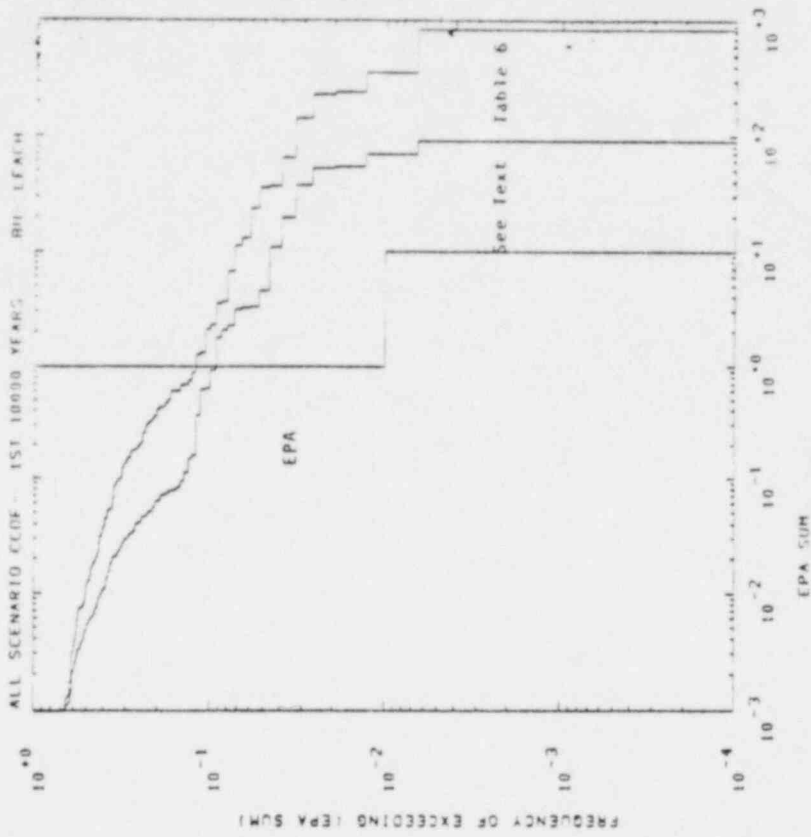


Figure 31

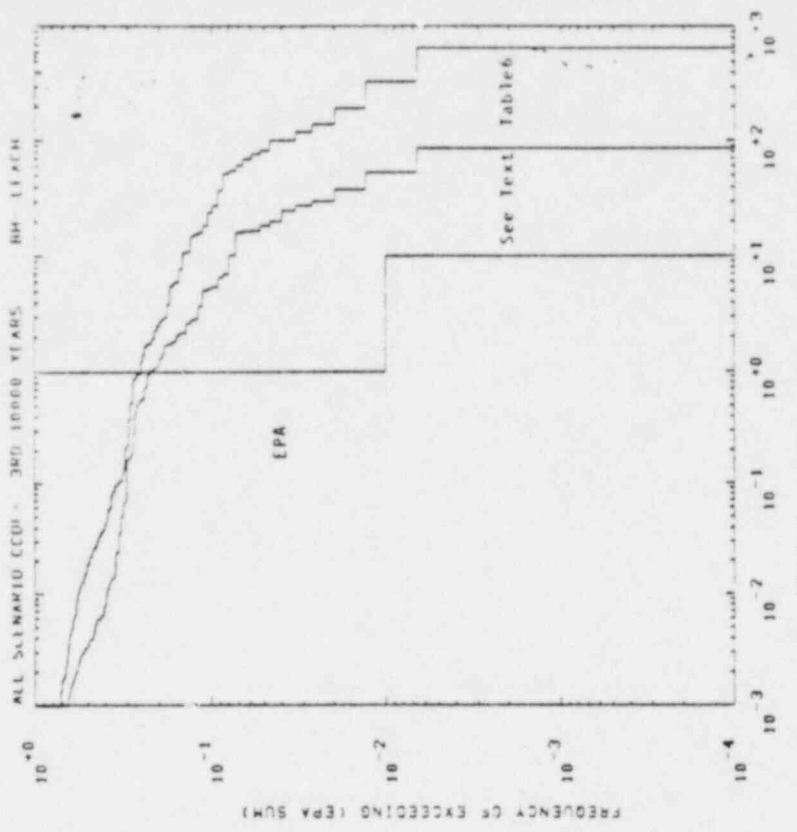


Figure 32

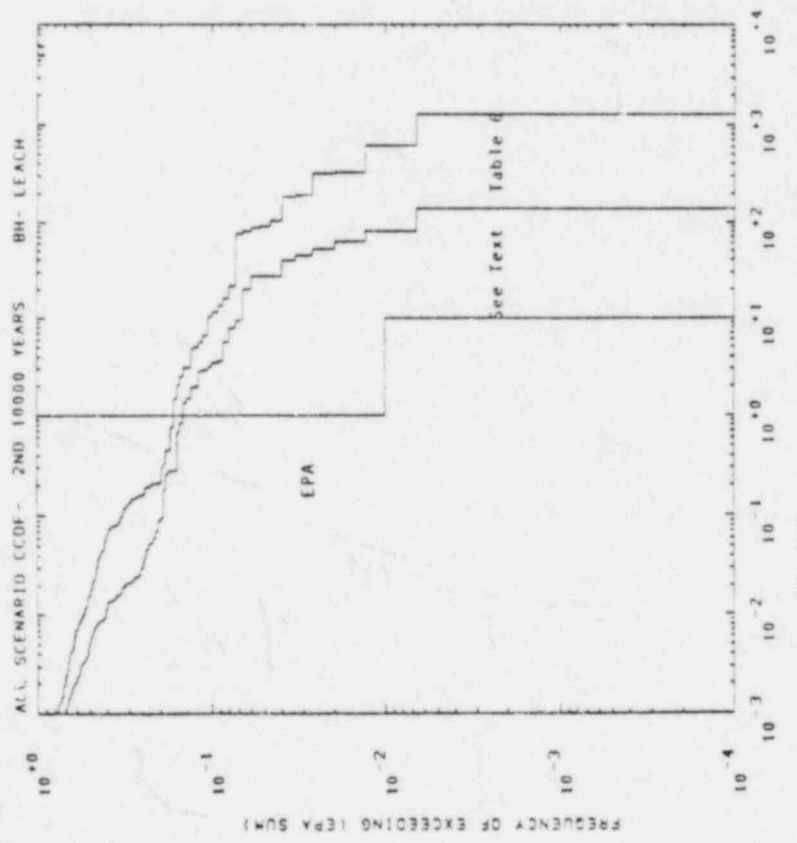


Figure 33

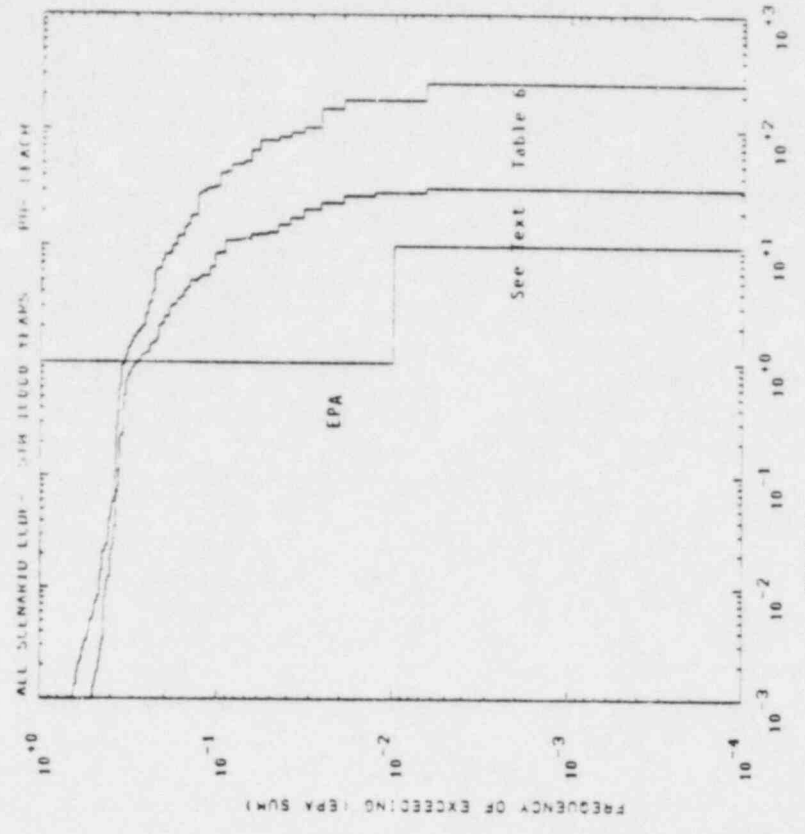


Figure 35

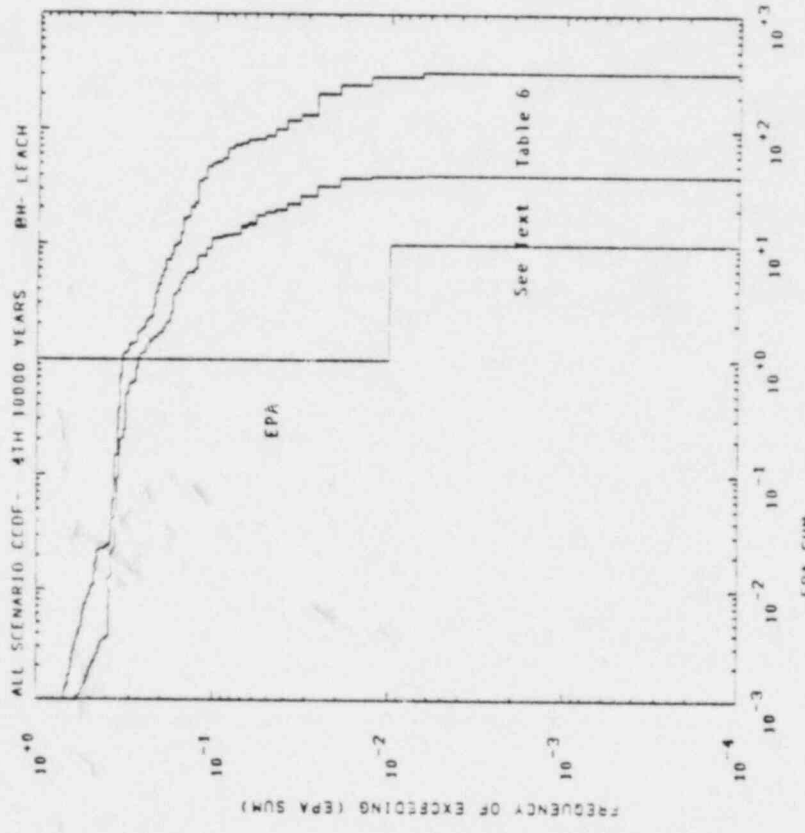


Figure 34

9. Conclusions

The analyses presented show how existing analysis tools could be used to assess compliance with the draft EPA Standard. A detailed development of probabilities of scenarios will be needed in order to perform a more realistic assessment. As site characterization proceeds, one may expect improvement in input data over that assumed in this analysis.

Ambiguities in the draft standard and assumptions necessary to assess compliance have been identified which will need to be clarified, justified, or further developed before a final assessment of compliance can be made.

Two interpretations of the draft standard have been presented which should be further discussed, especially in light of the uncertainties in both the scenario probability and estimated EPA Sum. Interpretation 1 is computationally the simpler since scenarios may be analyzed one-at-a-time as they are postulated. Due to the uncertainty in scenario probability, arguments as to whether or not compliance is achieved are reduced to two basic issues,

1. Assurance that the scenario probability is greater than 10^{-2} (the conservative assumption), between 10^{-4} and 10^{-2} (arguable if uncertainty in the probability is large), or less than 10^{-4} (negligible).
2. Confidence, that consequences are substantially less than the allowed maximum.

Interpretation 2 is somewhat more computationally difficult to utilize but seems to be more in the spirit of risk assessment as it has been applied to nuclear reactors, in that it considers all sources of a given consequence (EPA Sum). Uncertainty in scenario probability could be accommodated in this interpretation, at least in principle, by performing a sampling of a probability distribution assumed to describe each scenario. A CCDF would be constructed in the same manner from a probability versus EPA Sum plot, but the

estimated values of the EPA Sum would be scattered both along the EPA Sum and probability axes. A larger sampling error would be expected. Replicated sampling and construction of CCDF's would allow the estimation of confidence intervals about a resultant mean CCDF which could be compared to the draft EPA Standard. At this stage other sources of uncertainty such as numerical dispersion in computer codes could be included.

The results of analyses for this reference basalt site performed under Interpretation 1 showed a probability of a few percent of violating the draft EPA Standard for Scenario 2 without imposition of the 10CFR60 requirements on the release rate. Under Interpretation 2, the same analyses indicate compliance with the draft EPA Standard. Both of these results are subject to sampling error. Future analyses will explicitly address sampling error.

Analyses performed with different source models show the importance of the source term assumption on compliance estimates.

Appendix A

Radionuclide Retardation

1. Calculation of the Retardation Factor

The retardation factor R for an aqueous species or radionuclide traveling in a porous media is usually defined as:

$$R = \frac{\text{velocity of ground water}}{\text{velocity of radionuclide}} \quad (1)$$

The value of R can be calculated by:

$$R = 1 + K_d \cdot \rho \cdot \frac{(1 - \phi_{\text{eff}})}{\phi_{\text{eff}}} \quad (2)$$

where

K_d = the radionuclide distribution coefficient in cm^3/gm

ρ = grain density of rock in gm/cm^3

ϕ_{eff} = effective porosity that contributes to the flow path. In porous media $\phi_{\text{eff}} = \phi_{\text{total}}$.

For calculations of the retardation factor for solutes in fractured media, it is more convenient to define the retardation factor as follows. For a unit volume of rock:

$$R = \frac{M_T}{M_X} = \frac{\text{total mass of radionuclide in rock-water system}}{\text{mass of radionuclide in water}} \quad (3)$$

For porous media it can be shown that this expression is equivalent to Equation (2).

Let:

C_X = concentration of radionuclide in solution in gm/cm³

C_{MX} = concentration of radionuclide adsorbed by the rock in gm/gm

M_R = mass of nuclide in rock in grams

Then for a unit volume of porous rock

$$M_X = C_X \cdot \phi_{eff} \quad (4)$$

$$M_R = C_{MX} \cdot (1 - \phi_{eff}) \rho \quad (5)$$

$$M_T = M_X + M_R \quad (6)$$

From Equation (3)

$$R = \frac{M_R + M_X}{M_X} \quad (7)$$

substituting terms yields:

$$R = \frac{C_X \cdot \phi_{eff} + C_{MX} (1 - \phi_{eff}) \cdot \rho}{C_X \cdot \phi_{eff}} \quad (8)$$

$$R = 1 + \frac{C_{MX}}{C_X} \cdot \rho \cdot \frac{1 - \phi_{eff}}{\phi_{eff}} \quad (9)$$

Since (Equation 4.5)

$$K_d = \frac{C_{MX}}{C_X}$$

then

$$R = 1 + K_d \cdot \rho \cdot \frac{(1 - \phi_{eff})}{\phi_{eff}} \quad (2,10)$$

In general however, the fluid is not in contact with the entire rock mass. We introduce the utilization factor, ψ , to correct R for this effect:

$$R = \frac{C_X \phi_{eff} + \psi C_{MX} (1 - \phi_{eff}) \cdot \rho}{C_X \phi_{eff}} \quad (8b)$$

$$R = 1 + \psi K_d \cdot \rho \cdot (1 - \phi_{eff}) / \phi_{eff} \quad (11)$$

where ψ is the volume fraction of the rock that interacts with the fluid.

2. Estimation of Utilization Factor

In the reference repository we have assumed that most of the fractures are lined with secondary minerals.¹⁰ Under these conditions we can derive an expression for ψ and also simplify the expression for R. If we assume that the fluid in the fractures interacts only with secondary minerals, then

$$M_R = C_{SMX} \cdot V_{SM} \cdot \rho_{SM}$$

where ρ_{SM} and V_{SM} are the density and volume of secondary minerals in the unit volume of rock, respectively. C_{SMX} is the concentration of radionuclide adsorbed by the secondary minerals in gm/gm.

Let

$$V_{SM} = \left(\begin{array}{l} \text{volume of solid} \\ \text{rock in unit} \\ \text{volume of rock} \end{array} \right) \times \left(\begin{array}{l} \text{fraction of rock} \\ \text{composed of} \\ \text{secondary minerals} \end{array} \right)$$

$$V_{SM} = (1 - \phi_T) \cdot \psi \cdot \text{unit volume} \quad (12)$$

where

ϕ_T = total porosity.

If we assume that $\phi_T \approx \phi_{eff}$, then

$$R \approx \frac{C_X \cdot \phi_{eff} + \psi \cdot C_{SMX} \cdot (1 - \phi_{eff}) \cdot \rho_{SM}}{C_X \cdot \phi_{eff}}$$

$$R \approx 1 + \psi \cdot K_{dSM} \cdot \rho_{SM} \cdot \frac{(1 - \phi_{eff})}{\phi_{eff}} \quad (13)$$

Note that in this expression, K_d and ρ refer to the secondary minerals and that ϕ_{eff} refers to the basalt matrix. The utilization factor ψ is the volume fraction of the rock matrix occupied by secondary minerals.

Intuitively, we would expect that the amount of secondary mineralization in the basalt can be related to the volume of the fractures. At Hanford, for example, Long¹⁰ examined 3 flows in the Grande Ronde. He found that nearly all the fractures contained some filling and that > 75 percent of the fractures were filled completely. If we assume that the fractures that contribute to the effective porosity are on the average one-half filled, then since

"original" unfilled fracture porosity = 2 . residual porosity

Then

$$V_{SM} = \text{residual porosity} \sim \phi_{eff}$$

and

$$= \frac{V_{SM}}{V_{\text{solid rock}}} \approx \frac{\phi_{eff}}{(1 - \phi_{eff})} \quad (14)$$

This expression can be used to simplify Equation (13)

$$R = 1 + K_{dSM} \cdot \rho_{SM} \cdot \frac{\phi_{eff}}{(1 - \phi_{eff})} \cdot \frac{(1 - \phi_{eff})}{\phi_{eff}}$$

$$R = 1 + K_{dSM} \cdot \rho_{SM} \quad (15)$$

In the more general case, we can assume that the volume of secondary mineralization is a multiple (f) of the volume of residual connected pore space. Equations (14) and (15) become

$$\psi = \frac{f \cdot \phi_{eff}}{(1 - \phi_{eff})} \quad (14a)$$

$$R = 1 + f K_{dSM} \cdot \rho_{SM} \quad (15a)$$

Appendix B

Redox Conditions in the Reference Repository and Appropriate Values of K_d

A large amount of uncertainty in our estimates of radionuclide discharge is introduced by lack of knowledge about the geochemical environment that may be encountered by migrating nuclides and by the paucity of reliable values of radionuclide distribution coefficients (K_d 's) relevant to this study. In this section we will describe the assumptions we have made in characterizing the geochemical environment and in choosing appropriate values of K_d 's for our calculations.

1. Redox Conditions

The difficulties encountered in attempting to predict the Eh-pH environment of natural systems from either theoretical considerations, or from direct measurements, have been discussed in detail by several authors.^{11,12,13} Discussions of the probable nature of the geochemical environment within the Hanford Site and subsurface mines are given by Sato, Smith, and Guzowski, et al.^{11,14,15} Field measurements and theoretical calculations based on observed mineral assemblages in basaltic environments suggest that ground water in contact with basalt will have a low Eh (-0.40 to -0.55), high pH (9.4 - 10), and moderate temperatures (30 - 50°C). These Eh-pH conditions may be expected near the repository in part of Layer A in Figure 2 and along fresh basalt fractures exposed by faulting or drilling in other layers as described in the hypothetical disruption scenarios. In our characterization of the repository, we have not considered the oxidizing potential of air and foreign materials introduced into the basalt during operation and construction of the repository. The two interbeds I-V and I-M are assumed to be relatively active aquifer systems and are therefore assumed to be oxidizing and slightly alkaline.

In the "base" (no disruption) case, we have assumed that in all basalt layers groundwater flows through fractures lined with secondary minerals. The observed fractures fill consists of amorphous silica, zeolites, calcite, and nontronite.¹⁰ None of these minerals have

appreciable oxidizing power. Although nontronite contains Fe^{+3} , it forms under reducing conditions.¹⁶ At low pH, the dissolution of iron-bearing minerals in basalt and precipitation of ferric oxyhydroxides will proceed under reducing conditions.¹¹ For these reasons, we have assumed that the geochemical environment of partially filled fractures in basalt is reducing.

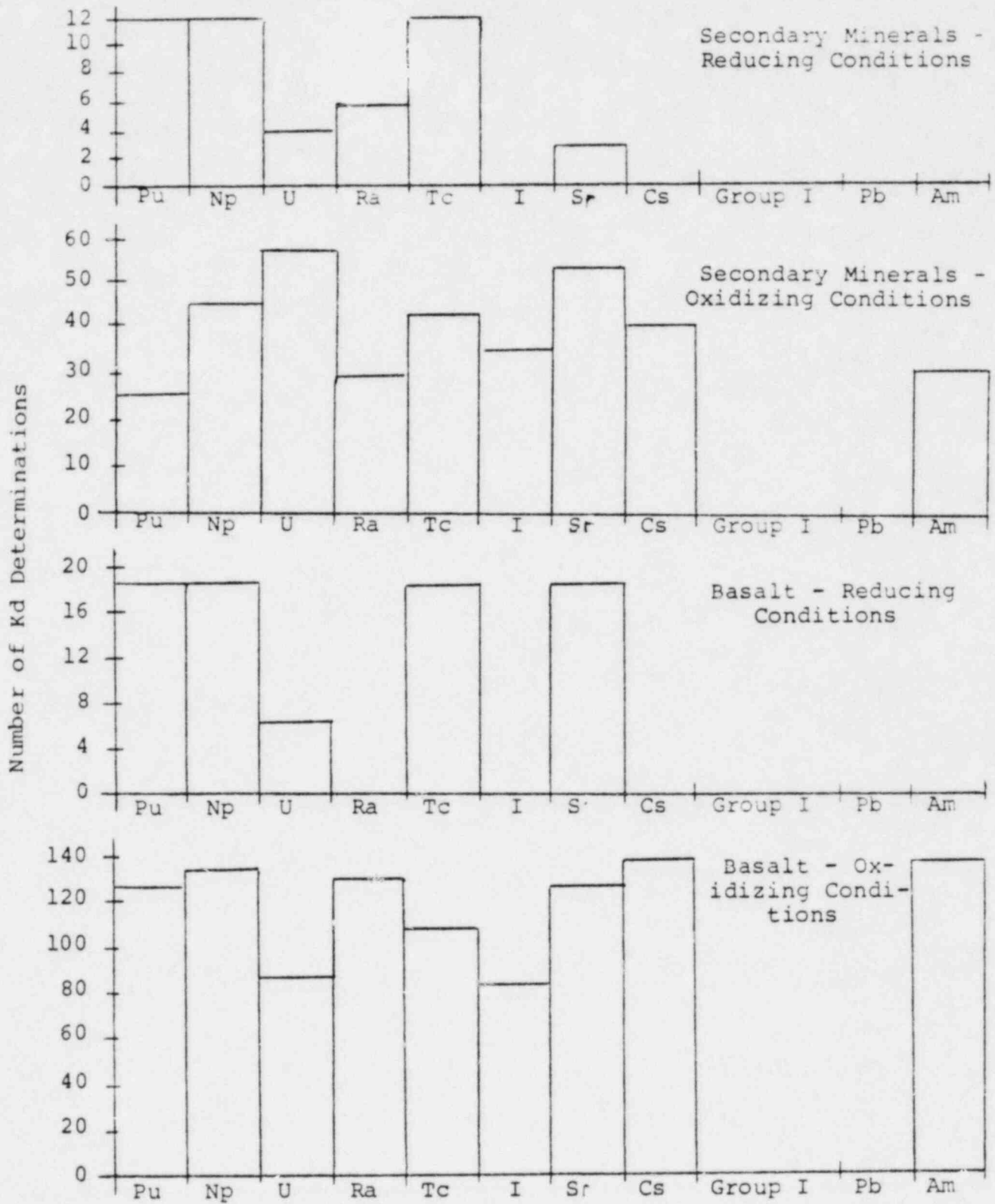
2. Available Data for Values of K_d

The large amount of experimental error reported for determinations of K_d 's and the questionable utility of this parameter for accurate calculations of radionuclide retardation has been discussed by several authors.¹⁵⁻²²

The values for the ranges of radionuclide distribution coefficients K_d that were used in this report are presented in Table 4 (main text). The data were supplied by several researchers and are reviewed in Guzowski, et al.¹⁵ Histograms of the number of determinations of K_d 's for each radionuclide for the substrates under several geochemical environments considered are shown in Figure B-1. It is clear that there are relatively few reliable determinations of K_d 's for the geochemical conditions relevant to this study. The large majority of data has been obtained for basalt under an oxidizing atmosphere, a condition that we do not feel is relevant to the geological system under consideration.

In most cases, the ranges of K_d values reported for reducing conditions overlap those reported for oxidizing conditions. For this reason we have used the more limited number of data obtained under oxygen-free conditions to estimate the ranges of K_d for reducing environments and we have supplemented these data with values obtained under oxidizing conditions where necessary. No data are available for several elements: Cm, Pa, Ac, Th, and Pb. Based on similarities in solubility, valence and ionic radii, the following chemical homologs have been assumed: (Am = Cm, Pa, Ac, Th) and (Pb = Ra).¹⁵ No values of the K_d 's of Cs, I, Ra, or Am in contact with basalt under reducing conditions are available. The K_d 's of these elements are assumed to be insensitive to redox conditions; values under oxidizing conditions were used for our calculations.

Figure 3-1.



Group I = Cm, Pa, Ac, Th:

Appendix C

An Approximate Treatment of Matrix Diffusion as a Retardation Mechanism

We have assumed that groundwater flow and radionuclide migration occur predominantly through numerous narrow vertical fractures in the basalt. We have also attempted to show the effect of such a flow assumption on the chemical sorption processes expected to retard radionuclide migration and enhance the containment capability of the repository. In doing so we have given up the traditional porous medium expression for the retardation factor of the form

$$R \approx \frac{\rho k_d}{\phi} (1 - \phi)$$

in favor of the form

$$R \approx \rho k_d$$

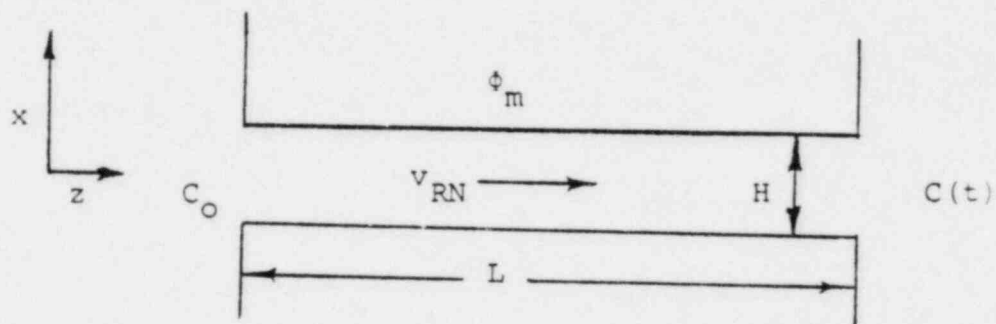
as discussed in Appendix A.

A few radionuclides are essentially unretarded by chemical sorption, i.e., $K_d \approx 0$. Specifically, ^{14}C and ^{99}Tc dominate the EPA Sum for most vectors producing large values of the EPA Sum. For scenarios involving major hydraulic connections between the subsurface facility and overlying aquifers, e.g., boreholes, these radionuclides may be of most concern in licensing considerations. In scenarios resulting in enhancement of the repository hydraulic properties, e.g., fractures in dense basalt, transport may still be dominated by flow through narrow fractures. For these cases we may have overestimated the releases by neglecting a potential retardation mechanism.

A number of authors have discussed the diffusion of contaminants into the rock matrix for cases similar to that which we have assumed, namely transport through narrow fractures in relatively impermeable rock.^{23,24,25} The treatment presented here is essentially that of Erickson and Fortney²⁶ who have used this effect in the design of radionuclide migration experiments in non-welded tuffs. We would like to estimate the potential importance of this mechanism in radionuclide retardation. The validity of

the method as derived and implemented here rests on a number of assumptions which will be made. Nevertheless, the results will demonstrate the potential importance of this retardation mechanism and the importance of understanding it better.

Consider the idealized fracture and geometry depicted in the following figure:



A fracture of width H and length L is assumed to exist in a rock matrix with a porosity, ϕ_m . At time $t = 0$ a constant radionuclide concentration, C_0 , is "turned on" at the fracture inlet. An expression for the time dependent concentration, $C(t)$, at the outlet is desired. The rock is assumed to be infinite in the x -direction with the contaminant concentration in the rock, $C_R(x, z)$, maintained at zero at $x = \pm \infty$. In the fracture, radionuclide transport is assumed to be purely advective with the contaminant transported at a speed, v_{RN} , with no variation of the concentration in the x -direction within the fracture. Dispersion in the z -direction in the fracture is neglected. In the rock, transport is assumed to be purely diffusive and in the x -direction. For this situation, transport in the fracture is assumed to be described by

$$\frac{\partial C}{\partial t} + V \frac{\partial C}{\partial z} + H \frac{\partial^2 C}{\partial x^2} = 0$$

where

$$Q = \int_0^{\infty} q(x, z, t) dx$$

and q is the contaminant concentration in the rock described by

$$\frac{\partial q}{\partial t} = \frac{D_{eff}}{R_R} \frac{\partial^2 q}{\partial x^2}$$

D_{eff} is the effective diffusion coefficient in the rock and R_R is the standard porous medium retardation factor for the rock. Matching contaminant flux in the x -direction at the fracture-rock interface gives the concentration of contaminant at the fracture exit ($z = L$),

$$C(t) = C_0 \operatorname{erfc}(\eta) \quad (C1)$$

where

$$\eta = \frac{\phi_m R_R L \sqrt{D_{eff}/R_R}}{H V R_N \sqrt{t - z/V R_N}}$$

A "breakthrough time", t_B , may be defined as that value of where $C(t_B)/C_0 = 1/2$. The effect of the early tail of the erfc -function will be addressed below. This value of η will be denoted by η_0 , which has a numerical value of approximately

$$\eta_0 = .48$$

The expression for η may be solved for t giving

$$t_B = \frac{L}{V_{RN}} + \left(\frac{\phi_m R_{RL}}{H V_{RN} \eta_0} \right)^2 \left(\frac{D_{eff}}{R_R} \right)$$

In the absence of diffusion into the rock matrix ($D_{eff} = 0$) radionuclides would be expected to appear at the exit in high concentration at time L/V_{RN} . Thus, we may define a retardation for this mechanism, R_{MD}

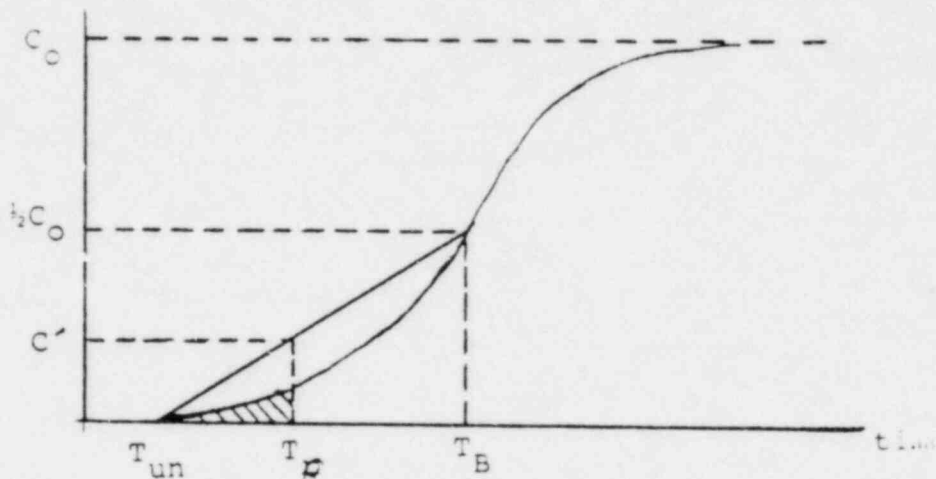
$$R_{MD} = t_B / \left(\frac{L}{V_{RN}} \right) = 1 + \frac{R_{RL} D_{eff}}{V_{RN}} \left(\frac{\phi_m}{H \eta_0} \right)^2$$

If there is some chemical retardation in the fracture then V_{RN} is retarded relative to the fluid velocity, V_{f1} , by the chemical retardation factor, R_{ch} , so that

$$R_{MD} = 1 + \frac{R_{RL} R_{ch} L D_{eff}}{V_{f1}} \left(\frac{\phi_m}{H \eta_0} \right)^2$$

As will be shown, retardation factors resulting from use of this form can be very large. Transport calculations have not been performed for times long enough to demonstrate this effect. Thus we do not have the results of numerical calculations of the total discharge to be compared to the EPA limits. It is not clear that the current version of the DVM transport model could be used for such a calculation due to the skewed shape of the breakthrough curve. We can, however, make a bounding estimate of the total integrated discharge based on simple considerations which should be applicable to one-member radionuclide decay chains such as ^{14}C and ^{99}Tc .

Consider the following breakthrough curve depicting the behavior of Equation C1,



- C_0 = maximum discharge rate
- C' = estimated bound of the discharge rate for times less than T_R in the absence of matrix diffusion
- T_{un} = time of transport in the absence of matrix diffusion L/V_{RN}
- T_R = regulatory time limit, e.g., 10^4 years
- t_B = estimated breakthrough time with matrix diffusion as a retardation mechanism

The shaded area represents the total integrated discharge, TID, we seek to bound. The only assumption necessary is that the shape of the discharge curve is curved upward, as depicted, for times less than t_B . This assumption has not been investigated, but seems reasonable.

The area shaded is bounded by the area of the triangle of base $(T_R - T_{un})$ and height, C' ,

$$TID \leq \frac{1}{2} C' (T_R - T_{un}) = \frac{1}{4} C_0 \frac{(T_R - T_{un})^2}{(T_B - T_{un})}$$

where the last step follows from similar triangles. The maximum discharge rate is given from the transport calculation performed without matrix diffusion.

No decay corrections have been considered. In fact, the correction terms already introduced are sufficient to significantly reduce the calculated discharges.

To implement these results for the multilayered reference basalt system, we will assume the radionuclide migration path to be made up of a series of idealized fractures through each of the layers of the reference repository (except the thin sandstone layer). The sub-surface facility is treated as an extended source releasing radionuclides through these idealized fractures. Discharges from the last set of fractures is collected by overlying aquifers. Lateral variations in properties are neglected. We seek an equivalent single fracture representation of the actual multi-layered system.

The fluid transport time is given by

$$T_{fl} = \sum_i \frac{L_i}{v_{fl,i}} = \frac{1}{q} \sum_i L_i \phi_{h,i}$$

layers

where q is the Darcy velocity which is the same in all layers, i , and L_i is the thickness of the i^{th} layer. $\phi_{h,i}$ is the effective porosity assumed to be dominated by fractures. The transport time for the migrating contaminant, T_B , is given by

$$T_B = \sum_i \frac{L_i}{v_i^{(md)}} = \sum_i \frac{L_i R_i^{(md)}}{v_{RN,i}} = \sum_i \frac{L_i R_i^{(md)} R_i^{(ch)}}{v_{fl,i}}$$

$$= \frac{1}{q} \sum_i L_i R_i^{(md)} R_i^{(ch)} \phi_{h,i}$$

so that

$$R_{eff} = \frac{T_B}{T_{f1}} = \frac{\sum_i L_i \theta_{h,i} R_i^{(ch)} R_i^{(md)}}{\sum_i L_i \theta_{h,i}}$$

Here, we have assumed the Darcy velocity and fluid velocity to be related by

$$V_{f1,i} = \frac{q}{\theta_i}$$

Finally, to implement these results, we will make the following assumptions.

1. $\theta_{m,i} = \theta_{h,i}$ an approximate relationship consistent with data on basalt¹⁵
2. $R_{ch} = 1 + K_d \rho$ as in Appendix A
3. $D_{eff} = 2 \times 10^{-7}$ cm²/sec
4. $H = .05$ cm

To demonstrate the effect of diffusion into the rock matrix on estimates of the integrated discharge, three vectors of Scenario II have been chosen which led to violations of the EPA draft standard. The integrated discharges for these vectors are summarized in Table C-1. Applying the approximate treatment yields results presented in Table C-2. Data used in these calculations are presented in Tables C-3, 4, and 5.

It should be noted from this summary of results that the estimated contribution to the EPA Sum is the estimated integrated discharge from time zero to T_R . Thus, for Vector 15, for example, we estimate the total, integrated to 50,000 years, divided by their EPA limits, and summed over all radionuclides to give a value of less than .140. Similarly, for Vector 62, the 50,000 year upper bound estimated for the EPA Sum is 0.2. The results for Vector 24 must be qualified. The method developed for this estimation is based on the treatment of a single-membered radioactive decay chain. All of the dominant contributors

to the EPA Sum in Vector 24 are members of longer decay chains. The effects of other chain members on these estimates has not been investigated quantitatively.

Other violating vectors for this scenario have been investigated with this method and similar improvement observed. The accuracy of the estimates would be improved by estimating discharges at times earlier than T_B and correspondingly larger values of η_0 . However, the treatment given is sufficient to demonstrate the potential importance of diffusion into the rock matrix as a diffusion mechanism.

Table C-1

SCENARIO II Discharges with Matrix RetardationVector 15

Period (years)	<u>0-10⁴</u>	<u>10-20,000</u>	<u>20-30,000</u>	<u>30-40,000</u>	<u>40-50,000</u>
EPA Sum	.68	.34	.079	1.27	2.55
Tc99	-	-	-	1.27	2.55
C14	.68	.32	.05		

Vector 24

EPA Sum	.093	.044	.015	1.02	6.97
236U				.19	1.42
238U				.25	1.61
234U				.55	3.61

Vector 62

EPA Sum	.81	1.57	3.46	1.42	-
Tc99	0	1.18	3.43	1.42	-
C14	.81	.39	-	-	-

Table C-2

Summary of Effects of Diffusion Into Rock Matrix on TID*. Contributions to the EPA Sum less than .001 are omitted. No corrections for decay have been included.

SCENARIO II

	Vector 15		Vector 24			Vector 62	
	Tc99	C14	234U	236U	238U	Tc99	C14
R _{eff}	6.4E11	2.1E4	2.3E9	2.3E9	2.3E9	2.0E9	1.8E4
T _{fl} (yr)	1.2E3	1.2E3	1.1E3	1.1E3	1.1E3	1.1E3	1.1E3
T _B (yr)	7.4E14	2.5E7	2.4E12	2.4E12	2.4E12	2.3E12	2.1E7
C ₀ (Ci/yr)	22.3	1.15	.22	.10	.093	33.2	1.4
Contributions to EPA Sum	<hr/>						
TR = 1.E4		.005					.007
2.E4		.021					.030
3.E4		.049					.070
4.E4		.088					.127
5.E4		.40					.200

*Total integrated discharge

C-10

Table C-3

SCENARIO II

Vector 15 Data Used to Estimate Retardation
Due to Diffusion Into the Rock Matrix

i	L_i	ϕ_i	V_i^{f1}	R_{host}	$R_{fracture}$	R_{md}
<u>Tc99</u>						
1	150.	.0537	2.449	.5859E+05	28.36	.3216E+10
2	150.	.0750	1.754	.4100E+05	28.36	.6132E+10
3	50.	.0129	10.23	.2552E+06	28.36	.6411E+08
4	60.	.0967	1.360	.3106E+05	28.36	.3981E+10
5	690.	.0887	1.483	.3416E+05	28.36	.3887E+11
6*	10.	.1639	.8026	33.91	33.91	1.000
7	690.	.625	2.105	.4988E+05	28.36	.1984E+11
8	200.	.0587	2.240	.5329E+05	28.36	.5101E+10
9	150.	.0600	2.193	.5212E+05	28.36	.3984E+10
<u>C14</u>						
1	150.	.0537	2.449	1.000	1.000	1936.
2	150.	.0750	1.754	1.000	1.000	5273.
3	50.	.0129	10.23	1.000	1.000	9.855
4	60.	.0967	1.360	1.000	1.000	4520.
5	690.	.0887	1.483	1.000	1.000	.4012E+05
6*	10.	.1639	.8026	1.000	1.000	1.000
7	690.	.0625	2.105	1.000	1.000	.1402E+05
8	200.	.0587	2.240	1.000	1.000	3375.
9	150.	.0600	2.193	1.000	1.000	2696.

*No matrix diffusion assumed in Layer 6.

SCENARIO II

Table C-4

Vector 24 Data Used to Estimate Retardation Due to Diffusion
 Into the Rock Matrix. Caveats in the text with regard to
 the uranium text should be noted.

i	L _i (ft)	Ø _i	f _i V _i	R _{host} ^{ch}	R _{fracture} ^{ch}	R _{md}
<u>U234, U236, U238</u>						
1	150.	.0484	2.619	2455.	10.20	.3678E+08
2	150.	.0440	2.878	2711.	10.20	.3058E+08
3	50.	.0125	10.09	9817.	10.20	.8559E+06
4	60.	.1017	1.246	1103.	10.20	.6139E+08
5	690.	.0675	1.876	1724.	10.20	.3231E+09
6*	10.	.1438	.8808	1317.	1317.	1.000
7	690.	.0639	1.981	1827.	10.20	.2907E+09
8	200.	.0552	2.297	2138.	10.20	.6329E+08
9	150.	.0708	1.790	1639.	10.20	.7687E+08

*No matrix diffusion assumed in Layer 6.

Table C-5

Vector 62 Data Used to Estimate Retardation
Due to Diffusion Into the Rock Matrix

i	L_i	θ_i	$\frac{f1}{V_i}$	R_{host}^{ch}	$R_{fracture}^{ch}$	R_{md}
<u>Tc99</u>						
1	150.	.0422	3.326	7215.	5.348	.3391E+08
2	150.	.0931	1.506	3095.	5.348	.1565E+09
3	50.	.0140	10.04	.2242E+05	5.348	.1277E+07
4	60.	.0694	2.021	4260.	5.348	.3570E+08
5	690.	.0786	1.784	3725.	5.348	.5213E+09
6	10.	.1694	.8276	76.98	76.98	1.000
7	690.	.0753	1.861	3899.	5.348	.4808E+09
8	200.	.0735	1.907	4002.	5.348	.1330E+09
9	150.	.0742	1.890	3964.	5.348	.1015E+09
<u>C14</u>						
1	150.	.0422	3.326	1.000	1.000	879.8
2	150.	.0931	1.506	1.000	1.000	9460.
3	50.	.0140	10.04	1.000	1.000	11.65
4	60.	.0694	2.021	1.000	1.000	1568.
5	690.	.0786	1.784	1.000	1.000	.2617E+05
6	10.	.1694	.8276	1.000	1.000	1.000
7	690.	.0753	1.861	1.000	1.000	.2306E+05
8	200.	.0735	1.907	1.000	1.000	6216.
9	150.	.0742	1.890	1.000	1.000	4789.

Appendix D

Calculation of Thermal Buoyancy Gradient

Consider a cylindrical volume of fluid with length L and average temperature T immersed in a medium of average temperature T_0 ($T > T_0$) (Figure D-1). The difference in temperature produces an upward force on the volume of fluid. The velocity of the fluid in the cylindrical volume can be described by:²⁷

$$v = \alpha \Delta T K \quad (D-1)$$

with

v = Darcy velocity of fluid

α = average coefficient of thermal expansion of fluid

$$\Delta T = T - T_0$$

K = hydraulic conductivity of medium

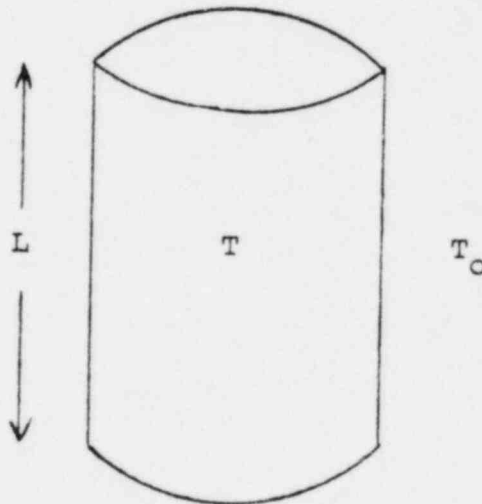


Figure D-1.

Water Column Assumed for Thermal/Buoyancy Calculation

Since Darcy velocity is equal to the product of hydraulic gradient (I) and conductivity, the upward gradient is given by

$$I = \alpha \Delta T \quad (D-2)$$

The temperature field around a repository at the Hanford Site (46,800 MTHM spent fuel) has been calculated for various times after closure. Figure D-2 presents the results of these calculations as 1,000, 4,000, and 30,000 years after repository closure.²⁸ The upward gradient for each time period is calculated as follows. The "disturbed zone" is assumed to be 4 km wide and has a height of 400 meters above the repository. The average temperature \bar{T} of this disturbed zone is calculated by

$$\bar{T} = \frac{1}{V} \int^V T dV.$$

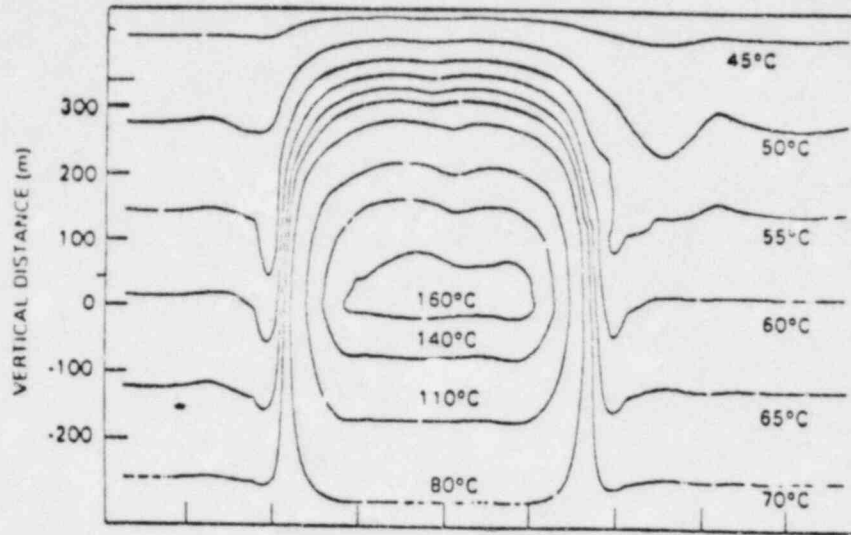
T_0 is the average background temperature of the disturbed zone calculated from the natural geothermal field. The hydraulic gradient is then obtained by using Equation (D-2), i.e., $I = \alpha (\bar{T} - T_0)$.

The results of the calculations are shown in Table D-1.

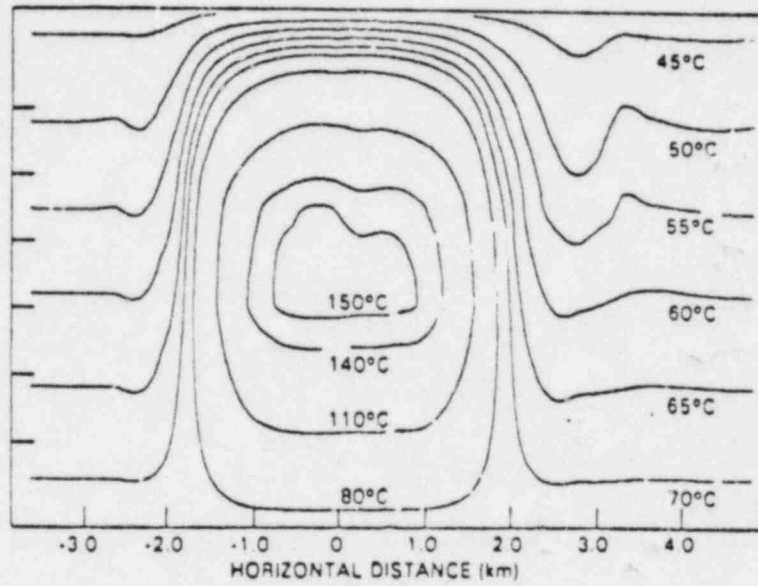
Table D-1
Hydraulic Gradients Produced by Thermal Effects

	$\bar{T} (^{\circ}\text{C})$	$T_0 (^{\circ}\text{C})$	$(1/^{\circ}\text{C})$	Gradient
1,000 year	98.2°	53.2°	608×10^{-6}	0.027
4,000 year	101.8°	53.2°	608×10^{-6}	0.030
10,000 year	64.3°	53.2°	513×10^{-6}	0.006

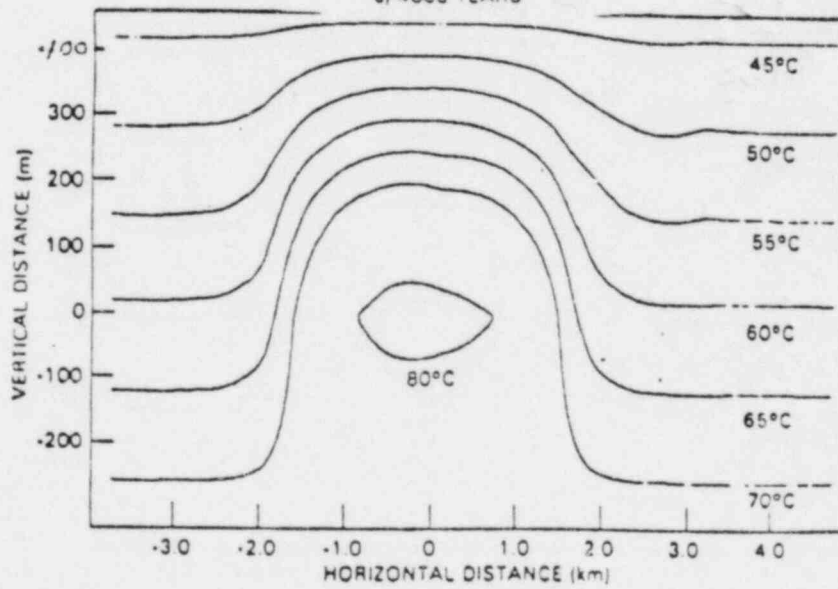
Isotherms Used in Calculating Thermal Bouyancy



d) 1000 YEARS



e) 4000 YEARS



f) 30000 YEARS

NOTE:
REPOSITORY LOCATED
AT (0, 0) COORDINATES

Figure D-2. (from Reference 28)

Appendix E

The Mixing Cell Source Model

In Source #3 we allow the backfilled regions to be modeled as a mixing cell in which flowing groundwater is assumed to mix with radionuclides in the volume of the mixing cell. The concentration of radionuclides released from the backfilled regions is then given by the uniform concentration in the mixing cell. This model can be calculated analytically for a single stable species.

Let

V = mixing cell volume,

C = radionuclide concentration in water in the mixing cell,

L = rate of radionuclide input into V from waste form leaching,

Q = water flow through V .

In this illustration we will assume the leach rate, L , to be constant for a period, τ , so that L is given by

$$L = \frac{N_0}{\tau}$$

where N_0 is the initial containment inventory.

The contaminant concentration in the mixing cell is described by

$$V \frac{dC}{dt} = L - QC \quad (E.1)$$

If we let

$$\lambda_0 \equiv Q/V$$

the solution of E.1 is

$$C(t) = \frac{N_0}{\lambda_0 V \tau} \left(1 - e^{-\lambda_0 t} \right) \quad (E.2)$$

For small t

$$C(t) = \frac{N_0}{V \tau} (t)$$

Thus the concentration of the radionuclide increases linearly from zero.

The asymptotic release rate QC_∞ can be obtained from Equation (E.1) with

$$\frac{dC}{dt} = 0,$$

$$QC_\infty = L$$

Thus, for long times, the release rate approaches a value governed by the rate of waste form leaching. The release rate from the mixing cell is then less than or equal to the release rate given by consideration of the waste form leaching along.

For decaying radionuclide chains, this model is implemented numerically in NWFT/DVM according to the compartment model shown in Figure E.1. Radionuclides remaining in the waste form are represented by Compartments, R. The waste form breakdown rate governs transfer from Compartments R to Compartments U. The inventory in the Compartments U is examined along with the water volume in the mixing cell and solubility limits to transfer all or part of that inventory into the mixing cell. The mixing cell inventory is denoted by Compartments N. The mixing cell is flushed constantly to give a release source (S) of

$$S_i = \lambda_0 N_i$$

When solubility limits are applied, radionuclides may be transferred from Compartments N to Compartments U, representing precipitation. For large solubility limits, Compartments U may be empty.

Horizontal transfer between radionuclides compartment, i , and compartments $i + 1$ or $i - 1$ represents decay and production.

The effect of various source models can be illustrated by considering the total integrated discharge of the contaminant, D_i ,

$$D_i = \int_0^t S_i \cdot dt$$

For a leach or solubility limited source, S_i is a constant. For the mixing cell, S_i is initially zero and approaches an asymptotic value determined by the leach or solubility limit. The discharge is illustrated in Figure E.2.

The integrated discharge is numerically equal to the area under the plot of S_i vs. t . Due to its low initial value, the mixing cell always gives lower values of S_i and D_i than leach or solubility limits, the shaded area indicating the magnitude of the reduction in D_i .

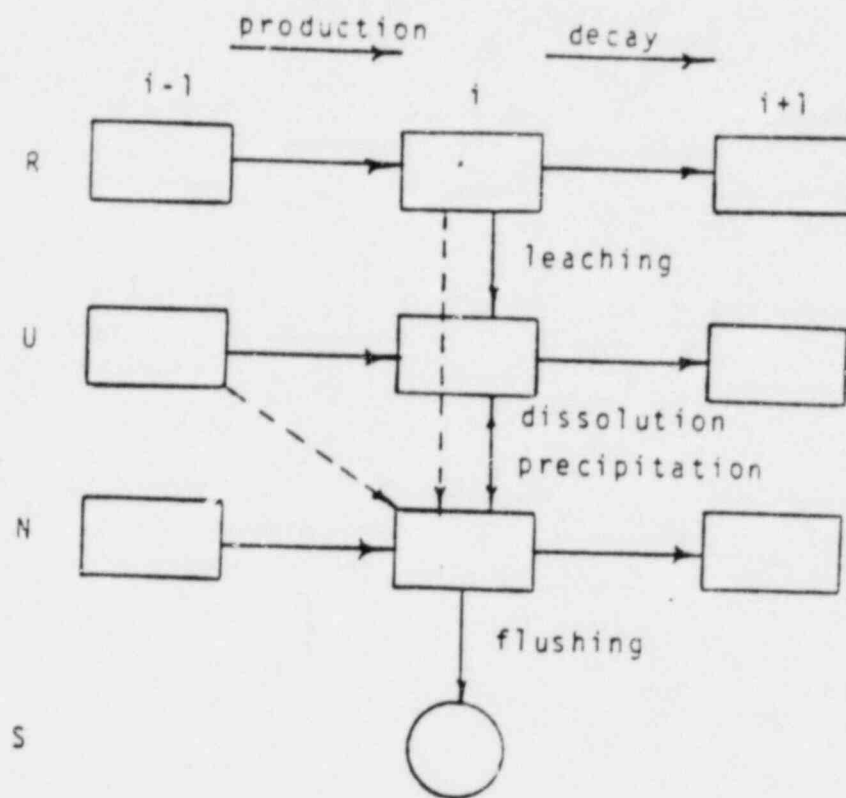


Figure E.1. Implementation of the Mixing Cell Source Model for NWFT/DVM.

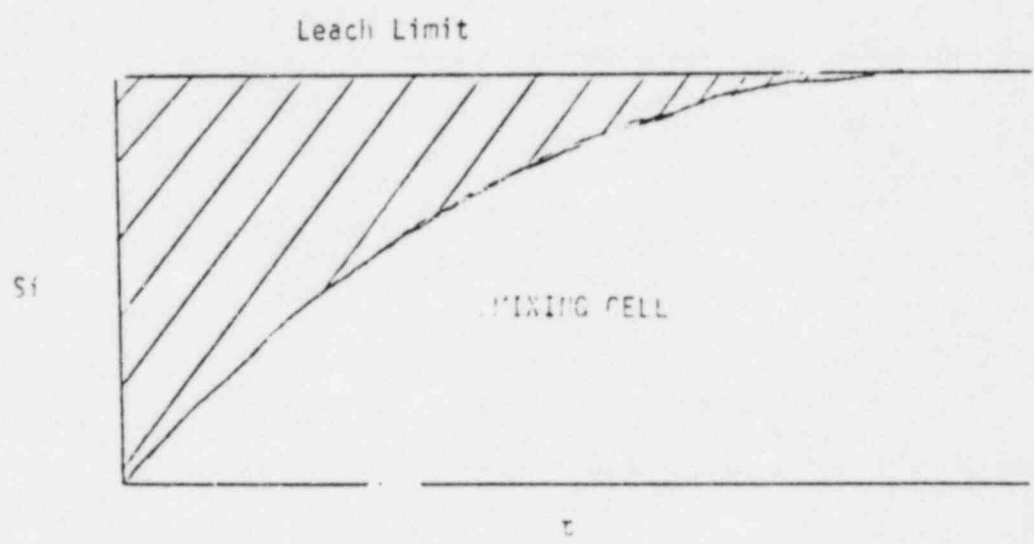


Figure E.2. Effects of the Mixing Cell Assumption on Integrated Discharge Relative to the Leach Limited Source Model

Appendix F

Rationale For the Selection of Scenarios Analyzed in Basalt

In these analyses we have chosen scenarios which are both credible and consistent with characteristics of a real basalt site currently being studied. It is felt that contaminant transport by groundwater to an aquifer is the dominant transport mode. The first selection process therefore involved examining scenarios involving groundwater transport to an aquifer. The path of this transport from the underground facility could either be upward or downward to an upper or lower aquifer respectively. An upward path was chosen for our analyses for the following reasons:

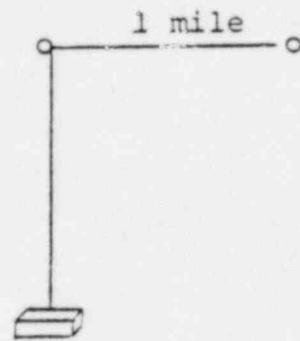
1. There is no indication that there exists a downward gradient from the subsurface facility to the lower aquifer in the real site.
2. Lack of knowledge of the characteristics of the lower aquifer for the real site. That is, data involving flow direction, discharge location, hydraulic properties are very limited and inconsistent.
3. Based on expert judgement, the groundwater travel time from the underground facility to the accessible environment via a lower aquifer would most probably be much longer than via an upper aquifer. In other words, the lower aquifer path would probably be of much less radiological consequence than the upper case.

No Disruption Scenario

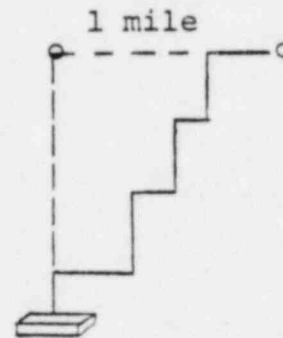
With an upward path chosen, a base case (no disruption) scenario was selected with the following rationale:

1. The cross-sectional area of the whole underground facility was used as the cross-sectional area of the upward flow column. This is the largest areal extent that can carry the wastes from the underground facility. This is a conservative approach.

2. Little or no natural upward gradient is indicated from the data from the real site. Therefore an upward gradient that could be produced by the thermal buoyancy resulting from waste heat was used in the analyses.
3. The "shortest" path to the accessible environment was selected. First, one mile down gradient in the first aquifer above the underground facility was chosen as the "accessible environment". Then a "vertical" path rather than a "Zig-Zag" path to the upper aquifer was used (see figures below).



Vertical Path



Zig-Zag Path

Each horizontal segment in the zig-zag path is a high conductivity zone in an interflow or an interbed layer. It was felt that the vertical segments in this path could be represented by one vertical segment as in the "vertical path" case. Available data on interflow and interbed zones of the real site suggest that the total travel time of groundwater in the horizontal segments would most probably be longer than that in the aquifer in the "vertical path" case. Therefore, a "vertical path" to the upper aquifer was chosen for our analyses.

Disruption Scenarios

The disruption scenarios we chose involved the introduction of a high conductivity zone between the underground facility and the upper aquifer. One scenario (Scenario II) involves a high conductivity zone of large areal extent and another scenario (Scenario III) a zone of small areal extent. For Scenario II the dense basalt layer containing the underground facility was assumed to be fractured by either earthquakes or stresses (mechanical or thermal) related to the proximity of the underground facility. The same rationale as (1), (2), and (3) in the "no disruption" scenario were applied here. Scenario III involves a small area of high conductivity. This could be a borehole, a degraded shaft or fractured rock around a borehole or a shaft. We feel that the two scenarios selected represent events of high or credible probability and possibly of high consequences for the time period of interest.

No massive disruption scenario, e.g., faulting, was considered in our analyses. Due to time constraint of this work, no detailed analysis of the probability of occurrence of massive disruption could be performed. We feel, however, that the probability of having a massive disruption through or near the underground facility at a site with these characteristics during the time period of interest should be very small.

References

1. Campbell, J. E., et al., 1980, "Risk Methodology for Geologic Disposal of Radioactive Waste: The Distributed Velocity Method of Solving the Convective-Dispersion Equation," SAND80-0717 (NUREG/CR-1376), Sandia National Laboratories.
2. Pepping, R. E., and Runkle, G. E., 1981, "Risk Methodology for Geologic Disposal of Radioactive Wastes: Decay Chain Representation for Geologic Transport of Radioactive Wastes," SAND81-0065 (NUREG/CR-2376), Sandia National Laboratories.
3. Fontes, J. C., Neretnieks, I., et al., "The Application of Isotope Techniques in the Assessment of Potential Sites for the Disposal of High-Level Radioactive Wastes, (In preparation), IAEA (Vienna).
4. Cranwell, R. M., et al., "Risk Methodology for Geologic Disposal of High-Level Radioactive Waste in Bedded Salt: Reference Site Analyses," SAND81-2573 (NUREG/CR-2452), Sandia National Laboratories.
5. Muller, A. B., Finley, N. C., and Pearson, F., Jr., 1981, "Geochemical Parameters Used in the Bedded Salt Reference Repository Risk Assessment Methodology," SAND81-0557, (NUREG/CR-1996), Sandia National Laboratories.
6. Iman, R. L., et al., 1980, "Latin-Hypercube Sampling (Program User's Guide)," SAND79-1473, Sandia National Laboratories.
7. "Environmental Radiation Protection Standards for Management and Disposal of Spent Nuclear Fuel, High-Level and Transuranic Radioactive Wastes," 40CFR191.
8. Egan, D. J., Environmental Protection Agency, Public Presentation at the Symposium on Uncertainties Associated With the Regulation of the Geologic Disposal of High-Level Radioactive Wastes, Gatlinburg, Tenn., March 9-13, 1981.
9. Cranwell, R. M., and Donath, F. A., "Probabilistic Aspects of Faulting in A Repository System," SAND80-0164, (In preparation), Sandia National Laboratories.

10. Long, P. E., 1978, "Characterization and Recognition of Intra Flow Structures, Grande Ronde Basalt," RHO-BWI-LD-10, Rockwell Hanford Operations, Richland, Washington.
11. Sato, M., 1960, "Geochemical Environments in Terms of Eh and pH," Econ. Geol. 55: p. 928-961.
12. Garrels, R. M., and Christ, C. L., 1965, Solutions, Minerals and Equilibria, Harper and Row, New York.
13. Stumm, W., and Morgan, J. J., 1970, Aquatic Chemistry, Wiley, New York.
14. Smith, M. J., et al., 1980, "Engineered Barrier Development for a Nuclear Waste Repository in Basalt," RHO-BWI-ST-7, Rockwell Hanford Operations, Richland, Washington.
15. Guzowski, R. V., Nimick, F. N., and Muller, A. B., 1982, "Repository Site Definition in Basalt: Pasco Basin, Washington," SAND81-2088, (NUREG/CR-2352), Sandia National Laboratories.
16. Harder, H., 1978, "Synthesis of Iron Layer Silicate Minerals Under Natural Conditions," Clay and Clay Minerals, 26: p. 65-72.
17. Erdal, B. R., et al., 1980, "Parameters Affecting Radionuclide Migration in Geologic Media," in Scientific Basis for Nuclear Waste Management, Vol. 2, C. J. M. Northrup, Jr., Ed., Plenum, N.Y., p. 609-616.
18. Wolfsberg, K., et al., 1979, "Sorption-Desorption Studies on Tuff," LA-7480-MS, Los Alamos National Laboratory.
19. Relyea, J. F., Rai, D., and Serne, R. J., 1979, "Interaction of Waste Radionuclides With Geomedia Program Approach and Progress," in Scientific Basis for Nuclear Waste Management, Vol. 1, G. J. McCarthy, Ed., Plenum, N.Y.
20. Relyea, J. F., et al., 1980, "Methods for Determining Radionuclide Retardation Factors: Status Report," PNL-3349, Battelle Pacific Northwest Laboratories, Richland, Washington.

21. Hostestler, D. D., et al., 1979, "Status of Sorption Information Retrieval System," PNL-3139, Battelle Pacific Northwest Laboratories, Richland, WA.
22. Reardon, E. J., 1981, "K_d's -- Can They Be Used to Describe Reversible Ion Sorption Reactions in Contaminant Migration?," Ground Water, 19: p. 273-286.
23. Neretnieks, I., 1980, J. Geophysical Research, 85: 88, p. 4379-4397.
24. Grisak, G. E., and Pickens, J. F., 1981, J. Hydrology, 52: p. 47-57.
25. Tang, D. H., et al., 1981, Water Resource Research, 17: 3, p 555-564.
26. Erickson, K. L., and Fortney, D. R., 1981, "Preliminary Transport Analyses for Design of the Tuff Radionuclide Migration Field Experiment," SAND81-1253, Sandia National Laboratories.
27. Merkin, J. H., 1979, International Journal of Heat Mass Transfer, 22: p. 1461-1462.
28. King, I. P., et al., 1981, "Parametric and Sensitivity Analysis of Waste Isolation in a Basalt Medium," RHO-BWI-C-94, Rockwell-International.

Technical Assistance for Regulatory Development:
A Simplified Repository Analysis in a Hypothetical
Bedded Salt Formation

R. E. Pepping

M. S. Chu

M. D. Siegel

Sandia National Laboratories
Albuquerque, New Mexico

with contributions from

Pei-Lin Tien

Adel A. Bakr

Science Applications, Incorporated
Albuquerque, New Mexico

Fin No. A-1165. Task 3

Table of Contents

	Page
I. Introduction	1
II. The Draft EPA Standard	3
III. Sequence of the Discussion	11
IV. The Hypothetical Repository	12
V. Radionuclide Release Scenarios and Probabilities	25
VI. Computer Models and Data Used for Scenario Analysis	35
A. The Ground Water Transport Scenarios: NWFT/DVM	35
B. Disinterment Scenarios	43
C. Construction of CCDF's	45
D. Sensitivity Analysis Results	60
VII. Conclusions	62
VIII. Appendix A. The Mixing Cell Source Model ..	A-1

Figures

	Page
1. Radionuclide Releases From Disruptions	6a
2. Complementary Cumulative Distribution Function (CCDF)	7
3. Compliance Estimation	9
4. Consequence Estimates With Sampled Input	10
5. General Setting of the Reference Site	13
6. Schematic Cross-Sections Across the Subbasin	14
7. Floor Plan of Reference Subsurface Facility ..	20
8. The U-Tube Flow Pattern	27
9. Scenario II Geometry	30a
10. Brine-Pocket Areas	34a
11. Flow and Transport Network Assumed by NWFT/DVM	35a
12. CCDF for the Direct Hit Scenario	47
13. CCDF for Brine Pocket Penetration Scenario ...	49
14. CCDFs for Groundwater Transport Scenarios With Source #1	51
15. CCDFs for Groundwater Transport Scenarios With Source #2	54
16. CCDFs for Groundwater Transport Scenarios With Source #3	57

Tables

	Page
1. Release Limits for the EPA Draft Standard	4
2. Stratigraphic Units, Lithology, and Thickness	16
3. Hydraulic Properties of the Units	19
4. Assumed Radionuclide Inventory	22
5. Lengths and Elevations for the Groundwater Transport Scenarios	36
6. Hydraulic Properties and Sampled Distributions	37
7. Source Model Assumptions	39a
8. Sorption Data	40
9. Solubility Limits	42
10. Repository Hazard Index	43
11. Probabilities and Consequences for Disinterment Scenario 1 (The "Direct Hit")..	46
12. Probabilities and Consequences for Disinterment Scenario 2 (The Brine Pocket)..	48a

I. Introduction

Background

The Environmental Protection Agency (EPA) has drafted a standard for protection against highly radioactive wastes to be stored underground. The standard, which will apply to all geologic repositories, is still being developed and an internal working draft is available [1]. The Nuclear Regulatory Commission (NRC) will enforce the standard, and is developing appropriate Federal regulations [2].

To assign quantitative, that is, numerical values to such factors as release of radionuclides from a geologic repository, the EPA used simple computer models [3]. The agency expects the NRC to use computer modeling to assess compliance with the EPA standard. To support NRC, Sandia National Laboratories (SNL) is developing computer models that may be used in such a compliance assessment [4]. We expect that NRC will use the models to evaluate applications to construct actual repositories.

The Department of Energy (DOE) is also involved in that it selects actual sites for geologic repositories and submits applications to construct them. To determine their suitability for waste disposal, the DOE is investigating basalt and tuff flows, bedded salt and granite formations, and salt domes. None of these geologic formations are characterized well enough to choose specific sites. Neither are they modeled in enough detail to evaluate any given site to the rigorous compliance requirements set down by the draft EPA standard. However, whatever information does exist can be supplemented with general information taken from such sources as similar formations or host-rock descriptions, hydraulic properties, and geochemical characteristics. We can then apply the models thus developed to evaluate a similar but hypothetical repository. Using the capability of SNL models as a base, we then determine how well the hypothetical site meets the draft EPA Standard: do they or do they not comply? Such questions we hope to answer below.

Hypothetical Repositories

To develop credible models, SNL uses information from several repositories hypothetically constructed in candidate host-rocks. In fact, results from such a hypothetical repository in a sequence of basalt flows have been informally presented [5]. We are presently analyzing repositories in the following formations:

- A sequence of basalt flows,
- A sequence of welded and non-welded tuff,
- A sequence of sedimentary rocks and bedded salt, the salt acting as the host-rock; this repository is the subject of this report.

All data on the hypothetical repositories have been taken from the open literature. Generally, however, the quality of such data is not high enough to accompany a characterization report of an actual site. Also, in some cases, data for a given rock unit had to be assumed from known properties of similar formations. Therefore, whatever results we arrived at must not be interpreted as a definitive statement on any specific site or formation.

Scenarios

To select scenarios for detailed analysis, we used the results of risk analysis methods development programs at SNL [6]. In that work a number of scenarios were identified that may be important in understanding risks from real repositories. Most of those scenarios involved flowing groundwater intruding into the backfilled regions of the repository. Various water-bearing geologic strata were the sources of groundwater as well as the potential paths for migrating radionuclides.

After considering the previous scenario development efforts and the details of the repository (discussed below) we chose two types of scenarios: groundwater transport and disinterment. In the first type of scenario radionuclides are presumed to be released at low rates over an extended period. Radionuclides are transported to the accessible environment by the natural, or slightly perturbed, groundwater flow system. In disinterment scenarios, radionuclides are transported rapidly to the accessible environment over a short period.

II. The Draft EPA Standard

The EPA assumes that natural or man-induced disruptions will cause the repository to release some radionuclides and that they will find their way to the accessible environment.* In Draft #19 of its standard, the EPA sets the limits for total integrated discharges that may be expected from such disruptions (Equation (1)):

$$\text{EPA Sum} = \sum_i \frac{Q_i}{\text{EPA}_i} \quad (1)$$

where: Q_i = total integrated release of radionuclide i
 EPA_i = release limit for radionuclide i .

The sum over i includes all radionuclide present in the waste. The proposed release limits are listed in Table 1.

We determine Q_i by estimating discharge rates to the surface and integrating those rates over 10,000 years, the period after sealing the repository that the draft EPA standard addresses. The draft EPA standard requires that $\text{EPA Sum} \leq 1.0$ and that it will not be exceeded at probability of greater than 0.01/10,000 years; these values result from the so-called "expected releases." The EPA also requires that $\text{EPA Sum} \leq 10.0$ at a probability greater than 0.0001/10,000 years -- the so-called "unlikely releases."

To enforce the EPA standard, the NRC must ensure that any repository is designed such that radionuclide releases are kept low and that the site is chosen such that disruptions that could lead to releases are not likely. However, to enforce compliance, the NRC must understand a particular planned repository well enough to quantify potential disruptions and to estimate releases that they cause. In other words, each potential disruption (i) must have a numerical value assigned to the probability that it will occur. Likewise, the amount of radionuclides thus released must have a numerical value in terms of Equation 1.

*The accessible environment is "any location on the surface where radionuclides may be released or any aquifer that may be contaminated by radionuclides at a distance of 1 mile from the perimeter of the underground facility."

Table 1

Cumulative Releases to the Accessible Environment
for 10,000 Years After Disposal

Radionuclide	Release Limit
Americium-241 - - - - -	10
Americium-243 - - - - -	4
Carbon-14 - - - - -	200
Cesium-135 - - - - -	2000
Cesium-137 - - - - -	500
Neptunium-237 - - - - -	20
Plutonium-238 - - - - -	400
Plutonium-239 - - - - -	100
Plutonium-240 - - - - -	100
Plutonium-242 - - - - -	100
Radium-226 - - - - -	3
Strontium-90 - - - - -	80
Technetium-99 - - - - -	2000
Tin-126 - - - - -	80
Any other alpha-emitting radionuclide - - - - -	10
Any other radionuclide which does not emit alpha particles - - - - -	500

The following are examples of i and how we can estimate their probabilities:

- * Inadvertant drill holes; we consider similar activities, such as present-day exploratory drilling in similar media.
- * Failure of shaft or borehole seals; thoroughly investigate properties of sealing materials.
- * Geologic faulting; investigate seismic activity at the site.

We can estimate radionuclide releases by modeling the processes that tend to transport nuclides. This aspect is covered in the following sections.

Where sufficient data are available the following procedures can be used to estimate how well an application complies with the draft EPA Standard [7]:

1. Examine each potential disruption (i ; hereafter called "a scenario") and estimate its probability, p_i . Next, use numerical modeling to estimate the consequences C_i , of that scenario. C_i is numerically equal to the EPA Sum obtained by evaluating Equation 1. Thus, after completing the analyses, you will have a set of doublets (p_i, C_i) that can be displayed graphically (Figure 1).
2. To start estimating compliance, integrate results from Step 1 to produce a Complementary Cumulative Distribution Function (CCDF) of the following consequences:

$$p > = \sum_i p_i \cdot U (C_i - C >) \quad (2)$$

where $p >$, $C >$ are the ordinate and abscissa of the CCDF respectively

$U(x)$ = unit step function,

$$U(x) = \begin{cases} 1 : x > 0 \\ 0 : x < 0. \end{cases} \quad (3)$$

The CCDF can be constructed from Figure 1, as shown in Figure 2.

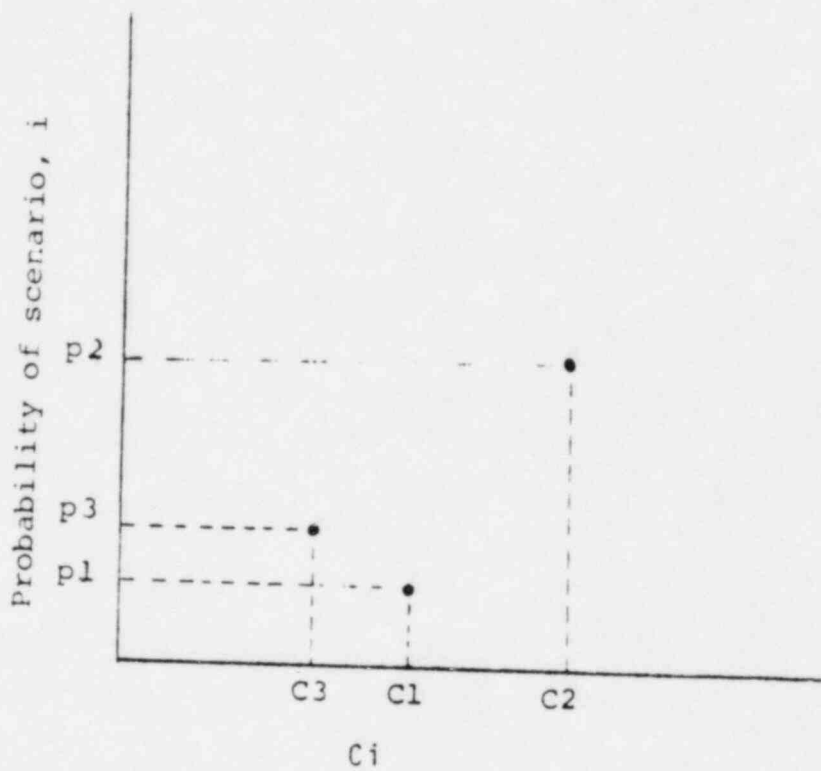


Figure 1. Expected EPA Sum, C_i , from Scenario i

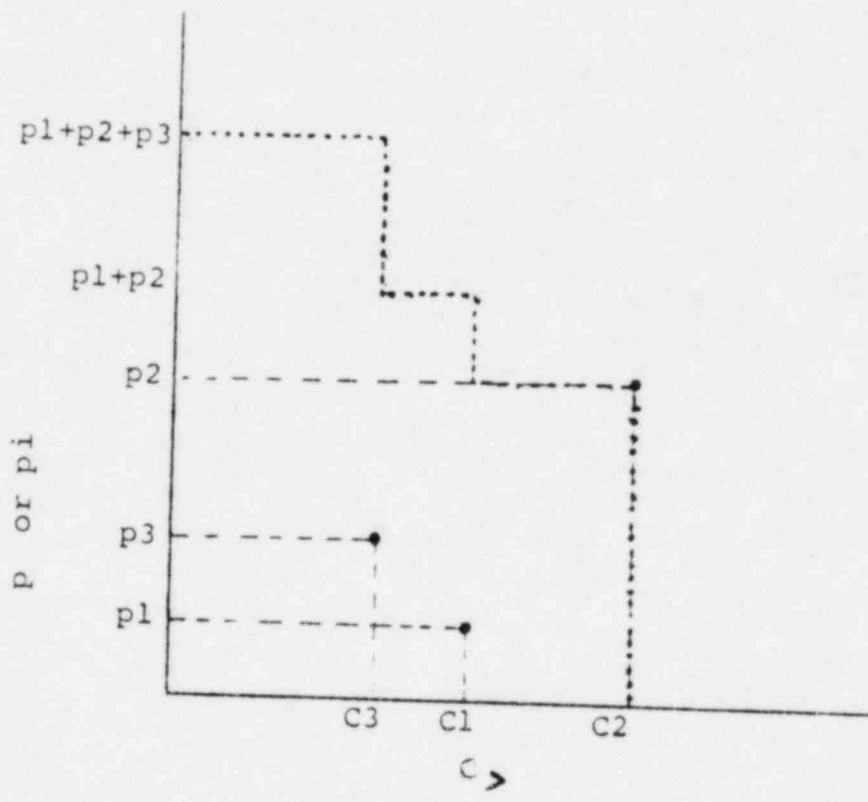


Figure 2. Complementary Cumulative Distribution Function (CCDF)

3. Lay Figure 2 over the CCDF implied by the EPA Standard (Figure 3). If Figure 2 falls outside the Standard's CCDF (shaded area in the figure), a violation is indicated.

When calculating estimates of the consequences mentioned in Step 2, there are built-in uncertainties that result from uncertainties in data inserted into the model for estimating releases. The following, for example, are some factors that may contain such uncertainties:

- hydraulic properties along paths for groundwater that could transport radionuclides;
- geochemical properties along the groundwater paths;
- when calculating groundwater transport rates, those very parameters that define the source of radionuclides.

The effect of such uncertainties as listed above is to produce a family of estimates, C_{ij} , where j denotes the j th estimate of the EPA Sum for a certain scenario, i (Figure 4). In the situation illustrated, which we use later, each C_{ij} has the same probability, p_i , as any other one. We accomplish this by using a sampling procedure to sample equally probable combinations of the input data such that, if N combinations of input data are chosen, the probability associated with C_{ij} , that is p_i' , is:

$$p_i' = \frac{p_i}{N} \quad (4)$$

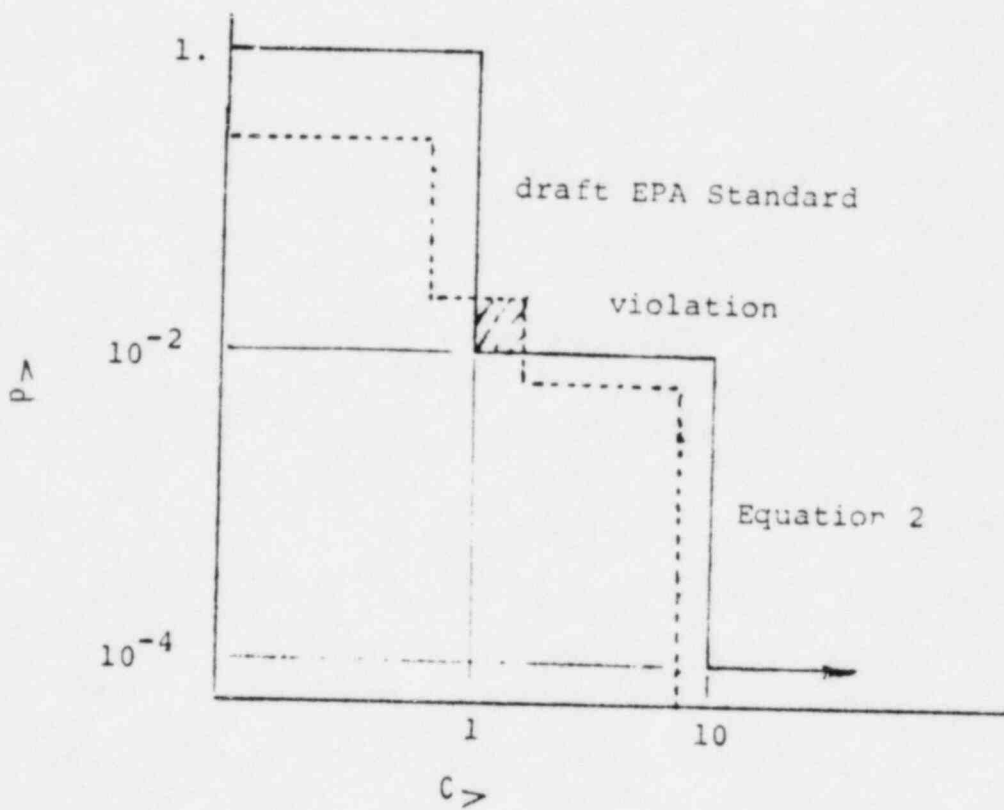


Figure 3. Compliance Estimation: Comparison of the Constructed CCDF With the Draft EPA Standard.

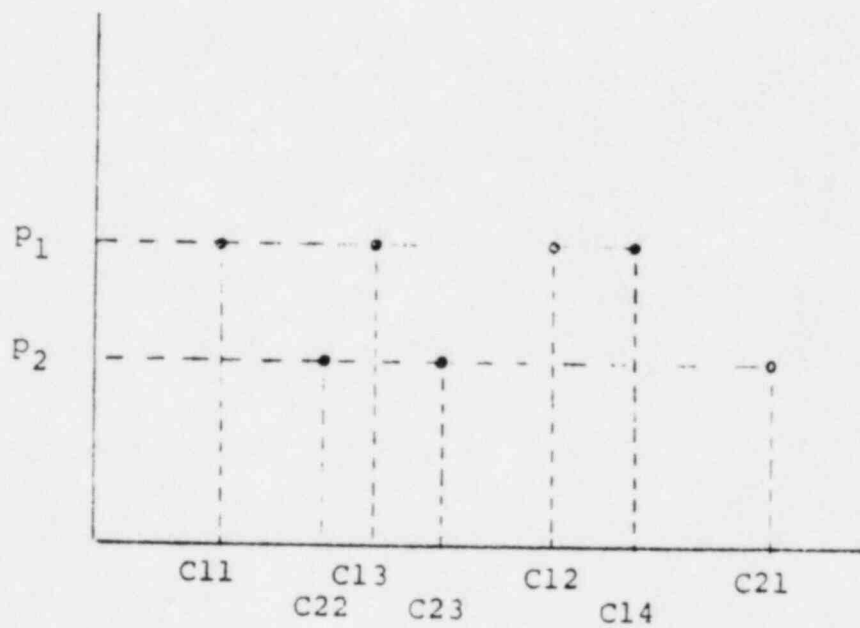


Figure 4. Consequence Estimates for Two Scenarios With Sampled Input.

III. Sequence of Discussion

Below we will discuss our findings as follows:

1. Description of the hypothetical repository --
 - rock types found at the site
 - hydraulic properties of the rock formations
 - properties of any aquifers
 - various sizes of all formations,
2. Scenarios -- such situations or potential states of the repository that may lead to release of radionuclides -- and their probabilities of occurrence,
3. Models -- description and details of their application to this analysis.
4. Required geochemical data,
5. Quantitative data -- numerical results from this analysis: how much, when, how long?

As we discuss our findings, we are assuming that the reader is familiar with the problems of disposal of radioactive wastes and the methods developed at SNL to address them. Nevertheless, we will endeavor to avoid highly technical language and will provide complete citations when we feel it will behoove the reader to seek further clarification from the open literature.

IV. The Hypothetical Repository

If we are to use the SNL models to verify compliance with the draft EPA Standard, we need a description of the repository to be licensed. The description should include the geologic, hydrologic, and geochemical properties of the site; the shape, size, and layout of the excavation, that is, the engineered underground facility; and the nature of the nuclear waste.

Bedded-Salt Site

The bedded-salt repository site is located in a subsidiary basin within a major sedimentary basin. The crust of the region sank, allowing sediments to accumulate. Beginning 300 million years ago, within this depressed region, small blocks of the crust were displaced along deep-seated faults, creating a system of subbasins separated by basement uplifts. The subbasin where the site is located (Figure 5) is bounded on the north by Uplift A and on the south by Arch M. River C, approximately 40 to 50 miles to the north, flows eastward and a small river, River R, about 25 miles to the east, flows northwest to southeast. The uplift and the arch are bounded by high-angle reverse faults that steepen with depth, indicating that the subbasin is a block of crust that was uplifted with respect to surrounding regions. The subbasin is situated within a tectonically stable region that is associated with a shield area to the north. Several faults strike northwest just south of the uplift, but the rest of the subbasin lacks evidence of faulting or volcanism.

Current seismicity in the region is localized along the uplift, which is the dominant structural feature and the focus of any seismic energy release; most earthquakes in the area have foci in the basement. In the past, only a few earthquakes with intensities between V and VI on the Modified Mercalli Intensity Scale have been registered, and none with destructive intensities of VII and above. Accordingly, this region is in Zone 1 on a seismic-risk map, which means that minor earthquake damage is expected in the next 100 years. However, the level of shaking hazards is expected to be less than 4 percent of that of the force of gravity.

Active subsurface dissolution is evident along the northern and eastern margins of the subbasin; collapse features such as sinkholes, depressions, small faults, and fractures are common within the salt dissolution zone, which is at least 10 miles from the site. The mean rates of salt dissolution range from 19 feet (6 m) to 1150 feet

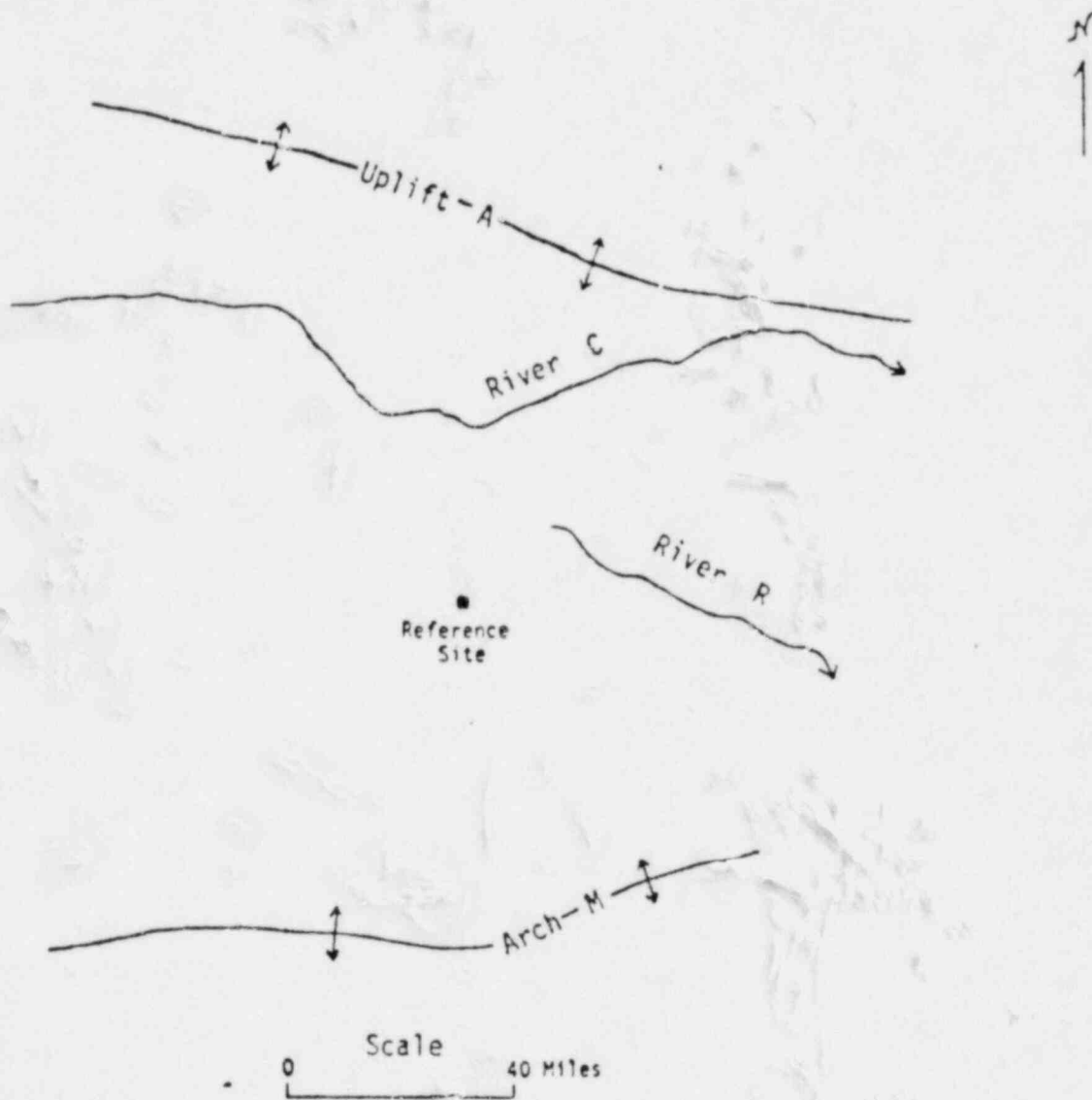


Figure 5. General Setting of the Beddal Salt Reference Site (Plan View).

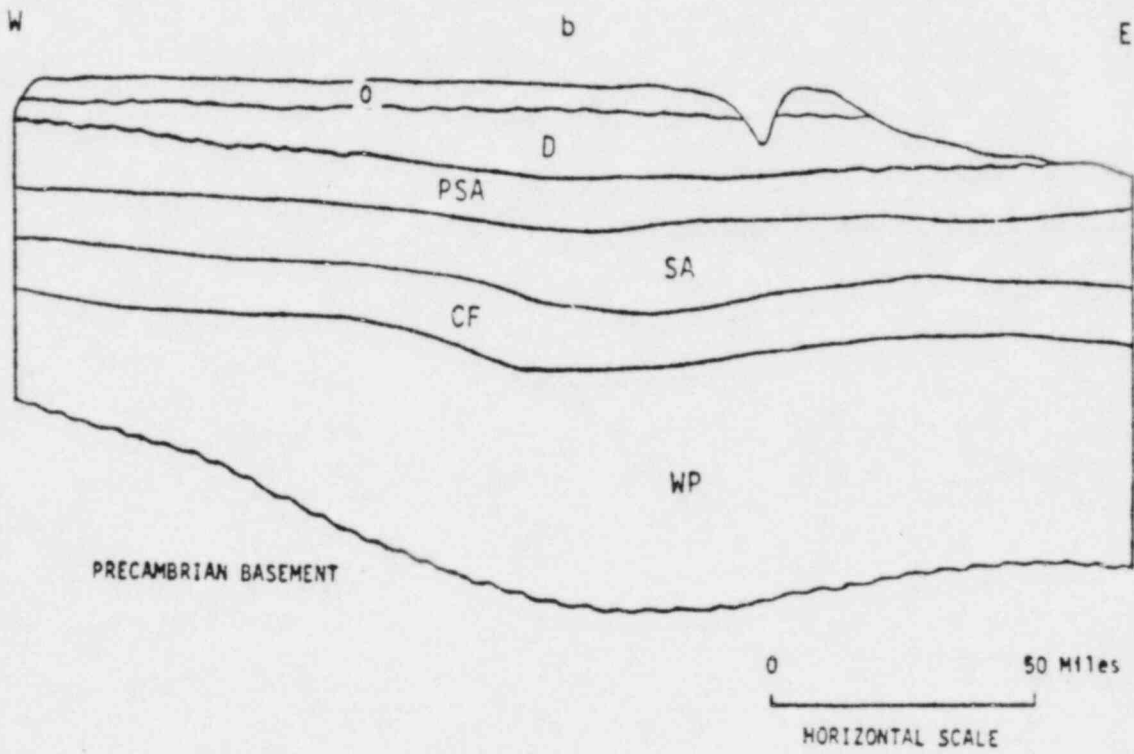
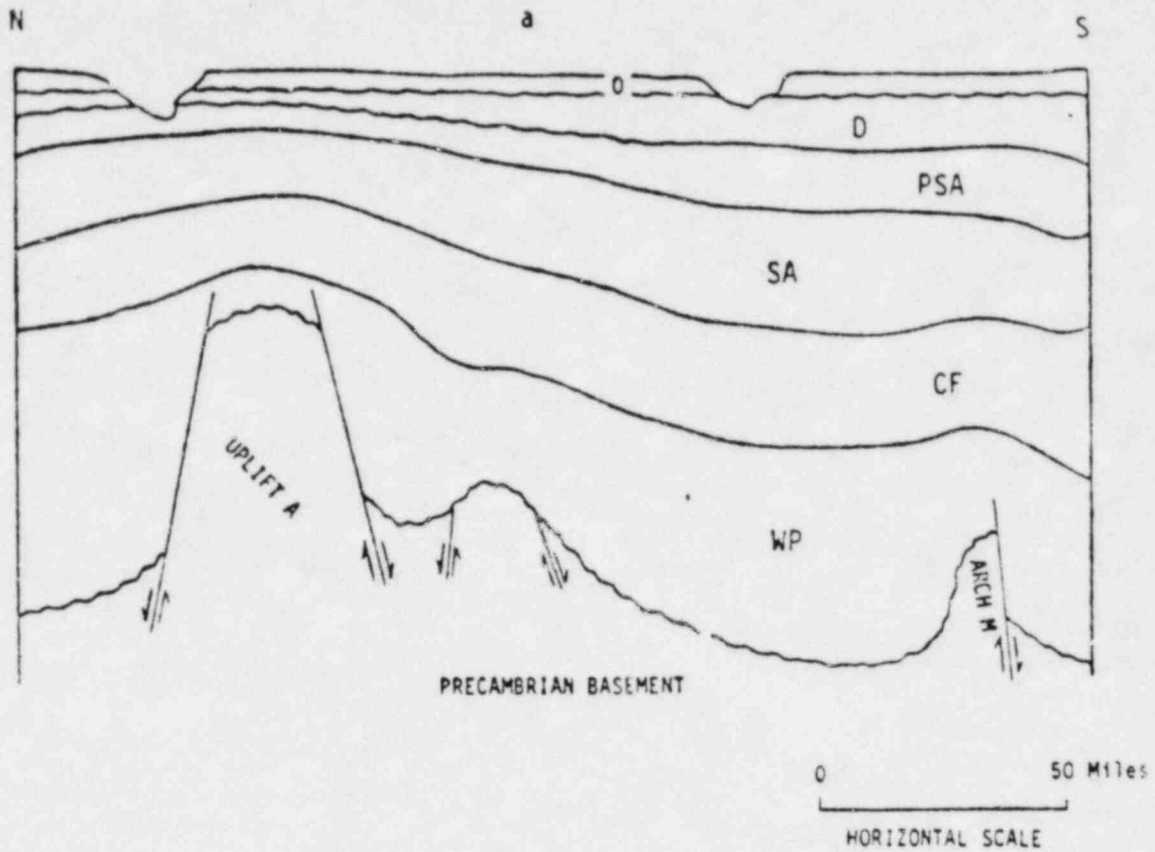


Figure 6. Schematic Cross-Section Across the Subbasin.

(350 m) per 10,000 years. Salt dissolution along the north side is slower than along the east side of the subbasin.

The subbasin is a relatively shallow, continental-interior basin. The Precambrian basement is at most 10,000 feet below the surface. The repository is located in the center of Unit SA, which consists of 1,000 to 1,200 feet of evaporites, mainly halite with small amounts of anhydrite and dolomite (Table 2). Unit SA is overlain by Unit PSA, which ranges in thickness from 550 to 850 feet and consists of siltstone, sandstone, salt and anhydrite. Unit PSA is an aquitard slowing the downward movement of groundwater. Overlying the unit is 300- to 900- foot-thick Unit D, which consists of sand and clay, and is a minor aquifer. Unit O, which overlays Unit D, is between 50 to 300 feet thick and is the major unconfined aquifer in the area. The major constituents of Unit O are sand and clay, with small amounts of gravel and some caliche that thinly covers the surface.

Below Unit SA is Unit CF, which ranges from 1,750 to 2,050 feet in thickness and is composed predominantly of halite, anhydrite, and clay. CF is also an aquitard. Below Unit CF is Unit WP, which is from 2,300 to 4,200 feet thick and consists mainly of shale, limestone, and sandstone. This unit, which is brine-saturated, is considered an aquifer but with such low conductivity that no pumping at all takes place.

Geochemical analyses of shale samples from Unit WP show an average 2.4 percent total organic carbon and as high as 5.38 percent sediments of the layers deposited after Unit WP. Kerogen color, which indicates thermal maturity when plotted against kerogen type, shows that samples from this unit are in transition between maturity and immaturity, and that those of post unit WP never reached temperatures high enough to generate hydrocarbons. This means that, since the site is away from any potential hydrocarbon reservoir, intensive exploration and drilling will not likely take place within the area.

About 50 miles west of the site, the shallow aquifers (Units O and D), are recharged at a rate of between 0.2 and 1.0 inches/year, but discharge along the eastern margin of the subbasin. In these aquifers, the groundwater flows slowly from west to east, several inches to a few feet per year. Flow in the overlying aquifers is driven by gravity. The aquifer Units O and D, dip over a range of 10 to 50 feet

Table 2

Stratigraphic Units, Lithology, and Thickness of
Hypothetical Repository Site

Unit	Thickness (Ft)	Lithology	% Thickness
0	50 - 300	silt clay	45
		sand gravel	50
		caliche	< 5
D	300 - 900	shale clay	30
		siltstone	7
		sandstone conglomerate	60
		limestone	< 3
PSA	550 - 850	anhydrite	7
		claystone	8
		salt	23
		mudstone	22
		siltstone	28
		sandstone	12

Table 2 (Cont'd)

Stratigraphic Units, Lithology, and Thickness of
Hypothetical Repository Site

Unit	Thickness (Ft)	Lithology	% Thickness
SA	1000 - 1200	dolomite	13
		anhydrite	22
		claystone	5
		salt	59
		mudstone	< 1
		siltstone	
		sandstone	
CF	1750 - 2050	dolomite	< 5
		anhydrite	20
		claystone	15
		salt	50
		mudstone	5
		siltstone	5
		sandstone	< 1
WP	2300 - 4200	limestone	55
		sandstone	9
		claystone shale	36

per mile. This results in a head gradient of 2 to 10×10^{-3} driving horizontal flow within Units O and D. Vertical gradients in Units O and D are downward and small in magnitude. The dispersivity of Units O and D is small, less than 100 feet, and typically tens of feet.

Unit WP recharges very slowly -- much slower than the shallow aquifers -- a few hundred miles west of the site and discharges several hundred miles southeast of the subbasin. The briny groundwater in this unit flows slowly, mostly from west to east, at a rate of a few inches per year. Its hydraulic gradient varies between 10 and 30 feet/mile, i.e., from 2 to 6×10^{-3} . The vertical hydraulic gradient, in this unit, however, is steep, about 1 foot/foot, and is directed upward

Table 3 lists ranges of horizontal and vertical hydraulic conductivities and porosities for each unit. Values of conductivities for the O and D units mean that approximately 50 percent of conductivity measurements made in these units would fall in the given range. For the remaining units, the values indicate that 85 percent of the measurements would fall in the given range.

Engineered Underground Facility

The DOE has conceived a design for a subsurface facility where nuclear wastes can be emplaced [8-10]. We will use this facility for our analyses. Since the facility has already been described elsewhere [11], we will present only the few gross features that are important to our analyses. The reader is cautioned that the repository is merely hypothetical, although we will assume it to be real for modeling purposes.

Dimensions -- The mined repository, which is located at a depth of 2,300 feet, has a storage area that extends over a 3,000 acres, rectangular area 15,370 by 8,600 feet (Figure 7). A shaft pillar area extends 2,000 feet horizontally away from the waste storage area, the "pan-handle" area shown in Figure 7.

Each storage room is 4,000 feet long by 17.5 feet wide, by 19 feet high. For our calculations, we will assume the height to be 15 feet because of creep closure that takes place over the operational life of the repository, that is, during the waste emplacement period. The central corridors, which are 18.5 feet wide, will also be calculated as being 15 feet high.

Table 3

Hydraulic Properties of Geologic Units

Unit	Horizontal Hydraulic Conductivity (ft/d)	Vertical Hydraulic Conductivity (ft/d)	Porosity (dimensionless)
O	4 - 25	0.4 - 3	0.1 - 0.2
D	0.4 - 2.5	0.04 - 0.25	0.05 - 0.1
PSA	10^{-5} - 10^{-2}	10^{-6} - 10^{-3}	0.01 - 0.05
SA	10^{-7} - 10^{-3}	10^{-8} - 10^{-4}	0.001 - 0.01
CF	10^{-6} - 10^{-3}	10^{-7} - 10^{-4}	0.005 - 0.05
WP	10^{-5} - 10^{-2}	10^{-6} - 10^{-3}	0.01 - 0.05

Capacity -- The mine can accept approximately 86,000 metric tons of unreprocessed spent fuel assemblies. This translates to about 204,000 canisters containing either one assembly from a pressurized water reactor (PWR) or two from a boiling water reactor (BWR). The cylindrical canisters, which are 14 inches in diameter and 15 feet long, are to be placed in vertical holes drilled into the floor of the storage rooms. Total volume of excavated salt is 1.56×10^8 feet³.

Backfill -- After waste emplacement is completed, the mine is backfilled with crushed salt, leaving a residual porosity of 20 percent.

Waste Inventory

The EPA Standard requires that all radionuclides in the waste inventory (Table 1) be considered. However, we have found through experience that a subset of the inventory (Table 4) is most important to estimate compliance. Therefore, we will use this subset in this study.

The inventory listed in Table 4 is that of the full repository at the time it is sealed closed ($t = 0$). Although the inventory varies from canister to canister because of reactor type (BWR/PWR), we will assume that each canister contains a uniform fraction of the entire inventory: 4.9×10^{-6} , that is, 1/204,000.

Table 4

Radionuclide Inventories (Ci) at Time of Closure ($t = 0$)

<u>Radioisotope</u>	<u>Half-Life (years)</u>	<u>Ci at $t=0$</u>	<u>Radioisotope</u>	<u>Half-Life (years)</u>	<u>Ci at $t=0$</u>
252Cf	.265E1	9.5E-2	249Cf	.352E+03	9.93E-1
248Cm	.352E6	8.03E-2	245Cm	.827E+04	3.34E4
244Pu	.828E8	1.15E-8	241Pu	.146E+02	4.4E9
244Cm	.181E2	1.19E8	241Am	.433E+03	2.0E8
240U	.161E-2	0	237U	.185E-01	1.06E5
240Np(m)	.120E-3	0	237Np	.214E+07	4.04E4
240Pu	.676E4	4.61E7	233Pa	.750E-01	4.04E4
236U	.239E8	3.16E4	233U	.162E+06	7.96E0
236Pu	.285E1	9.70E2	229Th	.730E+04	1.55E-2
232Th	.141E11	3.22E-5	225Ra	.405E-01	1.55E-2
232U	.72E2	2.06E3	225Ac	.274E-01	1.54E-2
228Ra	.67E1	8.95E-6	221Fr	.913E-05	6.77E-3
228Ac	.699E-3	8.95E-6	217At	.101E-08	0
228Th	.191E1	2.05E3	213Bi	.894E-04	6.77E-3
224Ra	.997E-2	2.05E3	213Po	.133E-12	0
220Rn	.177E-5	2.05E3	209Tl	.418E-05	1.49E-4
216Po	.475E-8	0	209Pb	.376E-03	6.77E-3
212Pb	.121E-2	2.05E3	209Bi	Stable	---
212Bi	.115E-3	2.05E3			
212Po	.951E-14	0			
208Tl	.589E-5	7.38E2			
208Pb	Stable				

Table 4 (Continued)

Radionuclide Inventories (Ci) at Time of Closure (t = 0)

Radioisotope	Half-Life (years)	Ci at t=0	Radioisotope	Half-Life (years)	Ci at t=0
250Cf	.131E+02	1.54E0	251Cf	.900E+03	2.83E-2
246Cm	.471E+04	6.64E3	247Cm	.164E+08	2.51E-2
242Pu	.379E+06	1.30E5	243Pu	.568E-03	0
238U	.451E+10	3.03E4	243Am	.765E+04	1.73E6
238Pu	.890E+02	3.08E8	243Cm	.320E+02	2.42E5
234U	.247E+06	9.95E4	239Np	.643E-02	1.73E6
234Th	.660E-01	3.03E4	239Pu	.244E+05	3.19E7
234Pa	.22E-7	3.03E4	235U	.710E+09	1.6E3
230Th	.800E+05	1.68E1	231Th	.292E-02	1.6E3
226Ra	.160E+04	8.09E-2	231Pa	.325E+05	3.39
222Rn	.105E-01	3.08E-2	227Ac	.216E+02	1.44
218Po	.580E-05	3.68E-2	227Th	.498E-01	1.41
218At	.634E-07	0	223Fr	.418E-04	8.90
217Rn	.111E-08	0	223Ra	.312E-01	1.43
214Pb	.510E-04	3.68E-2	219At	.171E-05	0
214Bi	.375E-04	3.68E-2	219Rn	.127E-06	6.32E-1
214Po	.520E-11	0	215Bi	.133E-04	0
210Tl	.247E-05	0	215Po	.570E-10	0
210Pb	.210E+02	1.78E-2	215At	.317E-11	0
210Bi	.137E-01	8.21E-3	215At	.317E-11	6.32E-1
210Po	.378E+00	1.66E-2	211Pb	.686E-04	6.32E-1
206Hg	.154E-04	0	211Bi	.409E-05	0
206Tl	.796E-07	0	211Po	.165E-07	6.30E-1
206Pb	Stable	---	207Tl	.911E-05	6.30E-1
			207Pb	Stable	---

Table 4 (Continued)

Radionuclide Inventories (Ci) at Time of Closure (t = 0)

<u>Radioisotope</u>	<u>Half- Life (years)</u>	<u>Ci at t=0</u>
14C	5730.	4.83E4
90Sr	28.8	4.24E9
99Tc	2.14E5	1.31E6
126Sn	1.0E5	5.15E4
129I	1.6E7	2.98E3
135Cs	3.0E6	3.33E4
137Cs	30.	6.65E9

V. Radionuclide Release Scenarios and Probabilities

The three scenarios with radionuclide transport that we analyzed were groundwater transport, drilling into a canister, and brine pocket penetration.

In all cases, the sealed repository is violated either because mineshaft seals fail or because exploratory drill holes penetrate the underground engineered facility. Therefore, the draft EPA Standard requires that each radionuclide release have an associated probability assigned to it. Since all scenarios that we considered were caused by either the shaft seal failing or by drilling, we had to determine the likelihood that either would happen.

Since Unit WP has low hydraulic conductivity and groundwater flows through it extremely slowly -- inches per year -- we will ignore it as a source of groundwater or a migration path.

Wells sunk into Unit WP could shorten the path of radionuclides to the accessible environment. However, because of its tightness, salinity, and overlying units of greater transmissivity, we do not feel that wells are likely to be drilled into the lower units for the extraction of water. Also, the natural discharge location for the unit is farther than 100 miles away. With the groundwater moving at 1 mile/1,000 years (5.28 inches/year) it would take over 100,000 years for the radionuclides to escape. This time is much greater than the 10,000 year limit set by the draft EPA Standard.

We should note that the objective of this study is to choose and analyze a set of representative scenarios. As will be shown the scenarios chosen will indeed be important scenarios in the compliance assessment of the assumed repository. This is not to say that they are the only scenarios. A full scenario development, characterization, and analysis is beyond the scope of this work.

Probability of Seal Failure

Without a detailed study of the properties of sealing materials, we can only assume a non-mechanistic probability to their failure. Thus, we assume that:

$$\left. \begin{array}{l} \text{Probability of} \\ \text{shaft seal failure} \\ \text{at 1000 years} \end{array} \right\} = 0.001$$

For our calculations, we also assume that the shafts seal remains defective throughout the calculation, that is, it is not resealed.

Groundwater Transport Scenarios

In order that the units (O and D) overlying the back-filled repository be able to transport radionuclides, two hydraulic conduits are required between them. One allows water to enter and contact the canisters. The other carries contaminated water back to the geologic units. The two conduits and the repository would thus form a U-shaped path, called a U-tube (Figure 8).

The vertical conduits could be formed along former mine shafts leading to the repository whose seals had failed. Another possibility would be inadvertent penetration by exploratory drill holes made by future generations seeking petrochemicals or evaporite minerals.

In Figure 8, the conduit to the left is either a mine shaft whose seal has failed, or a borehole. The one to the right is a borehole. Water is driven through the U-tube by the head difference between the vertical conduits and the units overlying the repository. The difference is caused by the water flowing horizontally through Units O and D.

Below, we analyze two variations of the characteristics of the overlying aquifer. In one we assume that Unit O is nearly saturated and that the vertical legs of Figure 8 connect with it. Water and radionuclides flow from the backfilled regions back into Unit O. Once there, the radionuclides are transported through the unit.

In the other variation, we assume that Unit O has been depleted, say for irrigation. Unit D is then the migration path for radionuclides, although more slowly because of its lower conductivity.

Probability of U-Tube Formation -- To determine the likelihood that a borehole will intrude into the repository, we first assume that the drilling rate into the 3,000-acre tract is 1.9×10^{-3} /year. This rate is relatively low for drilling into strata containing bedded salt [4]. However, it is a reasonable value considering the thermal maturity of the strata, discussed previously in the description of the report. The floor space of engineered facility covers a smaller area than that of its gross extent, typically

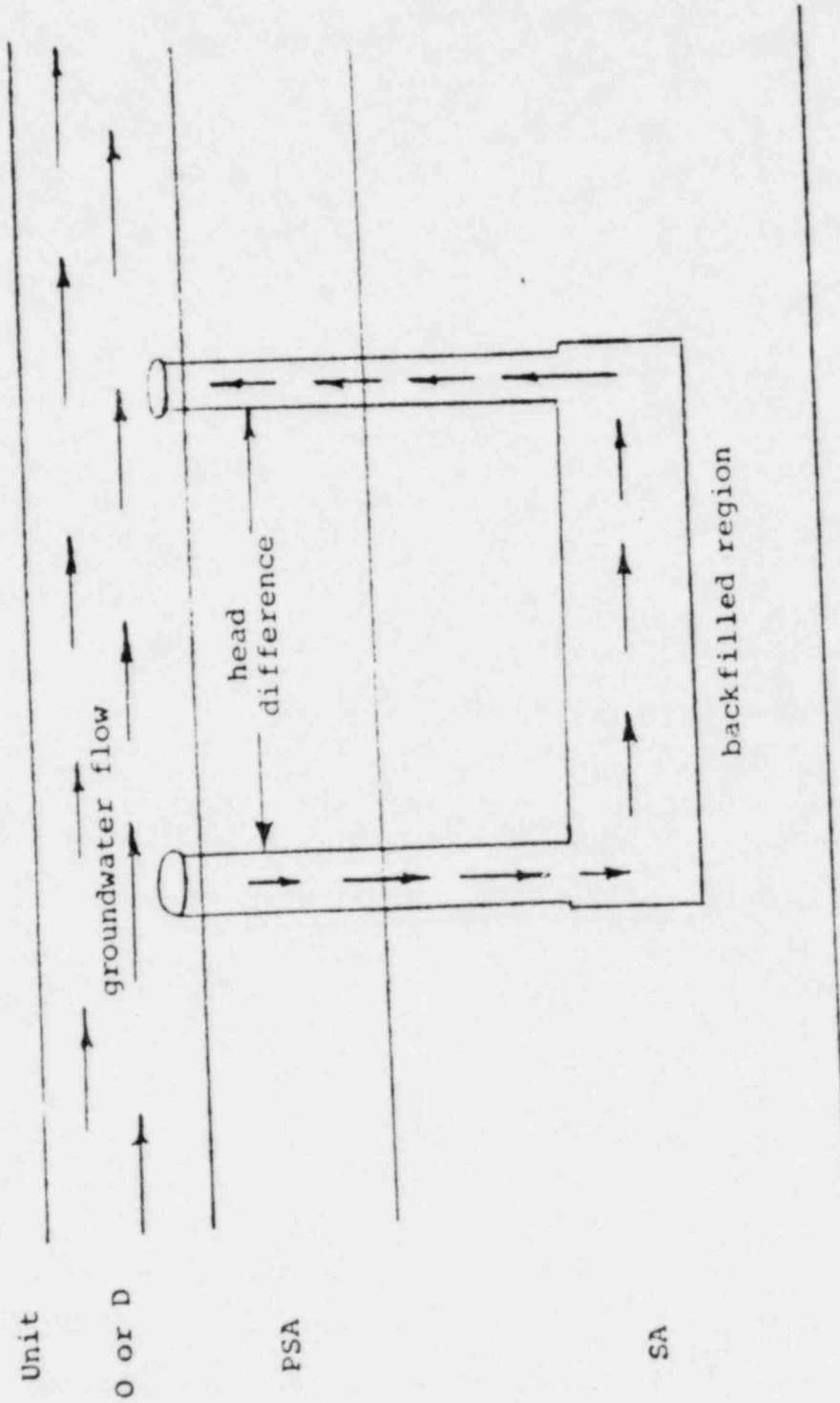


Figure 8. The U-Tube Flow and Migration Pattern for the Groundwater Transport Scenario.

25 percent or less. In the assumed design this fraction is less than 10 percent [8-10]. For the calculations presented in this report, we assumed this fraction to be about 15 percent so that the number of boreholes expected to penetrate the backfilled regions in 10,000 years is:

$$19 * 15\% \approx 3.$$

We can thus assume that three boreholes are expected to penetrate the backfilled regions during the 10,000 year period.

However, other factors enter the picture. If water is to flow through a U-tube, there must be enough driving head. For example, in the case where water originates in Unit 0 and returns loaded with radionuclides, there is a minimum distance that must separate the vertical legs of the U-tube. This distance is determined by applying the DNET Model [12]. The water in the U-tube's entry leg is fresh until it comes into contact with the salt. Therefore, the exit leg contains saturated brine, which is heavier. Given the hydraulic gradient of Unit 0, the minimum down-dip separation calculates as 11,500 feet.

In the case where water originates from and returns to Unit D, both vertical legs are filled with brine. Therefore, there is no difference in their weights and two or more holes, regardless of separation, may form a successful U-tube, as long as both penetrate the backfilled regions.

To implement all our assumptions, we further assume that exploratory drilling is a Poisson process with a distribution on the number of boreholes into the 450-acre (15 percent of 3,000) target area given by

$$P(N) = \frac{(\lambda T)^N e^{-\lambda T}}{N!}, \quad (5)$$

where: $\lambda T = 3.$

In the Unit 0 case, where we require a minimum distance of 11,500 feet, we must adjust the value of λT . The adjustment needed is a scaling of the value of λT by the ratio of the target area to 3,000 acres.

We will consider four variations on the U-tube scenario. In two of the variations, the Unit 0 will be assumed to transport the radionuclides. In the other two, Unit D will be assumed to transport the radionuclides. For each of the assumed major transporting units, two types of vertical conduits (Figure 8) will be considered. In all U-tube scenarios analyzed, the vertical conduit at the right in Figure 8 will be assumed to be formed by one or more boreholes. The conduit at the left of Figure 8 will be assumed to be one or more failed shaft seals, in one case, and one or more boreholes in the other. In the discussion that follows, probabilities for these scenarios will be given. In order to describe the hydraulic properties of the vertical legs, conditional probabilities will also be needed to describe the number of boreholes that may occur. These will also be given in the following discussion.

Scenario I -- Water originates in and returns to Unit 0. The entrance leg is a shaft whose seal has failed and the exit leg is one or more boreholes. Both legs are separated by at least 11,500 feet. The size of the target area (Figure 7) is approximately

$$\text{Area} = (17,000 - 11,500) \times 8,600 \text{ feet}^2 = 1,086 \text{ acres.}$$

Thus, we scale λT appropriately to get $(\lambda T)'$:

$$(\lambda T)' = \lambda T \frac{1,086 \text{ Acres}}{3,000 \text{ Acres}} = 1.09 \quad (6)$$

Using Equation (5), $P(0) = 0.34$ and the probability of one or more holes penetrating the target is

$$P_{\geq 1} = 1 - 0.34 = 0.66.$$

Therefore, the probability that Scenario I will occur is

$$P_1 = P_{\text{shaft}} * P_{\geq 1} = 0.001 * 0.66 = 0.00066. \quad (7)$$

We can now use Equation (5) to generate a conditional probability distribution on the number of boreholes in the 1,086 x 15 percent target area, $P_c(n)$, which will be needed for computing:

n	1	2	3	4	5	6	7	≥ 8
$P_c(n)$	0.56	0.30	0.11	0.03	0.01	0.0011	1.7×10^{-4}	nil

Scenario II -- Water originates from and returns to Unit 0. Both legs of the U-tube are two or more boreholes separated by at least 11,500 feet. Since any two boreholes separated by that distance can form a successful U-tube, we need a convolution of probabilities of boreholes in differential target areas at greater than minimum separation. To avoid this complicated computation, we present a simplified treatment to estimate the number of boreholes, ignoring the 2,000-foot-long "panhandle" of the repository since no waste is stored there (Figure 9).

The two 2,700 foot sections at each end of the repository are targets for the boreholes forming a U-tube with those at the opposite end. The size of each target area is thus 2,700 feet x 8,600 feet = 533 acres. Therefore, adjusting λT gives us

$$(\lambda T)' = \lambda T \cdot \frac{533}{3000} = 0.53. \quad (8)$$

The probability that there will be no boreholes in a target area that is 15 percent of 533 acres is 0.59 [Equation (5)], so that the probability of more than one boreholes at each end is

$$P_2 = (1 - .59)^2 = 0.17. \quad (9)$$

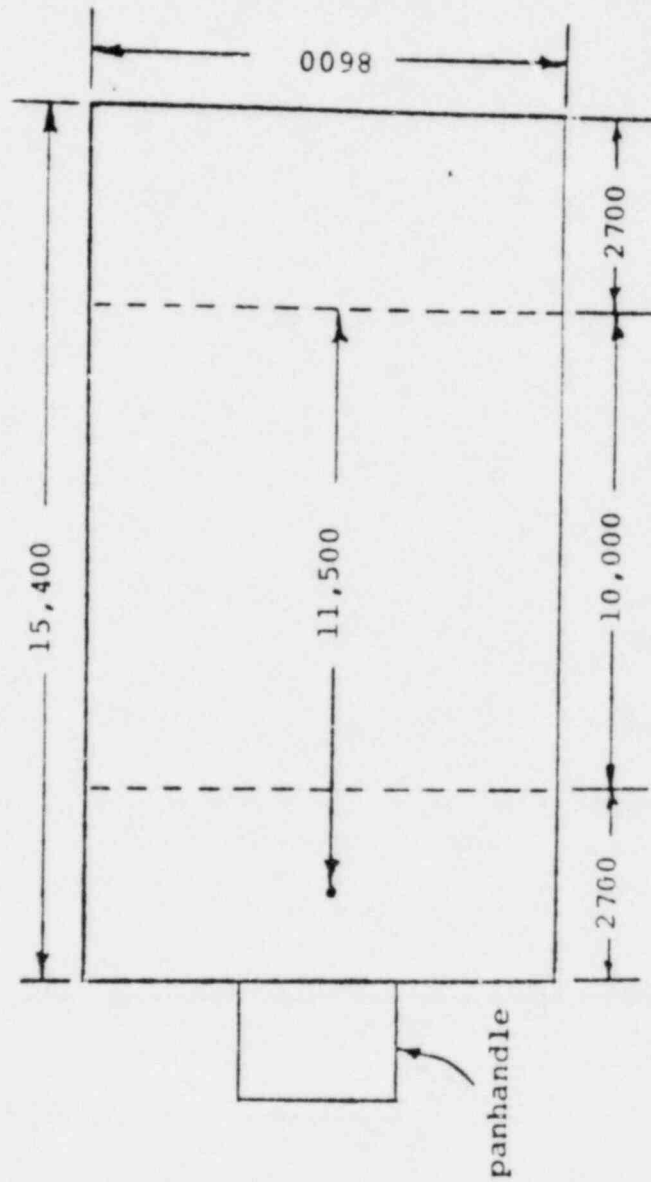


Figure 9. Scenario II geometry.

However, in order to perform our calculations, we need the distribution of the number of boreholes. This number can be generated from Equation (5) to give us a conditional probability distribution of boreholes in each target area:

n	1	2	3	4	5	6	<u>≥ 7</u>
P _C (n)	.7549	.2031	.0364	.0049	.0005	.00005	nil

Scenario III -- Water originates in and returns to Unit D. One leg of the U-tube is a shaft whose seal has failed and the other is one or more boreholes at any distance, not exceeding the size of the backfilled regions. We use the same calculations as for Scenarios I and II. However, we do not adjust for target area and use instead $\lambda T = 3$. Using Equation (5), we calculate the probability of one or more boreholes penetrating the target area as $P_{>1} = 0.95$ so that the probability of this scenario occurring is:

$$P_3 = P_{\text{shaft}} * P_{>1} = 0.001 * 0.95 = 0.00095. \quad (10)$$

Thus, the conditional probability distribution on the number of boreholes is:

n	P _C (n)	n	P _C (n)
1	0.16	6	0.05
2	0.24	7	0.02
3	0.24	8	0.01
4	0.18	9	0.003
5	0.11	10	0.001
		<u>≥ 11</u>	nil.

Scenario IV -- Water originates in and returns to Unit D. Both legs of the U-tube are boreholes with no minimum separation. No adjustment of λT is needed and we use $\lambda T = 3$. By using Equation (5), we calculate the probability of two or more boreholes penetrating the target area as $P_{>2} = 0.80 \equiv P_4$. The conditional probability of distribution is

n	P _C (n)	n	P _C (n)
2	0.28	7	0.03
3	0.28	8	0.01
4	0.21	9	0.003
5	0.13	10	0.001
6	0.06	<u>≥ 11</u>	nil.

Since we can not assume Unit C to be both saturated and depleted, we assume each of these possibilities to be equally probable. This translates to an additional 1/2 on the probabilities above. Also, we treat only one scenario at a time. For example, we do not consider a U-tube formed by a failed shaft seal which, after subsequent drilling, becomes a U-tube with boreholes providing additional water conduits. Thus, the shaft seal failures compete with boreholes for U-tube formation. Including the factors of 1/2 for Unit O vs Unit D scenarios, we calculate probabilities for the mutually exclusive scenarios, P',

$$P_1' = 1/2 P_1 (1 - 1/2 P_2)$$

$$P_2' = 1/2 P_2 (1 - 1/2 P_1)$$

$$P_3' = 1/2 P_3 (1 - 1/2 P_4)$$

$$P_4' = 1/2 P_4 (1 - 1/2 P_3)$$

In summary, the probability assigned to each scenario, pi', is:

Scenario	Pi	Pi'
1	.00066	.00030
2	.17	.0850
3	.00095	.00029
4	.80	.40

Disinterment

Scenario 1: The canister "direct hit."

In this disinterment scenario, the radionuclides move to the surface directly and rapidly. While sinking a borehole, possibly while exploring for minerals, the drill bit strikes a waste canister and brings a fraction of the contents to the surface.

In the scenarios previously described, we determine that in 10,000 years, 19 boreholes would have been expected over the 3,000 acre site. The same probability applies to

this disinterment scenario. Each borehole will have a fixed probability of making a "direct hit" on a canister. The probability is determined by comparing the area of the waste canisters with that of the facility.

Since there are 204,000 canisters, each with an end area of 1.15 foot², any drill bit penetrating the back-filled repository has a probability of hitting a canister of

$$P_{hit} = \frac{2.04 \times 10^5 \text{ canisters} \times 1.15 \text{ foot}^2/\text{canister}}{15,370 \text{ feet} \times 86,000 \text{ feet}} \quad (11)$$

$$= 1.2 \times 10^{-3}$$

For n boreholes, the probability of N direct hits will be given by a binomial distribution,

$$P(N,n) = \frac{n!}{N! (n-N)!} P_{hit}^N (1-P_{hit})^{n-N} \quad 0 \leq N \leq n. \quad (12)$$

Thus, the probability of N hits is:

$$P(N) = \sum_{n=1}^N p(n) \cdot P(N,n) \quad (13)$$

$$= \sum_n \frac{(\lambda T)^n e^{-\lambda T}}{n!} \cdot \frac{n!}{N!(n-N)!} P_{hit}^N (1 - P_{hit})^{n-N}$$

where $\lambda T = 19$

$$P_{hit} = 1.2E-3$$

A more detailed analysis of this scenario might include the spatial extent of the drill bit, the drilling direction, and the distribution of wastes within the canister.

Scenario 2: Brine-pocket penetration

We have not had time during this study to analyze this scenario in detail. However, it has been suggested as a potentially important scenario to be considered when analyzing risks from nuclear waste disposal [13]. The suggestion is that for an actual repository site, approximately 1 borehole in 25 will hit a brine pocket. Therefore, we use this number with some other assumptions to describe this scenario.

We use the probabilistic expression of Equation (13) because conceptually, the disinterment scenario is the same as that of the brine pocket penetration (Figure 10), the brine pocket now being the target, rather than the canister. Therefore, we have to develop an expression for P_{hit} .

As indicated in Figure 10, we assume that M brine pockets exist below the horizon of the subsurface facility, with an area, A_m . Each brine pocket is spherical with a cross-sectional area, a , projecting to the surface. We assume that the ratio of total brine pocket area, $M \cdot a$, to A_m is a constant, α ,

$$M \cdot a = \alpha A_m.$$

The constant, α , then gives the probability that a random drill bit will penetrate a brine pocket. The value of $\alpha = 1/25$ was given with no mention of the thickness of the salt layer [13]. However, since we are concerned only with the lower half of the salt layer, we will assume that

$$\alpha = 0.02$$

This value will be used for P_{hit} in Equation (13) to evaluate this scenario.

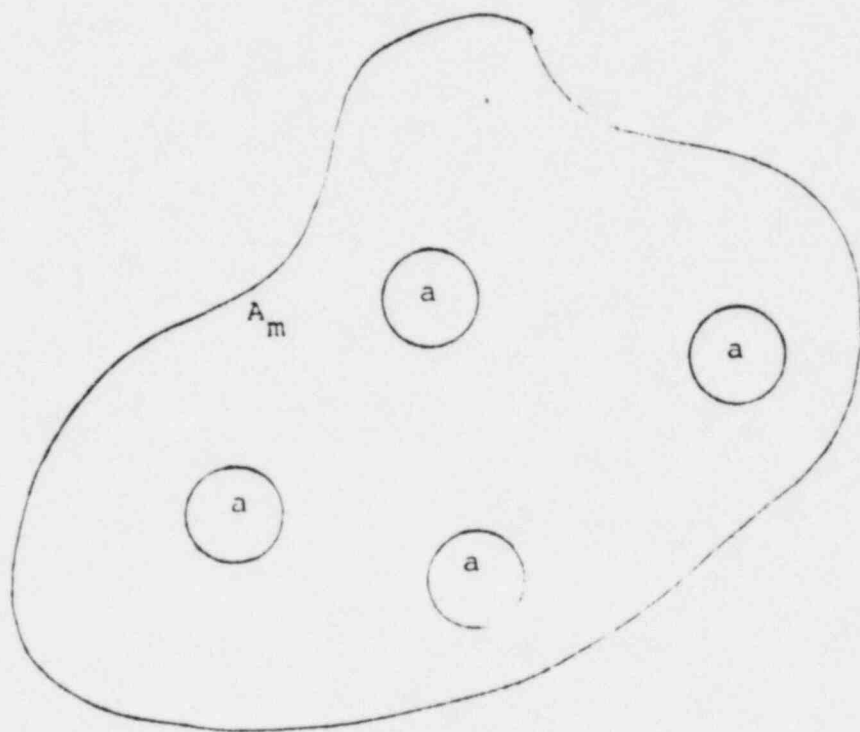


Figure 10. Reference Area, A_m , Containing M Spherical Brine Pockets. Each brine pocket has a projected area, a , at the surface.

VI. Computer Models (NWFT/DVM) Used for Groundwater Transport Scenarios

We used different models to estimate discharges expected from the various scenarios. For groundwater transport (U-tube) scenarios, we used the NWFT/DVM [14] model developed at SNL for the NRC. For the disinterment scenarios, we used more simplistic models.

A. The Groundwater Transport Scenarios NWFT/DVM

This model is used to calculate time-dependent discharge rates of radionuclides into the accessible environment for the four groundwater transport scenarios. Figure 11 shows the simple network of points and distances used in the calculations. In the figure, " l " indicates the length between junctions at elevations, " d ," and " p " is the hydraulic pressure of the aquifer.

The upper horizontal legs represent the overlying aquifer, either Unit O or Unit D, the vertical legs represent the borehole(s) or failed shaft, and the lower horizontal leg represents the backfilled region.

The numerical values assigned to the l 's and d 's vary from scenario to scenario. These values are presented in Table 5. Note that we have consistently assumed the maximum lateral separation between the vertical legs for simplicity. This is most important for Scenarios 3 and 4 since the vertical legs can be much closer. This assumption will generally tend to overestimate groundwater and radionuclide flow velocities in legs #5 and #6. This assumption is of little consequence until the actual vertical leg separation becomes so small that a significant fraction of the migration time is represented by transport through legs #5 and #6.

The cross-sectional area of the U-tube legs (l_4 , l_5 , and l_6) depends on whether the legs are mineshafts (2,000 feet²) or boreholes (0.8 foot²/hole). We also assume that the inlet and outlet pressures (p_1 and p_4) are zero since the aquifers are unconfined.

We used the Latin Hypercube Sampling Method [15] to select input data for flow and transport calculations (Table 6). For example, to calculate discharges in each

Table 5

Lengths and Elevations, l_j ; and d_j , Corresponding to Figure 10 for the Groundwater Transport Scenarios.

Index, i :	1	2	3	4	5	6	
Lengths	lengths, l_j (feet)						
Groundwater transport scenario	I	100,000	17,370	5,280	2,000	1,878	17,370
	II	102,000	15,370	5,280	1,986	1,878	15,370
	III	100,000	17,370	5,280	1,500	1,378	17,370
	IV	102,000	15,370	5,280	1,486	1,378	15,370
	Elevations, d_j (feet)						
Groundwater transport scenario	I	859	159	37	0	-1,841	-1,841
	II	859	145	37	0	-1,841	-1,841
	III	359	-341	-463	-500	-1,841	-1,841
	IV	359	-355	-463	-500	-1,841	-1,841

Table 6

Hydraulic Properties

Conductivities are assumed to be lognormally distributed. Porosities are assumed to be normally distributed. The given ranges specify the 0.001 and 0.999 quantiles of the assumed distributions.

<u>Property</u>	<u>0.001 Quantile</u>	<u>0.999 Quantile</u>
1. Hydraulic Conductivity (ft/day) of Unit 0	0.15	680.
2. Porosity of Unit 0	0.1	0.2
3. Hydraulic Conductivity (ft/day) of Unit D	0.015	68
4. Porosity of Unit D	0.05	0.1
5. Hydraulic Conductivity (ft/day) of Failed Shaft	0.05	50.0
6. Porosity of Failed Shaft	0.05	0.5
7. Hydraulic Conductivity (ft/day) of Boreholes	0.05	25.0
8. Porosity of Boreholes	0.05	0.5

groundwater transport scenario, we chose 50 combinations of input data (vectors) from the distributions in the table. We repeated this procedure three times so as to observe the effects of sampling error on the calculated discharges.

In order to avoid physically unreasonable combinations of porosity and hydraulic conductivity, we assumed a rank correlation of 0.7 when sampling these parameters for any feature [15]. Leg 6 is the backfilled repository, which is a hydraulic "short circuit" between legs 4 and 5 and has a hydraulic conductivity of 10^6 feet/day.

Model NWFT/DVM also requires that we assign a value to cross-sectional area of this "short circuit." Depending on the source model (see below), we assigned an end-view, cross-sectional area of 1.3×10^5 ft² if the entire waste inventory is available to access by groundwater. If the available fraction is proportional to the number of boreholes, the cross-sectional area can be deduced by the number of boreholes multiplied by the cross-sectional area of the penetrated storage room: 262.5 ft². Actually, since leg 6 is a "short-circuit" anyway, these assignments are of little practical value, but are assigned because the model requires them.

We have neglected dispersivity from our NWFT/DVM calculations. We feel this is justified since the dispersivity is small for the assumed repository. More importantly, the effect of dispersivity is to make the leading edge of the discharge curve more diffuse. Since we are calculating time-integrated discharges, we expect little error from the neglect of dispersion. The error is largest when integration begins or ends during the diffuse part of the discharge. The effect is to assign a portion of the discharge to the adjacent 10,000-year period.

In our calculations, we have assumed three models for NWFT/DVM, each describing a different source of nuclide release (Table 7). We did not perform detailed modeling of each source; the sources are simply assumptions chosen to demonstrate their efficacy.

Source #1 -- This source exceeds the minimum release rate required by NRC [10CFR60(2)], that is, 10^{-5} /year of the entire radionuclide inventory shown in Table 4. We have assumed that the inventory is homogeneously dispersed throughout the wastefrom so that if $N_i(t)$ denotes the i th radionuclide in the inventory at time, t , in the absence

of release, the release rate of that radionuclide is $(10^{-5}$ to $10^{-7}) \times N_i(t)$. We assume that the entire waste inventory is available for transport.

Source #2 -- This source resembles Source #1 in release rate, but the amount of waste available for transport is reduced. Each borehole allows only that waste in the particular backfilled storage room that it penetrates to be available for transport. This model would be valid if we assumed that flow through the backfilled regions would be localized to the vicinity of the borehole (there are 106 storage rooms).

Source #3 -- This source resembles Source #2 but allows the backfilled rooms to be modeled as a mixing cell where wasteforms are leached uniformly (Appendix A). The range of leach limits has been changed to allow a more rapid rate in the breakdown of wasteforms. The calculated discharges thus show how a less stable wasteform can be compensated if mixing mechanisms can be assumed. We also allow solubility limits to apply to radionuclide concentrations in the mixing cell.

Geochemical Data

We assume that retardation of radionuclides occur only in the aquifer units (O and D) of the transport path. The retardation factor, R, is thus given by

$$R = 1 + \rho K_d \frac{(1-\phi)}{\phi} \quad (14)$$

where

ρ = the assumed rock density (2.7 g/cm³)

ϕ = the unit's porosity (see Table 6)

K_d = the sorption equilibrium constant (Table 8)

Table 7

NWFT/DVM Source Models

Model Number	Source Type	Amount of Inventory Available for Access	Leaching (Release) Range (yr ⁻¹)	Leach Distribution
1	Leach Limited	1.00	10 ⁻⁵ to 10 ⁻⁷	Log Uniform
2	Leach Limited	$\frac{\# \text{ of boreholes}}{106^*}$	10 ⁻⁵ to 10 ⁻⁷	Log Uniform
3	Mixing Cell	$\frac{\# \text{ of boreholes}}{106}$	10 ⁻³ to 10 ⁻⁷	Log Uniform

*106 denotes the number of storage rooms in the repository

Table 8

 K_d - Assumptions

Element	percentiles of assumed lognormal distribution	
	0.001	0.999
Cm	10^2	10^5
Am	50	10^4
Pu	30	10^4
Np	2	400
U	.01	270
Th	10^3	10^5
Ac	10^2	10^5
Pb	100	500
Ra	100	500
Pa	0.01	10^4
Sr	1.0	2000
Cs	0.01	3000
I	0.01	100
Sn	0.01	500
Tc	0.01	3

^{14}C is assumed to be completely unretarded, ie. $K_d=0$.

The LHS method is also used to select values from the distributions for each input vector according to the distributions given in Table 8. Data appearing in Table 8 are taken from Reference 16 and supplemental information from the open literature.

Solubility limits are needed for Source #3 to treat concentration limits on each radionuclide. These data are presented in Table 9. Elements not appearing in Table 9 are assumed to have unlimited solubility.

Table 9

Solubility Limits (gm/gm)

The given ranges specify the 0.001 and 0.999 quantiles of an assumed lognormal distribution.

<u>Element</u>	<u>quantile</u>	
	0.001	0.999
Pu	1.6E-16	4.0E-4
U	1.6E-8	3.0E-2
Th	1.1E-9	5.8E-6
Ra	7.9E-12	1.3E-5
Np	1.3E-25	5.0E-7
Pb	2.5E-11	4.0E-5
Pa	1.4E-7	7.2E-4
Sn	6.3E-17	1.6E-4
Tc	1.9E-9	9.5E-5
Sr	2.2E-6	2.8E-3

B. Disinterment Scenarios

The disinterment scenarios are different enough from our usual analyses so that the manner in which we evaluated their consequences is discussed here. For each, the consequence of the scenario depends on the time of its occurrence and each consequence depends on the inventory at the time of penetration.

As a measure of the time-dependent consequence, Table 10 shows the hazard represented by the waste inventory in terms of EPA release limits. We obtained the table by evaluating Equation (1) for the entire inventory.

Table 10
Repository Hazard Index

Time (yr)	EPA Sum (Eq. (1))
1,000	8.3E7
1,500	4.3E6
2,000	2.5E6
5,000	8.9E5
10,000	6.4E5

In the direct hit scenario, for example, to use Table 10 to find the hazard on a per-canister basis, divide its value in the second column by 204,000 (the number of canisters). The disinterment scenarios have been described in terms of the number of boreholes expected to cause them, independent of when these boreholes occur. Since the consequences are time dependent, it is essential for consequence evaluation that a time of occurrence be assumed. The assumption made is that the N boreholes considered occur uniformly over the period of interest. For the "direct hit" scenario, the period is the 9900 years following loss of administrative control after 100 years. For the brine-pocket scenario, the period is the 9000 years following containment lifetime (1000 years) when all waste packages are assumed to fail simultaneously and completely. Thus, for N boreholes causing the scenarios, each is assumed to occur at a time, t_j , where

$$t_j = \begin{cases} \frac{9900}{N} \left(j - \frac{1}{2} \right) + 100 & \text{"direct hit"} \\ \frac{9000}{N} \left(j - \frac{1}{2} \right) + 1000 & \text{brine pocket} \end{cases} \quad (15)$$

In the "direct hit", we assume that a fraction, f_0 , of the canister contents are removed with:

$$f_0 = 1/4$$

Thus, a 1-borehole, direct hit occurs at 5150 years with a consequence (Table 10) of approximately,

$$C(1) \text{ direct hit} = 1/4 \cdot \frac{8.9 \times 10^5}{204,000} = 1.1 \quad (16)$$

For the brine pocket scenario, we assume the pressure in the pocket is relieved by expelling a fraction of its volume. This brine flows up the borehole into a backfilled room. We assume that the backfilled rooms have become resaturated before the waste packages fail at 1000 years. When the waste package fails, its contents are assumed to be released uniformly to the entire volume of water in the backfilled regions, at a constant rate over a period, τ . Thus, at time t_j the fraction of wastes that have been released is f_1 :

$$f_1 = \frac{t_j - 1000}{\tau}$$

We assume that the brine flow will be of short duration and will remove only those radionuclides in the water volume in the immediate vicinity of the borehole. No modeling was used to test this assumption. We assumed 1/40 of the water in the backfilled room is mixed with the flowing brine and released to the accessible environment. This choice corresponds to the water volume contained in a 100 foot length (50 feet either way from the borehole) of the 4,000 foot long room.

The consequence from this scenario is obtained by evaluating Equation 1 (through interpolation of Table 10) with the assumptions made,

$$C(N)_{\text{brine pocket}} = \sum_{j=1}^N \left(\frac{1}{40} \right) \left(\frac{t_j - 1000}{\tau} \right) \left(\frac{\text{Table 10}(t_j)}{106} \right) \quad (17)$$

We will assume $\tau = 100,000$ years. For example, a one-brine pocket scenario occurs at $t_j = 5,500$ years and has a consequence of approximately,

$$C(1)_{\text{brine pocket}} = \frac{1}{40} \left(\frac{4500}{100000} \right) \left(\frac{8.9 \times 10^5}{106} \right) = 9.45$$

Since both disinterment scenarios involve a relatively small fraction of the waste inventory, we do not consider them as competing with the groundwater transport scenarios. The boreholes that cause them, however, may also contribute to the U-tube formation. We have neglected the small perturbation the disinterment scenarios may have on the consequence of the groundwater transport scenarios.

C. Construction of the CCDFs

As we stated previously, assessing compliance with the draft EPA Standard should combine all scenarios to produce a final CCDF. For the scenarios analyzed, it is more illuminating to examine them individually. We will first present the disinterment scenarios followed by the groundwater transport scenarios. CCDFs for the groundwater transport scenarios have been constructed for each of the three source models described previously.

Disinterment Scenario 1: The "Direct Hit"

Equation (13) was evaluated to give probabilities, $P(N)$, of the N hit scenario. Equation (15) gives the time, t_j , for each of the N direct hits. Values from Table 10 were interpolated at t_j to give values of the EPA Sum, as illustrated in Equation (16). These results are presented in Table 11 and Figure 12. As can be seen in Figure 12, this scenario alone is enough to violate the draft EPA Standard.

Table 11

Probabilities (per 10,000 yr) and Consequences
for the "Direct Hit" Scenario*

N	P(N)	Consequence (EPA Sum)
0	.982	0
1	1.95E-2	1.09
2	2.04E-4	1.88
3	1.40E-6	2.65
4	7.08E-9	3.45

*Contributions with probabilities of less than 10^{-4} need not be considered.

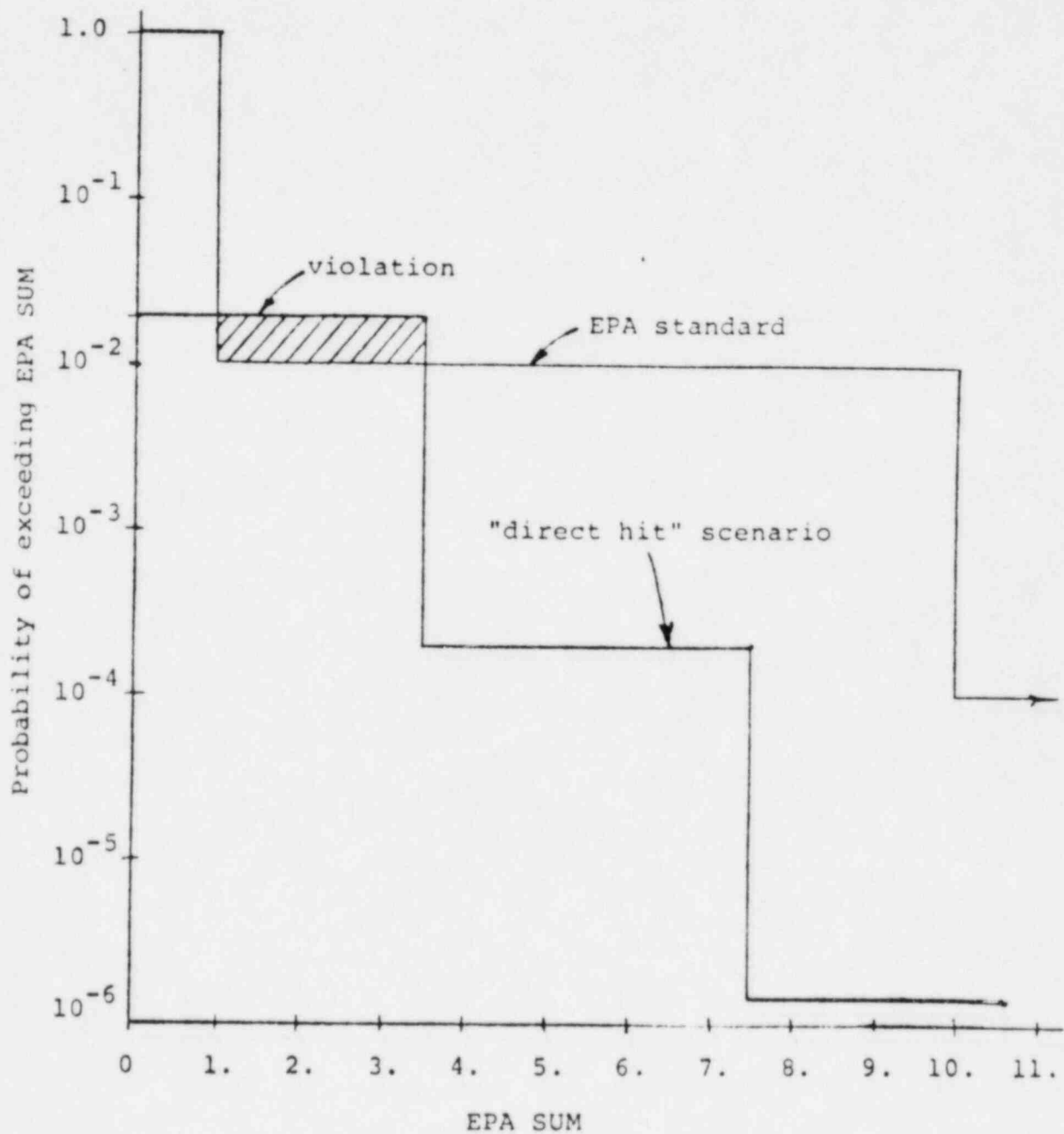


Figure 12. CCDF for Disinterment Scenario 1: The Direct Hit. The Shaded Area Indicates Violation of the Draft EPA Standard.

Brine-Pocket Penetration Scenario

Equation (13) was evaluated with $P_{hit} = .02$ probabilities, $P(N)$, of N brine pocket penetrations that release radionuclides. Equation (15) was used to evaluate t_j and the EPA Sum was evaluated according to Equation (17). Table 10 values were interpolated to give values at t_j . These results are tabulated in Table 11 and the resulting CCDF is presented in Figure 13. As can be seen from Figure 13, this scenario alone is enough to violate the draft EPA Standard.

Groundwater Transport Scenarios

We evaluated the groundwater transport scenarios for three source term assumptions discussed previously:

- Source #1: fractional release of 10^{-5} to 10^{-7} /year of entire inventory,
- Source #2: fractional release of 10^{-5} to 10^{-7} /year of a fraction of the inventory, that is given by considering the number of boreholes and assigning one roomful of waste to each borehole,
- Source #3: fractional release rate from the waste form of 10^{-3} to 10^{-7} with the same waste fraction assumption of Source #2. In addition we considered solubility limits and mixing assumed in the backfilled regions (Appendix A). This is the standard SNL source model assumption.

In addition, for these scenarios, we sampled the variables required for the analysis from the ranges given in Tables 6, 7, 8, and 9 by the LHS technique [15]. We chose 50 combinations of input and calculated an EPA Sum (Equation 1) for each. Also, we chose three independent samples to estimate the effects of sampling error.

We calculated radionuclide discharge rates for 50,000 years following waste emplacement. We intergrated these discharge rates over each of five 10,000 year periods and evaluated Equation (1). Thus, we calculated a CCDF for each of the five 10,000 year periods for each of the three independent samples and for each of the source term assumptions. When appropriate room number and release rates were also sampled. Figures, 14, 15, and 16 give the resulting CCDF's.

Table 12

Probabilities and Consequences
for the Brine Pocket Scenario

N	P(N)	Consequence (EPA Sum)
0	.942	0
1	.0565	9.21
2	.0017	24.0
3	3.39E-5	38.0

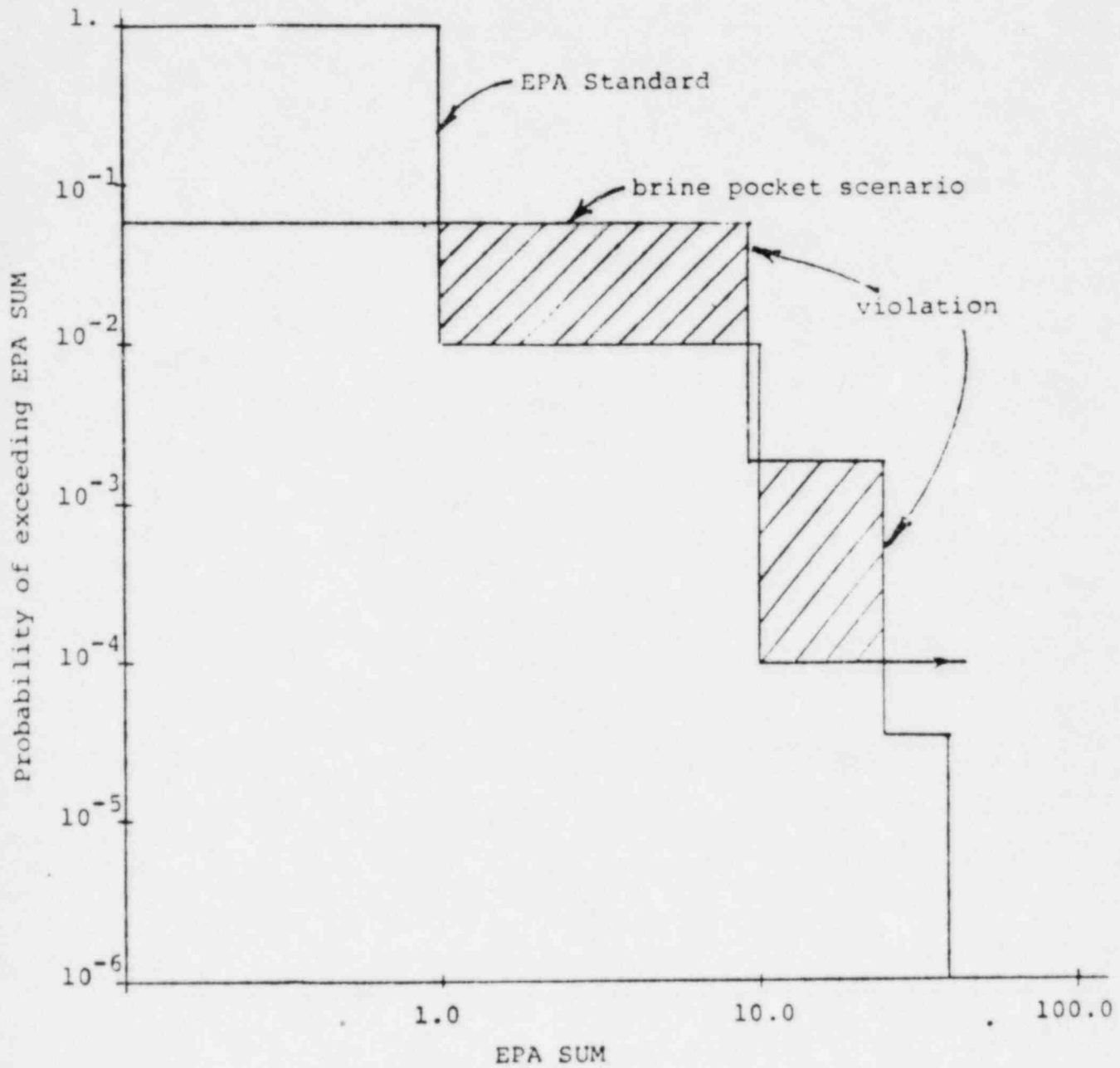


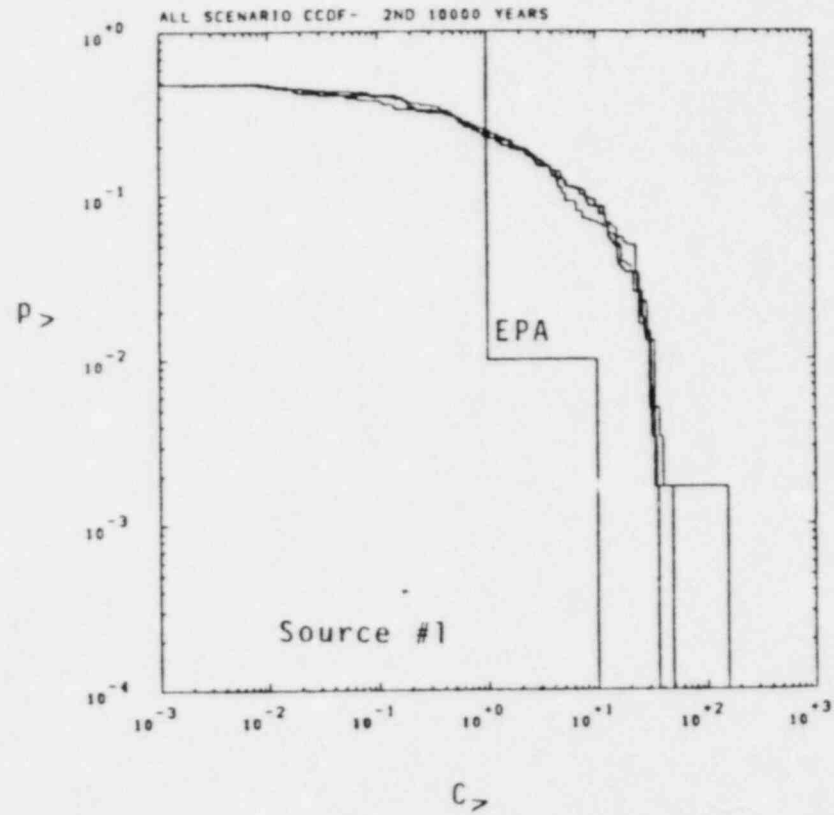
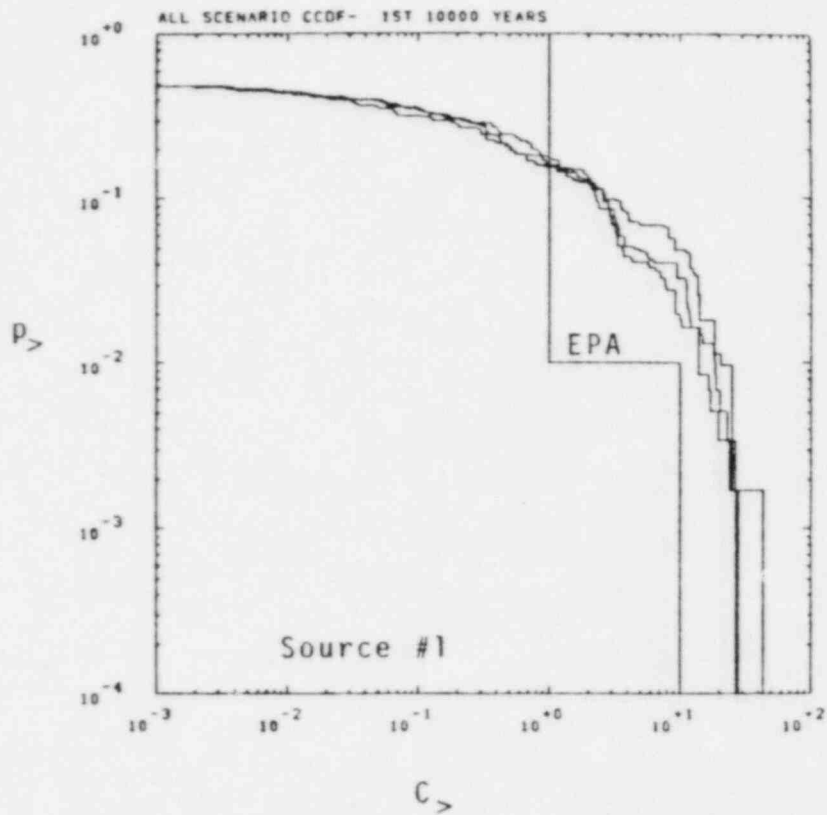
Figure 13. CCDF for the Brine Pocket Penetration Scenario. The Shaded Areas Indicate Violation of the Draft EPA Standard.

The three traces shown in each figure result from evaluation with the three independent samples. The vertical spread in these plots represents an estimate of sampling error associated with the LHS method. As can be seen, the sampling error is small over most of the curve.

All scenarios evaluated with Source #1, (Figure 14) yield large discharges. The results of these calculations indicate violation of the draft EPA Standard in each of the five 10,000 year periods.

The scenarios evaluated with Source #2 (Figure 15) yield less discharged, indicating that compliance may be achieved during the first 10,000 year period. The results indicate that the standard is violated in the other periods, although the magnitude of the violation is smaller. The results of the disinterment and brine-pocket scenarios should also be considered during the first 10,000 years.

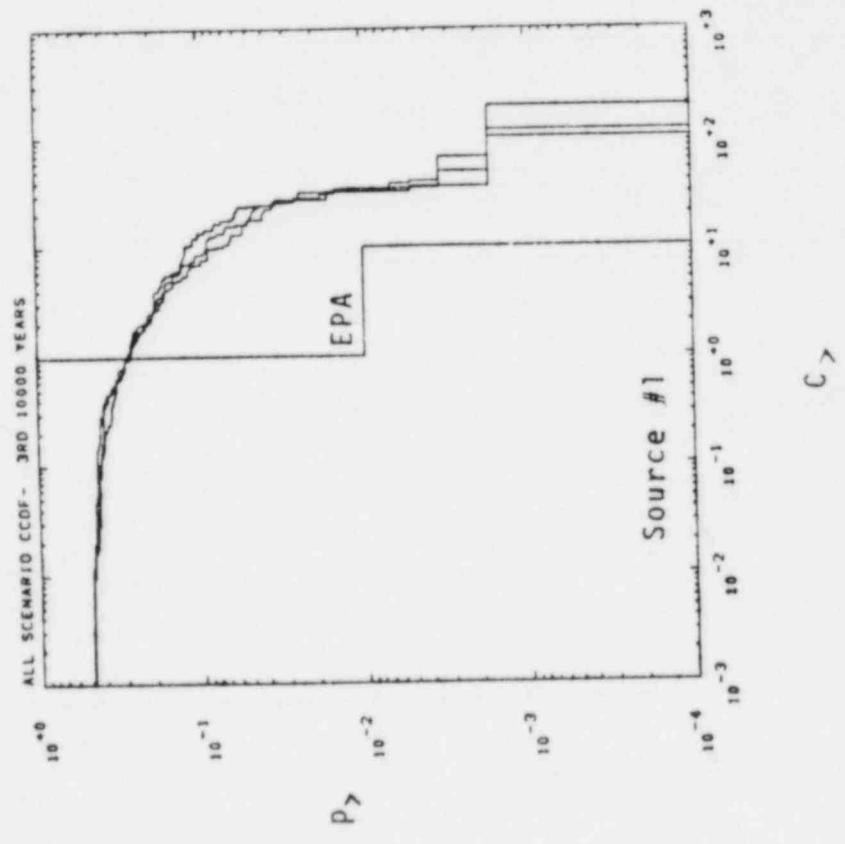
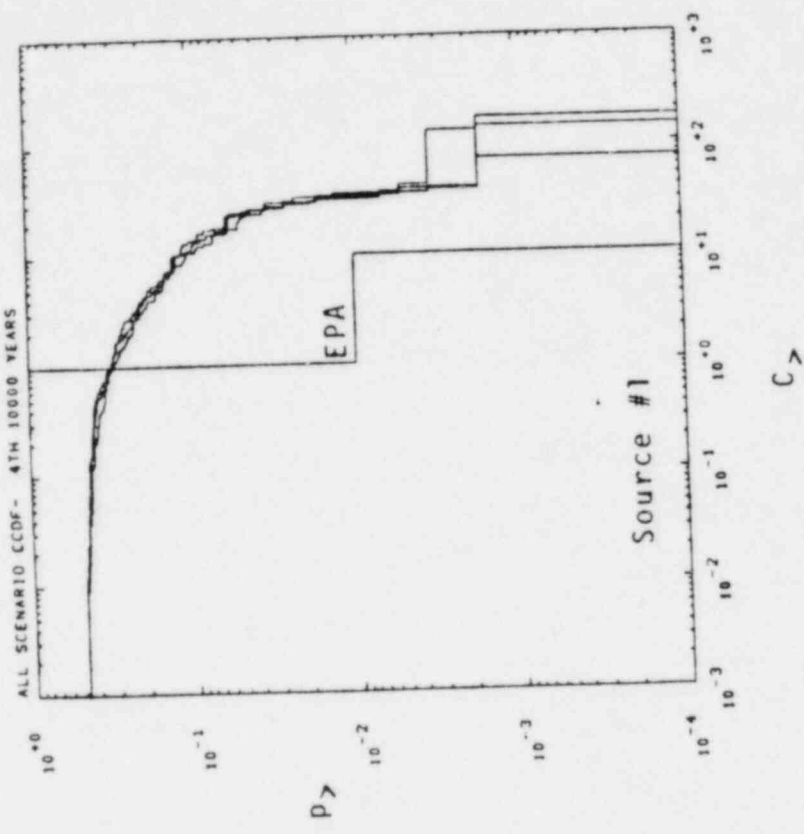
All scenarios evaluated with Source #3 indicate compliance may be achieved if the mixing cell assumption can be justified. As shown in Appendix A, the release rate with this type of source assumption should asymptotically approach that given by the waste form description alone (Table 7). Since we have assumed a less stable waste form, we can infer that the time required to achieve that asymptotic release rate was long compared to the times for which discharges were calculated. The importance of the release rate assumption is indicated by comparing Figures 14, 15, and 16.



(a)

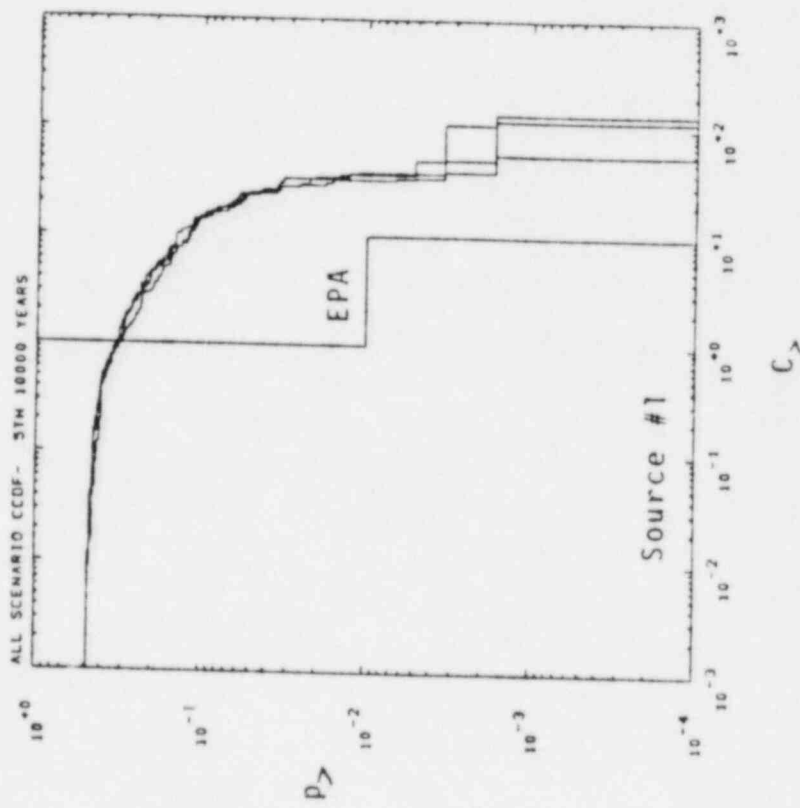
(b)

Figure 14. CCDFs for the Groundwater Transport Scenarios With Source #1.



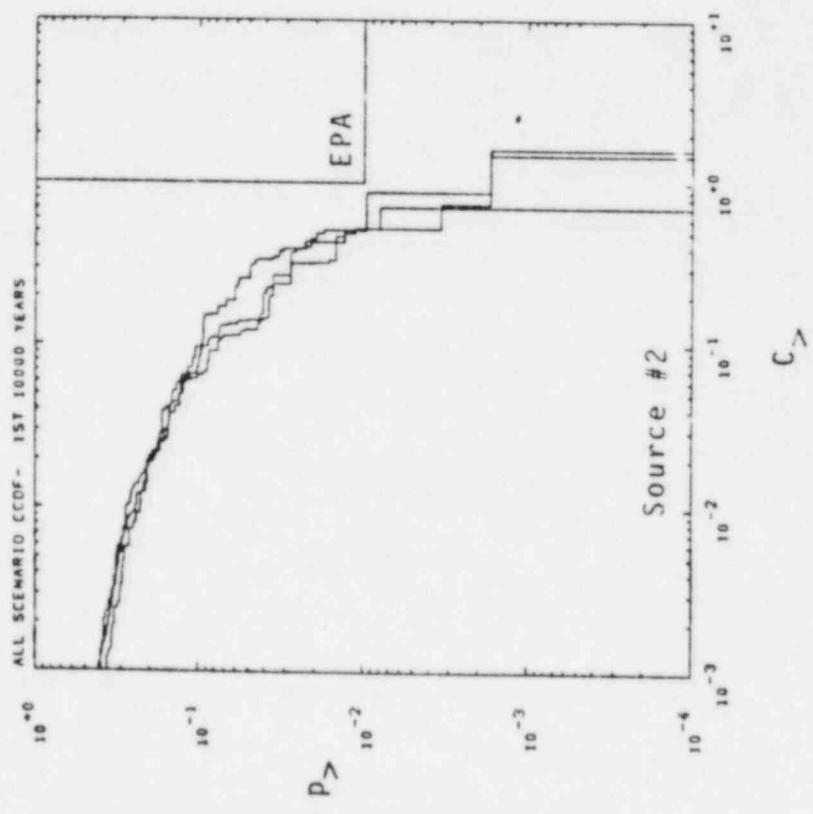
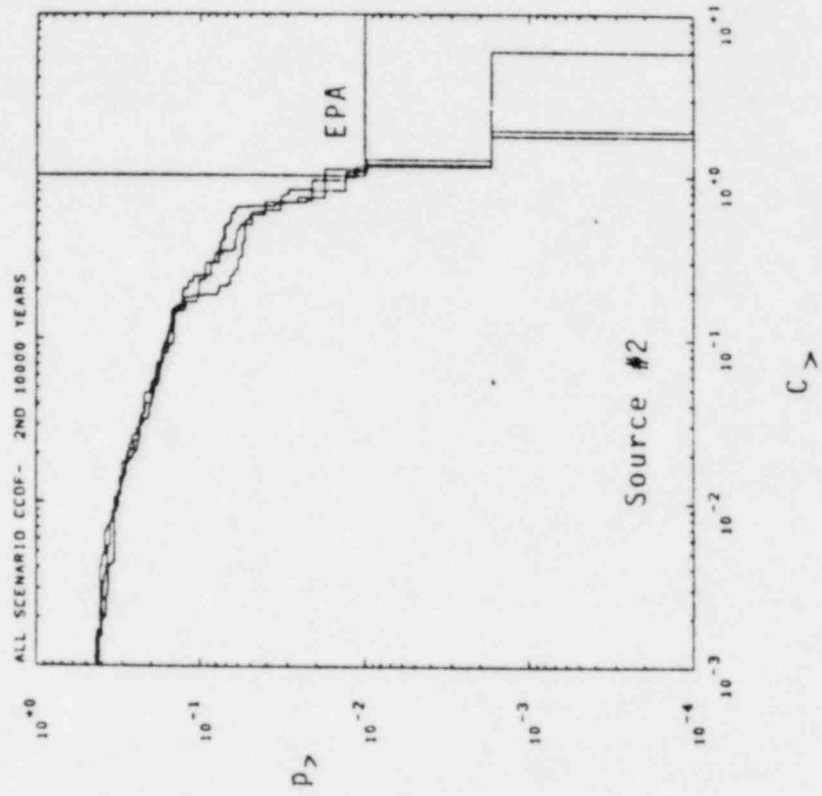
(c) (d)

Figure 14. CCDFs for the Groundwater Transport Scenario With Source #1.



(e)

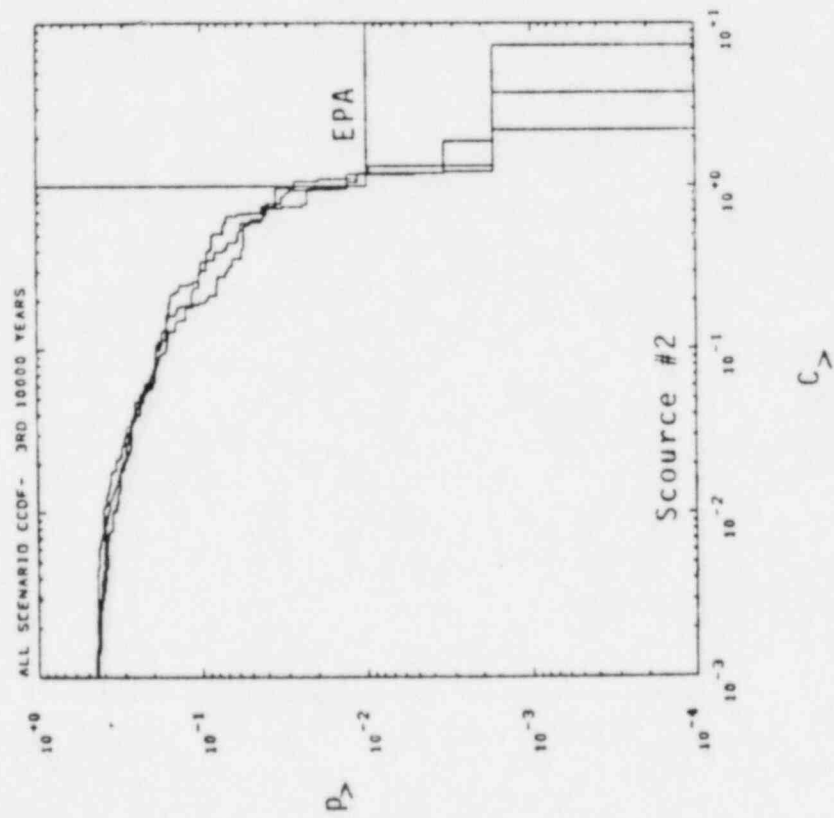
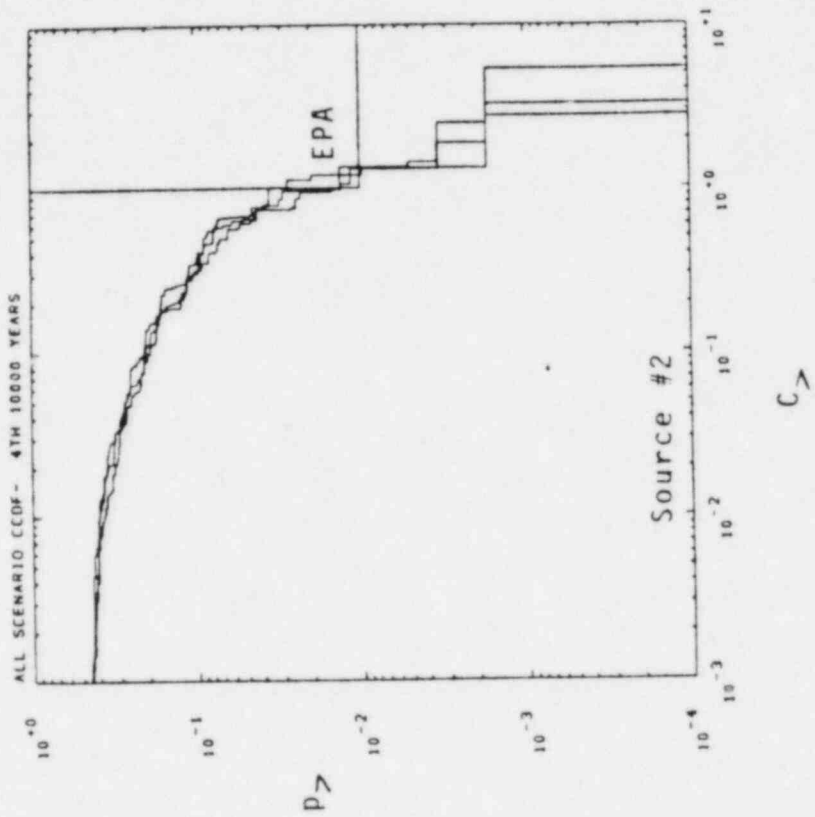
Figure 14. CCDFs for the Groundwater Transport Scenario With Source #1.



(a)

(b)

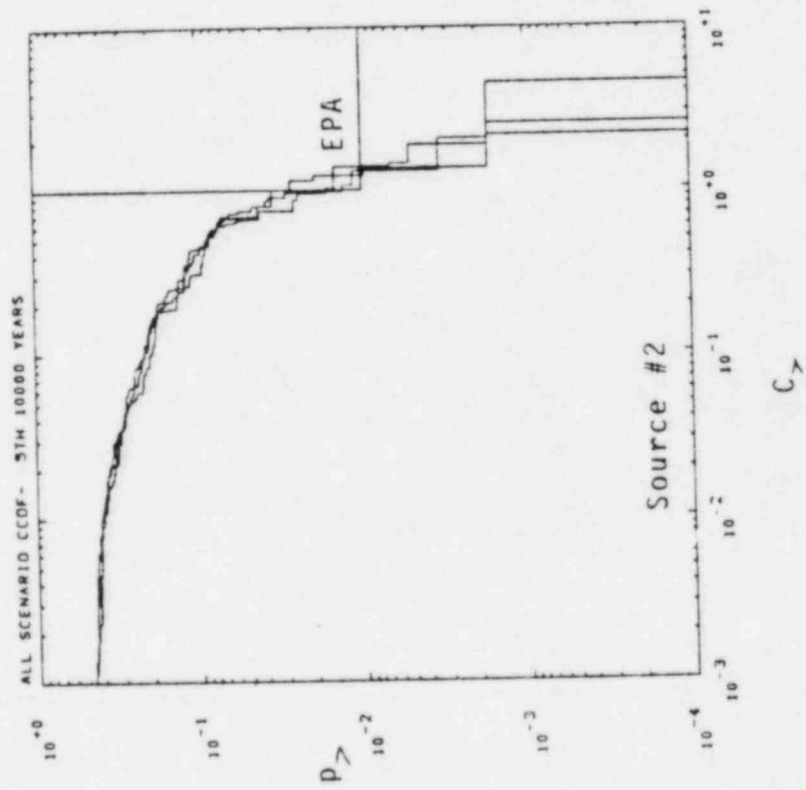
Figure 15. CCDFs for the Groundwater Transport Scenario With Source #2.



(c)

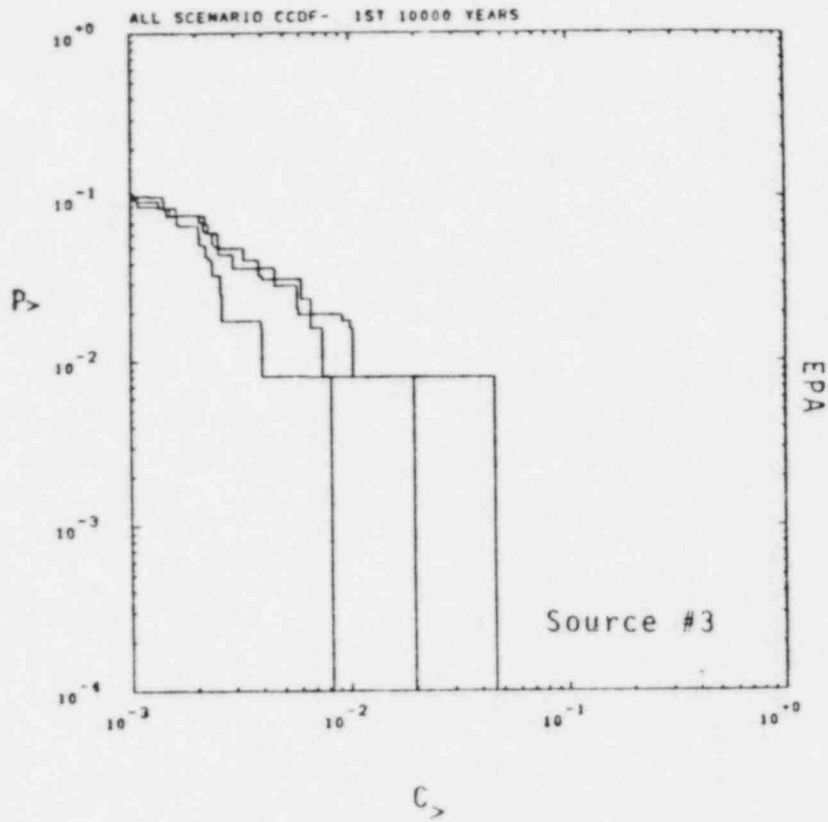
(d)

Figure 15. CCDFs for the Groundwater Transport Scenario With Source #2

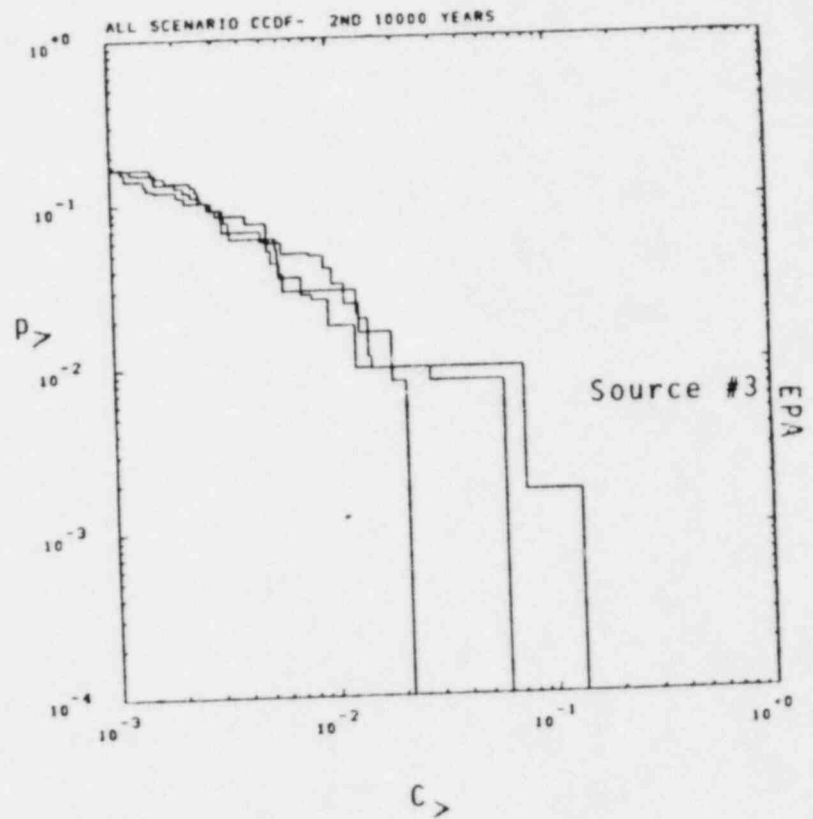


(e)

Figure 15. CCDFs for the Groundwater Transport Scenario With Source #2.

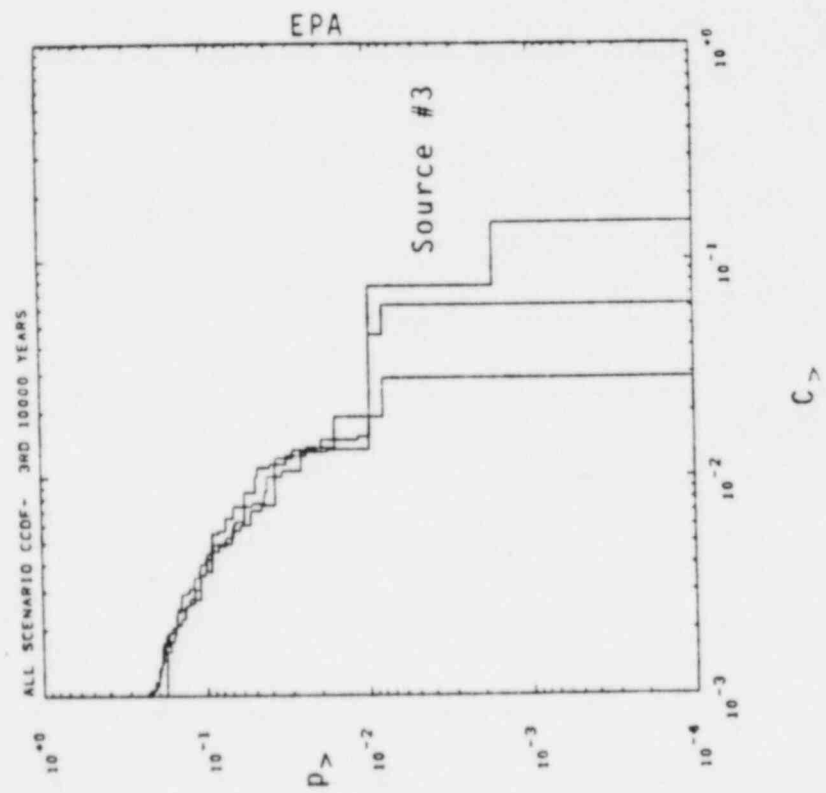
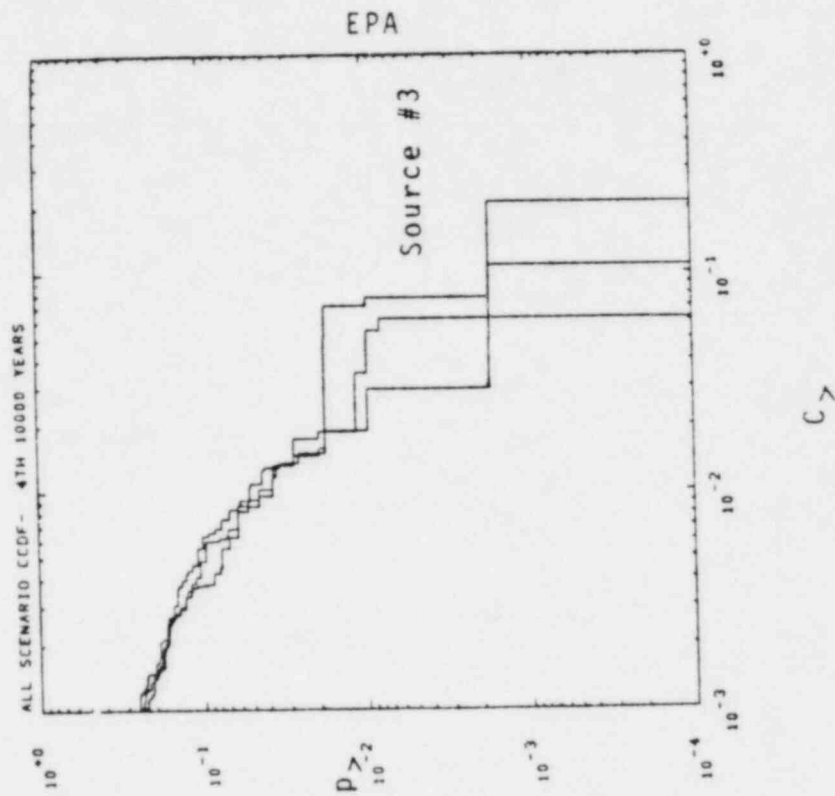


(a)



(b)

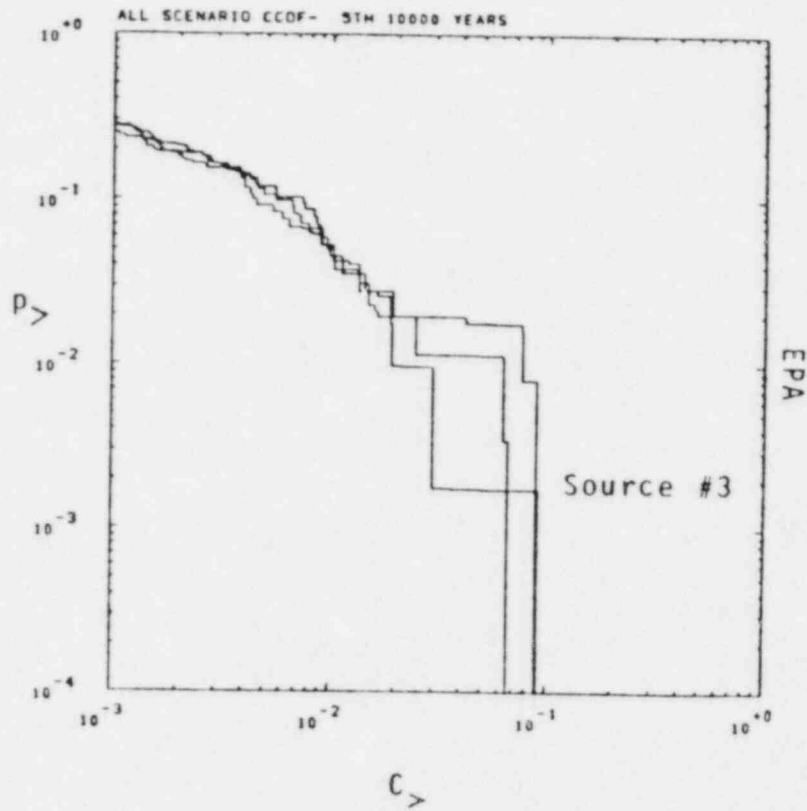
Figure 16. CCDFs for the Groundwater Transport Scenario With Source #3.



(d)

(c)

Figure 16. CCDFs for the Groundwater Transport Scenario With Source #3.



(e)

Figure 16. CCDFs for the Groundwater Transport Scenario With Source #3.

D. Sensitivity Analysis Results

For the groundwater transport scenarios we applied standard sensitivity analysis methods to the calculated discharges as measured by the EPA Sum (Equation 1) [17]. The results of this analysis indicate the relative importance of the various data used in the transport calculations (Tables 6 through 9). The important variables determined by this analysis are tabulated here:

Scenario	Source	
	#1 and #2	#3
1	$k_d(U), \tau$	$C_s(U), \tau$
2	$k_d(U), \tau$	$C_s(U), \tau$
3	$k_d(U), \tau, K_{ua}$	$C_s(U), \tau$
4	$k_d(U), \tau, K_{ua}$	$C_s(U), \tau$

In this table,

$K_d(U)$ = Uranium sorption equilibrium constant (Table 8),

τ = Leach period (reciprocal of Table 7),

$C_s(U)$ = Uranium solubility limit (Table 9),

K_{ua} = Hydraulic conductivity of the upper aquifer,
Unit O or D (Table 6).

The variables appearing in the table are those that control the time of first discharge (breakthrough) and the rate of discharge. For slowly varying discharge rates:

$$\left(\begin{array}{c} \text{Integrated} \\ \text{Discharge} \end{array} \right) \approx \left(\begin{array}{c} \text{Discharge} \\ \text{Rate} \end{array} \right) * \left(\begin{array}{c} \text{Breakthrough} \\ T - \text{Time} \end{array} \right)$$

where T denotes the end of the period of interest, e.g.,
T = 10,000 years.

For Source #3 the variables controlling the breakthrough time do not appear to be as important as for Sources #1 and #2. This is likely due to the shape of the leading edge of the discharge pulse. As shown in Appendix A, the mixing cell model gives a release rate (source term for NWFT/DVM) that is initially proportional to the leach rate, τ^{-1} , and increases linearly with time initially. For the leach limited sources, the discharge rate is nearly a step-function. Thus, we expect a larger sensitivity to variables controlling the time of breakthrough for sharply defined breakthroughs than for the slowly increasing breakthroughs typical of Source #3.

Of note is the appearance of Uranium -- specific variables, $k_d(U)$ and $C_s(U)$. Since we calculated discharges for a mixture of radionuclides, the variables influencing all radionuclides may be expected to be most important e.g., τ , K_{ua} . The appearance of element-specific variables indicates the dominance of the element(s) in the mixture.

VII. Conclusions

From the analyses presented here, we can draw several conclusions and make recommendations:

.Drilling in sedimentary basins indicates potentially serious consequences resulting from "direct hits" and we see no practical way to reduce the consequences of this scenario. They are fixed by the canister contents. Therefore, to reduce the seriousness of this scenario, steps would be needed to discourage drilling, perhaps with surface markers indicating the presence of the repository. Also, reducing the cross-sectional area of the canisters, as might be achieved by stacking canisters in storage holes, would reduce the probability of hitting the canisters by vertical drilling. The consequence, however, may be raised.

.Brine pockets in bedded salt may pose a significant problem in complying with the draft EPA Standard. Therefore, site characterization should directly address the question of identifying any brine pockets that may be present. If few brine pockets and low drilling rates can be expected, the probability of this scenario can be kept low.

Our modeling of this scenario is admittedly simplistic. Impermeable backfills may be expected in actual designs serving to limit the amount of waste that may mix with the flowing brine. Refining the description of this scenario is clearly needed. For example, we assumed $(1/40) \cdot 1/106$ of the entire waste inventory came into contact with the flowing brine. This fraction represents some 48 canisters distributed over a 100 foot length of the storage room. In fact, one may expect the brine to flow predominantly in the vicinity of the borehole, contacting a much smaller fraction of the waste and reducing the consequences of this scenario. The descriptions of flow along such a borehole and in the backfilled room, as well as the description of brine pocket characteristics require further analysis. One would expect a description in terms of the fraction of the waste contacted and the amount of flow expected; only such a description would be useful in analyzing such scenarios.

.The importance of the groundwater transport scenarios in contributing to estimates of compliance may be great

or small, depending on the source model chosen. Since all result from drilling, steps should be taken to keep future drilling rates low. Reducing the consequence may be achieved if the assumptions used in Sources #2 and #3 can be justified. Clearly, the fraction of waste available to flowing groundwater, solubilities, and mixing processes must be understood to estimate the importance of the contribution. Unfortunately, we have not analyzed any processes in the area adjacent to a repository. Such analysis would be needed to make definitive statements on these assumptions.

An important assumption has been made throughout this analysis and should be noted. We have assumed failed shafts and boreholes to remain open throughout the calculation, 50,000 years. In fact they would creep closed unless the groundwater flowing through them dissolved enough salt to keep the conduit open. We have not investigated this assumption in detail. The capability to address it is currently being developed with the DNET Model[12].

In general, we should note that we have not addressed the entire set of scenarios developed in Reference 6. We have addressed a subset of scenarios that we feel may be important. Judging from the results calculated, these scenarios are indeed important for any repository similar to the one we have assumed.

REFERENCES

1. Environmental Protection Agency, 40CFR191, Internal Working Draft 19, Federal Register, March 19, 1981.
2. Nuclear Regulatory Commission, 10CFR60 (Draft), Federal Register 46, No. 130, July 8, 1981.
3. Smith, D. J., et al., Population Risks From Disposal of High-Level Radioactive Wastes in Geologic Repositories (Draft), EPA 520/3-80-006, Environmental Protection Agency, February 1981.
4. Cranwell, R. M., et al., Risk Methodology for Geologic Disposal of High-Level Radioactive Waste in Bedded Salt: Reference Site Analyses, SAND81-2573 (NUREG/CR-2452), Sandia National Laboratories.
5. Pepping, R. E., M. S. Chu, and M. D. Siegel, Technical Assistance for Regulatory Development (Fin No. A-1165: Task 3), Sandia National Laboratories, Albuquerque, NM, December 1981, informal report.
6. Cranwell, R. M., et al., Risk Methodology for Geologic Disposal of Radioactive Waste: Scenario Formulation, Development, and Screening, SAND80-1429, (NUREG/CR-1667), Sandia National Laboratories, to be published.
7. Egan, D. J., Environmental Protection Agency, Public Presentation at the Symposium of Uncertainties Associated With the Regulation of the Geologic Disposal of High-Level Radioactive Wastes, Gatlinburg, TN, March 9-13, 1981.
8. Ritchie, J. S., A National Waste Terminal Storage Repository in a Bedded Salt Formation for Spent Unreprocessed Fuel: Conceptual Design Description, Report 78-58-R (Oakland, CA: Kaiser Engineers, December 1978).
9. Ritchie, J. S., A National Waste Terminal Storage Repository in a Bedded Salt Formation for Spent Unreprocessed Fuel: Conceptual Design Report, Vols. 1 and 2, Report 78-57-RE (Oakland, CA: Kaiser Engineers, December 1978).
10. Ritchie, J. S., A National Waste Terminal Storage Repository in a Bedded Salt Formation for Spent Unreprocessed Fuel: Twenty-Five-Year Retrievability, Special Study, Report 78-60-RE (Oakland, CA: Kaiser Engineers, December 1978).

REFERENCES (Continued)

11. Pepping, R. E., et al., Risk Analysis Methodology for Spent Fuel Repositories in Bedded Salt: Reference Repository Definition and Contributions From Handling Activities, SAND81-0219 (NUREG/CR-1931) Sandia National Laboratories, July 1981.
12. Cranwell, R. M., et al., Risk Methodology for Geologic Disposal of Radioactive Waste: The DNET Computer Code User's Manual, SAND81-1663 (NUREG/CR-2243) Sandia National Laboratories, January 1982.
13. Channell, J. K., Calculated Radiation Doses From Radionuclides Brought to the Surface if Future Drilling Intercepts the WIPP Repository and Pressurized Brine, EEG-11, Environmental Evaluation Group, Health and Environment Department, State of New Mexico, January 1982.
14. Campbell, J. E., et al., Risk Methodology for Geologic Disposal of Radioactive Waste: The Distributed Velocity Method of Solving the Convective-Dispersion Equation, SAND80-0717 (NUREG/CR-1376), Sandia National Laboratories, 1980.
15. Iman, R. L., et al., Latin-Hypercube Sampling (Program User's Guide), SAND79-1473, Sandia National Laboratories, 1980.
16. Muller, A. B., N. C. Finley, and F. Pearson, Jr., 1981, Geochemical Parameters Used in the Bedded Salt Reference Repository Risk Assessment Methodology, SAND81-0557, (NUREG/CR-1996), Sandia National Laboratories.
17. Iman, R. L., J. C. Helton, and J. E. Campbell, Risk Methodology for Geologic Disposal of Radioactive Waste: Sensitivity Analysis Techniques, Sandia Laboratories, SAND78-0912 (NUREG/CR-0390), October 1978.

VIII. Appendix A: The Mixing Cell Source Model

In Source #3 we allow the backfilled regions to be modeled as a mixing cell in which flowing groundwater is assumed to mix with radionuclides in the volume of the mixing cell. The concentration of radionuclides released from the backfilled regions is then given by the uniform concentration in the mixing cell. This model can be calculated analytically for a single stable species.

Let

V = mixing cell volume,

C = radionuclide concentration in water in the mixing cell,

L = rate of radionuclide input into V from waste form leaching,

Q = rate of water flow through V .

In this illustration we will assume the leach rate, L , to be given as a fractional rate, λ_L , of the remaining contaminant in the waste form,

$$L = \lambda_L N_0 e^{-\lambda_L t}$$

where N_0 is the initial contaminant inventory.

The contaminant concentration in the mixing cell is described by

$$V \frac{dC}{dt} = L - QC \quad (A.1)$$

If we let

$$\lambda_0 \equiv Q/V$$

the solution of A.1 is

$$C(t) = \frac{\lambda_L N_0}{(\lambda_0 - \lambda_L)V} \left(e^{-\lambda_L t} - e^{-\lambda_0 t} \right) \quad (A.2)$$

For small t

$$C(t) \cong \frac{\lambda_L N_0}{V} t$$

Thus the concentration of the radionuclide increases linearly from zero.

The asymptotic release rate QC_∞ can be obtained from Equation (A.1) with

$$\frac{dC}{dt} = 0,$$

$$QC_\infty = L$$

Thus, for long times, the release rate approaches a value governed by the rate of waste form leaching. The release rate from the mixing cell is then less than or equal to the release rate given by consideration of the waste form leaching alone.

For decaying radionuclide chains, this model is implemented numerically in NWFT/DVM according to the following compartment model.

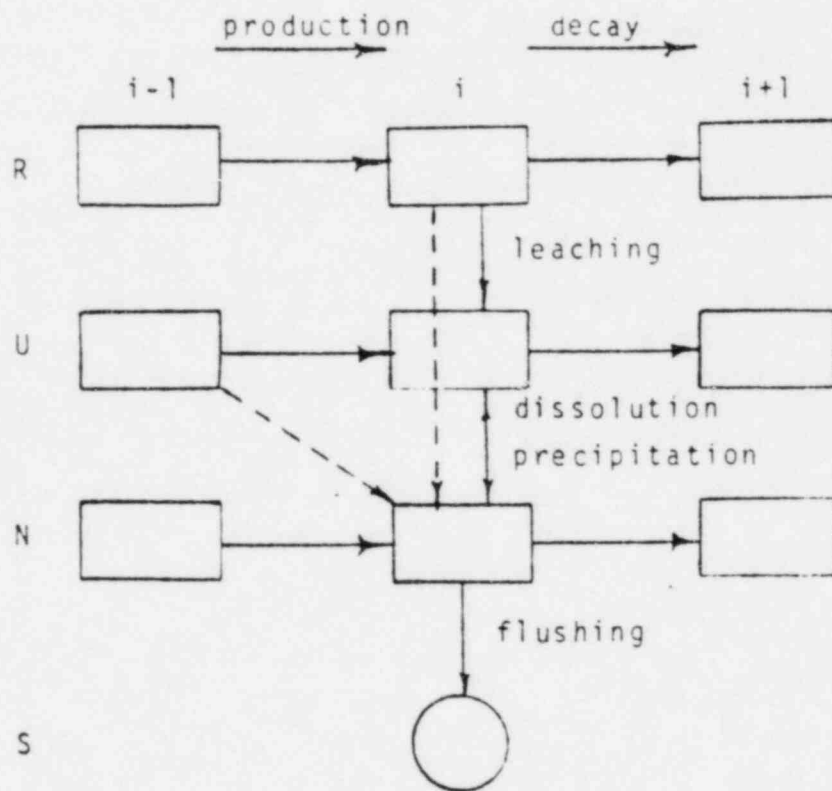


Figure A.1. Implementation of the Mixing Cell Source Model for NWFT/DVM.

Radionuclides remaining in the waste form are represented by Compartments, R. The waste form breakdown rate governs transfer from Compartments R to Compartments U. The inventory in Compartments U is examined along with the water volume in the mixing cell and solubility limits to transfer all or part of that inventory into the mixing cell. The mixing cell inventory is denoted by Compartments N. The mixing cell is flushed constantly to give a release source (S) of

$$S_i = \lambda_0 N_i$$

When solubility limits are applied, radionuclides may be transferred from Compartments N to Compartments U, representing precipitation. For large solubility limits, Compartments U may be empty. Then transfer to Compartments N may occur directly along the dotted paths of Figure A.1.

Horizontal transfer between radionuclides compartment, i , and compartments $i + 1$ or $i - 1$ represents decay and production.

Technical Assistance for Regulatory Development:
A Simplified Repository Analysis in
A Reference Tuff Site

Malcolm D. Siegel
Margaret S. Y. Chu

Sandia National Laboratories
Albuquerque, New Mexico 87185

With Contributions From:
K. L. Erickson *
M. Reade **

* Division 5843 Sandia National Laboratories
** C. G. S. Inc. Urbana, IL 61801

TABLE OF CONTENTS

	<u>Page</u>
1. Introduction	1
2. Geology and Hydrology of the Repository Site	2
2.1 Regional geology and hydrology	2
2.2 Local geology and hydrology	5
3. Waste and Repository Description	10
3.1 Waste	10
3.2 Subsurface facility	10
4. Site Geochemistry and Radionuclide Retardation	13
4.1 Geochemical environment	13
4.2 Sorption ratios	13
4.3 Solubility limits of radionuclides	15
4.4 Radionuclide retardation	15
5. Groundwater Transport Model	18
6. Description of Scenarios and Calculations	20
6.1 Introduction	20
6.2 Scenarios 1, 3, 4 and 1B: Alternate representa- tions of retardation in welded tuff layers	23
6.3 Scenario 5: Effects of changes in the water table on discharge	33
6.4 Scenario 6: Accessible environment at eight miles	41
6.5 Scenarios 2 and 2B: Importance of solubility limits to discharge	47
7. Conclusions	52
Appendix A -- Hydrogeologic Model of the Hypothetical Tuff Repository Site: Its Relationship to Data From the Nevada Test Site	54
A.1 Physical properties of welded tuff	54
A.2 Vertical hydraulic gradient	55
A.3 Horizontal hydraulic gradient	62
Appendix B -- Geochemistry and Radionuclide Retardation	64
B.1 Geochemical environment of the hypothetical tuff site	64
B.2 Radionuclide solubilities	65
B.3 Radionuclide sorption ratios	68

Appendix C -- Approximations for Adapting One-Dimensional Porous Media Radionuclide Transport Models to the Analysis of Transport in Jointed Porous Rock.	70
References	80

ABSTRACT

Potential radionuclide releases from a hypothetical tuff repository have been calculated and compared to the limits set by the EPA Draft Standard 40CFR191. The importance of several parameters and model assumptions to the estimated discharges has been evaluated. The areas that were examined included the radionuclide solubilities and sorption, the description of the local hydrogeology and the simulation of contaminant transport in the presence of fracture flow and matrix diffusion. The uncertainties in geochemical and hydrogeological parameters were represented by assigning realistic ranges and probability distributions to these variables. The Latin Hypercube sampling technique was used to produce combinations (vectors) of values of the input variables. Groundwater flow was described by Darcy's Law and radionuclide travel time was adjusted using calculated retardation factors. Radionuclide discharges were calculated using the Distributed Velocity Method (DVM). The discharges were integrated over five successive 10,000 year periods. The degree of compliance of the repository in each scenario was illustrated by the use of Complementary Cumulative Distribution Functions (CCDF).

Our calculations suggest the following conclusions for the hypothetical tuff repository: (1) sorption of radionuclides by zeolitized tuff is an effective barrier to the migration of actinides even in the absence of solubility constraints; (2) violations of the EPA Draft standard can still occur due to discharge of ^{99}Tc and ^{14}C . Retardation due to matrix diffusion, however, may eliminate discharge of these nuclides for realistic ground water flow rates; (3) in the absence of sorption by thick sequences of zeolitized tuff, discharges of U and Np under oxidizing conditions might exceed the EPA standard. Under reducing conditions, however, the low solubilities of these elements may effectively control radionuclide release.

1. INTRODUCTION

In the near future, the EPA is expected to issue 40CFR191, a draft standard for the geologic disposal of radioactive wastes. During a 180 day period, government agencies such as NRC are expected to comment on the standard. Sandia is funded by the NRC to provide information and insights useful in preparing these comments. The objective of this effort is to perform calculations similar to those performed by EPA in developing the draft standard. We have calculated integrated discharges of radionuclides in plausible scenarios. A number of media have been proposed as candidate hosts for nuclear waste repositories: bedded salt, domed salt, basalt, tuff and granite. This report documents analysis of a repository in the saturated zone of a volcanic tuff environment.

The conceptual model of the repository site is consistent with our current understanding of the characteristics of volcanic tuff environments currently being studied by the Department of Energy. It must be stressed that we have not attempted to accurately model any specific real site. At the present time the available data are not sufficient for this purpose. Large uncertainties exist in the characterization of the solubilities and sorption of radionuclides, in the description of the regional and local hydrogeology and in the mathematical treatment of contaminant transport due to fracture flow and matrix diffusion. We feel, however, that in this analysis, we have calculated reasonable upper limits of radionuclide discharge for a generic tuff repository under realistic conditions. In our calculations we have also attempted to evaluate the relative importance of the aforementioned areas of uncertainty to the estimated radionuclide release.

Appendices A through C describe in detail the assumptions and mathematical approximations that we used in our analysis. In Appendix A we discuss the data obtained from studies of Yucca Mountain at the Nevada Test Site which were used in setting realistic limits to hydrogeological parameters used in our calculations. The assumptions used to calculate hydraulic gradients for the hypothetical repository site are also discussed. In Appendix B, the geochemical environment at Yucca Mountain is described. The data which were used to estimate realistic values of radionuclide sorption ratios (R_d 's or K_d 's) and solubilities are also discussed. In some of our calculations we have used a retardation factor which includes the effects of matrix diffusion for ^{99}Tc , and ^{14}C and ^{129}I . Appendix C contains a derivation of the approximations we have used to adapt our one-dimensional porous media transport model to the analysis of transport in jointed porous rock.

2. GEOLOGY AND HYDROLOGY OF THE REPOSITORY SITE

2.1 Regional Geology and Hydrology

A map of the topographic setting and a regional cross-section of the repository are shown in Figures 1 and 2 respectively. The depository (point R) is located in Mountain A on the flanks of a large volcanic caldera. The depository horizon lies at a depth of approximately 3000 feet within a Tertiary volcanic tuff aquitard in the saturated zone. In Mountain A, the water table is 1500 feet below the surface and 1500 feet above the depository. The tuff aquitard is composed of layers of moderately welded to non-welded tuff units and extends several thousands of feet below the depository horizon. On a regional scale, the tuff aquitard is underlain by a Paleozoic clastic aquitard and a Paleozoic carbonate aquifer. The basal no-flow boundary of the regional groundwater system lies at the base of the carbonate aquifer.

Above the tuff aquitard lies a densely welded and highly fractured Tertiary tuff aquifer. This unit reaches a maximum thickness of about 1000 feet at Mountain A. In the washes adjacent to the mountain, the water table lies within the tuff aquifer. The piezometric surface approaches the land surface gradually along the A-D section in Figures 1 and 2; at point D water flows freely in wells at the surface.

The lateral boundaries of the regional groundwater system are approximately coincident with the edges of Figure 1. The areas north of Mesa A and Mesa B comprise the northern border of the system. The eastern and southeastern limits of the basin are marked by a series of mountains and ridges. A mountain range in the southwest marks another boundary of the system. The northwest border of the regional system is not well defined, however, the area to the west of Mesa A is known to belong to another hydrogeologic system.

Recharge to the ground water system through precipitation occurs only above the 5000 foot contour marked in Figure 1. Due to the high evaporation potential in this region, only about 15 percent of 15 inches of rainfall infiltrates to the water table in areas above this elevation. The ground water system is sluggish because of the small amount of recharge. The hydraulic gradients are low to moderate (10^{-4} to 10^{-3}) except in regions where the rocks in the saturated zone are relatively impermeable. The regional ground water flow is south-southeast through the repository and south-southwest in the southern portions of Figure 1.

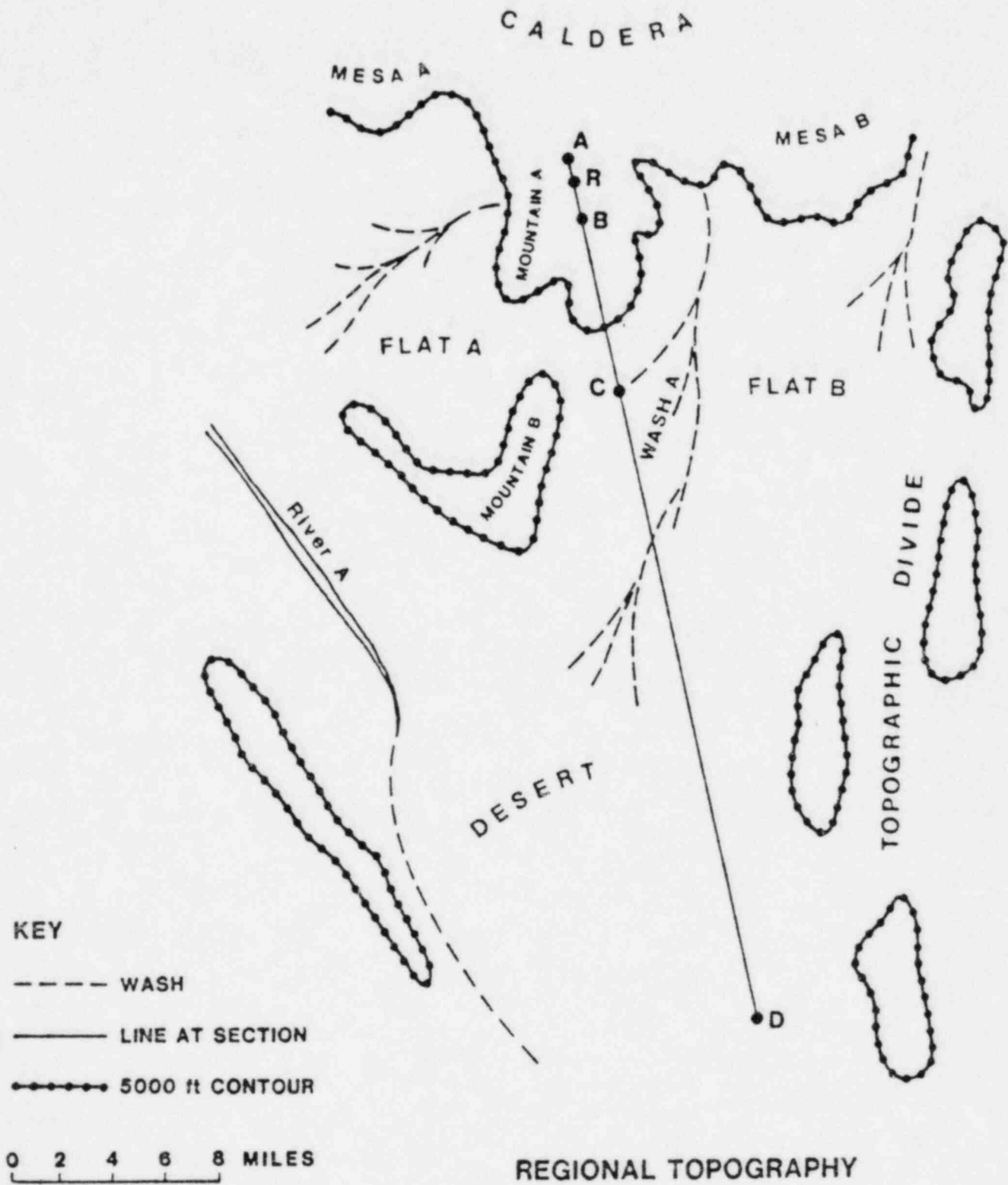


Figure 1. Regional topography of the hypothetical tuff repository site

REGIONAL CROSS SECTION

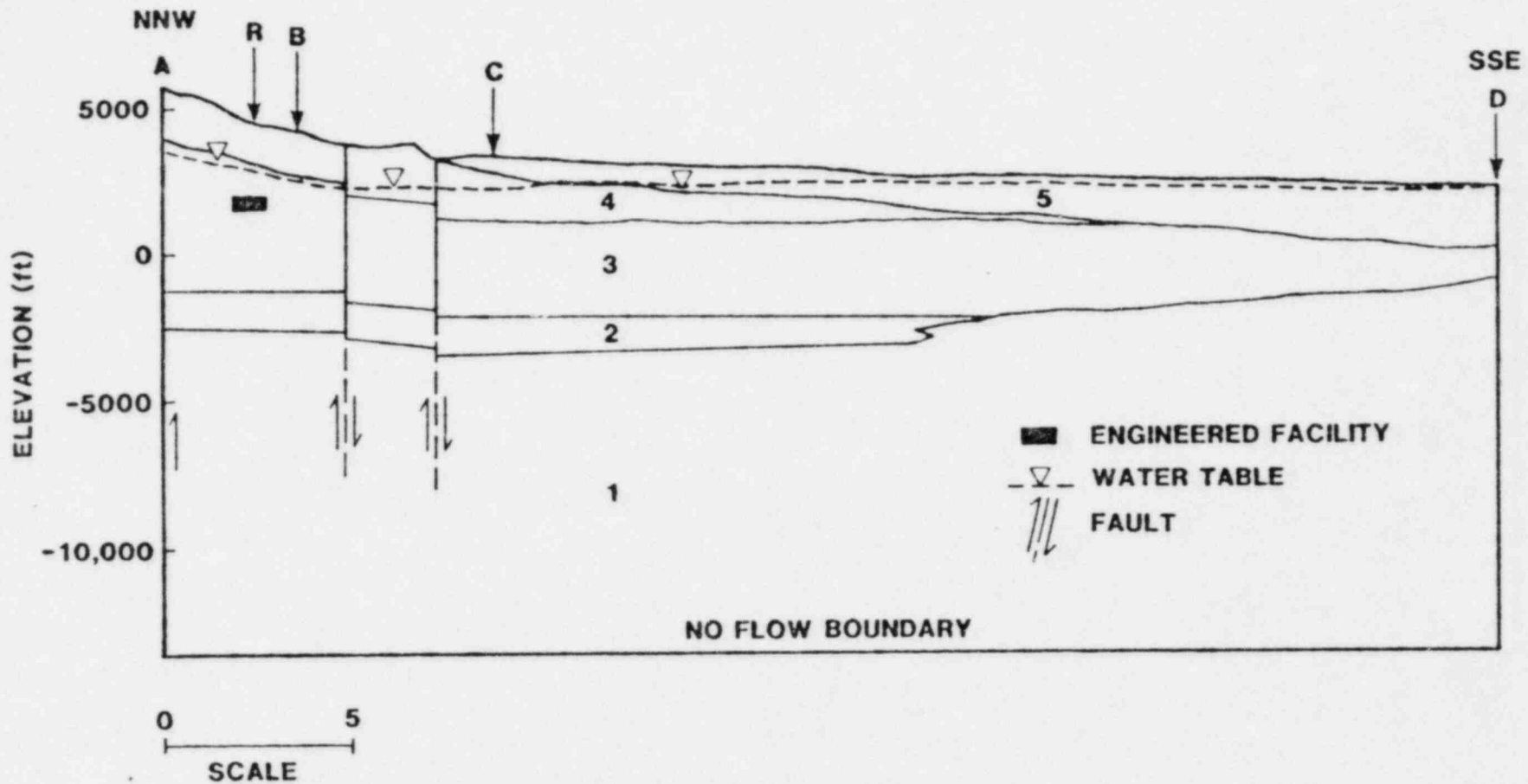


Figure 2. Regional Cross Section of Hypothetical Repository Site.

2.2 Local Geology and Hydrology

A detailed cross-section at the repository is shown in Figure 3. In Table 1, the stratigraphy for the site is described in more detail. An explanation of the petrological terms can be found in the section on Geochemistry.

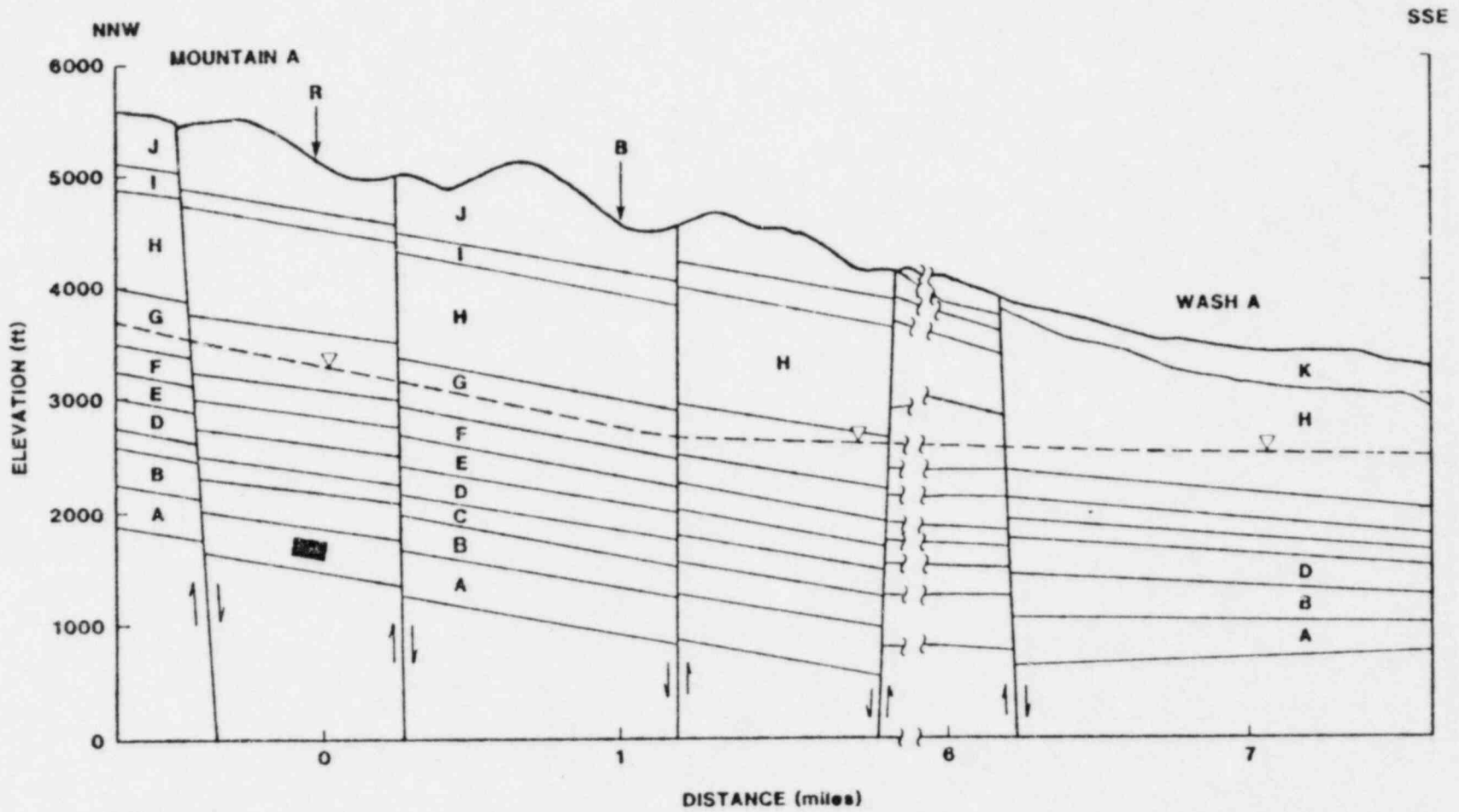
In the vicinity of the volcanic caldera, the tuff layers are underlain only by granitic batholiths; all pre-existing rocks have been destroyed by volcanic eruptions. The tuff units thin with increasing distance from the volcanic centers as shown in Figure 2.

The depository is located in the middle of Unit A, a densely welded member of the tuff aquitard. This unit is a devitrified tuff, composed primarily of alkali feldspar, tridymite and cristobalite. Layer B, directly above the depository horizon, is a non-welded zeolitized tuff composed primarily of clinoptilolite. The water table lies in layer G which is similar in composition to Layer B. Layers G and I have not undergone devitrification. They have retained their original glassy nature and are designated as "vitric" in Table 1.

The geochemical and hydrological characteristics of these layers are determined primarily by the mineralogy and the degree of welding of the rocks. The local flow system and radionuclide retardation will in turn be strongly influenced by these characteristics. In Table 2, the ranges and types of distribution for several hydrogeologic parameters are described for the different types of tuff. Data from pump tests, laboratory measurements of matrix porosity of intact cores, and calculations based on fracture aperture and density were used to bound reasonable limits for hydraulic conductivity and porosity. Observations of the orientation of fractures in volcanic tuffs at the Nevada Test Site (1,2) suggest that two sets of vertical fractures dominate the joint system. In our calculations, therefore, we have assumed that values of hydraulic conductivity and effective porosity in the vertical direction are twice the values in the horizontal direction. The assumptions and methods used to delimit the range of hydraulic properties are discussed in more detail in Appendix A.

The repository site is extensively block faulted, consequently, the water table lies in the tuff aquitard near Mountain A (an uplifted block) and in the tuff aquifer beneath the adjacent washes and flats (down-dropped blocks).

LOCAL CROSS SECTION



KEY


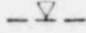

-  ENGINEERED FACILITY
-  WATER TABLE
-  FAULT

Figure 3. Local Cross Section of Hypothetical Tuff Repository Site.

Table 1
STRATIGRAPHY FOR TASK III TUFF

	<u>UNIT</u>	<u>DEGREE OF WELDING</u>	<u>ROCK TYPES</u>	<u>THICKNESS (FT)</u>	<u>COMMENT</u>
(Tuff Aquifer) K J I H		NA	ALLUVIUM	60-425	
		DENSE	DEVITRIFIED	145	
		NON WELDED	VITRIC	150	
		DENSE	DEVITRIFIED	900	WATER TABLE AT DISTANCE=8 MILES
(Tuff Aquitard) G F E D C B A		NON WELDED	ZEOLITIZED	475	WATER TABLE AT DISTANCE=0 MILES
		MODERATE	DEVITRIFIED	270	
		MODERATE	VITRIC	180	
		NON WELDED	ZEOLITIZED	150	
		DENSE	DEVITRIFIED	250	
		NON WELDED	ZEOLITIZED	300	
		DENSE	DEVITRIFIED	400	DEPOSITORY HORIZON
	MODERATE	ANALCIME	270		

Table 2

RANGES OF HYDROGEOLOGIC PARAMETERS

<u>Parameter</u>	<u>Densely Welded Tuff</u>	<u>Moderately Welded Tuff</u>	<u>Non-Welded Tuff</u>
Horizontal hydraulic conductivity (ft/day)''	2×10^{-5} -30 (LU)'	3×10^{-5} -5 (LN)	10^{-5} -2 (LN)
Horizontal effective porosity (%)''	4.4×10^{-4} -0.32 (LN)	0.03-22 (LU)	20-48 (N)
Horizontal hydraulic gradient	1×10^{-3} - 1×10^{-1} (LU)	1×10^{-3} -- 1×10^{-1} (LU)	1×10^{-3} - 1×10^{-1} (LU)
Vertical hydraulic gradient	1×10^{-2} - 4×10^{-2} (U)	1×10^{-2} - 4×10^{-2} (U)	1×10^{-2} - 4×10^{-2} (U)
Grain density (gm/cm ³)	2.3	2.2	1.7
Horizontal fracture porosity'' (%)	4.4×10^{-4} -0.32	0.0-0.06	---
Total Porosity (%)	3-10	10-38	20-50

' Type of distribution is indicated in parenthesis: (LU)-log uniform; (LN)-lognormal; (U)-uniform.

'' Values of these properties in the vertical direction are 2x the values in the horizontal direction.

The water table in the vicinity of the repository is indicated in Figure 3. Near Mountain A, the piezometric surface lies within Unit H and parallels the top of this layer. The horizontal hydraulic gradient near the repository lies within the range 10^{-1} to 10^{-3} . Approximately 2 miles from the repository, the water table enters the tuff aquifer (in Layer H) and the gradient decreases to 10^{-2} to 10^{-4} . This "hinge effect" is due to the combined effects of stratigraphy, contrasts in hydraulic conductivity and increased recharge at elevations above 5000 feet. In our calculations, however, we have sampled the horizontal gradient over a range of 10^{-1} to 10^{-3} for conservatism.

The blocks faulting can create local abrupt changes in head at vertical faults where relatively permeable water-bearing zones are abutted against impermeable layers. For the purpose of our calculations, however, we have ignored these local heterogeneities. The water lies more than 1000 feet below the surface at all points along section ARBC. Local changes in the water table will not substantially affect radionuclide transport on the scale of our model; the water table, therefore, is represented by straight lines in Figure 3.

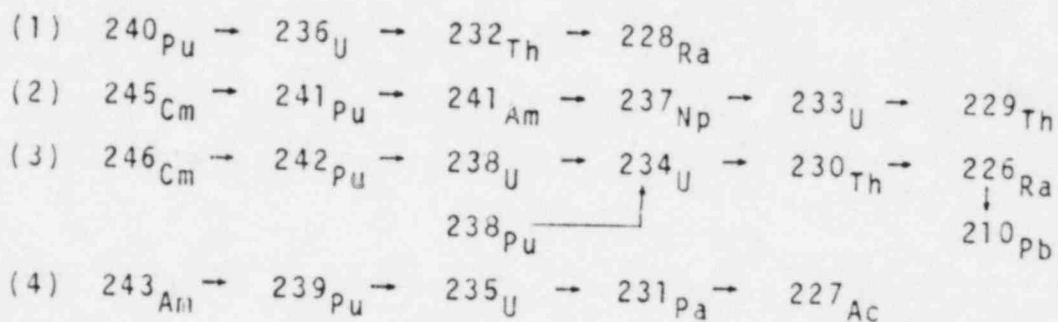
In all of the release scenarios (except scenarios 2 and 2B) we have assumed that radionuclides travel vertically from the engineered facility to the water table under the influence of thermal buoyancy related to the heat generated by the emplaced waste. We have also assumed that the volume of annual ground water flow through the repository is not large enough to appreciably perturb the regional flow system. Supply of ground water to the repository will be sufficient to saturate the repository at all times during the 50,000 year period of interest. This assumption adds another element of conservatism to our calculations and will be discussed further in Appendix A.

3. WASTE AND REPOSITORY DESCRIPTION

3.1 Waste

The inventory (Table 2) assumed in this work is equal to half the projected accumulation of 10-year-old spent fuel in the United States by the year 2010. This would contain a total of 103,250 BWR and 60,500 PWR assemblies; a total of 46,800 metric tons of heavy metal (MTHM). All radionuclides specified in the Release Limit Table of the EPA Standard are included in this inventory list.

Based on the inventory and toxicity of each radionuclide the following chains of radionuclides were considered:



The fission and activation product radionuclides ^{99}Tc , ^{129}I , ^{126}Sn , ^{90}Sr , ^{14}C , ^{135}Cs , and ^{137}Cs were also considered in this work.

All canisters containing the wastes are assumed to have a life of 1,000 years after emplacement. At year 1,000, all canisters fail simultaneously and radionuclide release begins. Radionuclide release is assumed to be determined by a constant rate of breakdown of the waste form. The waste matrix is assumed to dissolve at an annual rate of 10^{-3} to 10^{-7} of the original mass. Radionuclides are assumed to be uniformly distributed throughout the matrix so that their release rate is directly proportional to the matrix dissolution rate.

3.2 Subsurface Facility

The reference subsurface facility is a mined facility at a depth of 3,000 feet below the surface. A description of the facility is summarized in the following table.

Areal dimensions -- 2,000 acres ($8.71 \times 10^7 \text{ft}^2$)
(Reference 3, Table C1)

Height = 23 ft.

Rep. Volume = $8.71 \times 10^7 \times 23 = 2.0 \times 10^9 \text{ft}^3$

Extraction Ratio = 20% (Reference 3, p. 88)

Porosity of Backfill = 20%

* Porosity volume of depository = $8.0 \times 10^7 \text{ft}^3$

Table 3

INVENTORY OF REFERENCE REPOSITORY
(SPENT FUEL FROM 46,800 MTHM)

<u>Radionuclide</u>	<u>Half Life</u>	<u>Curies</u>
Pu240	6.76E3	2.1E7
U236	2.39E7	1.0E4
Th232	1.41E10	1.7E-5
Ra228	6.7	4.7E-6
Cm245	8.27E3	8.4E3
Pu241	14.6	3.2E9
Am241	433.	7.5E7
Np237	2.14E6	1.5E4
U233	1.62E5	1.8
Th229	7300.	1.3E-3
Cm246	4710.	1.6E3
Pu242	3.79E5	7.5E4
U238	4.51E9	1.5E4
Pu238	89.	9.4E7
U234	2.47E5	3.5E3
Th230	8.E4	0.19
Ra226	1600.	3.5E-4
Pb210	21.	3.3E-5
Am243	7650.	6.6E5
Pu239	2.44E4	1.4E7
U235	7.1E8	7.5E2
Pa231	3.25E4	0.25
Ac227	21.6	5.2E-2
Tc99	2.14E5	6.1E5
I129	1.6E7	1.5E3
Sn126	1.0E5	2.2E4
Sr90	28.9	2.4E9
C14	5730.	3.5E4
Cs135	2.0E6	1.3E4
Cs137	30.	3.5E9

4. SITE GEOCHEMISTRY AND RADIONUCLIDE RETARDATION

4.1 Geochemical Environment of the Hypothetical Tuff Site

The migration rate of radionuclide in the tuff repository site will depend on the interactions between the dissolved species and the rock matrix and between the different aqueous species in the liquid phase. Important geochemical parameters which must be characterized include the major and minor element composition, pH, Eh, and temperature of the ground water and the mineralogy of tuff layers through which the radionuclides migrate.

The lithology of each tuff unit in our hypothetical tuff site is described in Table 1. They are classified as zeolitized, vitric or devitrified. A more detailed discussion of the mineralogy may be found in Appendix B. The ground water in the repository site is assumed to be a sodium-potassium-bicarbonate water similar to that described by Winograd and Thordarson (4) at the Nevada Test Site. The Eh is assumed to be mildly oxidizing and the pH are between 7.2 and 8.3. The chemical composition of water from the vicinity of Yucca Mountain and the justification for the above assumptions are described in detail in Appendix B. The temperature assumed in the transport legs in the far field of the repository site is between 30 and 40°C. This range is based on the geothermal gradient at Yucca Mountain.

4.2 Sorption Ratios

The sorption ratio (R_d) is an experimentally determined ratio of the amount of radionuclide bound to a solid phase to the amount of nuclide in a volume of liquid in contact with the solid.

$$R_d \text{ (ml/gm)} = \frac{\text{gm radionuclides per gm rock}}{\text{gm radionuclide per ml water}}$$

Values for ranges of R_d for the different types of tuff found in the reference repository are given in Table 4. These ranges are based primarily on a review of the results of sorption ratio studies by scientists at Los Alamos Laboratories (5-10).

The degree of conservatism for these ranges is discussed in Appendix B. Elements for which no sorption data are published are enclosed in brackets in Table 4. They have been assigned to R_d values of chemical homologs for which data are available (11). To our knowledge, there are no acceptable data for

Table 4
RANGES OF R_d (ml/gm) VALUES SAMPLED BY LHS

<u>Element</u>	<u>Vitric Tuff</u>	<u>Devitrified Tuff</u>	<u>Zeolitized Tuff with Clinoptilolite</u>
Sr, [Ra, Pb, Sn]	117-300	50-450	290-213,000
Cs	429-8600	120-2000	615-33,000
Pu	70-450	80-1400	250-2000
Am, [Cm, Pa, Th, Ac]	85-360	190-4600	600-9500
Np	5-7	5-7	4.5-31
U	0-11	1-14	5-15
I, ^{14}C	0	0	0
Tc	0-2	0.3-1.2	0.15-2.0

Np sorption on vitric tuff; the sorption ratio range for devitrified tuff was assigned to this media.

4.3 Solubility Limits of Radionuclides

The solubility limits that were assigned to each element in this study are listed in Table 5. The values in this table are probably upper bounds for the solubilities of these elements in a volcanic tuff environment. The determination of solubilities of radionuclides in ground water associated with a repository in tuff requires experimental studies and calculations describing the possible interactions between nuclides and ligands over a range of temperatures, water compositions and redox conditions. The theoretical calculations are not within the scope of this contract and to our knowledge have not been carried out. Few experimental data describing radionuclide solubility in tuff are available at this time. Due to the time constraints of this contract, we have compiled this list of solubility values from a limited amount of experimental data and solubilities calculated from a limited review of thermochemical data (12-16). A discussion of the conservatism of these data may be found in Appendix B.

4.4 Radionuclide Retardation

The classical expression for retardation in porous media was used for layers of zeolitized tuff in all scenarios.

$$R = 1 + R_d \cdot \rho \cdot \frac{(1 - \phi)}{\phi} \quad (4.1)$$

Where ϕ is the effective porosity of the rock
 ρ is the grain density of the rock
 R_d is the radionuclide sorption ratio (ml/gm)

The calculation of retardation in moderately and densely welded tuff layers was different in each scenario. Detailed descriptions of the scenarios are found in the next section. In scenarios 3 and 4, expression 4.1 was used for moderately welded tuff layers. It was assumed that all radionuclides were unretarded in densely welded layers in scenarios 1, 3, 4, 5, and 6. In scenarios 1, 5, and 6 it was assumed that all radionuclides were unretarded in moderately welded tuff layers also.

Table 5
 ELEMENT SOLUBILITIES USED IN
 MIXING CELL CALCULATIONS

<u>Element</u>	<u>Solubility gm/gm</u>	<u>Reference</u>
Pu	2.4×10^{-4}	*
U	2.4×10^{-5}	15
Th	2.3×10^{-7}	13
Ra	2.3×10^{-8}	16
Cm	2.5×10^{-11}	*
Am	2.4×10^{-12}	15
Np	2.4×10^{-8}	15
Pb	2.1×10^{-6}	*
Pa	2.3×10^{-2}	13
Ac	no limit	*
Tc	no limit	*
I	no limit	*
Sn	1×10^{-3}	13
Sr	2×10^{-6}	13, 16
Cs	no limit	*
C	3×10^{-5}	*

* See discussion in Appendix B

In scenarios 1B, 2, 2B, and 5B matrix diffusion for Tc, ^{14}C , and I was included explicitly in the calculations of radionuclide retardation:

$$R = 1 + \phi_{m} \cdot \left(\frac{1-\epsilon}{\epsilon} \right) \cdot \left(1 + R_d \cdot \rho \cdot \left(\frac{1-\phi_{m}}{\phi_{m}} \right) \right) \quad (4.2)$$

Where ϕ_{m} = matrix porosity
 ϵ = fracture porosity
 ρ = grain density of rock matrix
 R_d = radionuclide sorption ratio (ml/gm)

The derivation of this expression and constraints on its use are discussed in Appendix C.

5. GROUNDWATER TRANSPORT MODEL

In the calculations of radionuclide transport it is assumed that groundwater flow is described by Darcy's Law:

$$q = Q/A = KI \quad (5.1)$$

where Q is the volumetric flow rate through an area A , normal to the flow direction, I is the hydraulic gradient, K is the hydraulic conductivity, and q is the Darcy velocity. When the flow passes through a series of layers with different hydraulic properties, an "effective" hydraulic conductivity may be calculated by

$$K = \frac{\sum_i L_i}{\sum_i \frac{L_i}{K_i}} \quad (5.2)$$

with

L_i = thickness of layer i

K_i = hydraulic conductivity of layer i

The total groundwater travel time is given by

$$\text{Time} = \sum_{i=1} \frac{L_i}{V_i} \quad (5.3)$$

where V_i is the interstitial groundwater velocity in layer i and is equal to q/ϕ_i , with ϕ_i being the effective porosity of layer i . We have assumed that ϕ_i and K_i are correlated with $r^2 = 0.70$. The geometry of the flow path is described for each scenario in Section 6.

When a radionuclide (RN) is transported by ground water, the radionuclide travel time (T_{RN}) is increased by its retardation factor. This is given by

$$T_{RN} = \sum_i \frac{L_i \cdot R_i^{RN}}{V_i} \quad (5.4)$$

where R_i^{RN} is the retardation factor of radionuclide RN in layer i.

The Distributed Velocity Method (DVM) (17) has been developed by Sandia to simulate long chains of radionuclides transported by ground water. In this study we calculated the average velocity of radionuclides using Equation (5.4). The DVM code was then used to calculate the discharges of radionuclides.

6. DESCRIPTIONS OF SCENARIOS AND CALCULATIONS

6.1 Introduction

The conceptual model of our hypothetical repository site is consistent with our current understanding of the characteristics of volcanic tuff environments being studied by the Department of Energy. We have not attempted to accurately model any particular real site; at the present time the available data are not sufficient for this purpose. Large uncertainties exist in the characterization of the solubilities and sorption of radionuclides, in the description of the regional and local hydrogeology and in the mathematical treatment of contaminant transport in the presence of fracture flow and matrix diffusion. In our calculations, we have attempted to evaluate the relative importance of these areas of uncertainty to the estimated radionuclide discharge. We have calculated radionuclide release for several scenarios using different combinations of the following assumptions:

- A. Release rate of radionuclides from the engineered facility
 - 1. limited by leach rate
 - 2. solubility limited
- B. Representation of retardation of radionuclides in moderately welded units
 - 1. no retardation
 - 2. porous media approximations with zeolite R_d 's
 - 3. porous media approximations with R_d 's for vitric or devitrified tuff
- C. Matrix diffusion
 - 1. no credit given for retardation
 - 2. calculation of retardation of ^{99}Tc , ^{129}I , and ^{14}C in welded units
- D. Distance to accessible environment
 - 1. one mile
 - 2. eight miles
- E. Flow path
 - 1. vertical path and gradient controlled by thermal pulse
 - 2. horizontal migration only
- F. Location of water table
 - 1. in zeolitized tuff
 - 2. in densely welded tuff (300 ft above present day level)

The characteristics of each scenario are summarized in Table 6. The release rate of radionuclides from the engineered facility was set equal to the leach rate (10^{-3} to 10^{-7} of the original inventory) in all scenarios except scenario 28. The mixing cell option of NWFT/DVM was used in the scenario 28 and will be described in more detail in Section 6.5.

The uncertainties in geochemical and hydrogeological parameters were represented by assigning realistic ranges and probability distributions to these variables. The Latin Hypercube Sampling Technique (18) was used to produce 105 combinations (vectors) of values of the input variables. Integrated radionuclide discharges for five successive 10,000 year periods were calculated as described in Section 5. A release ratio was calculated for each vector by dividing the magnitude of the discharge of each radionuclide by the corresponding EPA release limit (19) and then summing over all radionuclides. The results are presented as probability distributions of the release ratios for each scenario (Complementary Cumulative Distribution Functions) (6). The curve indicates the ability of the repository site to limit the release of radionuclides. They also illustrate how our ability to assess the compliance of a repository with the EPA Draft Standard is affected by the uncertainty in the input data.

We have not made quantitative estimates of the probability of occurrence of any of the scenarios. We have assumed only that each of the scenarios is an "anticipated event" (corresponding to a "reasonably foreseeable release" in the EPA Draft Standard (19)). We feel that the scenarios have a reasonable probability of occurrence within the 10,000 year regulatory period.

The water table is at least 1,000 feet below the land surface at all points within the hypothetical repository site of our analyses. All of the scenarios require that a well be drilled at least to the depth of the water table and that the radionuclides are withdrawn continuously for 10,000 years or longer. We have based our subjective estimate of the probability of drilling at the hypothetical tuff site on estimates of the water, hydrocarbon and heavy metal ore potential of the Nevada Test Site. Our estimate of the probability of a pluvial period and subsequent rise in the water table at the repository site (Scenario 5) is based on information concerning past climatic changes at NTS.

Table 6
 DESCRIPTIONS OF SCENARIOS

SCENARIO	DISTANCE BETWEEN DEPOSITORY AND POINT OF DISCHARGE		REPRESENTATION OF RETARDATION IN WELDED UNITS DENSELY AND MODERATELY WELDED MODERATELY WELDED ONLY				VERTICAL GRADIENT CONTROLLED BY THERMAL PULSE		CLIMATIC CHANGE CAUSES 300 FT RISE IN WATER TABLE	
	1 MILE PUMP	8 MILE PUMP	MATRIX DIFFUSION MODEL	FRACTURED MEDIUM WITH NO RETARDATION	POROUS MEDIUM WITH ZEOLITES	POROUS MEDIUM WITH DEVITRIFIED TUFF OR VITRIC TUFF	YES	NO	YES	NO
#1	X			X			X			X
#1B	X		X				X			X
#2	X		X					X		X
#2B	X		X					X		X
#3	X				X		X			X
#4	X					X	X			X
#5	X			X			X		X	
#5B	X		X				X		X	
#6		X		X			X			X

* Scenarios 2 and 2B differ from each other in their treatment of the source term. Scenario 2 was a leach limited source term with no solubility limits. In scenario 2B we used the mixing cell option of NWFT/DVM which allows solubility limits to constrain the rate of radionuclide release from the repository.

6.2 Scenarios 1, 3, 4, and 1B: Alternate representations of retardation in welded tuff layers

Scenario 1 - The "Base Case"

Scenario 1 can be considered the base case scenario in our analyses of the hypothetical tuff site (Figure 4). The major geological barriers to radionuclide migration are the layers of zeolitized tuff above the repository. The magnitude of the vertical hydraulic gradient is determined by a buoyancy effect of water heated by the repository as described in Appendix A. Ground water and radionuclides from the repository will travel along the vertical gradient to the top of the water table then migrate horizontally down the horizontal hydraulic gradient. The horizontal gradient is calculated as the sum of the regional gradient plus a component related to the upwelling heated water from the repository.

At a distance of one mile from the repository, a well pumps water from this upper saturated unit. The major barrier to horizontal transport of the radionuclide is retardation in the zeolitized layer G. Layers of zeolitized tuff are treated as porous media in the fluid transport and retardation calculations. Layers of moderately or densely welded tuff are treated as porous media in the transport calculations but it is assumed that no retardation occurs in these layers. Since no credit is given to retardation in the welded units, the calculated discharge is an upper bound for release associated with the fluid transport path described above.

Scenarios 3 and 4 -Porous media approximations for moderately welded tuff layers

Scenarios 3 and 4 differ from scenario 1 only in the treatment of retardation in the moderately welded tuff layers (Figures 5 and 6). In both scenarios these layers are treated as porous media. Moderately welded tuffs are characterized by physical and chemical properties that are intermediate between densely welded devitrified tuffs and nonwelded zeolitized tuffs. In scenario 3, R_d values of zeolitized tuff (Table 4) are used to calculate retardation factors. These calculations provide a lower bound to discharge from the site for scenarios 1, 3, and 4. R_d values for vitric tuffs and devitrified tuffs are used to calculate retardation in layers E and F respectively in scenario 4. Values of all other variables are the same as in corresponding vectors of scenario 1.

Scenario 1B - Matrix diffusion in welded tuff layers

Scenario 1B (Figure 7) differs from scenario 1 only by the inclusion of matrix diffusion in calculations of radionuclide retardation in moderately and densely welded tuff layers. The calculation of a retardation factor which includes the effects of matrix diffusion has been described in Equation 4.2 and in Appendix C. At present, it can only be shown that this expression is valid for radionuclides with $R_d = 0$ (K. Erickson, personal communication). For scenario 1B, therefore, retardation due to matrix diffusion was considered only for ^{129}I , ^{99}Tc and ^{14}C (see Table 4).

Results

Radionuclide discharge rates for each vector were calculated. Discharge rates were integrated for 10,000 year periods from 0 to 50,000 years. The results of the calculations are presented as complementary cumulative distribution functions for each 10,000 year period in Figures 8A-8E. (20) The number of vectors that violate the EPA Standard, the maximum violation and the sum of the release ratio over all vectors are presented in Table 7. For these scenarios, all violations of the EPA Standard are due to discharges of ^{99}Tc and ^{14}C . The effect of retardation in the moderately welded units on the integrated discharge can be assessed by comparing the values for scenarios 3 and 4 to corresponding values for scenario 1. It can be seen that discharge is decreased for the first 40,000 years and increased in the period from 40,000 to 50,000 years relative to scenario 1. Comparison of the results for scenario 1B with those for scenario 1 shows that although discharge of the radionuclides is decreased significantly by matrix diffusion, violations of the EPA release limit still occur.

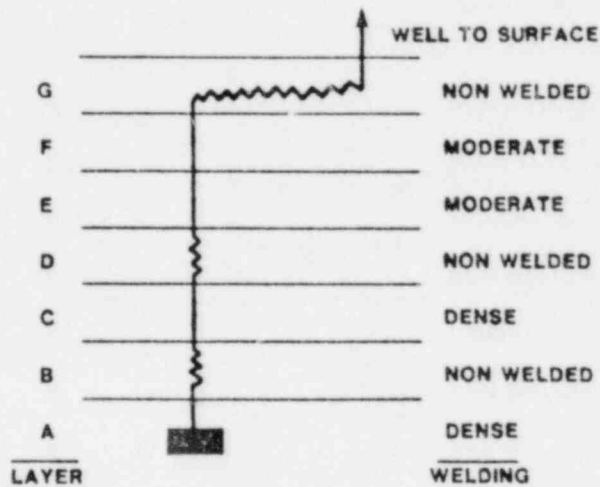
The characteristics of the three vectors whose radionuclide discharges violate the EPA Standard are shown in Table 8. When these values of hydraulic gradient and darcy velocity are compared to the ranges of hydrogeologic parameters sampled by the LHS for input, it can be seen that the high radionuclide discharges are due primarily to large groundwater fluxes. These annual groundwater discharges range from 2 percent to 7 percent of the present day recharge of the Pahute Mesa groundwater system at the Nevada Test Site (21, 22). In Appendix A it is shown that this fraction is unrealistically high for Yucca Mountain. Therefore, we can conclude that violation of the EPA Standard for a groundwater flow path similar to Scenario 1B is very unlikely.

SCENARIO 1

1 mile well; moderate = fractured; thermal buoyancy; no pluvial

LEG	LAYERS	WELDING - RETARDATION	LENGTH (ft)
1	A	dense - no retardation	200 v
2	B	nonwelded - porous - zeolites	300 v
3	C	dense - no retardation	250 v
4	D	non-welded - porous - zeolites	150 v
5	E	moderate - no retardation	180 v
6	F	moderate - no retardation	270 v
7	G	nonwelded - porous - zeolites	5280 h

FLOW PATH






- KEY
-  DEPOSITORY
 -  LAYERS WITH NO RETARDATION
 -  LAYERS WITH RETARDATION

Figure 4

SCENARIO 4

1 mile well; moderate = porous, vitric or devitrified tuff, thermal buoyancy

LEG	LAYERS	WELDING - RETARDATION	LENGTH (ft)
1	A	dense - no retardation	200 v
2	B	nonwelded - porous - zeolites	300 v
3	C	dense - no retardation	250 v
4	D	non-welded - porous - zeolites	150 v
5	E	moderate - porous - vitric	180 v
6	F	moderate - porous - devitrified	270 v
7	G	nonwelded - porous - zeolites	5280 h

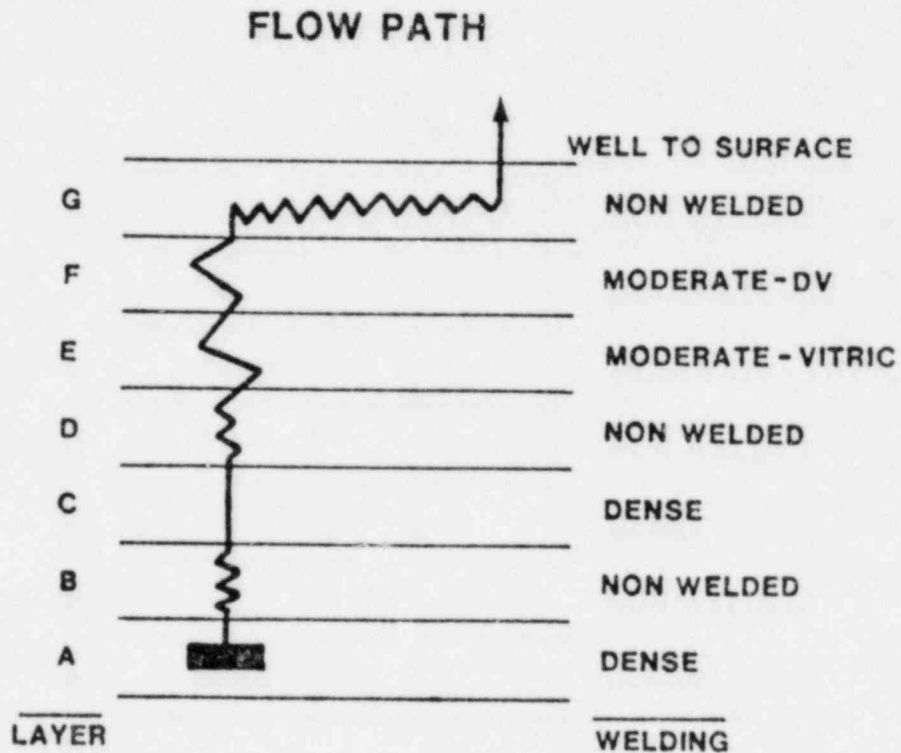


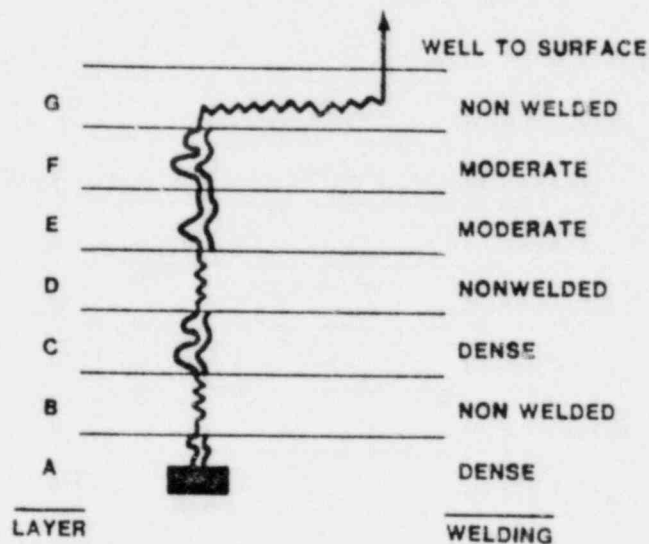
Figure 6

SCENARIO 1B

1 mile well; matrix diffusion; thermal buoyancy; no pluvial

LEG	LAYERS	WELDING - RETARDATION	LENGTH (ft)
1	A	dense - matrix diffusion	200 v
2	B	nonwelded - porous - zeolites	300 v
3	C	dense - matrix diffusion	250 v
4	D	non-welded - porous - zeolites	150 v
5	E	moderate - matrix diffusion	180 v
6	F	moderate - matrix diffusion	270 v
7	G	nonwelded - porous - zeolites	5280 h

FLOW PATH



- KEY
- DEPOSITORY
 - LAYERS WITH MATRIX DIFFUSION
 - LAYERS WITH RETARDATION (POROUS MEDIA)

Figure 7

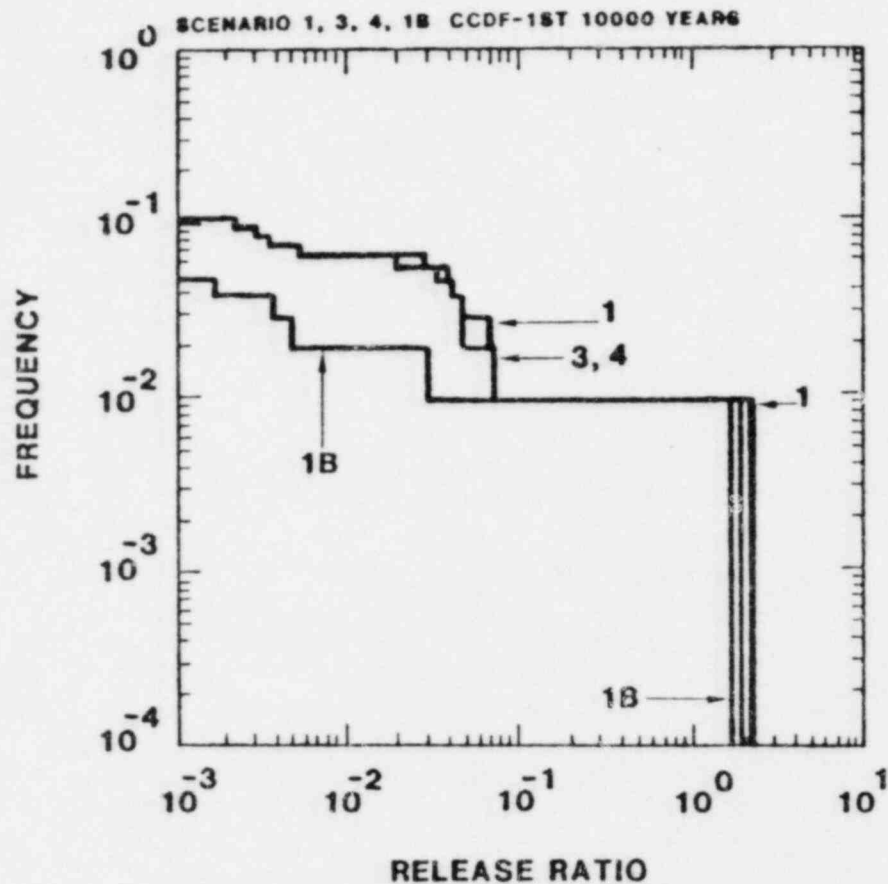


Figure 8.a

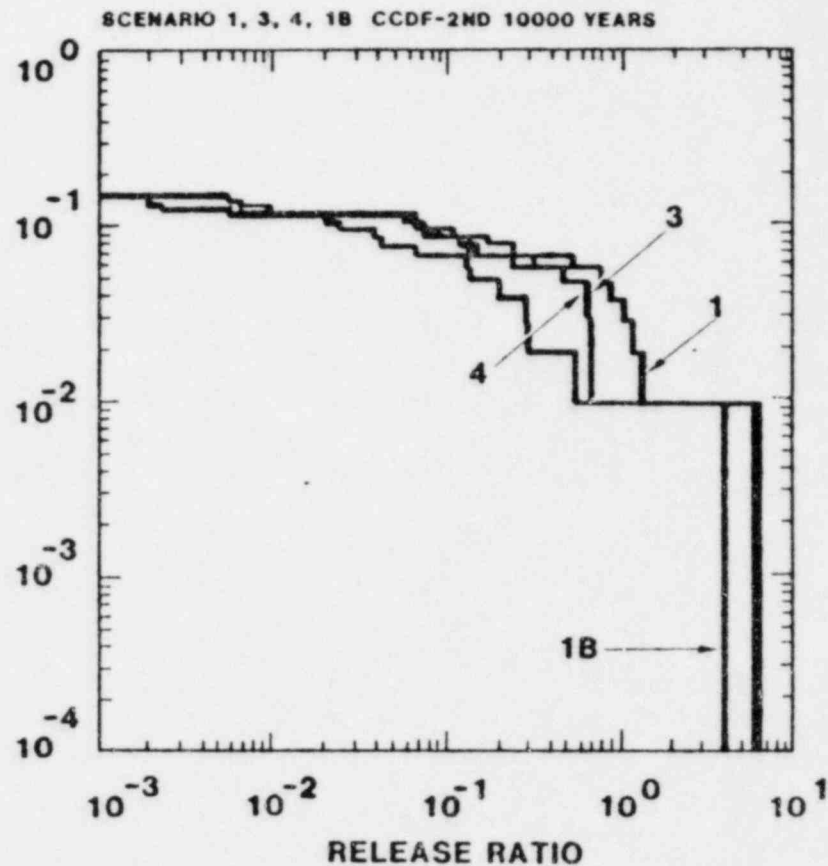


Figure 8.b

Figure 8. Complementary Cumulative Distribution Functions for Scenarios 1, 1B, 3, and 4: Alternate Representations of Retardation in Welded Tuff Units.

1 = base case; 1B = base case with matrix diffusion; 3 = zeolites; 4 = vitric or devitrified

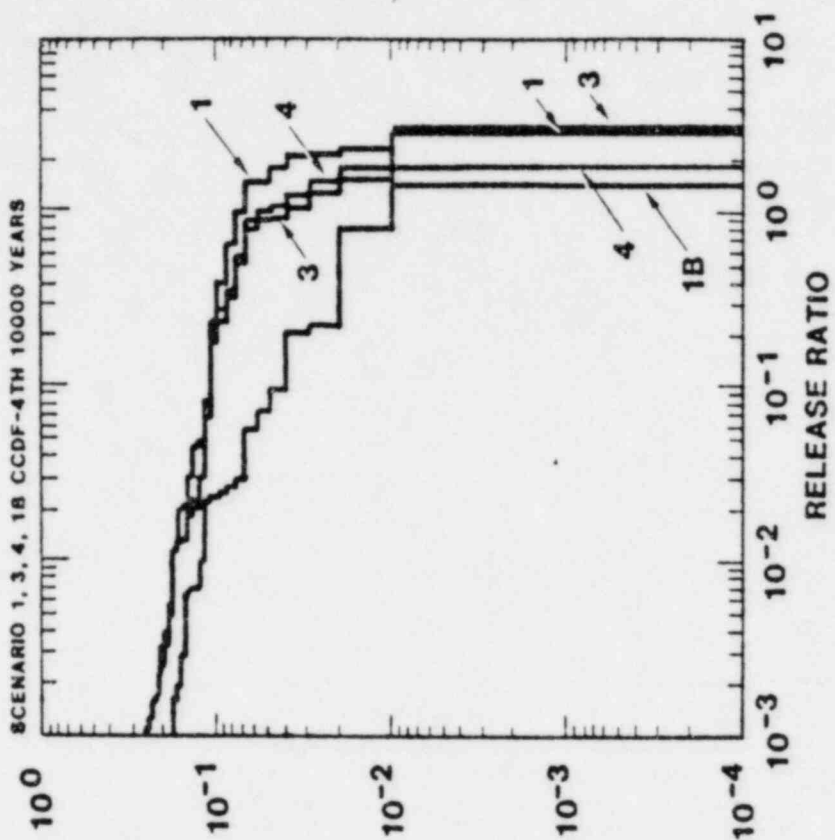


Figure 8.c

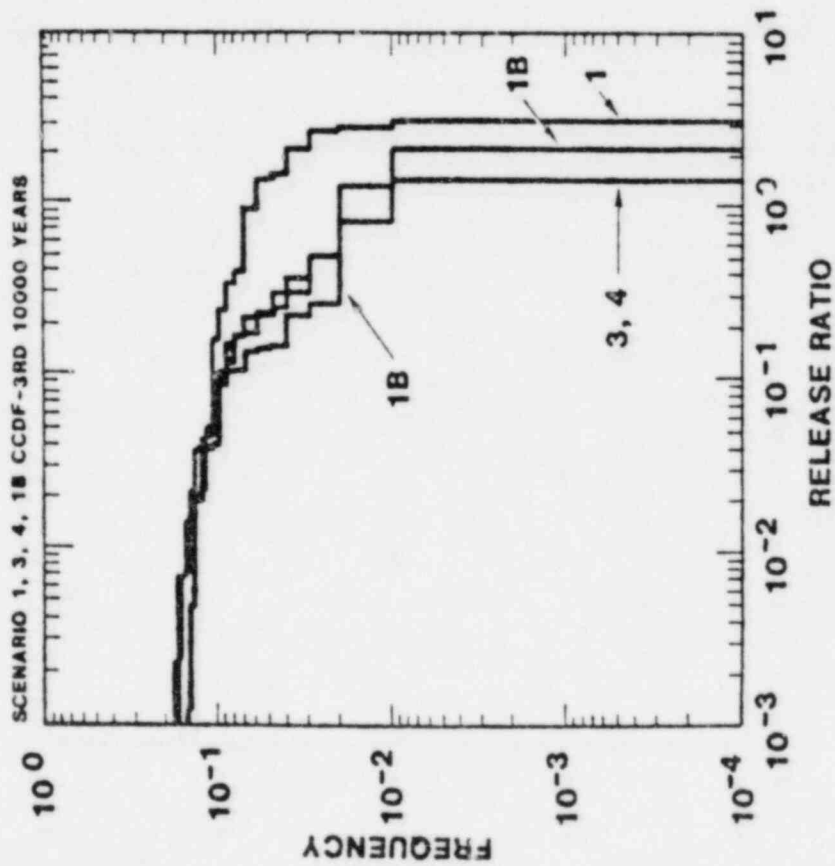


Figure 8.d

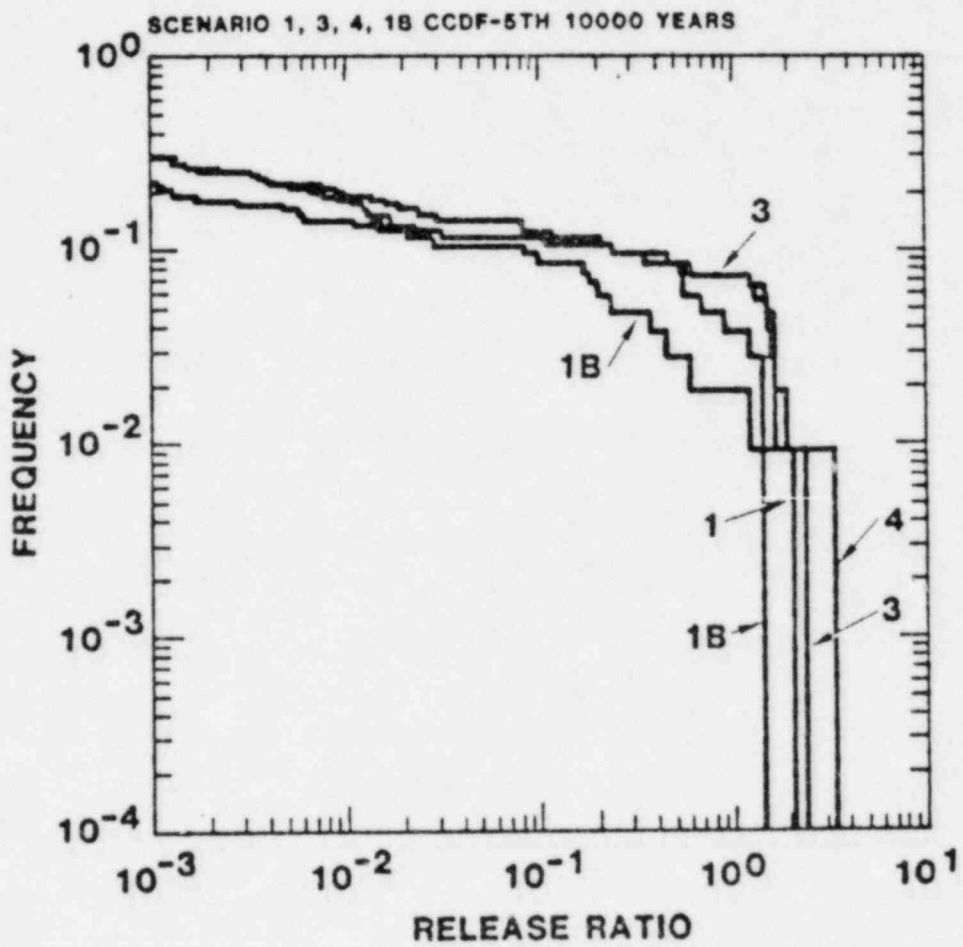


Figure 8.e

Table 7

NUMBER OF VIOLATING VECTORS, MAXIMUM OF RELEASE RATIOS AND SUM OF RELEASE RATIOS
OVER ALL VECTORS FOR EACH 10,000 YEAR PERIOD

Scenario	0-10,000yr	10,000-20,000yr	20,000-30,000yr	30,000-40,000yr	40,000-50,000yr
1	1*	4	7	8	4
	2.4**	5.9	3.1	2.9	2.0
	2.5***	12.1	16.5	17.0	10.7
3	1	1	1	4	8
	1.9	6.2	1.4	3.1	2.3
	2.2	10.2	4.8	12.0	14.4
4	1	1	1	6	8
	1.9	6.1	1.4	1.5	3.4
	2.1	10.1	4.6	10.6	15.6
1B	1	1	2	1	2
	1.7	3.9	2.2	1.5	1.5
	1.8	5.7	5.0	3.1	5.2

* number of violating vectors

** maximum release ratio

*** sum of release ratios

Table 8
 PROPERTIES OF VECTORS WHICH VIOLATE EPA STANDARD
 IN SCENARIO 1B

VECTOR	3	24	51
PARAMETER			
Maximum R* for Tc	10827	7570	14364
Average vertical darcy velocity (ft/yr)	0.32	0.13	0.41
Vertical hydraulic gradient	0.04	0.03	0.03
Average horizontal darcy velocity (ft/yr)	0.17	0.88	0.36
Horizontal hydraulic gradient	0.02	0.08	0.02
Total groundwater travel time (yr)	10197	3781	6069
Discharge** (ft ³ /yr)	2.7x10 ⁷	1.1x10 ⁷	3.6x10 ⁷
Maximum release ratio***	1.2	3.9	1.5

*R = retardation factor

**annual recharge of regional ground water system is approximately 5x10⁸ ft³/yr

***maximum during 50,000 year period

6.3 Scenario 5: - Effects of changes in the water table

In scenario 5, the water table has risen 300 feet during a pluvial period and occurs in the densely welded tuff of layer H. Radionuclides migrate from the depository to this layer under the influence of the vertical hydraulic gradient (Figure 9). The zeolitized tuff of layer G is not a barrier to horizontal radionuclide migration in this scenario. In this calculation we have assumed that no retardation occurs in layer H. Ground water and dissolved radionuclides are pumped from the aquifer from a well located one mile from the depository. In all other respects, this scenario is equivalent to scenario 1.

Scenario 5B (Figure 10) differs from scenario 5 by the inclusion of matrix diffusion in calculations of radionuclide retardation in the moderately and densely welded layers A, C, E, F, and H. As in scenario 1B, retardation by matrix diffusion was considered only for ^{129}I , ^{99}Tc , and ^{14}C .

Results

The results of the calculations for scenario 5 are presented in Figures 11A-11E and in Table 9. It can be seen that the lack of retardation in the horizontal transport leg has resulted in discharges that are much larger than those calculated for scenario 1. Violation of the EPA Release limit results from discharges of ^{236}U , ^{233}U , ^{235}U , ^{238}U , ^{234}U , ^{228}Ra , ^{237}Np , ^{99}Tc , and ^{14}C . In the first 10,000 year period, discharge is entirely due to releases of ^{99}Tc and ^{14}C .

After 30,000 years, releases of other radionuclides comprise the major part of the discharge.

Results from scenario 5B are summarized in Figures 11A-11E and in Table 9. Matrix diffusion decreases the discharges of ^{99}Tc and ^{14}C to levels below the EPA release limit during the first 10,000 years. After 20,000 years, the release of ^{236}U , ^{228}Ra , ^{237}Np , ^{233}U , ^{229}Th , ^{238}U , ^{234}U , ^{210}Pb , ^{235}U and ^{227}Ac exceed the EPA Standard.

The properties of the vectors which violate the EPA Standard in scenario 5B are described in Table 10. The large radionuclide releases associated with vectors 3, 24, and 51 are due to their large groundwater discharge and short travel times. In vectors 72 and 85, the high horizontal darcy velocity is indicative of the short travel time associated with the horizontal legs

SCENARIO 5

1 mile well; moderate = fractured; thermal buoyancy; pluvial

LEG	LAYERS	WELDING - RETARDATION	LENGTH (ft)
1	A	dense - no retardation	200 v
2	B	nonwelded - porous - zeolites	300 v
3	C	dense - no retardation	250 v
4	D	non-welded - porous - zeolites	150 v
5	E	moderate - no retardation	180 v
6	F	moderate - no retardation	270 v
7	G	nonwelded - porous - zeolites	475 v
8	H	dense - no retardation	5280 h

FLOW PATH

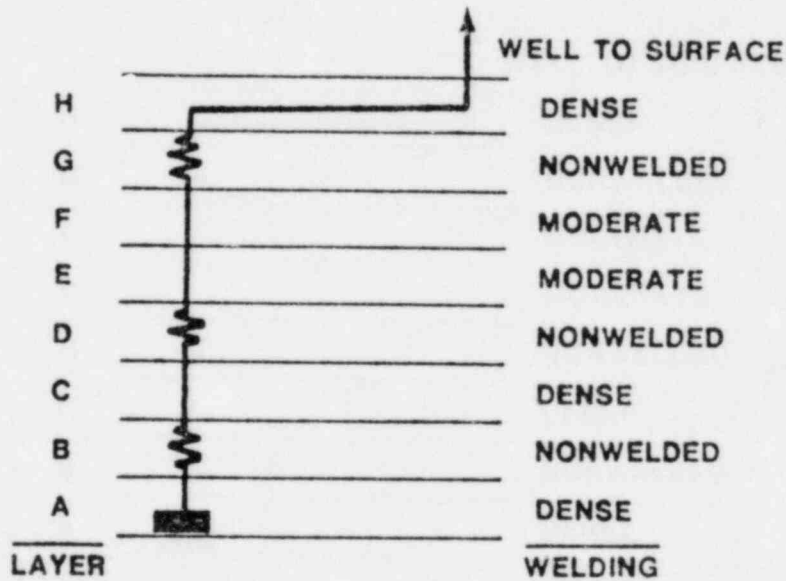


Figure 9

SCENARIO 5B

1 mile well; matrix diffusion; thermal buoyancy; pluvial

LEG	LAYERS	WELDING - RETARDATION	LENGTH (ft)
1	A	dense - matrix diffusion	200 v
2	B	nonwelded - porous - zeolites	300 v
3	C	dense - matrix diffusion	250 v
4	D	non-welded - porous - zeolites	150 v
5	E	moderate - matrix diffusion	180 v
6	F	moderate - matrix diffusion	270 v
7	G	nonwelded - porous - zeolites	475 v
8	H	dense - matrix diffusion	5280 h

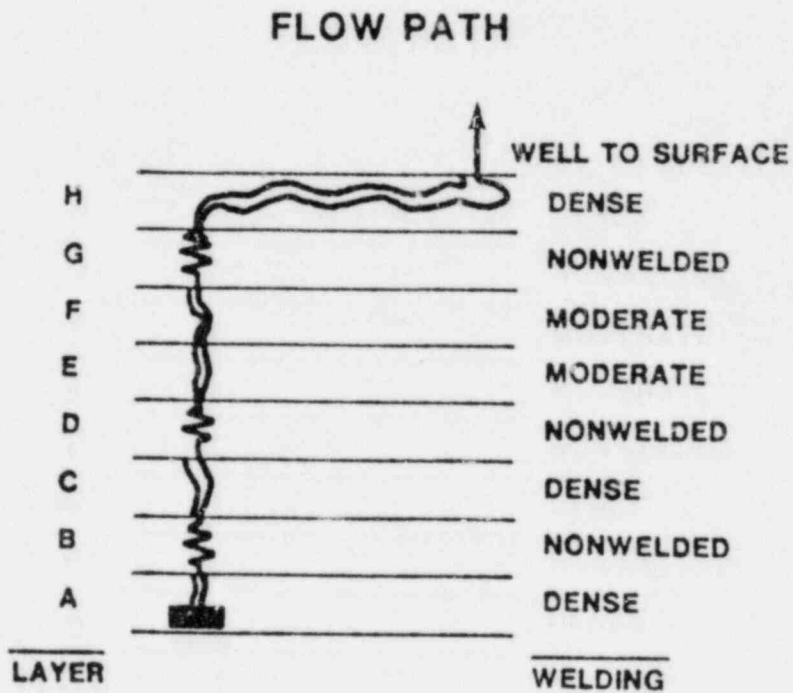


Figure 10

Table 9

NUMBER OF VIOLATING VECTORS, MAXIMUM OF RELEASE RATIOS AND SUM OF RELEASE RATIOS
OVER ALL VECTORS FOR EACH 10,000 YEAR PERIOD

Scenario	0-10,000yr	10,000-20,000yr	20,000-30,000yr	30,000-40,000yr	40,000-50,000yr
5	3*	6	11	14	16
	7.9**	6.2	20.9	43.7	54.0
	13.4***	29.6	54.2	102.1	178.8
5B	0	1	3	4	4
	0.90	2.1	19.3	42.1	53.4
	1.1	5.9	28.8	75.9	153.0
6	0	1	1	4	3
	0.1	1.5	1.6	4.4	2.2
	0.1	2.5	3.7	12.5	7.6
2	11	14	19	20	19
	207	85	87	57	55
	667	392	461	424	434
2B	8	10	16	17	19
	22	24	21	20	21
	62	114	116	123	130

* number of violating vectors

** maximum release ratio

*** sum of release ratios

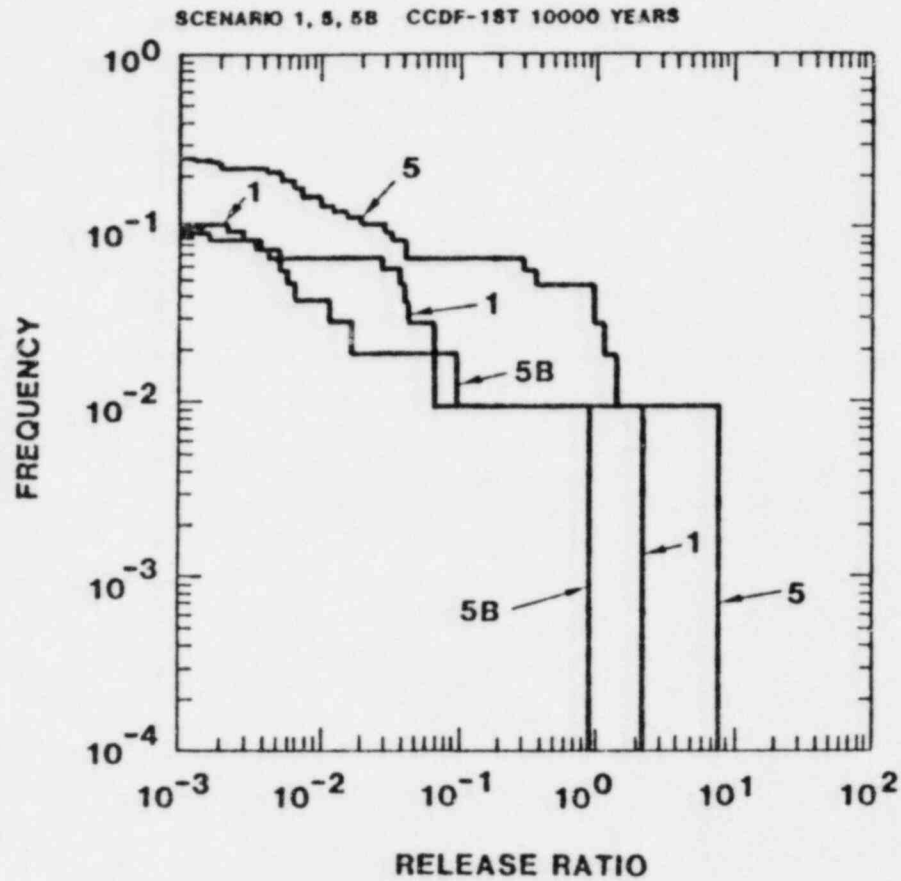


Figure 11a.

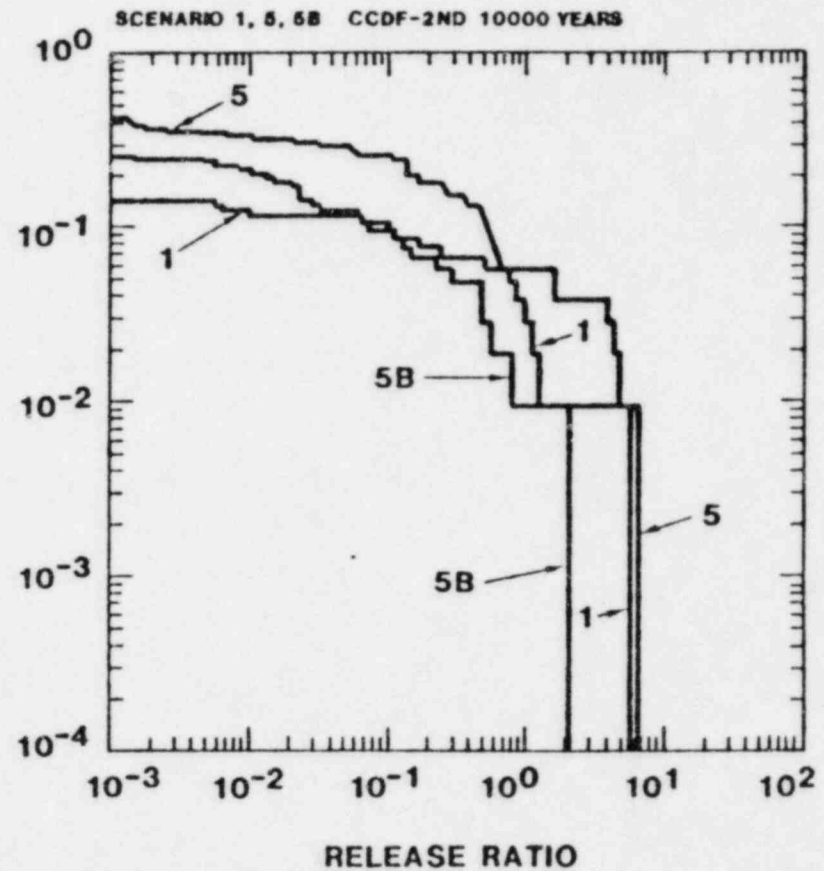


Figure 11b.

Figure 11. Complementary Cumulative Distribution Functions for Scenarios 1, 5 and 5B: Effects of Changes in the Water Table on Discharge.

1 = base case; 5 = water table rise; 5B = water table rise with matrix diffusion.

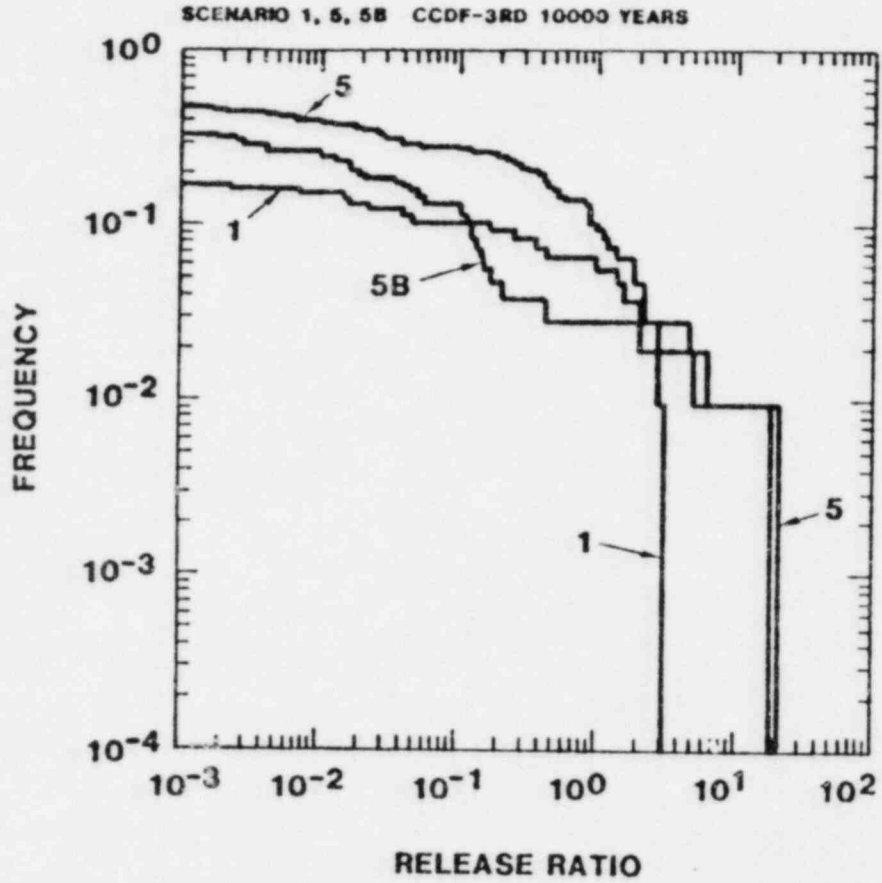


Figure 11.c

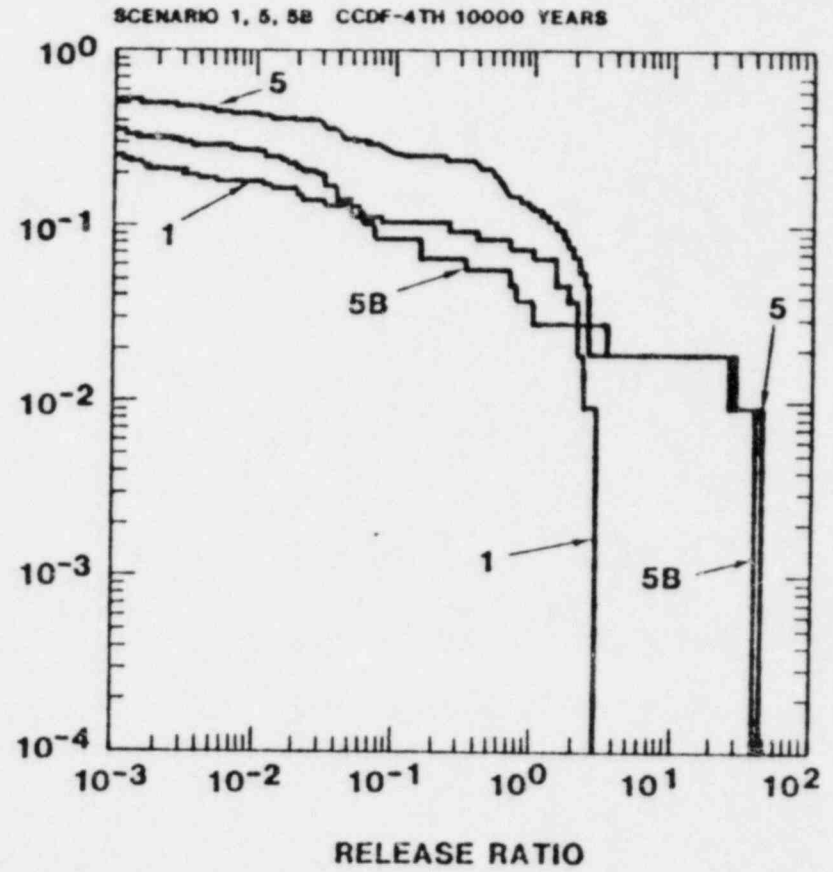


Figure 11.d

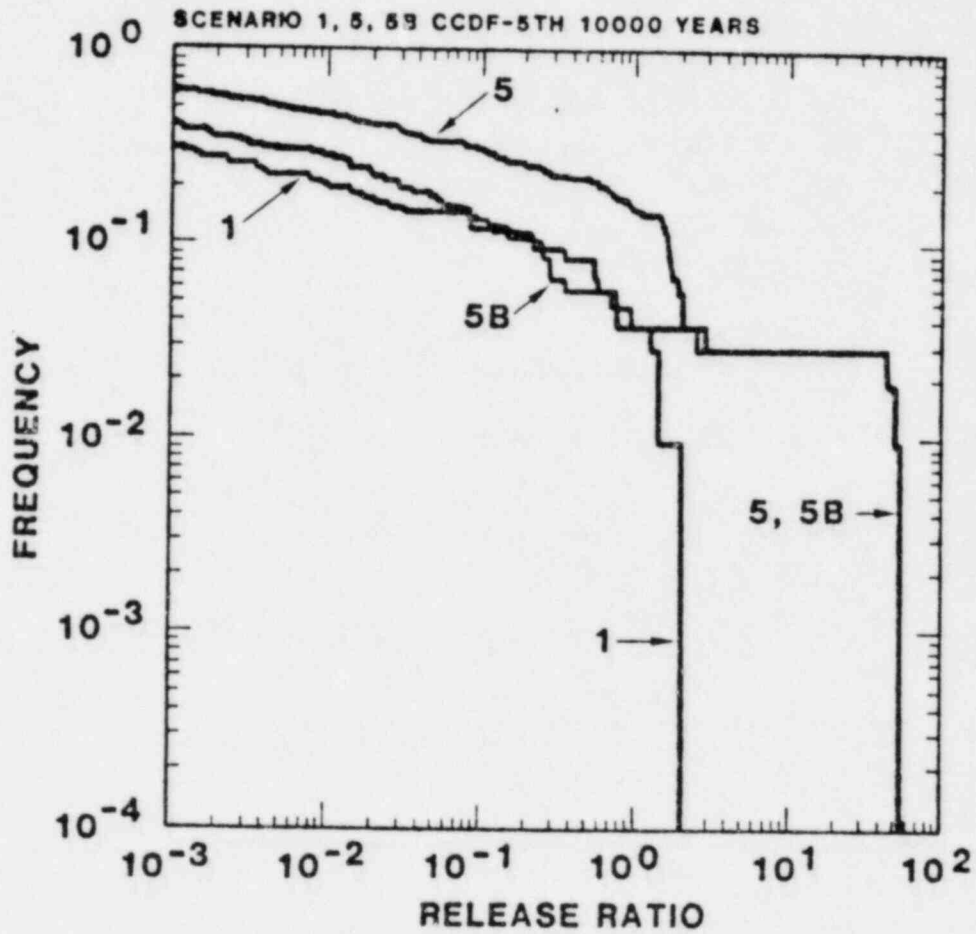


Figure 11.e

Table 10

PROPERTIES OF VECTORS WHICH VIOLATE EPA STANDARD
IN SCENARIO 5B

VECTOR	3	24	51	72	85
<hr/>					
PARAMETER					
Maximum R for U	32	27	23	47	35
Maximum R for Np	41	37	39	52	68
Maximum R for Tc	10827	20063	26659	13866	14888
Average vertical darcy velocity (ft/yr)	0.3	0.16	0.43	0.04	0.07
Vertical gradient	0.04	0.03	0.03	0.03	0.04
Average horizontal darcy velocity (ft/yr)	0.03	0.002	2×10^{-4}	1.5	169
Horizontal gradient	0.02	0.08	0.02	0.02	0.03
Total groundwater travel time (yr)	1024	2585	2203	7877	4939
Discharge (ft ³ /yr)	2.7×10^7	1.4×10^7	3.8×10^7	3.5×10^6	6.1×10^7
Maximum release ratios					
U234	16	26	19	0	0
Np237	8.7	7×10^{-5}	12	0	0
Tc99	0	0	0	2.6	3.5
TOTAL	44.4	48.7	53.4	2.6	3.5

(0.03-0.6yr). Although the retardation factors for Tc in leg 8 are high for these vectors (5076 and 2569 respectively), the high darcy velocity indicates that this leg is not a barrier to migration of this radionuclide.

6.4 Scenario 6 - Accessible environment at eight miles

At the hypothetical repository site, the water table passes from the nonwelded zeolitized aquitard (layer G) into the overlying densely welded aquifer (layer H) at a distance of approximately two miles from the depository. In scenario 6, we have postulated that a well eight miles from the depository withdraws ground water and radionuclides from this aquifer. This scenario differs from scenario 1 by the additional one mile transport in the nonwelded unit and by six miles of transport in the densely welded tuff layer. No retardation occurs in the densely welded layer.

Results

The results of the calculation are presented in Figures 13A-13E and in Table 9. It can be seen that the additional seven miles of travel through layers G and H reduce the discharge during the first 10,000 years to levels below the EPA release limit. Discharges of the unretarded radionuclides ^{99}Tc and ^{14}C in vectors 12, 76, 77, and 105, however, exceed the EPA limit after 10,000 years. Due to time constraints, the effect of matrix diffusion on discharge was not calculated for the flow path of scenario 6. It was shown previously in scenario 1B that matrix diffusion in 900 feet of welded tuff decreased the discharge of ^{99}Tc and ^{14}C for the above vectors below the EPA Standard. It can be assumed, therefore, that matrix diffusion would eliminate all violations of the EPA Standard for a flow path similar to scenario 6.

SCENARIO 6

8 mile well; moderate = fractured; thermal buoyancy; no pluvial

LEG	LAYERS	WELDING - RETARDATION	LENGTH (ft)
1	A	dense - no retardation	200 v
2	B	nonwelded - porous - zeolites	300 v
3	C	dense - no retardation	250 v
4	D	non-welded - porous - zeolites	150 v
5	E	moderate - no retardation	180 v
6	F	moderate - no retardation	270 v
7	G	nonwelded - porous - zeolites	11000 h
8	H	dense - no retardation	31000 h

FLOW PATH

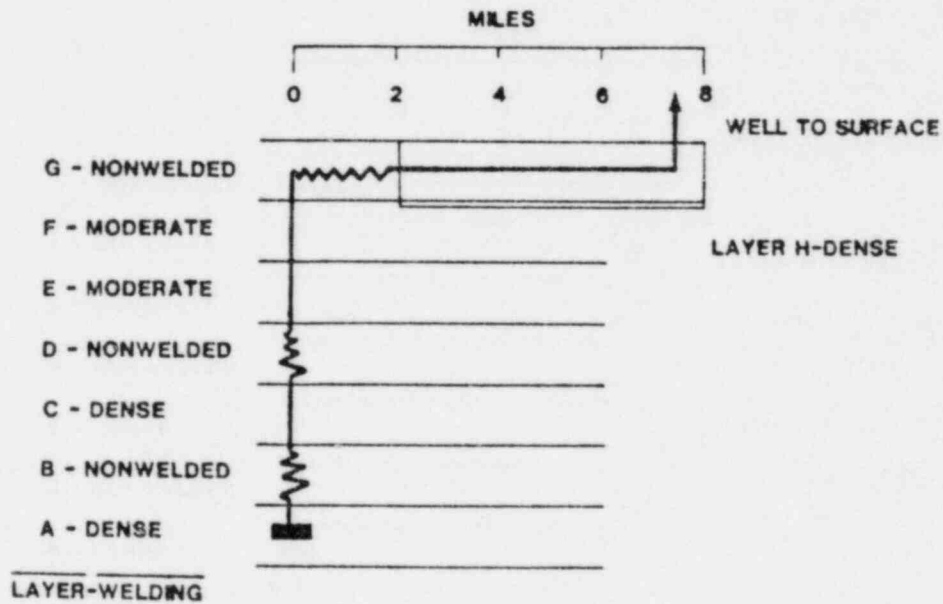


Figure 12

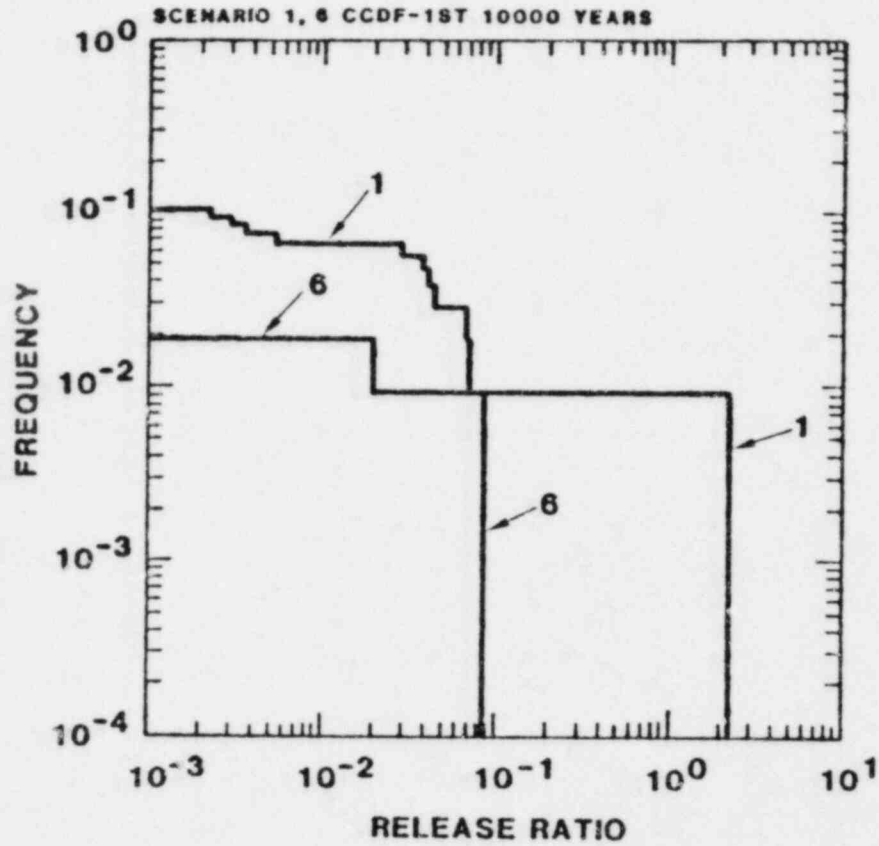


Figure 13.a

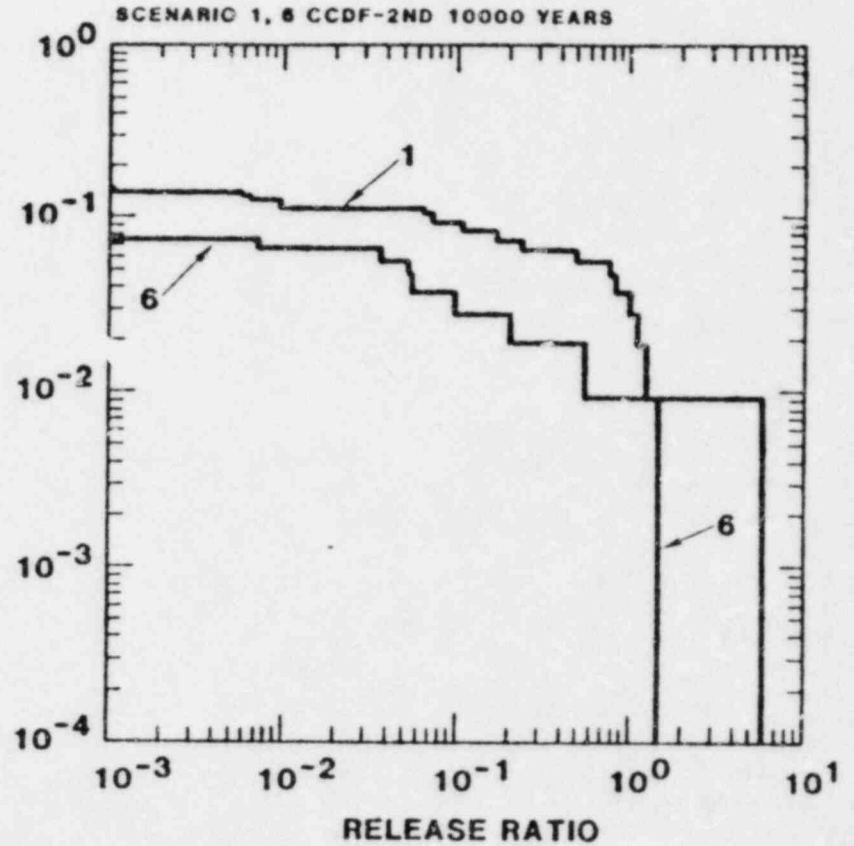


Figure 13.b

Figure 13. Complementary Cumulative Distribution Functions for Scenarios 1 and 6: Accessible environment at eight miles.

1 = base case; 6 = 8 miles

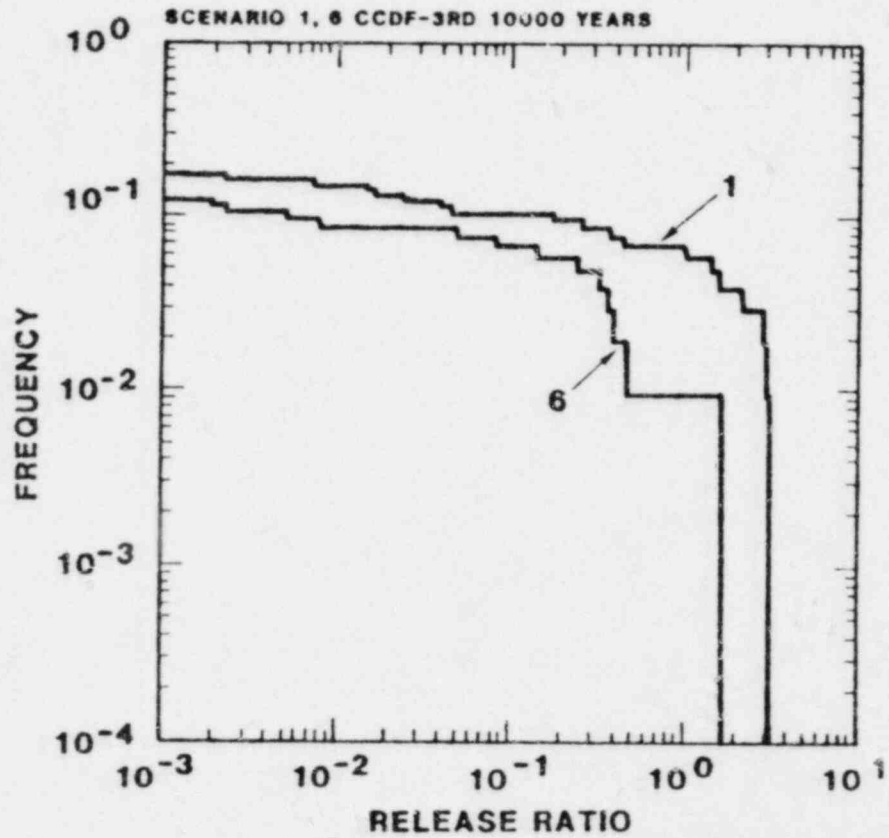


Figure 13.c

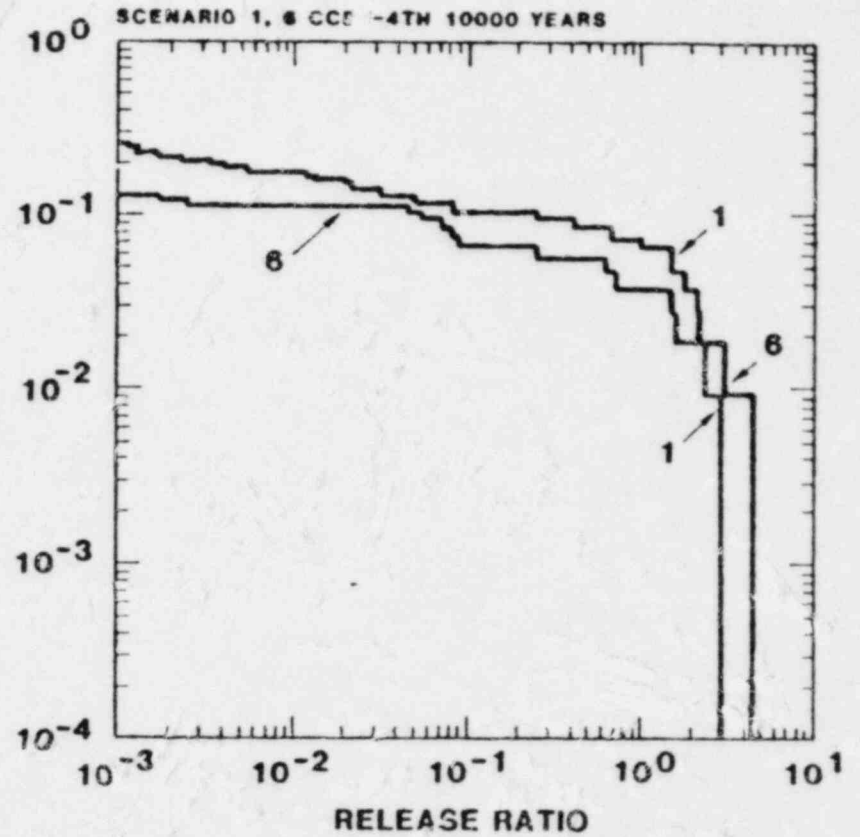


Figure 13.d

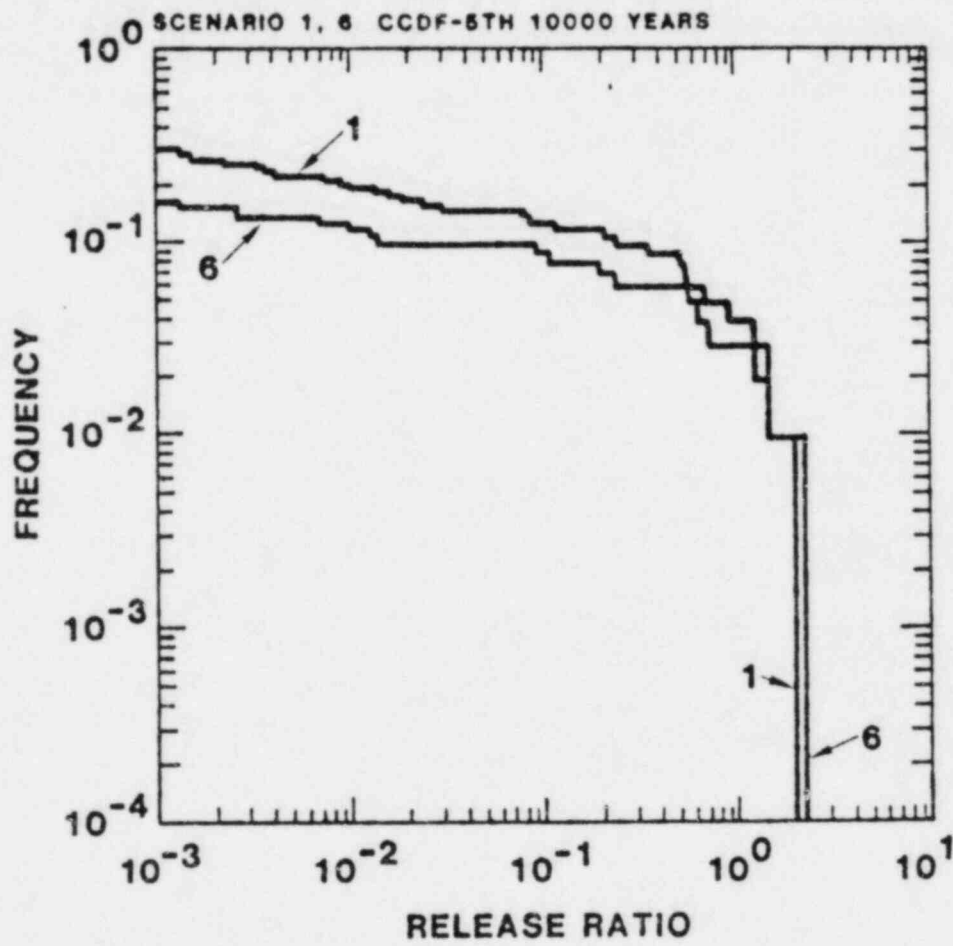


Figure 13.e

6.5 Scenarios 2 and 2B - Importance of solubility limits to discharge

We consider scenario 2 (Figure 14) our "worst case" scenario. The source term is entirely leach-limited; the solubility limits of radionuclide are not specified. Ground water migrates laterally from the depository. Due to the block faulting and dip of the tuff units in the repository site, the lateral fluid flow path cuts across several stratigraphic layers. At a distance of one mile from the depository, water and radionuclides are pumped by a well that extends to a depth of 3,000 feet. Technitium, ^{129}I and ^{14}C are retarded by matrix diffusion in the densely welded layers A and C. Layer B is highly sorbent zeolitic tuff which retards the movement of the other isotopes. This scenario has a shorter path length and thinner sequence of zeolitized tuff than the other scenarios.

Scenario 2B differs from scenario 2 only in the calculation of the source term. We have used the mixing-cell option at NWFT/DVM for this scenario (17,23). For each time step, the mass of a radionuclide that is assumed leached from the waste form is compared to the maximum amount that is consistent with a user-specified solubility limit. The solubility limits are listed in Table 5 and are discussed in detail in section 4.3 and in Appendix B. The smaller of these two amounts of radionuclide is transported in that time step.

Results

Results of calculations for scenarios 2 and 2B are summarized in Figures 15A-15E and in Table 9. Discharges in scenario 2 are the highest calculated in this study and lead to large violations of the EPA Standard. During the first 10,000 years, releases of ^{234}U , ^{237}Np , ^{238}U and ^{236}U account for 94 percent of the sum of the EPA release ratios. During the fifth 10,000 year interval they continue to dominate discharge and account for 85 percent of the violation of the EPA Standard. The importance of solubility limits in controlling discharge in scenario 2B can be seen in the figures and table. The sum of the release ratios for all uranium species is reduced by an order of magnitude and Np discharge is decreased by a factor of 30 for the first 10,000 year interval. Discharge of these radionuclides, however, still are in excess of the EPA standard. The solubilities that were assumed for uranium and neptunium were based on experimental studies under oxic conditions. They are upper bounds for the solubilities; under reducing conditions the solubilities of U and Np are 8 and 3 order of magnitudes lower respectively. We feel that the

SCENARIOS 2 and 2B

1 mile borehole; matrix diffusion; no thermal buoyancy or pluvial

LEG	LAYERS	WELDING - RETARDATION	LENGTH (ft)
1	A	dense - matrix diffusion	2600 h
2	B	nonwelded - zeolitized	300 v
3	C	dense - matrix diffusion	2600 h

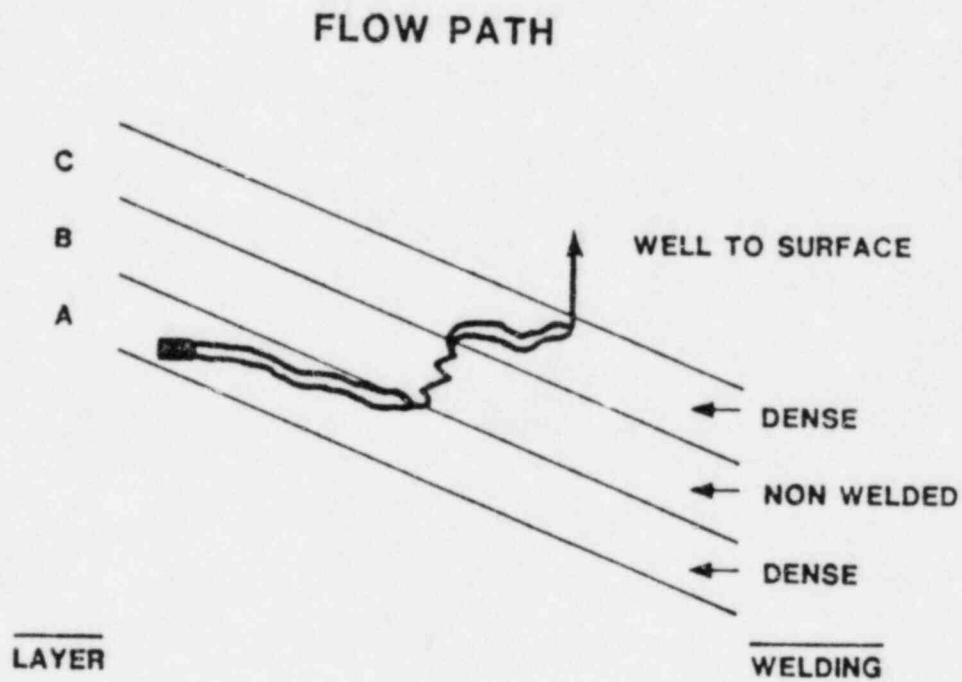


Figure 14

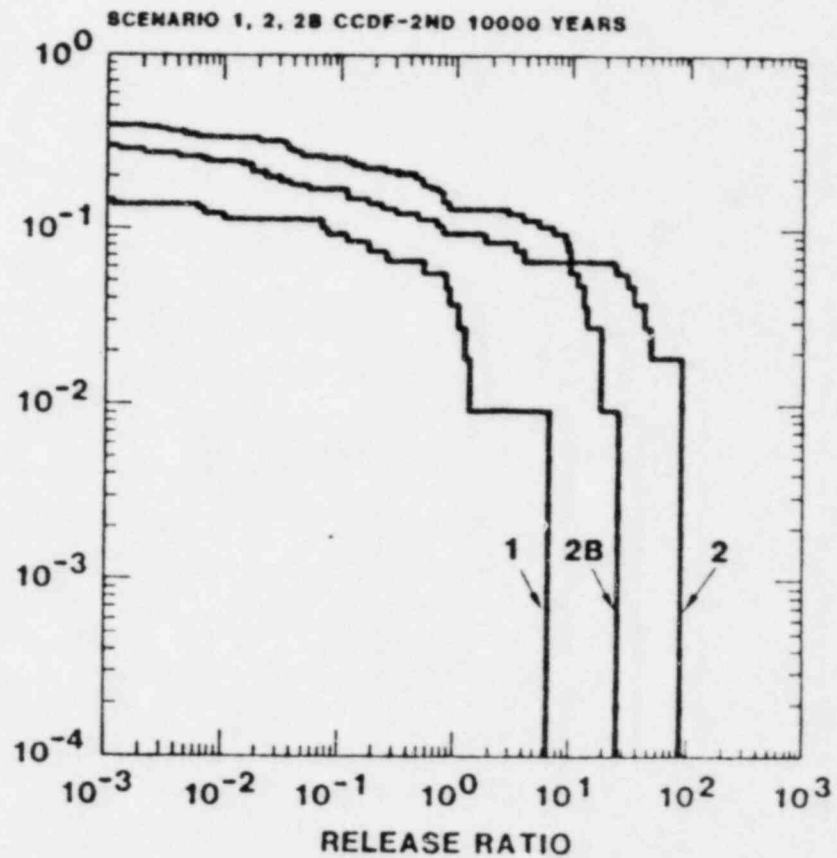
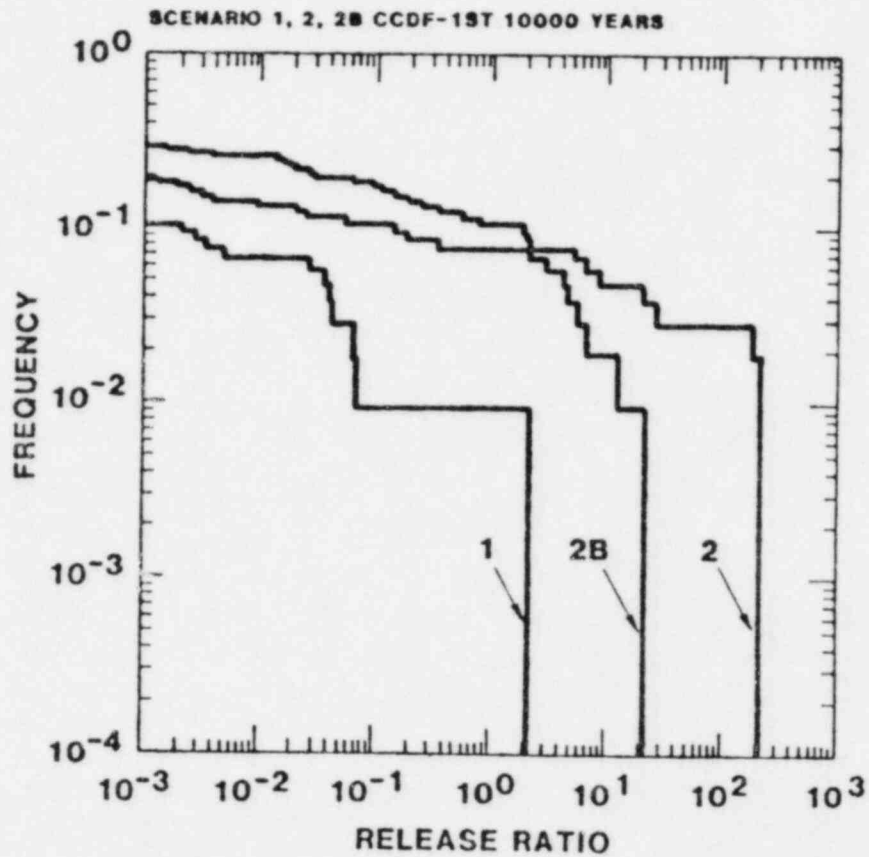


Figure 15.a

Figure 15.b

Figure 15. Cumulative Complementary Distribution Functions for Scenarios 1, 2 and 2B: Importance of Solubility Limits to Discharge.

1 = base case; 2 = leach limited; 2B = solubility-limited

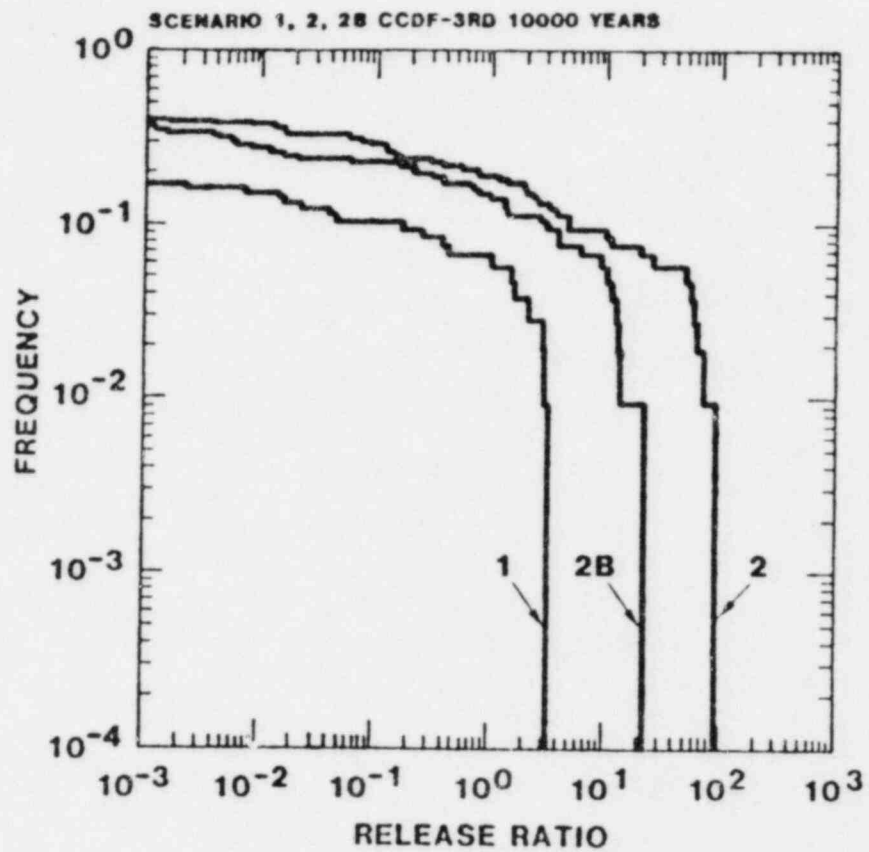


Figure 15.c

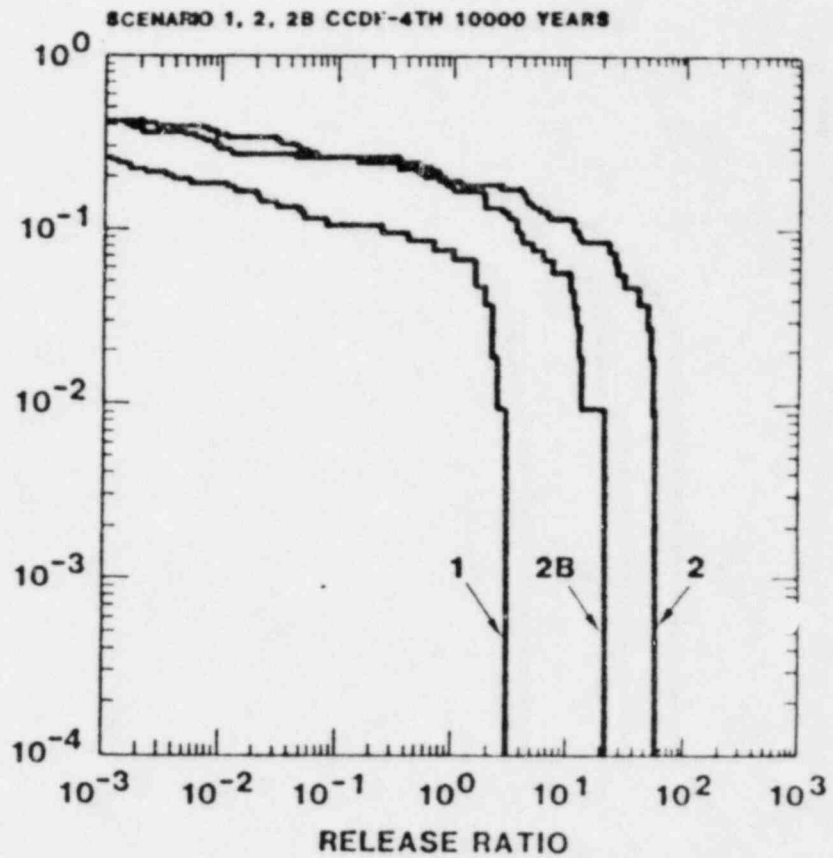


Figure 15.d

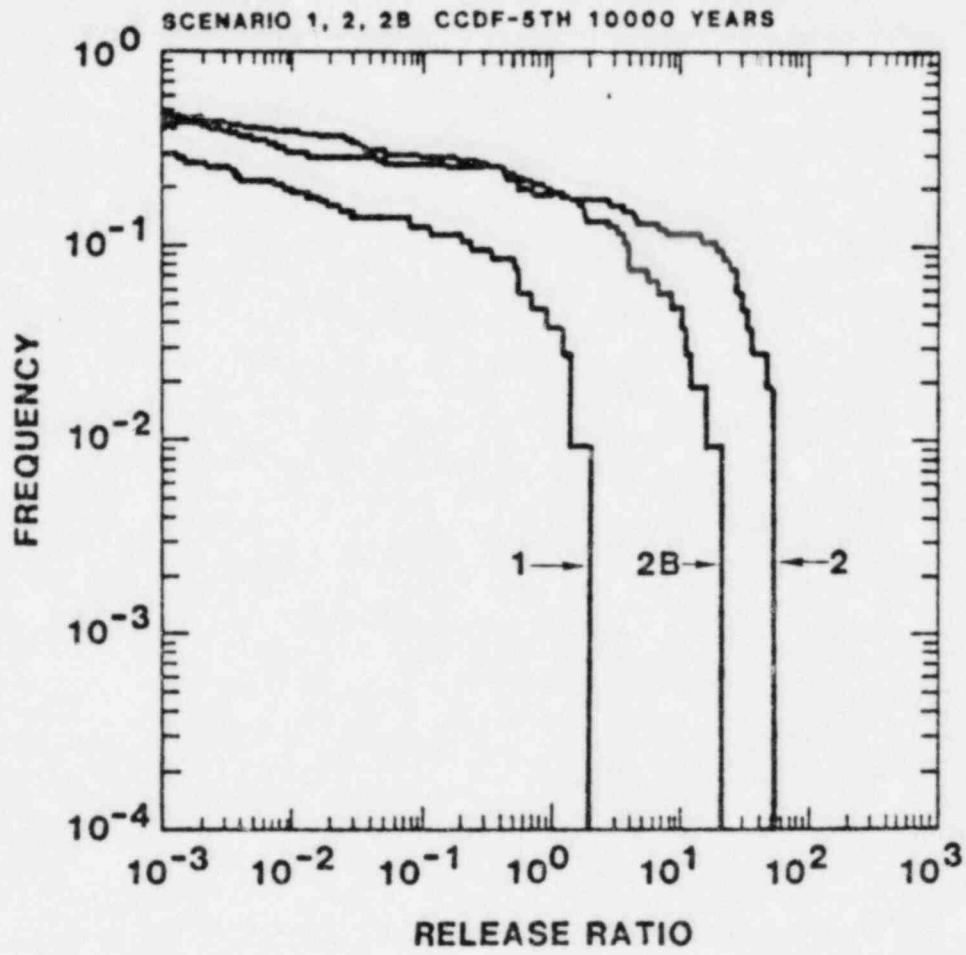


Figure 15.e

transport of radionuclides along the flow path described in scenarios 2 and 2B is less likely than transport as described in the other scenarios. The calculated violations of the EPA Standard, therefore, should not be interpreted as an indication that releases from a repository in tuff are likely.

7. CONCLUSIONS AND RECOMMENDATIONS

Estimates of potential radionuclide releases from HLW storage facilities in geologic formations are an integral part of the technical basis for the regulation of nuclear waste disposal. At present, the available data is insufficient to accurately model any real repository sites. Large uncertainties exist in the characterization of the solubilities and sorption of radionuclides, in the description of the regional and local hydrogeology and in the mathematical treatment of containment transport in the presence of fracture flow and matrix diffusion. We feel, however, that it is possible to place realistic upper limits on radionuclide discharge for a generic hypothetical tuff repository. We have also attempted to assess the importance of the variation of several variables and model assumptions to the calculations of radionuclide release from a repository in the saturated zone of a volcanic tuff site.

Our calculations suggest the following conclusions for the hypothetical tuff repository described in this paper:

- 1) Sorption of radionuclides by several thousand feet of zeolitized tuff may be a sufficient barrier to migration of actinides even in the absence of solubility constraints.
- 2) All violations of the EPA Draft Standard in the "base case" are due to discharge of ^{99}Tc and ^{14}C . Retardation due to matrix diffusion, however, could eliminate discharge of the nuclides for realistic groundwater flow rates.
- 3) If the radionuclides do not flow through thick sequences of zeolitized tuff, discharges of U and Np under oxidizing conditions may be much larger than the EPA limits. Under reducing conditions, however, the low solubilities of these elements may reduce discharges of these elements to levels below the EPA limit.

We feel that the following topics merit further investigation by the NRC:

- 1) Detailed calculations of limiting solubilities of uranium, neptunium and radium under geochemical conditions expected at the tuff site.

- 2) Calculations of the potential retardation of actinides due to matrix diffusion in welded tuff.
- 3) Calculations of the sensitivity of radionuclide discharges on assumptions about radionuclide speciation.
- 4) A study of the frequency of oil and water drilling and mineral exploration in area like Yucca Mountain. All of the scenarios examined in this involve human intrusion. A study of the probability of such activities in areas like Yucca Mountain would yield valuable insights about the safety of such a repository site.

APPENDIX A

HYDROGEOLOGICAL MODEL OF THE HYPOTHETICAL TUFF REPOSITORY SITE AND ITS RELATIONSHIP TO DATA FROM THE NEVADA TEST SITE

A major objective in the program of simplified repository analyses performed at Sandia is the definition of a hypothetical site which exhibits hydrogeological characteristics which might be found at real potential repository sites. We have defined our reference tuff site to be consistent with available hydrogeologic data from the Nevada Test Site. Where certain data are not available from the real site, we have postulated properties that are physically reasonable for the reference site. We have not attempted to accurately represent the Nevada Test Site in our analyses; instead we have modelled a hypothetical site which is internally self-consistent.

A.1 Physical properties of welded tuff

The tuff units at the reference tuff repository are described as densely welded, moderately welded or non-welded. Densely welded tuff units are highly fractured; the blocks between fractures have low interstitial matrix porosity. Non-welded tuff units have few fractures but have a high matrix porosity. This dual porosity of the rock must be considered when modeling fluid flow. We have used data from the UE25a-1 drill core log to obtain reasonable values of fracture density, aperture width and orientation in the tuff units (1,2). The maximum, minimum and median of the range of values of these parameters for different tuff lithologies are shown in Table A-1.

We have represented the fracture system as two sets of perpendicular vertical fractures. Values of horizontal fracture porosity (ϵ_h) here calculated by

$$\epsilon_h = N_a b / \sin (90^\circ - \theta)$$

where N_a is the observed fracture density in the core, θ is an estimate of the average inclination of the fractures from the horizontal plane, and b is the fractures aperture width observed under a petrographic microscope. Horizontal hydraulic conductivity for a parallel array of planar fractures is given (24) by:

$$K_H = \left(\frac{\rho g}{\mu} \right) \left(\frac{N_a b^3}{2 \sin 90 - \theta} \right)$$

where:

- ρ = density of water = 1.0 gm/cm³
- g = 9.81×10^4 cm² sec⁻¹
- μ = viscosity of water = 1.0 centipoise

In our joint system, fluid flowing in the horizontal direction will effectively encounter only one set of fractures. Fluid flowing in the vertical direction will encounter both sets of fractures. For this reason, values of hydraulic conductivity and fracture porosity in the vertical direction are twice the horizontal values.

The hydraulic conductivity is very sensitive to changes in fracture aperture. In welded zones, the majority of fractures were 5-20 microns wide; the maximum observed width was 150 microns. Fractures in non-welded zones were generally filled with secondary minerals. For these units, aperture widths of 0-5 microns are probably realistic and were used to estimate the hydraulic properties in Table A-1. Results of calculations using a 150 microns aperture width are also shown in the table. Ranges of values of total porosity are presented and are taken from data in References 4 and 25.

In Figure A-1, the ranges of values of matrix hydraulic conductivity of unfractured cores of tuff measured in the laboratory are compared to the values calculated from fracture properties. The values are based on data compiled in References 4, 22, and 25. Values of the bulk hydraulic conductivity as measured by actual pump tests at the Nevada Test Site are also shown. Data obtained in these tests reflect contributions from fluid flow in both the fractures and in the rock matrix between joints. It can be seen that flow in fractures may dominate the bulk hydraulic conductivity of densely welded tuffs whereas fluid flow in the porous rock matrix dominates the properties of non-welded units. Both fracture flow and porous flow are important for moderately welded tuffs. The insights gained from Figure A-1 were used to estimate reasonable ranges for effective porosity and hydraulic conductivity for the Latin Hypercube Sample. The data ranges and the shape of their distributions are tabulated in Table 2 of the main text. The shapes of the frequency distributions were estimated by comparing the median values to the upper and lower limits of the data ranges of the different types of hydraulic conductivity and porosity.

A.2 Vertical Hydraulic Gradient

There are insufficient data in the open literature at present to estimate vertical hydraulic gradients at the Nevada Test

Table A-1
 PROPERTIES OF FRACTURED TUFF

	Densely Welded Tuff	Moderately Welded Tuff	Non-Welded Tuff
Fracture Aperture - b (microns)			
min	5	5	0
median	12	12	5
max	150	150	5 (150)
Apparent Fracture Density - N_a (ft^{-1})			
min	0.2	0	0
median	1.2	0.4	0.1
max	4.8	0.8	0.3
Inclination of Fractures from Horizontal (θ)			
	42°	45°	80°
Horizontal Fracture Porosity - c (%)			
min	4.4×10^{-4}	0	0
median	6.4×10^{-3}	2.2×10^{-3}	9.5×10^{-4}
max	0.32	0.06	2.8×10^{-3} (0.09)
Horizontal Fracture Hydraulic Conductivity (K_H)			
min	2.6×10^{-5}	0	0
median	2.1×10^{-3}	7.5×10^{-4}	5.5×10^{-5}
max	16.7	2.9	1.7×10^{-4} (4.5)
Total Porosity (%)			
	3-10	10-38	20-50

Site with an acceptable degree of certainty. In our reference site, we have assumed that the vertical gradient in the vicinity of the repository will be dominated by a thermal buoyancy gradient related to heat generated by the decay of the radioactive waste. The calculation of the thermal buoyancy gradient is described below.

Consider a cylindrical volume of fluid with length L and average temperature T immersed in a medium of average temperature T_0 ($T > T_0$), (Figure D-1). The difference in temperature produces an upward force on the volume of fluid. The velocity of the fluid in the cylindrical volume can be described (26) by:

$$v \sim \alpha \Delta T K \quad (A-1)$$

with

v = Darcy velocity of fluid

α = average coefficient of thermal expansion of fluid

$\Delta T = T - T_0$

K = hydraulic conductivity of medium

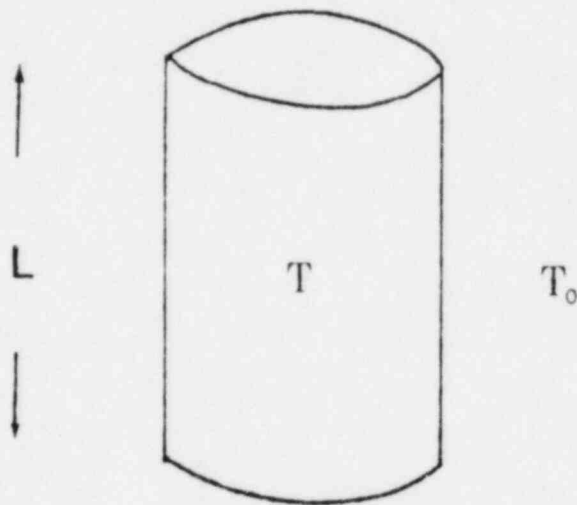


Figure (A-2)

Since Darcy velocity is equal to the product of hydraulic gradient (I) and conductivity, the upward gradient is given by

$$I = \alpha \Delta T \quad (A-2)$$

The temperature field around a repository in tuff for spent-fuel at 75 kW/Acre thermal loading has been calculated (3).

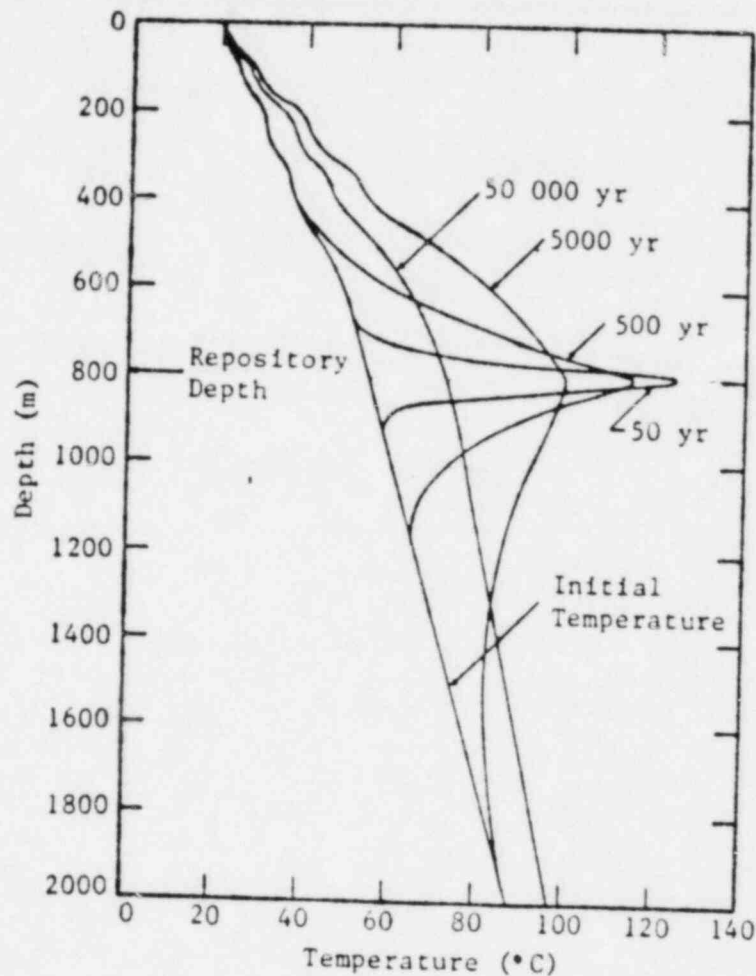


Figure (A-3) Far Field Temperature Profile Along the Vertical Centerline for GTL of 75 kW/Acre

Figure A-3 shows the temperature profile along the vertical centerline of the repository as a function of depth and time after closure. The "disturbed zone" is assumed to extend from the repository to 470 meters below surface where the water table lies. The average temperature of this disturbed zone is calculated by:

$$\bar{T} = \frac{1}{L} \int T \, dL$$

L is the distance from the repository to the water table and is equal to 330 meters. T_0 is the average background temperature of the same zone as calculated from the natural geothermal field. The ambient temperature at the repository horizon is 50°C. Under these assumptions, the hydraulic gradients calculated are shown in Table A-2:

Table A-2

<u>Time After Closure</u>	<u>\bar{T} (°C)</u>	<u>T_0 (°C)</u>	<u>α (1/°C)</u>	<u>Gradient</u>
500 y.	73°	50°	6.01×10^{-4}	1.4×10^{-2}
5,000 y.	85°	50°	6.68×10^{-4}	2.3×10^{-2}
50,000 y.	65.4°	50°	5.54×10^{-4}	8.5×10^{-3}

More recent field work indicates that the ambient rock temperature at the repository horizon will be 35°C (27). Table A-3 shows the calculated upward gradient when this temperature is assumed.

Table A-3

<u>Time</u>	<u>\bar{T} (°C)</u>	<u>T_0 (°C)</u>	<u>α (1/°C)</u>	<u>Gradient</u>
500 y.	73°C	30°C	6.01×10^{-4}	2.6×10^{-2}
5,000 y.	85°C	30°C	6.68×10^{-4}	3.7×10^{-2}
50,000 y.	65.4°C	30°C	5.54×10^{-4}	1.9×10^{-2}

Thermal histories at 307 and 711 meters below the surface for a repository with a 100 kW/Acre thermal loading have been calculated and are presented in Figure A-4 (27). From these curves, it is apparent that the peak temperature occurs before 10,000 years after closure of the facility. The hydraulic gradient at 500 years for an average ambient temperature of 50° was selected as a lower bound for our calculations. The gradient at 5,000 years with the average ambient temperature of 30° was used as the upper bound for the vertical hydraulic gradient. A range of vertical hydraulic gradients of 1×10^{-2} to 4×10^{-2} was sampled by the Latin Hypercube Sample technique for the transport calculations.

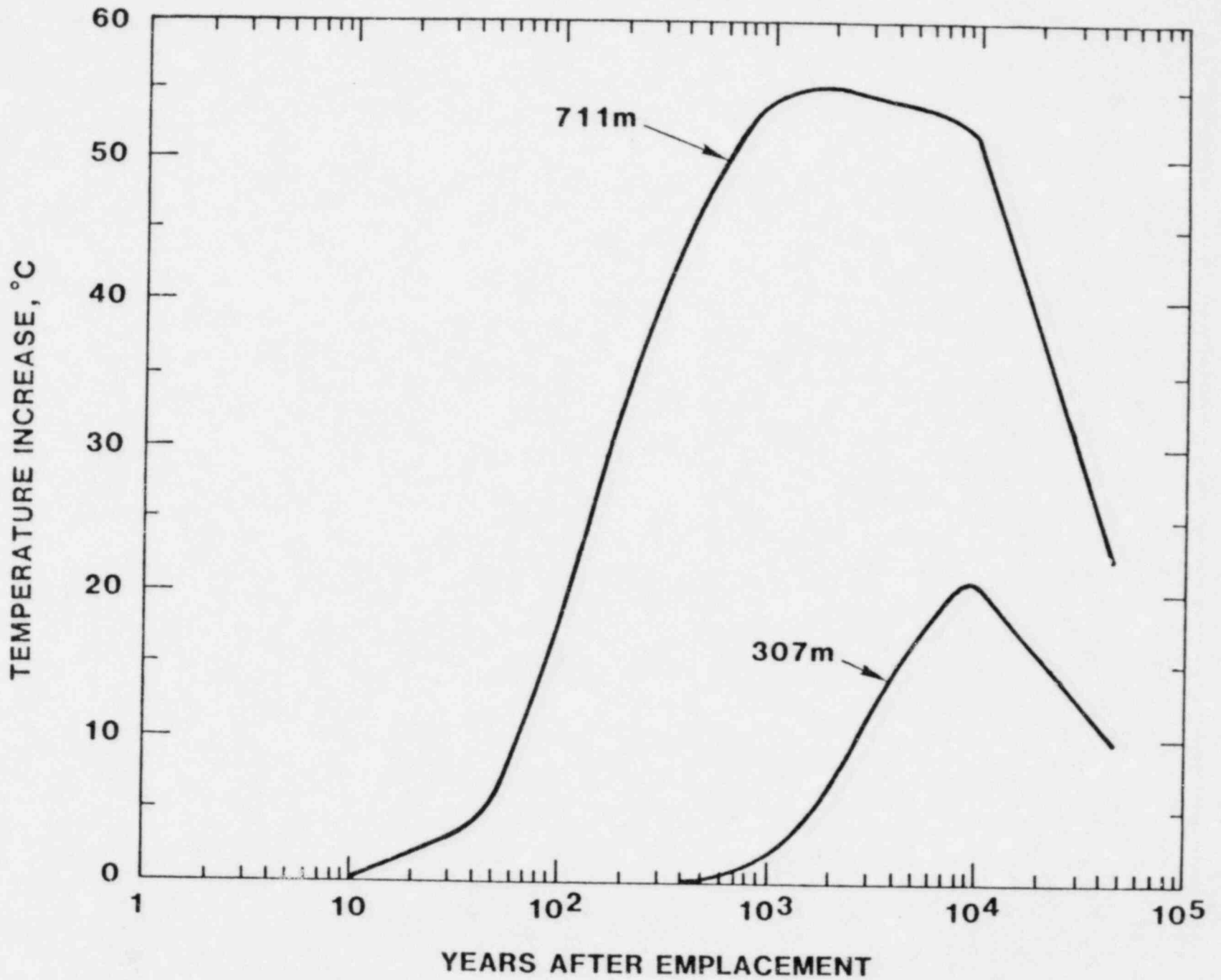


Figure A-4. Temperature increase histories at 307 and 711 meters below the surface of the earth for SF at 100 kW/acre.

The volume of annual recharge at the repository site places a constraint on the maximum flow through the repository under the influence of this thermal gradient. The maximum vertical discharge calculated from the vectors sampled by the LHS technique was 3.6×10^7 ft³/yr (vector #51). This is approximately 7 percent of the volume of ground water moving through the Pahute Mesa ground water system. The area of the repository comprises less than 0.1 percent of the area of this flow system. Although all of the recharge in this system is limited to areas above 5000 feet elevation, this volume of groundwater flow through the repository is probably unrealistically high. As discussed in Section 6 (Table 7), nearly all of the vectors whose radionuclides releases violated the EPA Standard in scenarios 1, 3, 4, 5, 6, 1B, and 5B were characterized by similarly unrealistic flows. Most of the other vectors considered in these calculations had ground water discharges at least an order of magnitude smaller than vector #51.

A.3 Horizontal Hydraulic Gradient

We have considered two contributions to the horizontal hydraulic gradient in our calculations. One component is the regional gradient of the undisturbed site. Static water levels from four wells near Yucca Mountain were used to estimate ranges of the regional horizontal gradient. Three of the wells have similar static water levels (~2400 ft) while the fourth and only well which is actually on Yucca Mountain has an anomalously high head (~3400 ft) (22, 28). The range of regional hydraulic gradients was set to span the highest and lowest valued that could be calculated from these data. The LHS routine, therefore, sampled a range of 10^{-1} to 10^{-3} .

The second component to the horizontal gradient is a local gradient related to the local rise in the water table above the repository due to the thermal bouyancy effect described previously. We can place an upper bound on this rise in water table (ΔZ) by assuming that the heated water in the cylinder described in Figure A-2 is constrained to expand only in the upward (Z) direction. By applying Archimedes Principle, we can show that the height of the heated cylinder can be related to the height of a cylinder of water of equal weight at the background temperature T_0 . Since the height of the cylinder of water at temperature T_0 equals the distance from the repository to the water table we can calculate ΔZ as follows:

$$w = \pi r^2 g \rho (L + \Delta Z) = \pi r^2 g \bar{\rho} L \quad \text{Archimedes Principle} \quad (\text{A-3})$$

$$\Delta Z = L(\rho/\bar{\rho} - 1) \quad (\text{A-4})$$

where

- $\rho, \bar{\rho}$ = average density of water at T_0 and T respectively
- L = height of cylinder of water at temperature T_0
- r = radius of cylinder of water
- ΔZ = rise of water table
- w = weight of water in both cylinders

If V equals the volume of the cylinder of water at temperature T_0 , then

$$w = \rho V = \bar{\rho} (V + \Delta V) \quad (\text{A-5})$$

$$\Delta V = \alpha V \Delta T \quad (\text{A-6})$$

$$\bar{\rho} = w/V(1 + \alpha \Delta T) = \rho / (1 + \alpha \Delta T) \quad (\text{A-7})$$

where ΔT and ΔV refer to differences in temperature and volume between the two cylinders and α is the average coefficient of thermal expansion of the fluid. Substituting (A-7) into (A-4) we obtain:

$$\Delta Z = L \alpha \Delta T \quad (\text{A-8})$$

We have shown that $\alpha \Delta T$ is equal to I_v , the vertical hydraulic gradient (equation A-2). We can therefore calculate ΔZ for each input vector in our calculations by using the value of I_v sampled by the LHS technique. The horizontal hydraulic gradient (I_H) used in our transport calculations is set equal to the sum of the regional gradient and the local gradient:

$$I_H = I_{HS} + I_v L/X \quad (\text{A-9})$$

where:

- I_{HS} = value of regional horizontal hydraulic gradient sampled by the LHS
- I_v = value of vertical gradient sampled by LHS
- L = sum of vertical leg lengths in transport path
- X = sum of horizontal leg lengths in transport path

APPENDIX B

GEOCHEMISTRY AND RADIONUCLIDE RETARDATION

B.1 - Geochemical environment of the hypothetical tuff site

The mineralogy of each rock unit at the hypothetical tuff site is described in Table 1. The mineralogy and chemical composition of a tuff unit depend in part upon its cooling history and degree of post-depositional alteration. Vitric tuffs are porous tuffs which are composed of pumice or fragments of glass shards which have undergone a moderate to slight degree of welding. Their chemical composition is simple; the sum $\text{SiO}_2 + \text{Al}_2\text{O}_3 + \text{K}_2\text{O} + \text{Na}_2\text{O}$ is greater than 95 weight percent. Minor elements include Ca, Mg, Cl, F and transition metals. Alteration of the glass to clay is ubiquitous in minor amounts and locally may be nearly complete. Devitrified tuffs are chemically very similar to vitric tuffs but are quite different in their mineralogy and physical properties. They are composed primarily of fine-grained aggregates of sanadine and cristobalite. They may contain phenocrysts of amphiboles, clinopyroxene and feldspar as well as lithic clasts. Low temperature alteration of devitrified tuffs is not significant; access of ground water to the rocks is limited by the low interstitial porosity. Zeolitized tuffs are the products of low temperature alteration of non-welded volcanic ash. They are composed primarily of the zeolites clinoptilolite, mordenite, and analcime.

An average chemical composition of the ground water (6) is shown in Table B-1. The water is classified as a sodium-potassium-bicarbonate water by Winograd et. al. (4). Locally the composition of ground water is dependent upon lithology. Waters associated with vitric tuffs are highest in silica, sodium, calcium and magnesium whereas ground water in zeolitic tuffs is depleted in the bivalent cations (29). The pH of these waters ranges from near-neutral to slightly alkaline (7.2-8.5). The Eh of the groundwaters in the repository horizon is unknown. Dissolved oxygen contents from several shallow wells from the Nevada Test Site are fairly high (~ 5 ppm) (30). The concentrations of several redox indicators and the alteration features of the mafic minerals in several units indicate that oxidizing conditions prevailed at one time below the water table (9). Negative redox potentials and low levels of dissolved oxygen, however, have been measured in sections of a drill hole in the Crater Flat Tuff (31). These observations are consistent with measured values of sulfide in the ground-water and the occurrence of pyrite (FeS_2) in the rock matrix. The measurements are subject to a large amount of

TABLE B-1

ANALYSES OF WATERS FROM THE NEVADA TEST SITE (mg/l)

<u>Well Species</u>	<u>J-13</u> ¹	<u>USW-H1</u> ²	<u>USW-VH1</u> ²
Na ⁺	47.00	74.90	97.10
K ⁺	4.70	5.10	4.30
Ca ⁺²	13.00	7.20	10.30
Mg ⁺²	2.00	0.40	1.90
Ba ⁺²	0.20	0.01	0.04
Sr ⁺²	0.06	0.02	0.08
HCO ₃ ⁻ + CO ₃ ⁻²	130.00		
Cl ⁻	7.70		
SO ₄ ⁻²	21.00		
NO ₃ ⁻²	5.60		
F ⁻	1.70		
SiO ₂	61.00	11.00	53.40
pH	7.1-8.3	-	-
TDS	> 294.00		

¹ LA-7480-MS - reference 6

² LA-8847-PR - reference 8

uncertainty and must be confirmed by further investigations. In light of this uncertainty, we assumed that the ground waters at the hypothetical repository are oxidizing. The importance of redox to both the solubilities and Rd values for the radionuclides that were considered in our calculations will be discussed below.

B.2 Radionuclide Solubilities

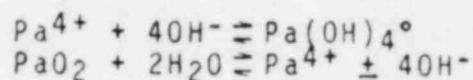
As discussed in Section 4.3, we have attempted to estimate upper bounds for the radionuclide solubilities at the tuff repository. These limits were set after a limited review of available experimental data and theoretical calculations. Most of the redox-sensitive elements are least soluble under reducing conditions. In light of the uncertainty concerning the redox conditions at Yucca Mountain and in order to ensure that our calculated releases are conservative, we have used the estimated radionuclide solubilities for oxidic conditions in our calculations.

The estimated solubility limit for each element is discussed below. In our calculations, a pH = 8 and a ground water composition similar to J-13 water (Table B-1) were assumed.

- Pu: Experimental studies reviewed by Wood and Rai (15) suggest that Pu solubility is relatively insensitive to redox conditions. They suggested a value of 4×10^{-10} M from their data. A more conservative value of 10^{-3} M (2.4×10^{-4} gm/gm) was used in order to account for the possible dominance of a Pu-carbonate complex (31).
- U: Uranium solubility could be very high if considerable CO_3^{2-} is present. However, the ground water composition at NTS (6,8) does not support this possibility. We have used the experimental data presented in (15) to set the U solubility limit at 2.4×10^{-5} gm/gm. Under reducing conditions the solubility would be approximately 8 orders of magnitude lower.
- Th: The dominant species at Th is probably $\text{Th}(\text{OH})_4^\circ$ at pH's above 5 (13,32,33). We used the reaction:
- $$\text{Th}(\text{OH})_4^\circ \rightleftharpoons \text{ThO}_2(\text{s}) + 2\text{H}_2\text{O}$$
- to estimate the solubility limit at 2.3×10^{-7} gm/gm at pH=8. The solubility is not sensitive to redox.
- Ra: Radium is another element whose solubility is relatively insensitive to redox. Its solubility is controlled primarily by $\text{RaSO}_4(\text{s})$ or $\text{RaCO}_3(\text{s})$. The value from (16) is a very conservative upper bound for Ra solubility at the tuff site.
- Cm: Few data are available to estimate Cm solubility in natural waters. In a 0.1M NaCl solution at pH=3, the Cm solubility was 10^{-11} M. The solubility decreases at lower pH (14). A conservative value of 10^{-10} M (2.5×10^{-11} gm/gm) was used in the calculations.
- Am: Am solubility has been studied by Wood and Rai (15). They suggest that a value of 7×10^{-12} M is reasonable over a wide range of redox conditions. Complexing by Cl^- , SO_4^{2-} , or NO_3^{2-} will not be significant.
- Np: Neptunium is least soluble under reducing conditions (10^{-10} M) (15). At an Eh = +0.26 and pH=7 the solubility of $\text{NpO}_2(\text{c})$ is approximately 2.4×10^{-8} gm/gm.

Pb: $PbCO_3$ or $PbSO_4$ will limit the solubility of lead in an oxic tuff environment to less than 10^{-6} M. If any sulfide is present, PbS will precipitate and further decrease the solubility.

Pa: Little data are available for protoactinium solubility in natural waters. We use the reactions:



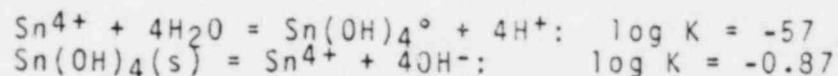
to set the solubility limit at 2.3×10^{-2} M.

Ac: We had no data to estimate the solubility of actinium; we therefore assumed that it had no solubility limit for in calculations.

Tc: Tc is least soluble under reducing conditions and precipitates as TcO_2 . Under oxidizing conditions it is probably present as TcO_4^- and is very soluble. We have assumed that it is not limiting solubility in our calculations (13, 16).

I, Cs: These elements probably have no limiting solubilities under repository conditions (13, 16).

Sn: We have assumed that these redox-insensitive reactions determine the solubility of tin (13, 16):



Sr: The solubility of Sr is probably set by strontianite $SrCO_3$ (13, 16). At pH=8, the reported 130 ppm of $HCO_3^- + CO_3^{2-}$ (Table B-1) is dominantly bicarbonate and $[CO_3^{2-}]$ is about 10^{-5} M. Log Ksp of $SrCO_3$ is -9.6 which means the solubility of Sr is about 2×10^{-6} gm/gm.

C: We set the solubility limit of ^{14}C at a level consistent with the concentration of HCO_3^- in J-13 water (~26 ppm carbon).

B.3 Radionuclide Sorption Ratios

The ranges of radionuclide distribution coefficients (Rd) used in our calculations are listed in Table 4. The values were chosen after a review of the published experimental studies that were conducted at Los Alamos National Laboratories through June, 1981. (5-10).

Rd values from batch experiments obtained under the following conditions were included in the ranges shown in Table 4.

temperature = 22°C
solid: solution ratio = 1:20
atmosphere = oxidizing
particle size = 106-500 microns
water = J-13 water pre-equilibrated with the rock sample.
rocks = samples from UE25a-1, G-1 and J-13 drill holes.

Parametric studies by L.A.N.L. scientists (5-10) suggest that the measured Rd values are dependent upon all of the parameters listed above. The conservatism of the data collected under these experimental conditions with respect to natural conditions expected at the tuff repository site is described in Table B-2.

For several elements, Rd values obtained under these experimental conditions can vary up to 3 orders of magnitude between samples of the same bulk mineralogy. The measured Rd values are strongly dependent upon the abundance of minor minerals such as montmorillonite, the duration of the experiment and upon the method used to measure the concentration of the sorbed radionuclide. Values obtained from desorption experiments are almost always significantly higher than those obtained from sorption experiments. The data ranges in Table 4 bracket the highest average Rd values obtained from desorption experiments and the lowest average sorption Rd value. Each average value that was considered is the mean Rd value for a single rock sample for several experiments which lasted from 3 to 12 weeks.

date May 13, 1982

Albuquerque, New Mexico 87185

to M. D. Siegel - 4413

Ken

from K. L. Erickson - 5843

subject Approximations for Adapting One-Dimensional Porous Media Radionuclide Transport Models to the Analysis of Transport in Jointed Porous Rock

This memorandum describes the basic ideas and results given in the informal notes provided you on 2 April 1982 and subsequently discussed by us on 20 and 21 April. The following remarks are confined to transport through a single, uniform jointed geologic medium. However, additional analyses since our meeting of 20 April indicate that similar results probably can be proved for a series of dissimilar jointed media.

Consider a region of jointed porous rock through which fluid flow occurs primarily in the joints and convective radionuclide transport in the porous matrix of the rock is negligible. Let the joints be linear, have rectangular cross-sections of approximately constant and uniform dimensions, have continuous physical and chemical properties, and be such that fluid flow is essentially one-dimensional with uniform average velocity v . Let the porous matrix be fully saturated, and let radionuclide retardation (relative to convective fluid flow in the joints) result from molecular diffusion in the pore water and simultaneous sorption by the solid phases. Furthermore, let the regions of porous rock bounded by the joints have approximately uniform shape and volume V_p . In the paragraphs below, criteria are developed for determining when transport in such jointed media can be approximated as transport through an equivalent porous medium whose porosity is defined by joint aperture, frequency, and orientation. Then, the appropriate expression is defined for the retardation factor R to be used in such equivalent one-dimensional porous media models having the form

$$\frac{\partial C}{\partial t} + \frac{v}{R} \frac{\partial C}{\partial z} = \text{dispersion and decay terms} \quad (1)$$

where C is the radionuclide concentration (assumed cross-sectionally uniform) in the flowing fluid in the joints; t is time, and z is the coordinate in the direction of fluid motion.

For a uniform region of jointed porous rock, as described above, assume: (1) fluid flow is laminar and velocity profiles can be replaced by the average velocity; (2) joint apertures are sufficiently small so that fluid-phase radionuclide diffusion perpendicular to the joint walls can be approximated as a quasi-steady-state process and represented by a linear-driving-force expression; (3) local sorption equilibrium exists at the interface between flowing fluid and bulk rock and between pore water and solid phases of the porous matrix; (4) sorption of radionuclides results from a reversible process such as adsorption or ion exchange; (5) solution-phase radionuclide concentrations are due only to dissolved species and are sufficiently dilute to be within the linear region of the sorption isotherm and sufficiently dilute for Fick's law with constant diffusion coefficient to be a reasonable approximation; (6) effects due to competing chemical reactions and surface diffusion are negligible, and (7) parameter values are constant. Furthermore, initially assume that mass transfer by dispersion in the direction of flow is small relative to that by convection. Then for a radionuclide which is present in the initial inventory but which is not subsequently produced as a daughter product, transport is described by the following equations:

(material balance for the fluid in the joint)

$$\frac{\partial C}{\partial t} + v \frac{\partial C}{\partial z} = - \frac{1}{m} \frac{\partial q}{\partial t} - \lambda C - \frac{\lambda}{m} q \quad (1)$$

(flux expression at interface between flowing fluid and bulk rock)

$$\frac{\partial q}{\partial t} = \frac{1}{R_f} (C - q_s/\bar{K}) - \lambda q \quad (2)$$

(material balance for the porous rock)

$$\frac{\partial q_i}{\partial t} = D_e \nabla^2 q_i - \lambda q_i \quad (3)$$

where

$$q = \frac{1}{V_p} \int_{V_p} q_i \, dV_p \quad (4)$$

and where D_e is the effective radionuclide diffusion coefficient in the porous rock; \bar{K} is the bulk sorption distribution coefficient between porous matrix and external solution; m is the void volume (based on joint aperture, frequency, and orientation) per unit volume of porous matrix; R_f is an effective interfacial resistance to mass transfer; q_i is the local concentration in the porous rock; q_s is the value of q_i at the interface between matrix and flowing fluid; λ is the radionuclide decay constant, and the Laplacian ∇^2 is defined in a coordinate system convenient for describing diffusion in the porous matrix.

Using the following initial and boundary conditions, Rosen (1952, 1954) solved Eqs. 1-4 for flow around spheres and $\lambda = 0$:

$$q_i(r, x, 0) = 0 \quad \text{for} \quad 0 \leq r \leq b, \quad x \geq 0 \quad (5)$$

$$u(0, \theta) = C(0, \theta)/C_0 = \begin{cases} 0 & , \quad \theta = t \leq 0 \\ 1 & , \quad \theta = t > 0 \end{cases} \quad (6)$$

where r is the radial coordinate and b is the radius of the spheres. Erickson (1981) gives a similar solution for a fluid flowing through a single fracture between two parallel, semi-infinite plates in which radionuclide diffusion was primarily perpendicular to the fracture and limited to a finite penetration depth. By substituting the appropriate expression for m , that is $\epsilon/(1 - \epsilon)$, the solution for flow through a system of joints forming several continuous plate-like regions of porous matrix (see Fig. 1) is obtained from the single-fracture result.

The exact solutions for the spherical and plate-like geometries are in the form of infinite integrals requiring numerical evaluation. However, for sufficiently large values of z/v , the infinite integrals approach relatively simple asymptotic expressions. In particular, if R_f is very small so that the radionuclide concentration in the fluid in the joint is essentially cross-sectionally uniform, then for flow around spherical regions of porous matrix

$$C/C_0 = \frac{1}{2} \left[1 + \operatorname{erf} \left(\frac{3\sigma\theta/2 - \gamma x}{2(\gamma x/5)^{1/2}} \right) \right] \quad (7)$$

and for flow around plate-like regions

$$C/C_0 = \frac{1}{2} \left[1 + \operatorname{erf} \left(\frac{2\sigma\theta - \gamma x}{2(\gamma x/3)^{1/2}} \right) \right] \quad (8)$$

provided that the effective bed length γx is greater than 50. For spherical regions, $c\theta = 2D_e(t - z/v)/b^2$, $\gamma x = 3D_e\bar{K}z/vmb^2$, and b is the radius of the spherical regions. For plate-like regions, $c\theta = D_e(t - z/v)/2b^2$, $\gamma x = D_e\bar{K}z/vmb^2$, and b is now the half-thickness of the plate-like regions. A criterion for determining when radionuclide concentrations in the fluid in the fractures can be considered cross-sectionally uniform is developed after the following discussion regarding Eqs. 7 and 8.

In general, it was felt that a system of plate-like regions of porous rock might be more representative of actual systems. Therefore, the following discussion is based on Eq. 8, although similar considerations naturally apply to Eq. 7.

The right side of Eq. 8 is symmetrical about the value of $C/C_0 = 0.5$. If for a given value of t , $t_{0.01}$ is defined as the elapsed time required for C/C_0 to reach a value of 0.01, and $t_{0.5}$, $t_{0.99}$, and $\theta_{0.5}$ are defined analogously, then from Eq. 8 and appropriate values of the error function

$$\frac{t_{0.99} - t_{0.01}}{\theta_{0.5}} = \frac{6.6}{(3\gamma x)^{1/2}} \quad (9)$$

and for $\gamma x > 50$

$$\frac{t_{0.99} - t_{0.01}}{\theta_{0.5}} < 0.54 ,$$

This implies that as γx becomes large, the spread in the breakthrough curve becomes small relative to the distance its midpoint has traveled, because the time interval by which the value of $C/C_0 = 0.01$ precedes the value of $C/C_0 = 0.5$ and the interval by which the value of $C/C_0 = 0.99$ trails become small relative to $\theta_{0.5}$ or $(t_{0.5} - z/v)$. For example, when $\gamma x > 50$, the intervals are about twenty-five percent or less of $\theta_{0.5}$. Furthermore, from Eq. 8

$$t_{0.5} = (1 + \bar{K}/m)z/v \quad (10)$$

and

$$v_{0.5} = v/(1 + \bar{K}/m) . \quad (11)$$

Therefore, as γx becomes large the solution to Eqs. 1-4 when $\lambda = 0$ approaches

$$C(z,t) = C[0,t - (1 + \bar{K}/m)z/v] \quad (12)$$

which is of the same form as the solution to Eq. 1 when the decay and dispersion terms are negligible, that is

$$C(z,t) = C(0,t - Rz/v) \quad (13)$$

For $\lambda > 0$ in Eqs. 1-4 and C_0 replaced by $C_0 e^{-\lambda t}$ in Eq. 6, the solution to Eqs. 1-4 is $e^{-\lambda t} U_0(z,t)$, where $U_0(z,t)$ is the solution for $\lambda = 0$. Similar remarks also apply to the solution of Eq. 1 in the form

$$\frac{\partial C}{\partial t} + \frac{v}{R} \frac{\partial C}{\partial z} = -\frac{\lambda}{R} C \quad (14)$$

where $C(0,t > 0) = C_0 e^{-\lambda t}$. Hence, for a radionuclide initially present in the inventory but not produced as a daughter by decay, Eqs. 1-4 ($\lambda \geq 0$) can be approximated by Eq. 1 if γx is sufficiently large; if R is taken as $(1 + \bar{K}/m)$, and if dispersion effects are small relative to convective transport. Due to the inherent uncertainties associated with analyses of radionuclide transport in geologic media, a twenty-five percent spread in the concentration profile about $t_{0.5}$ is probably not serious, and values of $\gamma x > 50$ are probably sufficiently large for Eqs. 1-4 to be approximated by Eq. 1.

For the simplest case of diffusion into a porous matrix in which the total porosity ϕ is available to the diffusion of radionuclides which is sufficiently well described by Eq. 3 using $D_e = D/\alpha^2(1 + \rho K_D/\phi)$, the criterion $\gamma x > 50$ and the retardation factor $R = 1 + \bar{K}/m$ can be defined in terms of more fundamental parameters as follows

$$\gamma x = D_e \bar{K} z / v m b^2 > 50$$

or

$$\frac{z}{v} > 50 \frac{b^2 \alpha^2}{D \phi} \left(\frac{\epsilon}{1 - \epsilon} \right) \quad (15)$$

and

$$R = 1 + \bar{K}/m = 1 + \left(\frac{1 - \epsilon}{\epsilon} \right) \left[\phi \left(1 + \frac{\rho}{\phi} K_D \right) \right] \quad (16)$$

where D is the diffusion coefficient for the radionuclide in aqueous solution (assumed constant); K_D is the distribution coefficient for sorption equilibrium between pore water and solid phases of the matrix (units of ml/gm); α is a tortuosity factor for the matrix, and ρ is the bulk dry density of the matrix ($\rho = (1 - \phi)\rho_s$ where ρ_s is the average grain density of the matrix material).

The preceding development was based on the assumption that radionuclide concentrations in the flowing fluid were cross-sectionally uniform. A criterion for the validity of that assumption is that the average fluid residence time in the joints is much greater than the characteristic time required for a concentration gradient to decay to near zero. The average fluid residence time in the fractures is z/v . Now, let H denote joint aperture, and assume that the characteristic decay time for a concentration gradient can be approximated by the equilibration time for a plane sheet of thickness $H/2$ and having one face maintained at a constant concentration. Then the characteristic decay time would be $H^2/4D$ (Crank, 1975), and the desired criterion is

$$z/v \gg H^2/4D \quad (17)$$

In summary, for a radionuclide which is initially present in the inventory and not subsequently produced by decay, transport through a single, uniform, jointed porous medium can be described approximately by Eq. 1 provided that

$$z/v \gg H^2/4D \quad (17)$$

and

$$z/v > 50 \frac{b^2 \alpha^2}{D\phi} \left(\frac{\epsilon}{1 - \epsilon} \right) \quad (15)$$

The value for the retardation factor R in Eq. 1 is given by

$$R = 1 + \left(\frac{1 - \epsilon}{\epsilon} \right) \left[\phi \left(1 + \frac{\rho}{\phi} K_D \right) \right] \quad (16)$$

As given previously, b is the half-thickness for the plate-like regions between joints; D is the radionuclide diffusion coefficient (assumed constant) in aqueous solution; H is the joint aperture; K_D is the distribution coefficient for sorption equilibrium between pore water and solid phases of the porous

matrix; $\bar{K} = \phi(1 + \rho K_D/\phi)$; $m = \epsilon/(1 - \epsilon)$; v is the average fluid velocity in the joints; z is the spatial coordinate in the direction of bulk fluid motion; α is a tortuosity factor for the porous matrix; ϵ is the porosity associated with the joints; $\rho = (1 - \phi)\rho_s$ and is the bulk dry density of the porous matrix material; ρ_s is the average grain density of the matrix material, and ϕ is the porosity of the porous matrix.

However, it should be emphasized that the applicability of Eqs. 15-17 depends on how closely a real system is approximated by the ideal system and assumptions from which the equations were developed. In particular, the treatment given for diffusion of radionuclides into the porous matrix may not be adequate in certain situations; particularly if very "tight" porosity is involved.

REFERENCES

Crank, J., The Mathematics of Diffusion, 2nd ed., pp. 49-53, Clarendon Press, Oxford, 1975.

Erickson, K. L., A Fundamental Approach to the Analysis of Radionuclide Transport Resulting from Fluid Flow Through Jointed Media, SAND80-0457, Sandia National Laboratories, Albuquerque, NM, 87185.

Rosen, J. B., "Kinetics of a Fixed Bed System for Solid Diffusion into Spherical Particles," J. Chem. Phys., V. 20, 3 (1952).

Rosen, J. B., "General Numerical Solution for Solid Diffusion in Fixed Beds," Ind. and Eng. Chem., V. 46, 8 (1954).

KLE:5843:1s

Distribution:

4410 D. J. McCloskey
 4413 M. S. Y. Chu
 4413 R. M. Cranwell
 4413 N. R. Ortiz
 4413 R. E. Pepping
 5840 N. J. Magnani
 5843 C. J. M. Northrup
 5843 K. L. Erickson

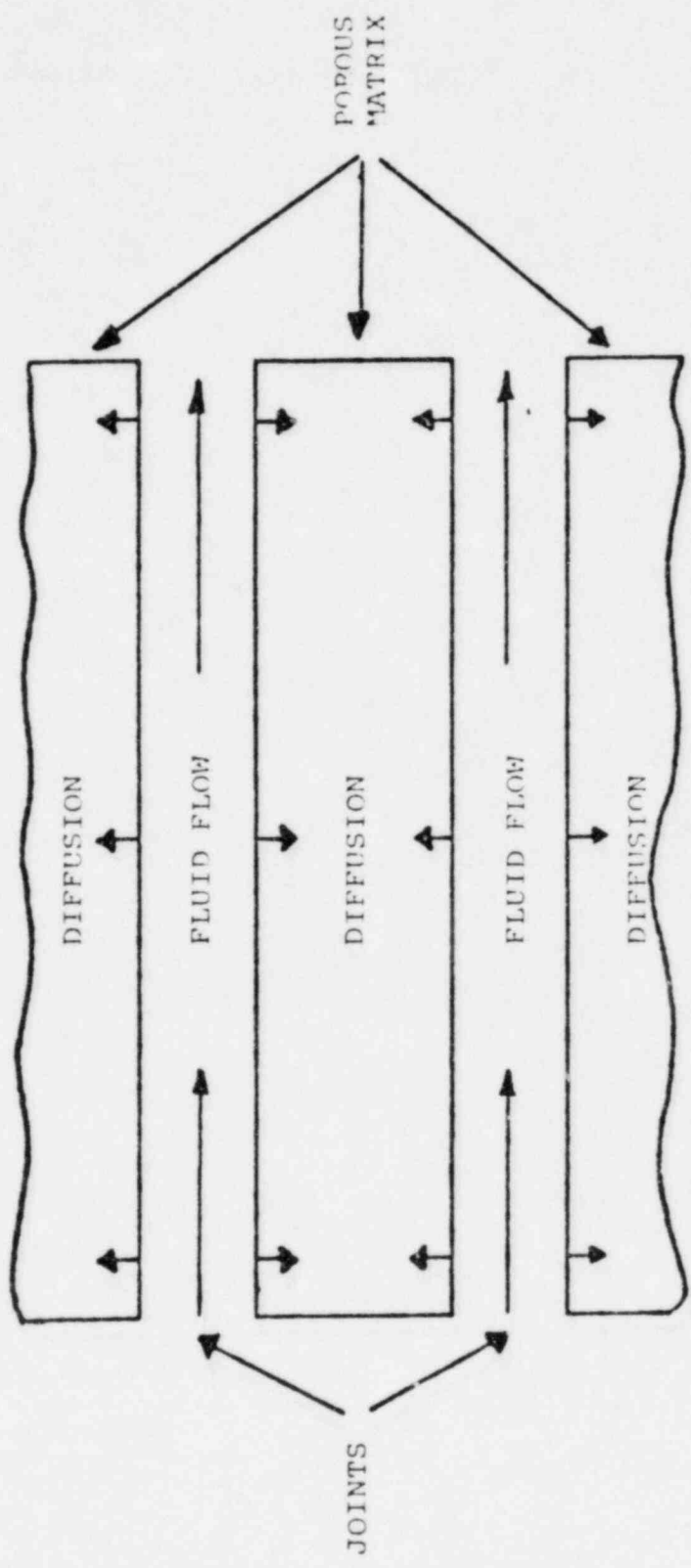


Fig. 1. Schematic diagram of fluid flow through joints and diffusion into the porous matrix.

ATTACHMENT 1

TO: Stewart Silling
FROM: Malcolm Siegel
RE: Calculation of Effective Retardation Factor (\bar{R}) for Matrix Diffusion

1. For retardation factor in NWFT/DVM runs use: (\bar{R}):

$$\bar{R} = 1 + \phi \cdot \left(\frac{1-\epsilon}{\epsilon} \right) \cdot \left(1 + \rho \frac{(1-\phi)}{\phi} \cdot K_D \right)$$

where:

K_D = distribution coefficient in ml/gm
 ϕ = matrix porosity of unfractured blocks
 ρ = grain density of rock
 ϵ = fracture porosity = $2Nb$ for our system where
 N = fracture density; b = fracture aperture

2. This expression is good when the following criterion (1) holds:

$$z/v \geq 50 \cdot (1/N^2D) \cdot (\alpha^2/\phi) \cdot (\epsilon/1-\epsilon) = \gamma_x$$

where:

D = ionic diffusion constant
 α = tortuosity
 z = path length in fractured media
 v = Darcy velocity \div fracture porosity

The criterion was evaluated for densely and moderately welded tuff units, for individual beds as well as for the entire welded tuff thickness. The maximum, median and minimum values of the ranges used for the LHS input variables were used to evaluate the expression (γ_x).

ATTACHMENT 1

	<u>γ_x max</u>	<u>γ_x min</u>	<u>γ_x median</u>
z	200 ft	200 ft	100 ft
ϵ	6.4×10^{-3}	8.8×10^{-6}	1.3×10^{-4}
ϕ	0.03	0.10	0.06
N	6.5 ft^{-1}	0.27 ft^{-1}	1.6 ft^{-1}
K	60 ft/day	4×10^{-5} ft/day	4.2 ft/day
i	4×10^{-2}	1×10^{-2}	2×10^{-2}
v	375 ft/day	0.045 ft/day	0.646 ft/day
z/v	0.533 day	4.4×10^3 day	155 day
γ_x	0.19 day	0.045 day	0.031 day

where:

i = vertical hydraulic gradient

D = 10^{-5} cm²/sec = 3.39×10^{-1} ft²/yr

$\alpha = 1.0$

K = hydraulic conductivity in LHS range for densely welded units

v = iK/ϵ

It can be seen from these calculations that the criterion $z/v \geq \gamma_x$ holds for the conditions encountered at the tuff site.

References:

- (1) Erickson, K. L., 1981, A Fundamental Approach to the Analysis of Radionuclide Transport Resulting from Fluid Flow through Jointed Media, SAND80-0457. (See p. 19-2 and work backwards. See also reference 14 in his bibliography.)

REFERENCES

1. Spengler, R. W., Muller, D. C., and Livermore, R. B. 1979, Preliminary Report on the Geology and Geophysics at Drill Hole UE25a-1 Yucca Mountain, Nevada Test Site. U. S. G. S. Open File Report 79-1244, 43p.
2. Sykes, M. L., Heiken, G. H., and Smyth, J. R. 1979, Mineralogy and Petrology of Tuff Units from the UE25a-1 Drill Site, Yucca Mountain, Nevada: Los Alamos National Laboratory. LA-8139-MS, 76p.
3. Johnstone, J. K., and Wolfsberg, K. eds. 1980, Evaluation of Tuff as a Medium for a Nuclear Waste Repository: an Interim Status Report on the Properties of Tuff, Sandia National Laboratories Report; SAND80-1464, 142p.
4. Winograd, I. J. and Thordarson, W. 1975, Hydrogeologic and Hydrochemical Framework, South-Central Great Basin, Nevada-California, with Special Reference to the Nevada Test Site, U. S. G. S. Prof. Pap. 712-C, 126p.
5. Wolfsberg, K. 1978, Sorption-Desorption Studies of Nevada Test Site Alluvium and Leaching Studies of Nuclear Test Debris, Los Alamos Scientific Laboratory Report LA-7216-MS, 33p.
6. Wolfsberg, K., Baynurst, B. P., et al. 1979, Sorption-Desorption Studies on Tuff I. Initial studies with samples from the J-13 Drill Site, Jackass Flats, Nevada, Los Alamos Scientific Laboratory Report LA--7480-MS, 60p.
7. Vine, E. N., Aguilar, R. D., et al. 1980, Sorption-Desorption Studies on Tuff II. A continuation of studies with samples from Jackass Flats, Nevada, and initial studies with samples from Yucca Mountain, Nevada, Los Alamos Scientific Laboratory Report LA-8110-MS, 75p.
8. Erdal, B. R., Daniels, W. R. and Wolfsberg, K., eds. 1981, Research and Development related to Nevada Nuclear Waste Storage Investigations, January 1 - March 31, 1981, Los Alamos Scientific Laboratories Report LA-8847-PR.

9. Wolfsberg, K., Aguilar, R. D., et. al. 1981, Sorption-Desorption Studies on Tuff III. A continuation of studies with samples from Jackass Flats and Yucca Mountain, Nevada, Los Alamos National Laboratory Report LA-8747-MS.
10. Erdal, B. R., Daniels, W. R., Vaniman, D. T., and Wolfsberg, K. 1981, Research and Development related to the Nevada Nuclear Waste Storage Investigations, April 1 - June 30, 1981, Los Alamos National Laboratory Report LA-8959-PR, 65p.
11. Guzowski, R. V., Nimick, F. B., and Muller, A. B. 1982, Repository Site Definition in Basalt: Pasco Basin, Washington, SAND81-2088, NUREG/CR-2352, Sandia National Laboratories, 88p.
12. Ogard, A. E. 1982, Personal communication.
13. Nimick, F. 1982, letter report on solubilities of radio-nuclides in basalt. Sandia National Laboratories.
14. Rai, D and Serne, R. J. 1978, Solid Phases and Solution Species of Different Elements in Geologic Environments, Battelle, Pacific Northwest Laboratories Report PNL-2651, 140p.
15. Wood, B. J. and Rai, Dhanpat 1981, Nuclear Waste Disposal: Actinide Migration from Geologic Repositories, Battelle, Pacific Northwest Laboratories Report PNL-SA-9549, 33p.
16. Muller, A. B., Finley, N. C., Pearson, F. J. 1981, Geochemical Parameters used in the Bedded Salt Reference Repository Risk Assessments Methodology, Sandia National Laboratories, SAND81-0557, NUREG/CR-1996, 86p.
17. Campbell, J. E., Longsine, D. E. and Cranwell, R. M., Risk Methodology for Geologic Disposal of Radioactive Waste: The NWFT/DVM Computer Code Users Manual, SAND81-0836, Sandia National Laboratories, November 1981.

18. Iman, R. L., Davenport, J. M. and Zeigler, D. M., Latin Hypercube Sampling (Program Users Guide). SAND79-1473, Sandia National Laboratories, January, 1980.
19. Environmental Protection Agency, 40CFR191, Draft 19, Federal Register, March 19, 1981.
20. Cranwell, R. M. et. al. Risk Methodology for Geologic Disposal of Radioactive Waste: Final Report, SAND81-2573, NUREG/CR-2452, Sandia National Laboratories, to be published.
21. Rush, F. E. 1970, Regional ground-water systems in the Nevada Test Site area, Nye, Lincoln, and Clark Counties, Nevada: Nevada Department of Conservation and Natural Resources, Water Resources - Reconnaissance Series Report 54, 25p.
22. Reade, M. T. 1982, letter report on geology and hydrology of the Nevada Test Site. C. G. S. Inc.
23. Longsine, J. 1982, Unpublished manuscript.
24. Freeze, R. A. and Cherry, J. A. 1979, Groundwater, Prentice-Hall Inc., Englewood Cliffs, N.J., p. 74.
25. Guzowski, R. 1982, oral presentation for NRC on Hydrology at Nevada Test Site.
26. Merkin, J. H. 1979, Free Convection Boundary Layers on Axi-Symmetric and Two-Dimensional Bodies at Arbitrary Shape in a Saturated Porous Medium, Int. J. Heat Mass Transfer, 22:1461-1467.
27. Interim Reference Repository conditions for spent fuel and commercial high level nuclear waste repositories in Tuff, Sept. 1981. Battelle Project Management Division (ONW1) NWTS-12.
28. Rush, G. 1982, Personal Communication.

29. White, A. F., Claassen, H. C. and Benson, L. V. 1980, The Effect of Dissolution of Volcanic Glass on the Water Chemistry in a Tuffaceous Aquifer, Rainier Mesa, Nevada, Geological Survey Water-Supply Paper 1535-Q, 34p.
30. Winograd, I. J. and Robertson, F. N. 1982, Deep Oxygenated Ground Water Anomaly or Common Occurrence?, Science, in press.
31. Erdal, B. 1982, NRC field trip to NTS and project reviews.
32. Serne, J. 1982, personal communication.
33. Baes, C. F. and Mesmer, R. E., 1976. The Hydrolysis of Cations, Wiley Interscience, John Wiley and Sons, New York, N. Y., p.166.

SAND82-1275

Technical Assistance for Regulatory Development:

Radionuclide Concentrations for the
Basalt and Bedded Salt Repositories

R. E. Pepping

Sandia National Laboratories
Albuquerque, N. M. 87185

May 1982

Fin No. A-1165 Task 3

Table of Contents

	Page
I. Introduction	1
II. Assumed Plume Description	2
III. Use of 10CFR20	16
IV. Computation Results	22
V. Conclusions	64
VI. References	67

Figures

	Page
1. The Gaussian Plume	5
2. The $4n + 0$ Series	18
3. The $4n + 1$ Series	19
4. The $4n + 2$ Series	20
5. The $4n + 3$ Series	21
6. Basalt Scenario 1: the base case, mean and maximum versus time	29
7. Basalt Scenario 2: fractures in dense basalt, mean and maximum versus time	30
8. Basalt Scenario 3: the borehole, leach limited, mean and maximum versus time	31
9. Basalt Scenario 3: the borehole, mixing cell, mean and maximum versus time	32
10. CCDF for Basalt Scenario 1, maximum concentrations	33
11. CCDF for Basalt Scenario 2, maximum concentrations	34
12. CCDF for Basalt Scenario 3 (Leach Limited), maximum concentrations	35
13. CCDF for Basalt Scenario 3 (Mixing Cell), maximum concentrations	36
14. Bedded Salt Scenario 1, Source 1, mean and maximum versus time	43
15. Bedded Salt Scenario 2, Source 1, mean and maximum versus time	44
16. Bedded Salt Scenario 3, Source 1, mean and maximum versus time	45
17. Bedded Salt Scenario 4, Source 1, mean and maximum versus time	46
18. Bedded Salt Scenario 1, Source 2, mean and maximum versus time	47

Figures (Continued)

	Page
19. Bedded Salt Scenario 2, Source 2, mean and maximum versus time	48
20. Bedded Salt Scenario 3, Source 2, mean and maximum versus time	49
21. Bedded Salt Scenario 4, Source 2, mean and maximum versus time	50
22. CCDF for Bedded Salt Scenario 1, Sources 1 and 2, maximum concentrations	51
23. CCDF for Bedded Salt Scenario 2, Sources 1 and 2, maximum concentrations	52
24. CCDF for Bedded Salt Scenario 3, Sources 1 and 2, maximum concentrations	53
25. CCDF for Bedded Salt Scenario 4, Sources 1 and 2, maximum concentrations	54
26. Bedded Salt Scenario 1, Source 3, mean and maximum versus time	55
27. Bedded Salt Scenario 2, Source 3, mean and maximum versus time	56
28. Bedded Salt Scenario 3, Source 3, mean and maximum versus time	57
29. Bedded Salt Scenario 4, Source 3, mean and maximum versus time	58
30. CCDF for Bedded Salt Scenario 1, Mixing Cell, maximum concentrations	59
31. CCDF for Bedded Salt Scenario 2, Mixing Cell, maximum concentrations	60
32. CCDF for Bedded Salt Scenario 3, Mixing Cell, maximum concentrations	61
33. CCDF for Bedded Salt Scenario 4, Mixing Cell, maximum concentrations	62

Tables

	Page
1. Dispersion Properties of Transporting Units	8
2. Radionuclide Inventories and 10CFR20 Limits	15
3. Important Radionuclides in Basalt Scenarios	28
4. Important Radionuclides in Bedded Salt Scenarios	63
5. Estimated Probabilities of Exceeding 10CFR20	65

1. Introduction

The Nuclear Regulatory Commission (NRC) has contracted Sandia National Laboratories (SNL) to provide technical assistance for the development of regulatory standards for nuclear waste disposal. In this project simplified repository analyses of hypothetical geologic repositories have been performed. To date, analyses of bedded salt and basaltic repositories have been performed and reported [1,2]. An analysis of a reference repository in a tuff flow is underway.

These analyses use computer models to simulate the transport of radionuclides to the biosphere which results from postulated breaches of the repository. The model used for these calculations is the NWFT/DVM model developed by SNL for use by NRC [3]. NWFT/DVM calculates radionuclide specific discharge rates to the biosphere in Curies/day for the long periods expected for such releases, tens of thousands of years. The result of such calculations may be used with other computer models to estimate the environmental distribution and health effects from such releases.

In the previous analyses performed in this project, we have been working with the draft EPA Standard (40CFR191) [4].

This draft standard requires time-integration of the calculated discharge to estimate total Curie releases over a 10,000 year period. In order to understand the implications of the calculated discharge rates, additional computations have been requested of SNL by NRC. Specifically, in this document we will report the estimations of radionuclide concentrations in the groundwater transporting the radionuclides. The interest in these calculations is two fold. Since the groundwater represents a potential source of drinking water, a standard already exists which places limits on the maximum allowable radionuclide concentrations, specifically, 10CFR20 [5]. Calculations of this type may be necessary in the assessment of the expected performance of a real repository. Furthermore, at this time the potential exists for significant modification of the draft EPA Standard from its present form. Thus, in order to better understand the implications of these releases and to compare the calculated concentrations to the only existing related standard (10CFR20), these calculations are necessary.

II. Assumed Plume Description

The computational model employed, NWFT/DVM, calculates radionuclide discharges to the biosphere resulting from

postulated breaches of the geologic repository e.g., borehole penetration and fault formation. This calculation is performed by numerically solving the convective-dispersion equation in one dimension, for a radionuclide chain,

$$D_z \frac{\partial^2 C_i}{\partial z^2} - V \frac{\partial C_i}{\partial z} + R_{i-1} \lambda_{i-1} C_{i-1} - R_i \lambda_i C_i = R_i \frac{\partial C_i}{\partial t} \quad (1)$$

where

C_i = i^{th} radionuclide chain member concentration

V = groundwater velocity

R_i = retardation factor for i^{th} radionuclide

λ_i = i^{th} radionuclide decay constant

$D_z = \alpha_L V$ = diffusion constant in the longitudinal (z) direction

α_L = longitudinal (z) dispersivity.

The calculated solution of Equation 1 is sufficient for estimation of radionuclide discharge rates at some point in the biosphere.

In order to estimate radionuclide concentrations in the flowing groundwater, Equation 1 must be extended into three dimensions,

$$D_x \frac{\partial^2 C}{\partial x^2} + D_y \frac{\partial^2 C}{\partial y^2} + D_z \frac{\partial^2 C}{\partial z^2} - V \frac{\partial C}{\partial z} = R_i \frac{\partial C}{\partial t} \quad (2)$$

where, for convenience, the contaminant has been assumed to be nonradioactive.

The situation we evaluate is depicted in Figure 1. A point source (borehole) or line source (fault, fracture zone) is assumed to release radionuclides to groundwater flowing in the z-direction. After some time a stable plume develops ($\frac{\partial C}{\partial t} = 0$) over the half-plane, $y \geq 0$. Away from the leading edge of the concentration profile in the z-direction ($z \approx Vt/R_1$), at some distance, z_0 , the solution of Equation (2) is given by

$$C(x,y,z_0) = \frac{\dot{C}_0}{2\pi\sigma_x\sigma_y V} \exp \left[-\frac{1}{2} \left(\frac{x^2}{\sigma_x^2} + \frac{y^2}{\sigma_y^2} \right) \right] \quad (3)$$

for point-sources, and

$$C(x,y,z_0) = \frac{\dot{C}_0}{2w V \sqrt{2\pi}\sigma_x} \exp \left[-1/2 \left(\frac{x}{\sigma_x} \right)^2 \right] \\ \times \left\{ \operatorname{erf} \left(\frac{y+w}{\sqrt{2}\sigma_y} \right) - \operatorname{erf} \left(\frac{y-w}{\sqrt{2}\sigma_y} \right) \right\} \quad (4)$$

for line sources of width $2w$ on the y-direction. In Equations 3 and 4,

$$\sigma_x^2 = 2D_x z_0 / V = 2\alpha_x z_0$$

$$\sigma_y^2 = 2D_y z_0 / V = 2\alpha_y z_0$$

and \dot{C}_0 is related to the radionuclide source strength. \dot{C}_0 will be derived later.

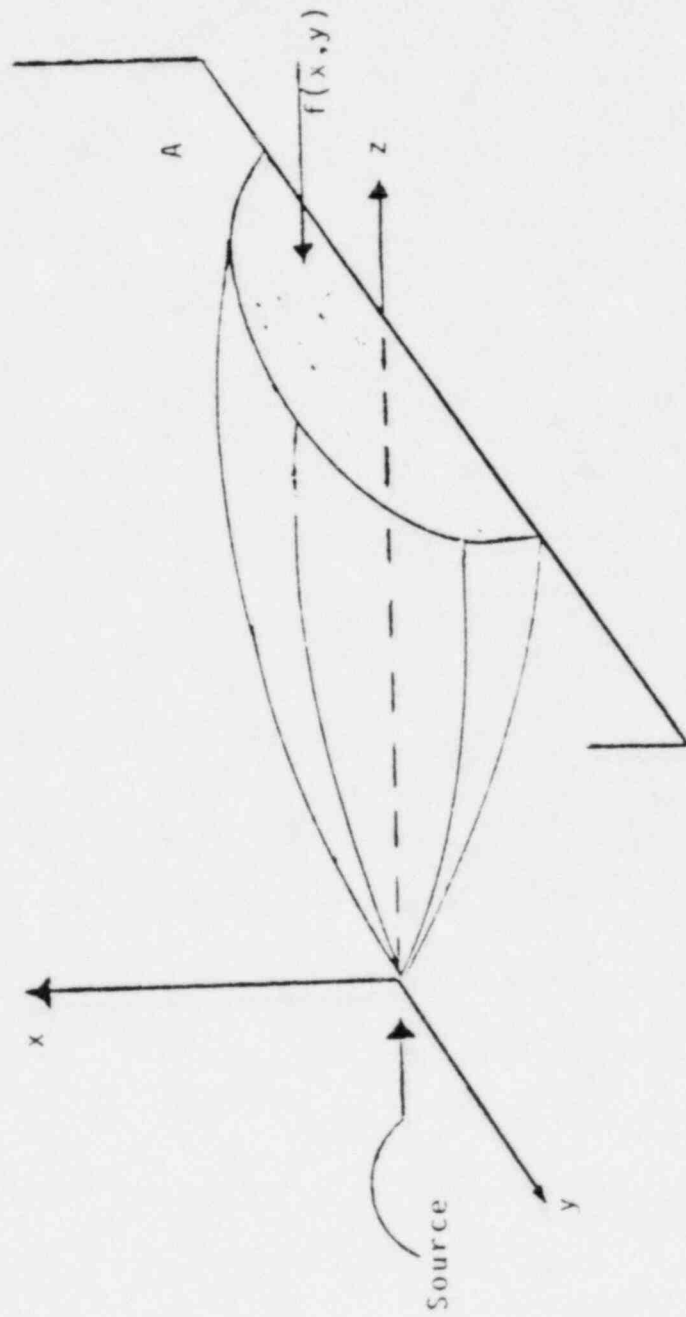


Figure 1. The Gaussian Plume

We will further assume that the medium is isotropic so that

$$D_x = D_y$$

and

$$\alpha_x = \alpha_y = \alpha_T$$

where τ is the transverse dispersivity. Hence, we can drop the subscripts on α and note

$$\sigma^2 = 2 \alpha_T z_0$$

Both Equations 3 and 4 are of the form,

$$C(x,y,z_0) = \frac{\dot{C}_0}{V} f(x,y,z_0)$$

where $f(x,y,z_0)$ describes the spatial dependence in the half-plane located at some distance from the source, z_0 . The function, $f(x,y,z_0)$, is normalized to 1/2 since only the upper half-plane, depicted in Figure 1, transmits radionuclides. NWFT/DVM calculates the radionuclide discharge across the half-plane depicted in Figure 1, D , which may be related to $C(x,y,z_0)$ by

$$\dot{D} = \int_A C(x,y,z_0) dQ = q \int C(x,y,z_0) dx dy = q \frac{\dot{C}_0}{V} \int f(x,y,z_0) dx dy = \frac{q \dot{C}_0}{2V}$$

Hence,

$$\dot{C}_0 = \frac{2V\dot{D}}{q} \quad (5)$$

In developing Equation 5,

Q = volumetric flow rate

q = Darcy velocity,

and q is assumed to be constant across A . Equations 3, 4 and 6 may thus be used to calculate the maximum concentrations. These occur on axis ($x=y=0$),

$$C_{\max} = \begin{cases} \frac{\dot{D}}{\pi\sigma^2q} & \text{point sources} \\ \frac{\dot{D}}{\sqrt{2\pi}\sigma wq} & \text{line sources} \end{cases} \quad (6)$$

We note that \dot{D} , the NWFT/DVM result, is in fact time-dependent. The assumption of steady-state spatial distributions must then be qualified. We are actually assuming a quasi-steady-state solution in which the radionuclide source varies sufficiently slowly with time that Equations 3 and 4 adequately describe the solution to Equation 2.

The plume model used in these calculations has two associated assumptions that should be noted. Both

Equations 3 and 4 show a Gaussian behavior in the x-direction. The assumption of such behavior is valid as long as the plume's lateral extent (a few σ_x) is less than the thickness of the transporting aquifer. The plume width in the x-direction may be measured in terms of σ_x , the width parameter, where

$$\sigma_x^2 = 2 \alpha_T z_0 \quad (7)$$

Making the assumption

$$\alpha_T = \frac{1}{10} \alpha_L$$

Equation 7 becomes,

$$\sigma_x^2 = \frac{\alpha_L z_0}{5}$$

In these calculations we will address the case, $Z_0 = 5,280$ feet.

The values of α_L used in the calculations varied between transporting media analyzed [1, 2].

Table 1

Dispersion Properties of Transporting Units

Medium	Basalt	Bedded Salt	Bedded Salt
Transporting Unit	R	O	D
α_L range	50 feet	1-50 feet	10-100 feet
α_L distribution	fixed	Log uniform	Log Uniform
$\sigma_{x,max}$	230 feet	230 feet	325 feet
Thickness of Transporting Unit L_x	200 feet	300 feet	500 feet

The distributions chosen are used by a sampling technique to select specific values of α_L for each input vector. The values of $\sigma_{x,max}$ are comparable to the thickness of the transporting unit.

In cases where σ_x is much greater than the thickness of the transporting unit, denoted by L_x , the usual assumption is to replace

$$\frac{1}{\sqrt{2\pi}\sigma_x} \exp \left[-\frac{1}{2} \left(\frac{x}{\sigma_x} \right)^2 \right]$$

in Equations 3 and 4 by L_x^{-1} . The model then describes a plume which is well mixed in the x-direction. Our situation then is neither of the cases,

$$\sigma_x \ll L_x \qquad \text{Gaussian in X}$$

nor

$$\sigma_x \gg L_x \qquad \text{well mixed in X}$$

Hence, we are in the "grey" region between the two models.

With log uniform distributions, the sampling method selects a majority of small values of α_L . Hence, we expect Equations 3 and 4 to be adequate for most vectors. For a few vectors, however, the model may be in error.

The maximum concentration may be expected to be between the values given by the two models,

$$C_{\max} = \frac{\dot{C}_0}{2\pi\sigma_x\sigma_y v} \quad \text{Gaussian}$$

$$C_{\max} = \frac{\dot{C}_0}{L_x\sqrt{2\pi}\sigma_y v} \quad \text{well-mixed}$$

for point-sources, and

$$C_{\max} = \frac{\dot{C}_0}{2w\sqrt{2\pi}\sigma_x v} \quad \text{Gaussian}$$

$$C_{\max} = \frac{\dot{C}_0}{2wL_x v} \quad \text{well-mixed}$$

for line sources. We will use the Gaussian model and note that, for a few vectors, the calculated value and another value given by multiplying by a factor,

$$\frac{\sqrt{2\pi}\sigma_x}{L_x}$$

bound the correct value. The factor is of the order of unity.

Choice of C_{max}

We have chosen C_{max} , as given by Equation 6, to present the results of these calculations. It is useful in that it provides a quantity that can be easily manipulated in response to questions relating to regulatory development. For example, a more interesting quantity may be an average concentration across some width of the aquifer including the plume. For example, essentially all of the plume is contained in a "pipe" of diameter 6σ . The area of a plane through that pipe is

$$\frac{1}{2} \pi (3\sigma)^2$$

where the factor of $1/2$ comes from considering only the half-plane shown in Figure 1. An average concentration is then given by,

$$\bar{C} = \frac{2\dot{D}}{9\pi\sigma^2q} = \frac{2}{9} C_{\max}$$

for point sources, and

$$\bar{C} = \frac{\dot{D}}{3\sigma(2w)q} = \frac{\sqrt{2\pi}}{3} C_{\max}$$

for line sources.

The choice of an even larger area gives larger quantities of groundwater discharge and correspondingly lower concentrations.

Thus C_{\max} is a useful quantity, from a computational point-of-view, which may be scaled to include other effects and assumptions.

Implementation

Radionuclide discharge rates were calculated with NWFT/DVM. Because of uncertainty in the data used by NWFT/DVM, Latin Hypercube Sampling (LHS) was used to select multiple sets of input (vectors) to calculate discharge rates, one discharge rate as a function of time for each radionuclide and each input vector. Latin Hypercube Sampling provides an unbiased estimate of

the cumulative distribution function of the model output (discharge rate at each time) [6].

Among the quantities sampled by LHS are hydraulic properties and dispersivities. These are used to calculate q and σ in Equation 6. To evaluate α_T ($\sigma^2 = 2\alpha_T Z_0$) we make the usual assumption relating the longitudinal and transverse dispersivity,

$$\alpha_T = \frac{1}{10} \alpha_L$$

Thus, the NWFT/DVM results and the LHS chosen input vectors may be used to evaluate Equation 6 for each postulated scenario.

In the bedded salt analyses [2] multiple borehole scenarios were considered. The assumption was made in the results presented here that all released radionuclides issued from a single borehole. This assumption is conservative in that it gives a concentration, C_{max} , as given by Equation 6. For N boreholes, the concentration may be as low as C_{max}/N depending on the distance between boreholes. For the scenarios examined, N was generally less than ten.

Table 2

Radionuclide Inventories and 10CFR20 Limits

Radionuclide	Initial Curies	RCG or RCG _{eff} (Ci/m ³)
<u>4n + 0</u>		
240 Pu	4.61E7	5.E-6
236 U	3.16E4	3.E-5
232 Th	3.22E-5	2.E-6
228 Ra	8.95E-6	2.85E-8
<u>4n + 1</u>		
245 Cm	3.34E4	4.E-6
241 Pu	4.4E9	2.E-4
241 Am	2.E8	4.E-6
237 Np	4.04E4	3.E-6
233 U	7.96E0	3.E-5
229 Th	1.55E-2	3.76E-7
<u>4n + 2</u>		
246 Cm	6.64E3	4.E-8
242 Pu	1.30E5	5.E-6
238 U	3.03E4	1.33E-5
238 Pu	3.08E8	5.E-6
234 U	9.95E4	3.E-5
230 Th	1.68E1	2.E-6
226 Ra	8.09E-2	2.88E-8
210 Pb	1.78E-2	8.73E-8
<u>4n + 3</u>		
243 Am	1.73E6	4.E-6
239 Pu	3.19E7	5.E-6
235 U	1.6E3	2.6E-5
231 Pa	3.39	9.E-7
227 Ac	1.44	3.35E-7
<u>Fission/Activation Products</u>		
137 Cs		2.E-5
135 Cs		1.E-4
129 I		6.E-8
126 Sn		3.E-6
99 Tc		3.E-4
90 Sr		3.E-7
14 C		8.E-4

III. Use of 10CFR20

An existing Federal Regulation, 10CFR20 [5], regulates radionuclide concentrations in drinking water by specifying a recommended concentration guide (RCG) in Curies/m³ H₂O for each radionuclide. For mixtures of radionuclides, such as we are considering, the standard required

$$1 \geq \sum_i \frac{C_i}{RCG_i}$$

where the sum over i denotes summation over all discharged radionuclides, C_i is the concentration of the i^{th} radionuclide, and RCG_i is given by 10CFR20 as shown in Table 4. Thus we will calculate a quantity $f(c)$,

$$f(c) = \sum_i \frac{C_i}{RCG_i} \quad (8)$$

In order to include the short-lived radionuclides excluded from the groundwater transport problem, we define an effective recommended concentration guide for the transported parent, $RCG_{i,eff}$,

$$\frac{1}{RCG_{i,eff}} = \sum_j \frac{f_j}{RCG_j} \quad (9)$$

The sum in Equation 9 includes all daughters of radionuclide i not included in the groundwater transport problem. The f_j relate the activity of the j^{th} daughter to that of the transported parent, i . They deviate from unity due to branching. The $RCG_{i,\text{eff}}$ are shown in Table 2. Figures 2 through 5 show the four actinide decay chains that were transported and include the short-lived daughters which must be included in Equation 9. The f_j may be calculated analytically but were inferred empirically from an ORIGEN calculation [7].

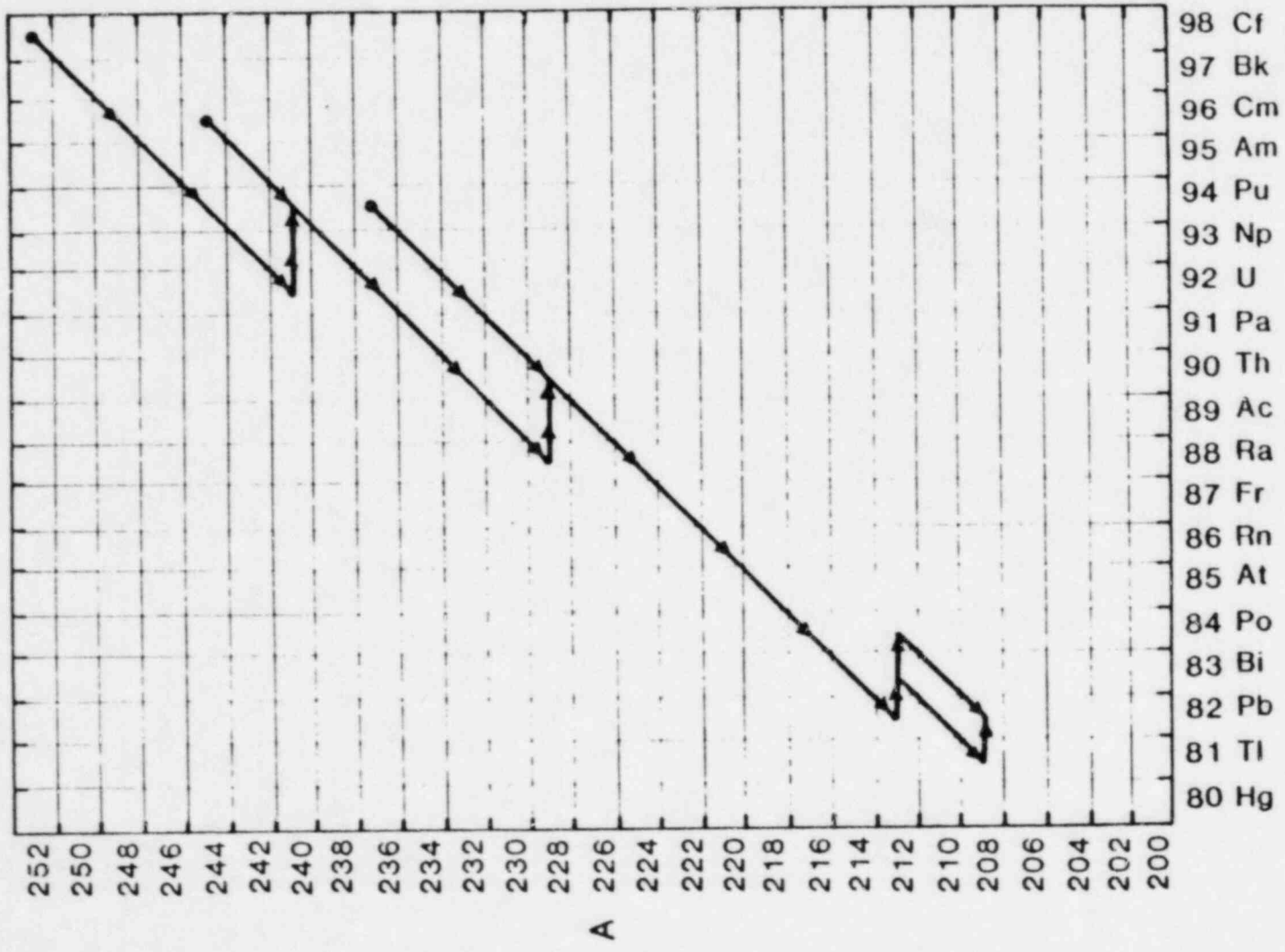


Figure 2. The 4n + 0 Series

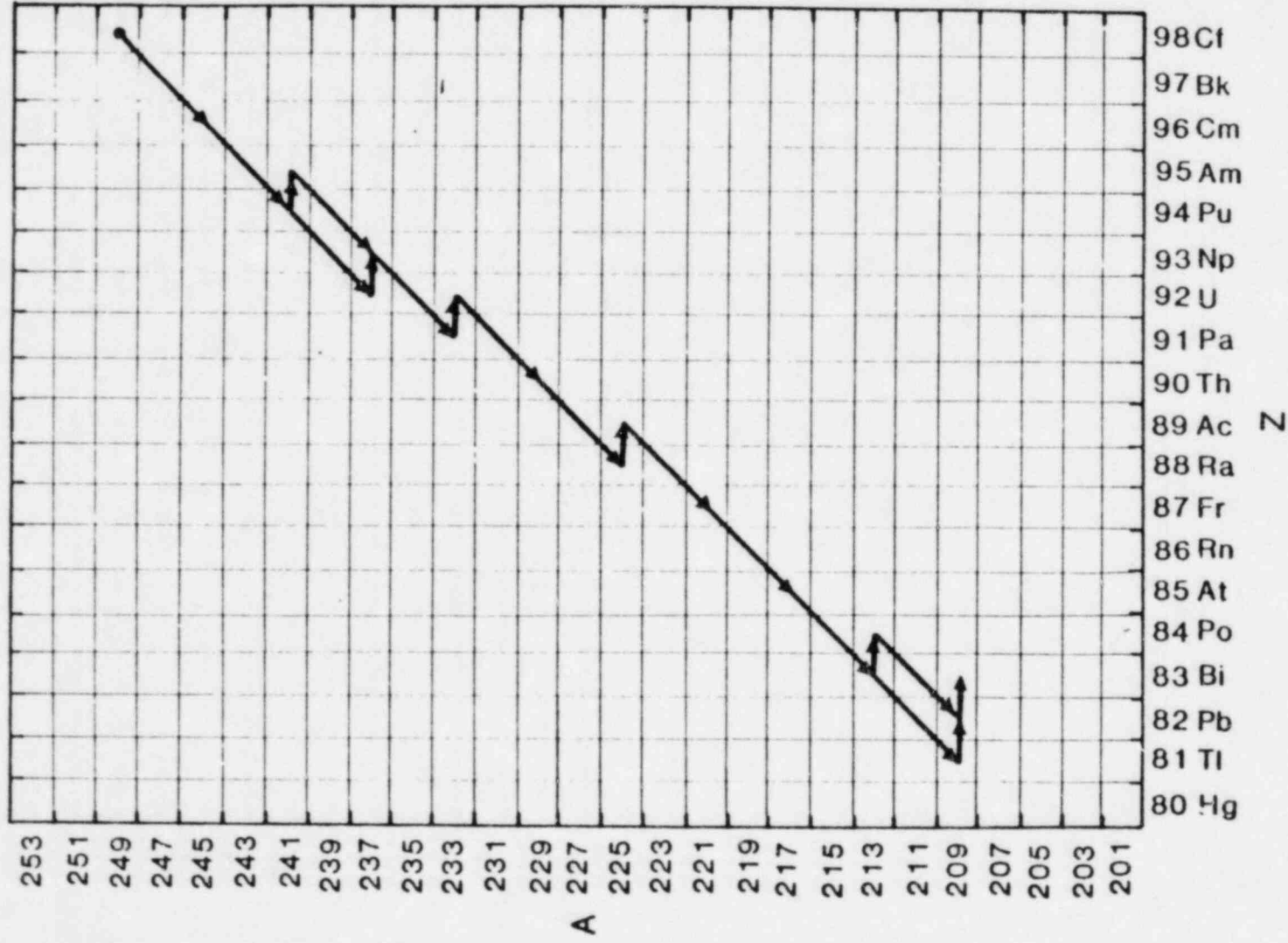


Figure 3. The 4n + 1 Series

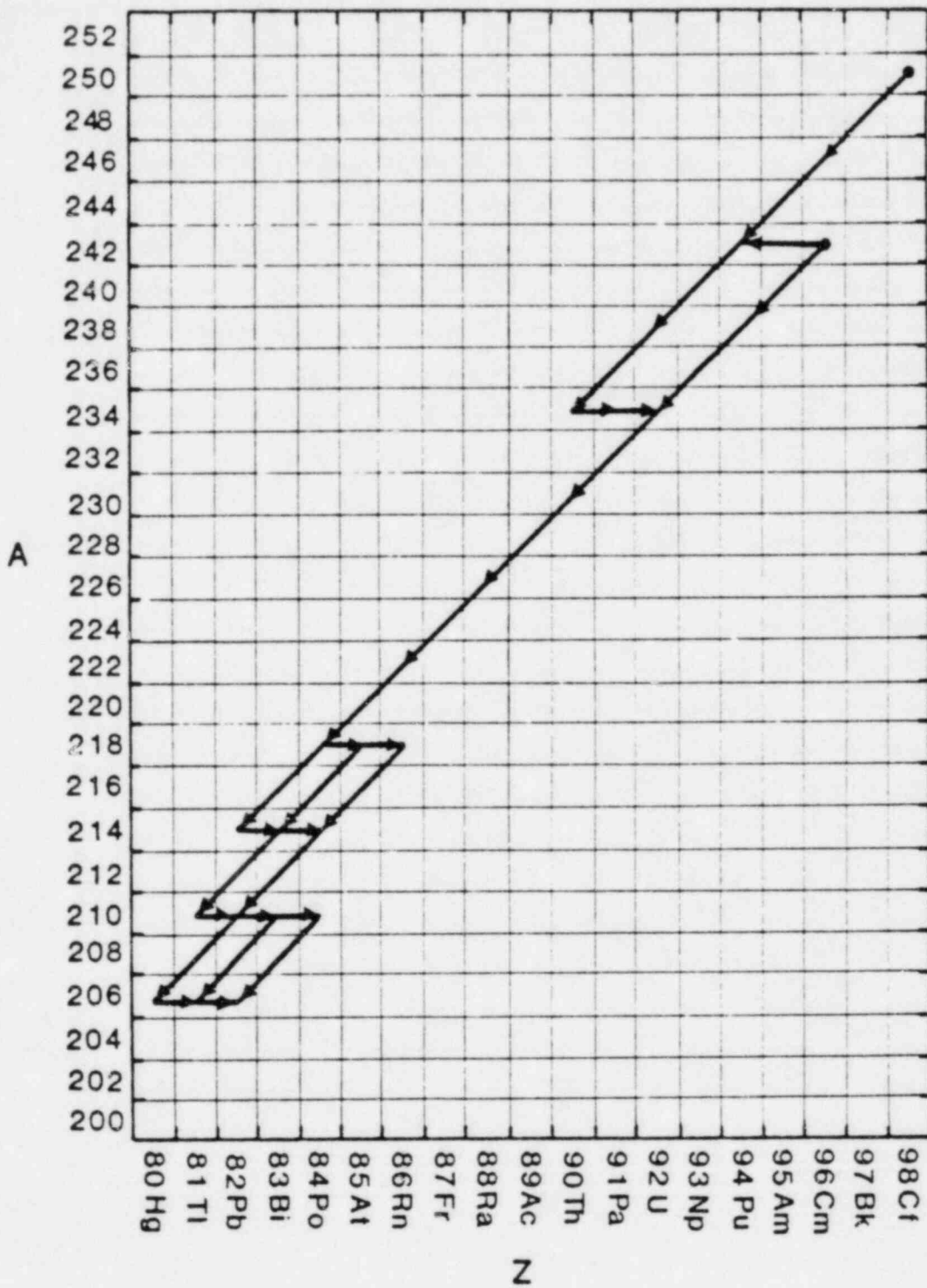


Figure 4. The $4n + 2$ Series

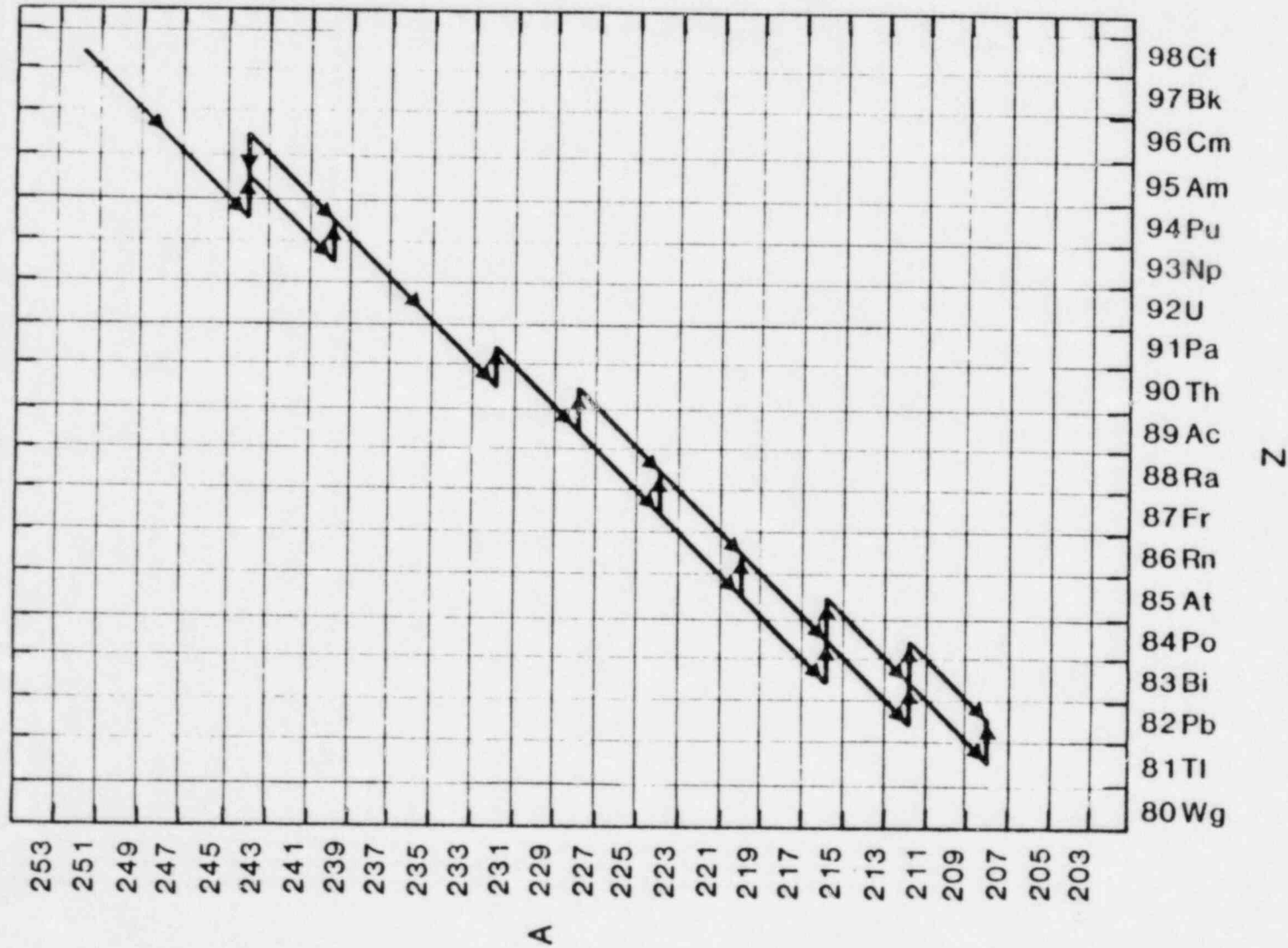


Figure 5. The 4n + 3 Series

IV. Computation Results

The methods developed in the preceding discussion were applied to results from two analyses previously reported [1, 2]. The first analysis reported [1] examined a hypothetical geologic repository in basalt. The second [2] examined a hypothetical bedded salt repository.

In the basalt analysis, three scenarios* were examined. In addition, one scenario was evaluated using two models for the radionuclide source term for the groundwater transport model. The scenarios analyzed were

Scenario	Description	Source
1	undisturbed case	leach limited
2	fractures in dense basalt	leach limited
3	borehole penetration	leach limited
4	borehole penetration	mixing cell

Scenarios 1 and 2 involved vertical flow and radionuclide migration to an overlying aquifer. The cross-sectional area of the column of flowing water was

*A scenario is defined as a unique set of events or processes which lead to radionuclide release. Each scenario has an associated flow geometry and transport variables, as determined by LHS, which are assumed to remain constant throughout a 50,000 year transport calculation.

large, comparable to the area of the subsurface facility, and treated as a line source of radionuclides into the overlying aquifer. Scenarios 3 and 4 were treated by assuming point-sources of radionuclide discharge into the overlying aquifer.

All input vectors for Scenarios 1 and 2 were evaluated with a leach-limited source assumption as selected by a source-term selection algorithm in NWFT/DVM. For Scenario 4, this algorithm selected the mixing cell model. For comparison, a leach limited source was imposed and the scenario was evaluated as Scenario 3.

In the analysis of the bedded salt repository, four groundwater transport scenarios were examined [2]. Each scenario involved borehole penetrations and failed shaft seals making a U-tube flow path. Each scenario was evaluated with three different source models. These models were described previously [2] and are summarized here. All scenarios were assumed to represent point sources of radionuclides discharging into the overlying aquifer.

- Source #1: the entire radionuclide inventory is assumed to be available for transport. The radionuclides are released at leach-limited rates sampled from the range, 10^{-5} - 10^{-7} /year.
- Source #2: a restricted fraction of the radionuclide inventory is assumed to be available for transport. The fraction is given by assigning one roomful of waste to each borehole in the input vector determined by LHS. There are 106 rooms in the reference design. Such an assumption may be valid if groundwater flow was confined to the immediate vicinity around the borehole. The leach rate range sampled is the same as for Source #1.
- Source #3: Source #2 is assumed but in addition, the backfilled rooms are treated as a mixing cell. Radionuclide release then occurs at a rate sensitive to the radionuclide concentration in the mixing cell. (This is the standard SNL source assumption.) For this source, leach rates were sampled from the range, 10^{-3} - 10^{-7} year.

Data used in the groundwater transport calculation was reported previously [1,2]. Data selection (input vectors) was made by the LHS method.

The results of these calculations are presented in figures that follow. Each input vector of the NWFT/DVM calculation produces discharge rates which are used to evaluate Equations 6 and 8 at each time. There are simply too many input vectors to present the results for each of them. We have chosen four forms to present results:

- 1) At each time, the values of Equation 8 are examined for the whole set of vectors to determine a mean value.
- 2) At each time, the values of Equation 8 are examined for the whole set of vectors to determine a maximum value.
- 3) For each vector, the maximum value of Equation 8 (over time) is recorded. Since each input vector chosen by the LHS method is equally probable, the result can be used to estimate the distribution of maximum values of Equation 8 that may occur any time during the 50,000 year interval. The probability that the scenario will occur is not included in this construction.

- 4) For each vector calculated, the dominant contributors to Equation 8 were recorded. This result was tabulated for each vector and scenario in summary tables. The tables indicate the number of vectors that the given radionuclide had a first or second ranking. An entry in the tables does not necessarily mean that the vector produced a large value of Equation 8.

Basalt Scenarios: Mean Values

In Figures 6a through 9a, mean values of Equation 8 versus time are shown. Scenarios 1 and 2 are noticeably lower than Scenario 3 for the leach limited cases. All of the basalt scenarios are characterized by relatively rapid transport through the overlying aquifer. Also, for leach limited sources, the rate of radionuclide release is independent of the quantity of water flowing through the backfilled regions. Thus it appears that the differences between Scenarios 2 and 3 can be explained in terms of two causes: (1) the earlier breakthrough time associated with the borehole, and (2) the larger dilution volumes associated with the line source.

The mixing cell source term of Scenario 4 greatly reduces the expected concentrations and shows the importance of the source term assumption. The concentrations are

actually lower than those of the undisturbed case with a leach limit, Scenario 1. Ordinarily, the undisturbed case gives a small consequence compared to that of the disturbed case. For Scenarios 1 and 4 this does not appear to be the case. Scenario 4 is presented only as a demonstration of the importance of the source. Some combination of the two scenarios may be a more appropriate choice for this analysis.

Maximum Values

Figures 6b through 9b show the maximum value of Equation 8 for the four scenarios. Most of the discussion of the mean values is appropriate here also.

Maximum Value Distributions

The maximum values of Equation 8 for each vector at any time are plotted as a Complimentary Cumulative Distribution Function (CCDF) giving the fraction of input vectors producing values of Equation 8 exceeding a value denoted as CSUM. The CCDFs are shown in Figures 10 through 13. Noting the requirements of 10CFR20, the value of unity in these figures is a reference. All 100 input vectors produced values of CSUM less than unity for Scenarios 1 and 4. Scenario 2 gives approximately 3

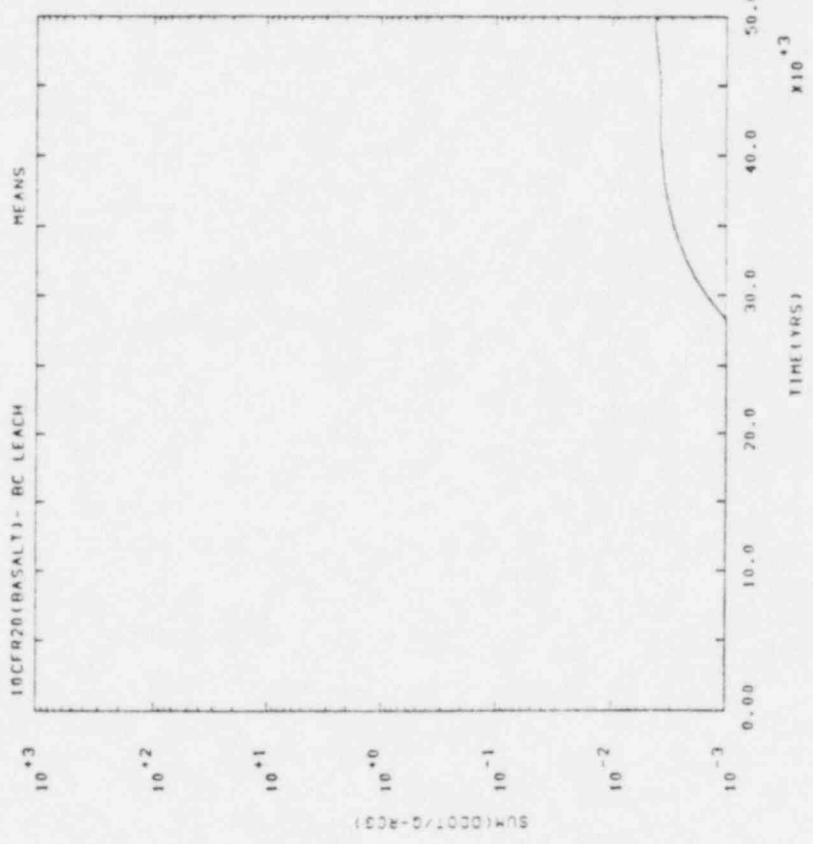
percent of the vectors exceeding unity. Scenario 3 gives about 30 percent of the vectors exceeding unity.

Important Radionuclides

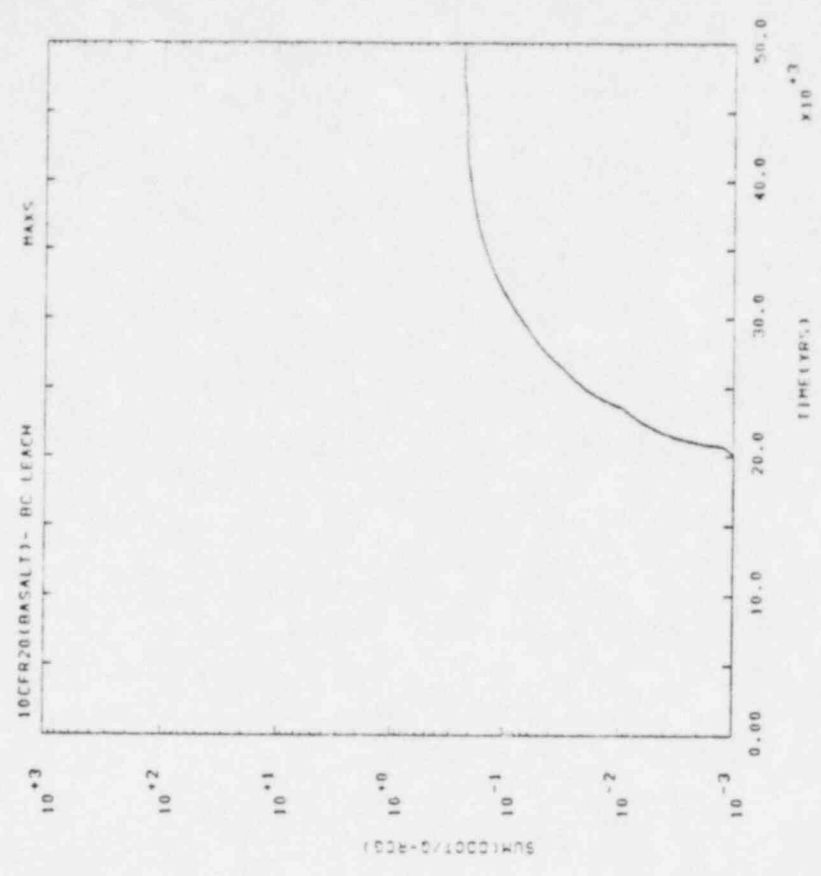
The individual radionuclides' contributions to Equation 6 were examined at each time and for each vector. The dominant two radionuclides were recorded at each time to produce a list of radionuclides that were important at some time during the calculation of that vector. These results are shown in Table 3. An entry in this table indicates that the radionuclide had a first or second ranking for the specified number of vectors.

Table 3
Important Radionuclides for Basalt Scenarios
(100 vectors, maximum)

Radionuclide	Scenario			
	1	2	3	4
240Pu			33	12
241Am			1	1
237Np			35	19
233U			5	
229Th			6	
238U			1	
234U			8	10
226Ra			46	43
210Pb			33	38
243Am			3	11
239Pu			31	11
227Ac			1	
99Tc	8	63	20	27
126Sn		1	1	
129I	58	99	100	96
14C	99	99	100	100



(a)



(b)

Figure 6. Basalt Scenario 1: the base case, mean and maximum versus time

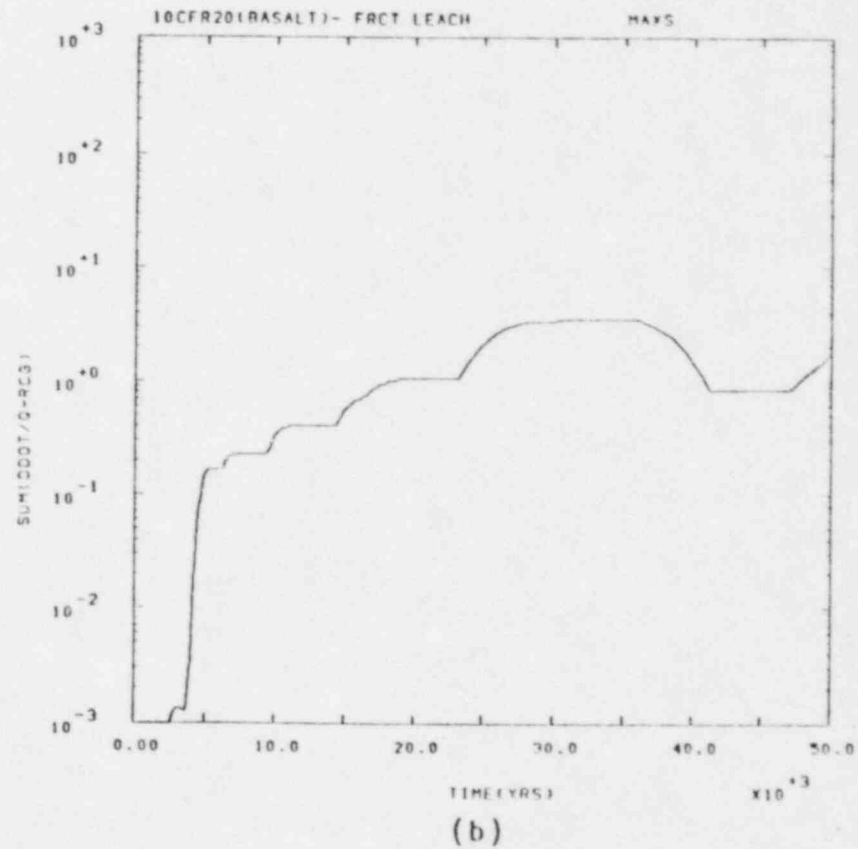
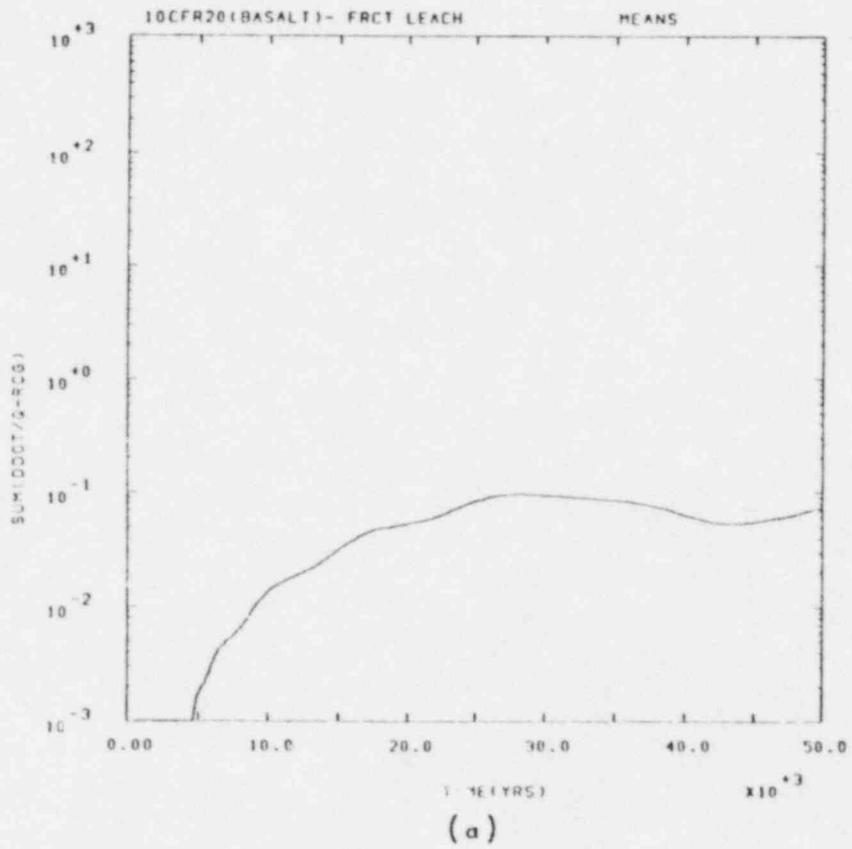
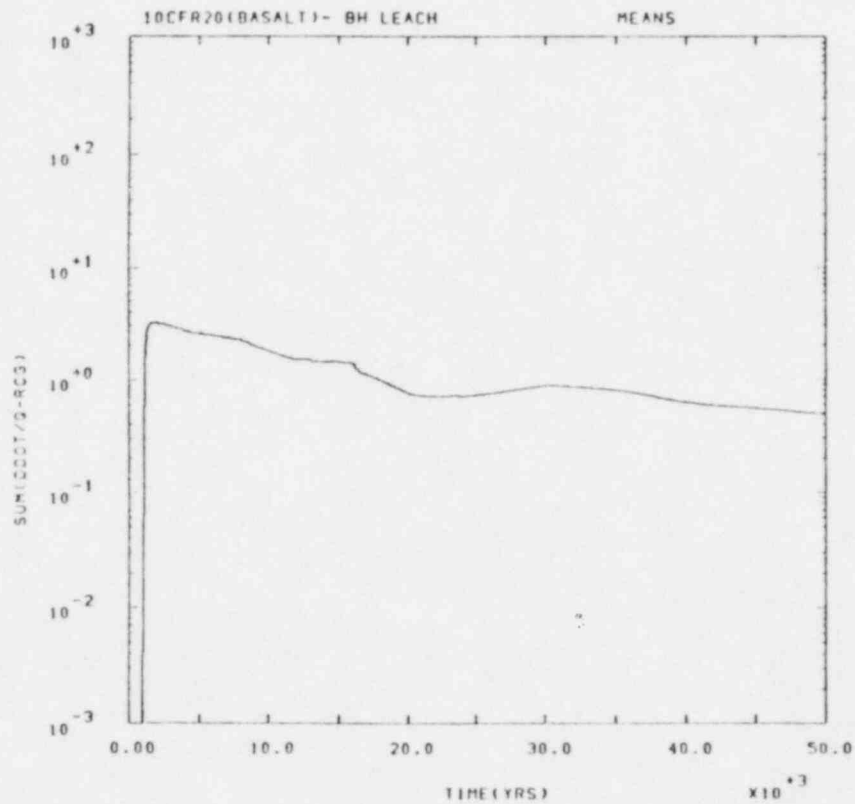
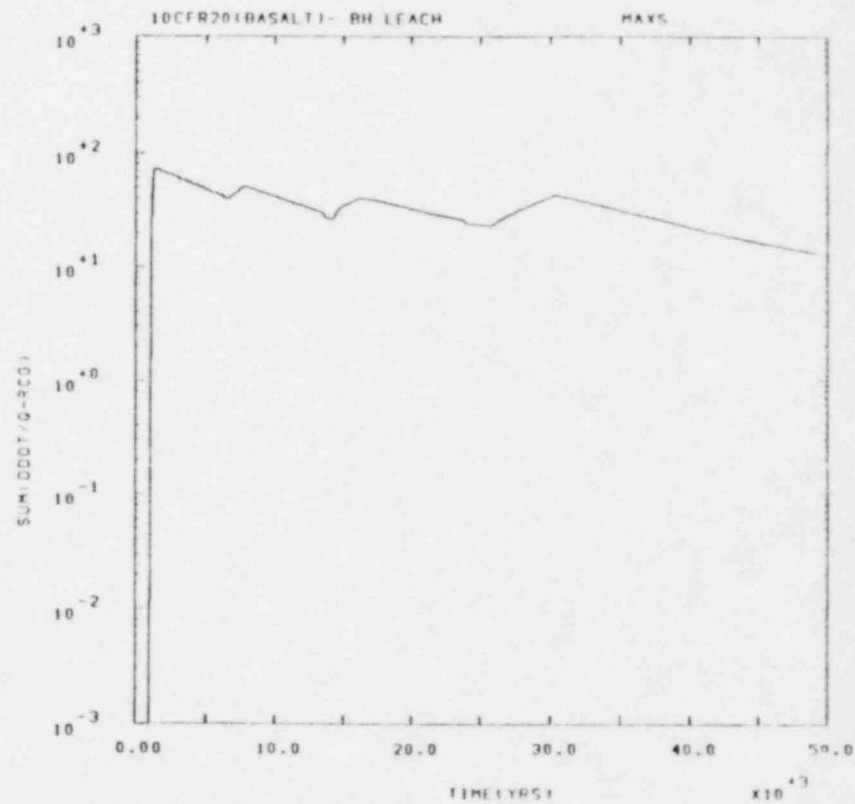


Figure 7. Basalt Scenario 2: fractures in dense basalt, mean and maximum versus time

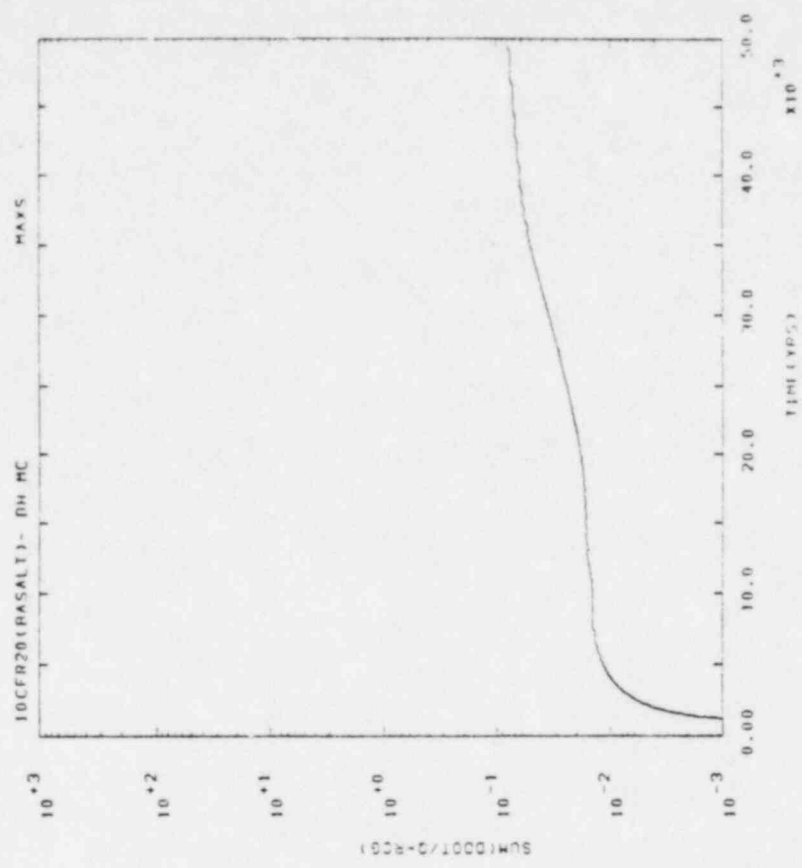


(a)

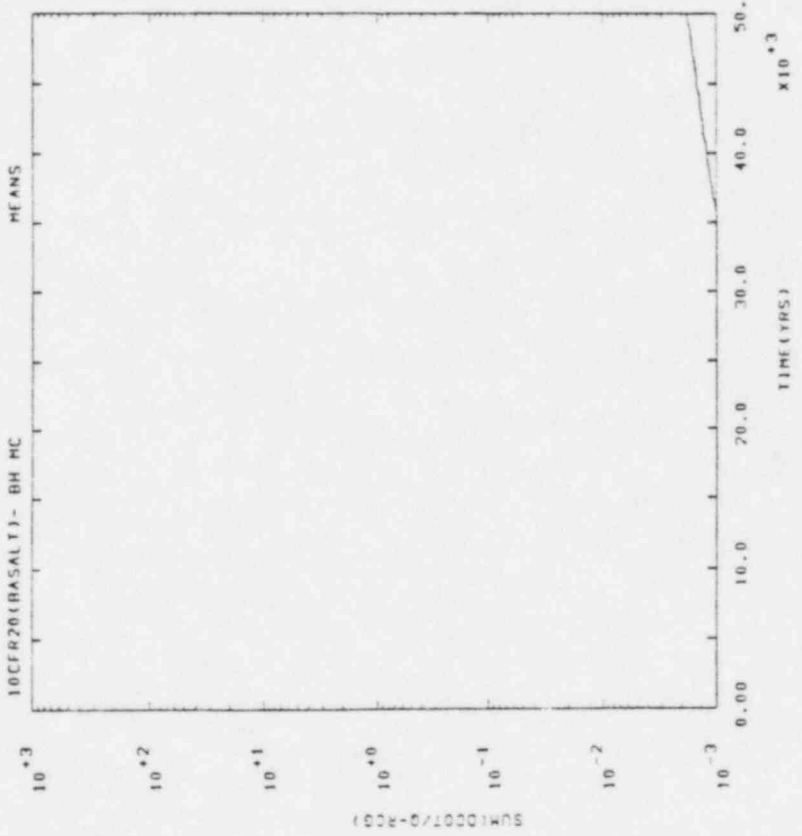


(b)

Figure 8. Basalt Scenario 3: the borehole, leach limited, mean and maximum versus time



(a)



(b)

Figure 9. Basalt Scenario 3: the borehole, mixing cell, mean and maximum versus time

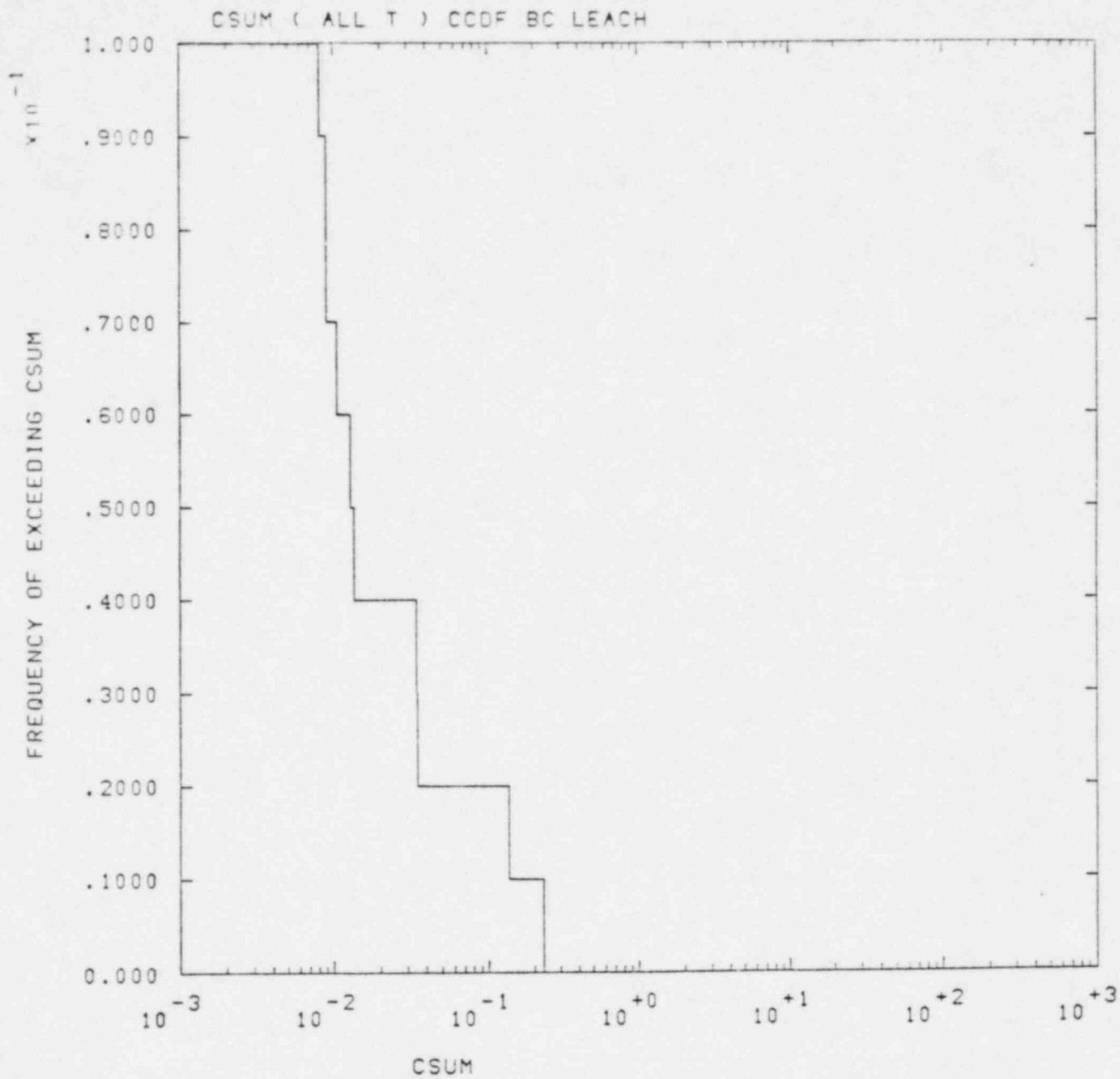


Figure 10. CCDF for Basalt Scenario 1, maximum concentrations

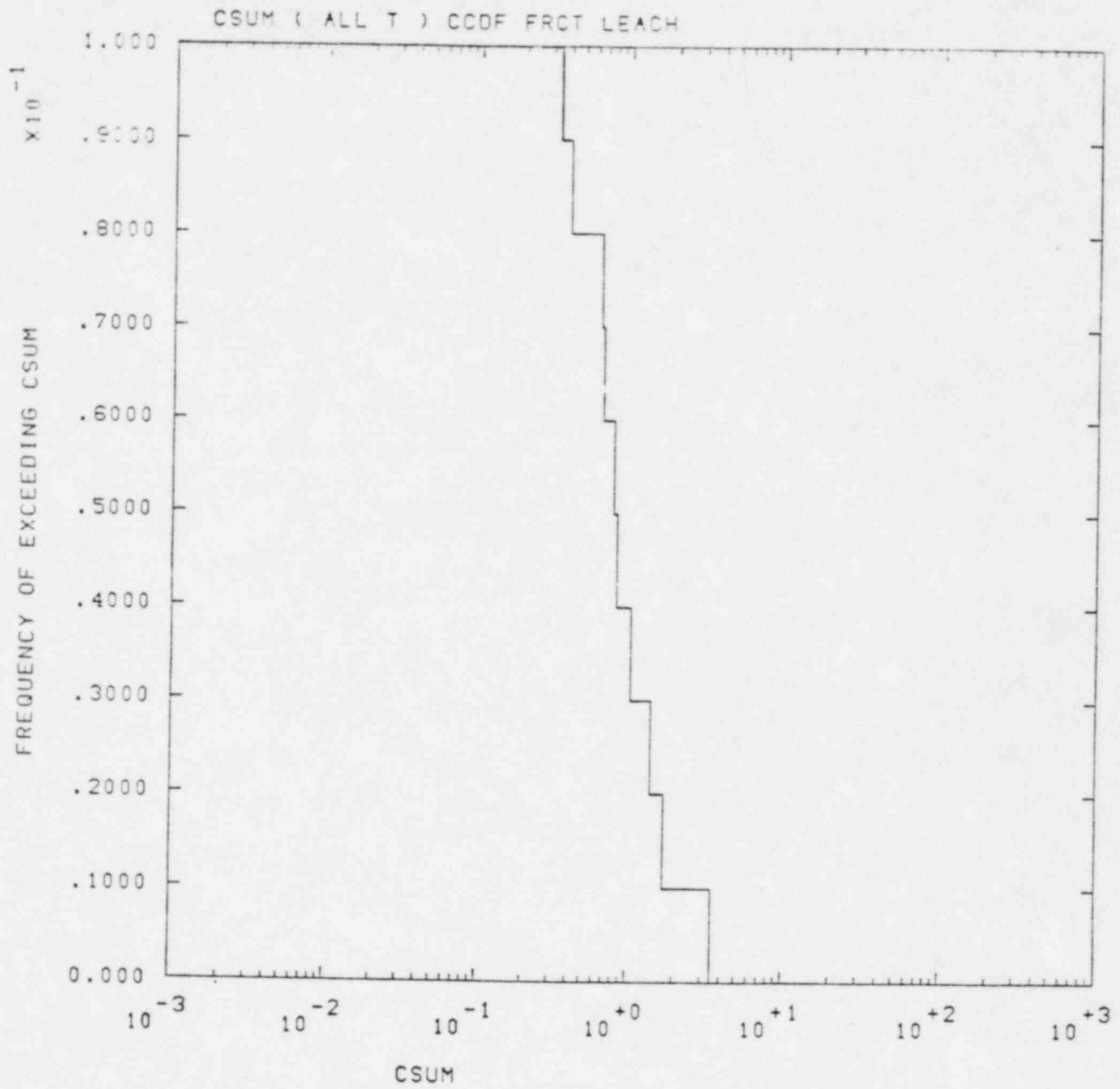


Figure 11. CCDF for Basalt Scenario 2, maximum concentrations

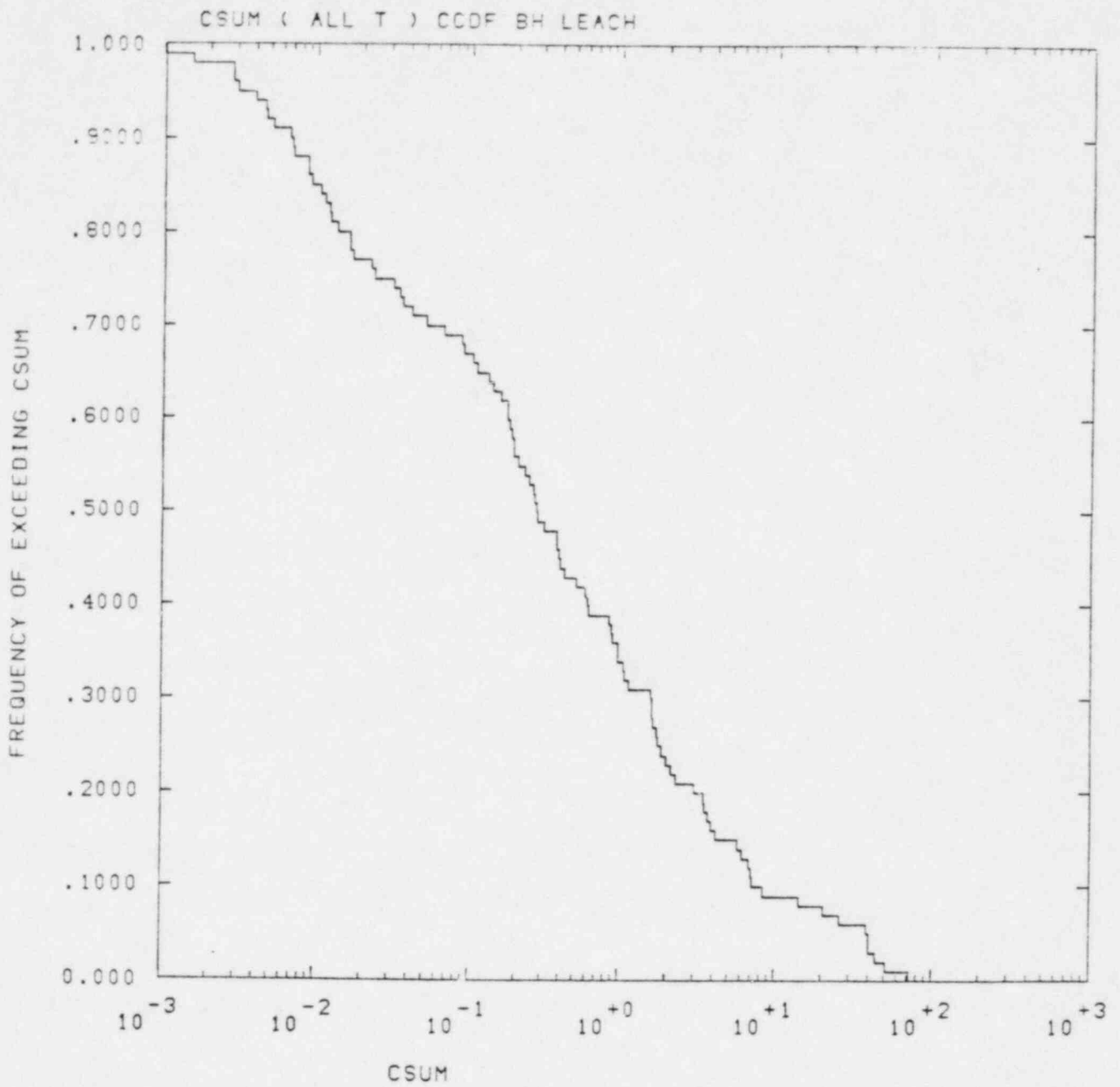


Figure 12. CCDF for Basalt Scenario 3 (Leach Limited), maximum concentrations

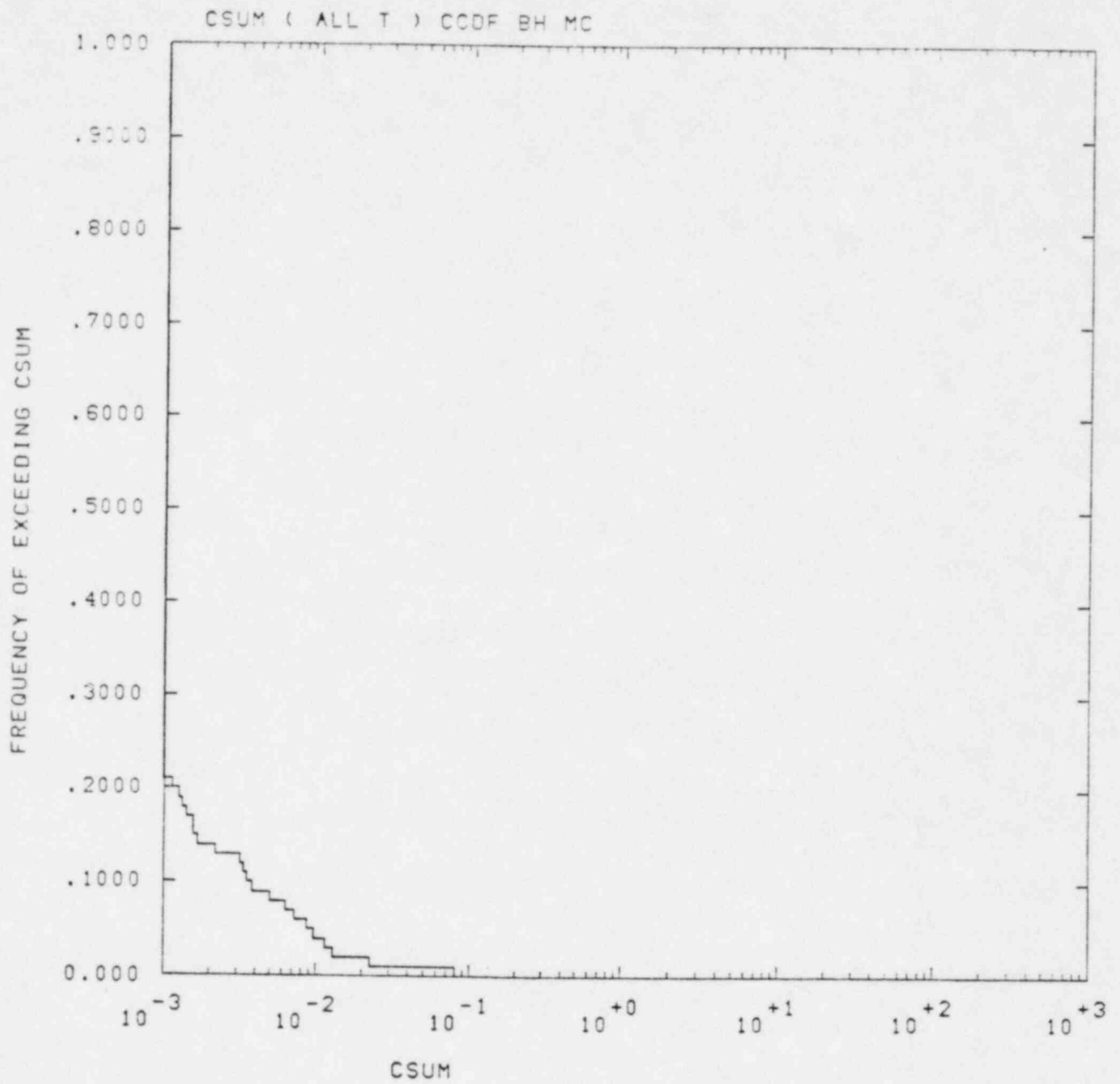


Figure 13. CCDF for Basalt Scenario 3 (Mixing Cell), maximum concentrations

Bedded Salt Scenarios

Before discussing the numerical results of the analyses of the bedded salt scenarios, we will discuss some of the general behavior expected of Equation 6 since the bedded salt scenarios seem to demonstrate them so clearly. The scenarios analyzed involve different combinations of failed shafts and boreholes with radionuclide transport to the accessible environment occurring through one of two possible overlying aquifers. In all scenarios, failed boreholes release radionuclides to the overlying aquifer and are modeled as point sources.

In the bedded salt scenarios, replicated sampling was used to estimate the magnitude of sampling error. In doing so, independent samples of input data were evaluated with the models described. The results of evaluations with each set are presented simultaneously. By doing this, the variation in calculated results due simply to sampling error are demonstrated.

Three sources were assumed in these analyses, two of which are leach limited. The third source assumed models the backfilled region as a mixing cell. Radionuclides are assumed to be released from the waste packages at a specified rate (the leach rate) into the mixing cell where they mix with groundwater. Release rate for the groundwater transport calculation are governed by their

concentrations in the mixing cell and their residence time in the cell. The residence time in the mixing cell is in turn governed by the rate of groundwater flow through the cell and its flow velocity. This source model has been described in appendices to References 1 and 2.

The first two sources assume radionuclide release rates from the backfilled regions to occur at leach limited rates. Only the fraction of wastes accessed by the flowing groundwater is assumed to vary, as discussed previously. For leach limited sources, the characteristics of groundwater flow through the backfilled regions do not influence the release rate. All other things being the same, the release rate is then simply related to the fraction of waste accessed. We take care of the "all other things being equal" condition by using the same input vectors for all calculations, the same conductivities, sorption constants, porosities, etc., for each analysis.

For the leach limited sources, Equation 6 may be used to estimate the behavior expected in the calculated results. The relationships derived will be crude, based on mean values, but will be useful in making order-of-magnitude estimates of the behavior expected as the source model assumption or scenario are varied.

From Equation 6 we expect the variables affecting q and i to affect the calculated results. The Darcy velocity, q , is given by,

$$q = Ki$$

where K is the hydraulic conductivity, a sampled quantity, and i is the hydraulic gradient in the aquifer assumed to be constant at .007. For Scenarios 3 and 4, the value of K was chosen to be 1/10 of the value for the same input vector in Scenarios 1 and 2. The dispersivities, which affect σ , are chosen according to the LHS method from the distributions shown in Table 1. A single loguniform distribution was sampled to determine a value of the dispersivity from the assumed range in Table 1. Thus, a sampled value of $\alpha = 1.0$ feet in Scenarios 1 and 2 was transformed to give a value of $\alpha = 10$ feet in Scenarios 3 and 4.

The distributions shown in Table 1 and the value of K assumed may be used to estimate the expected relative behavior. Letting a subscript, n , denote the scenario and m denote the source, the value of Equation 6 for a similar scenario with a leach limited source may be estimated relative to a reference scenario

$$C_{\max, n, m} = \left(\frac{q_{\text{ref}}}{q_m} \right) \left(\frac{\sigma_{\text{ref}}^2}{\sigma_n^2} \right) \frac{(\text{access fraction})_{n, m}}{(\text{access fraction})_{\text{ref}}} C_{\max, \text{ref}}$$

$$= \left(\frac{K_{ref}}{K_n} \right) \left(\frac{\alpha_{ref}}{\alpha_n} \right) \frac{(\text{access fraction})_{n,m}}{(\text{access fraction})_{ref}} \cdot C_{max,ref}$$

For example, for Source #1 we assumed all access fractions to be unity. Taking Scenario 1 as the reference, Scenario 2 would be expected to give a very similar result since both scenarios assume transport to occur through the same unit (same K and α). The Scenario 3 result could be estimated from Scenario 1 by estimating the α -ratio by the geometric means of the Table 1 extremes,

$$\left(\frac{K_1}{K_3} \right) \left(\frac{\alpha_1}{\alpha_3} \right) = 10 \left(\frac{7.07}{31.6} \right) \approx 2.2$$

For the scenarios analyzed, this term is always unity or 2.2.

The access fraction for Source 2 (and for Source 3) was determined from an estimated number of boreholes leading to the scenario [2]. The accessed fraction was proportional to this number. Thus, the relative access fraction (relative to unity) can be estimated from the number of boreholes expected. Each borehole was assumed to access one of 106 rooms full of waste.

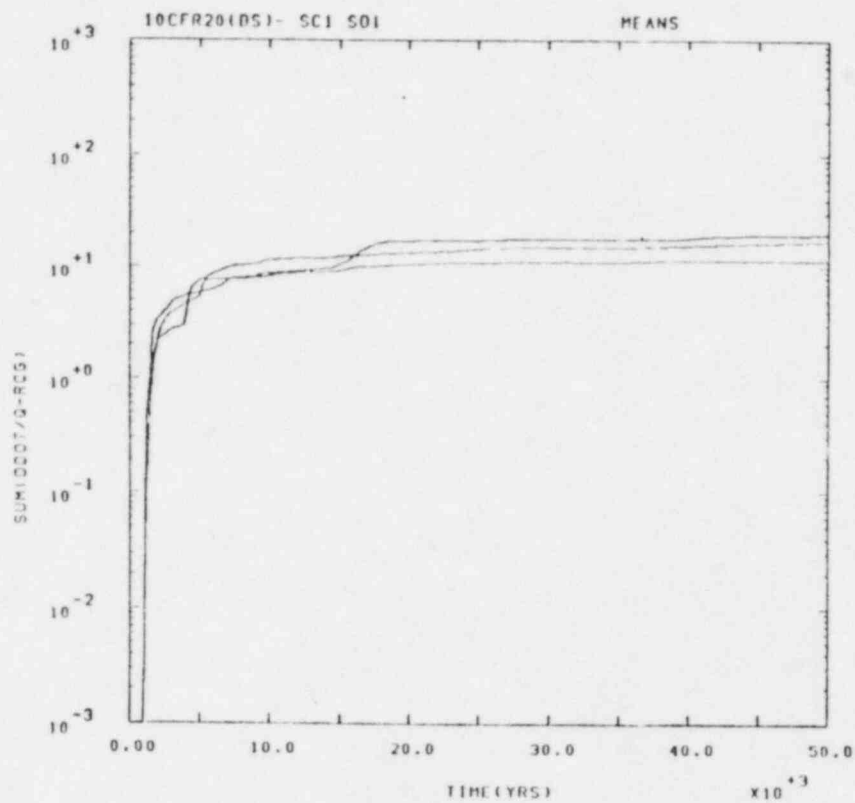
Scenario	Expected Access Fraction			
	1	2	3	4
Source 1	1.0	1.0	1.0	1.0
2 or 3	.015	.024	.030	.034

Numerical Results

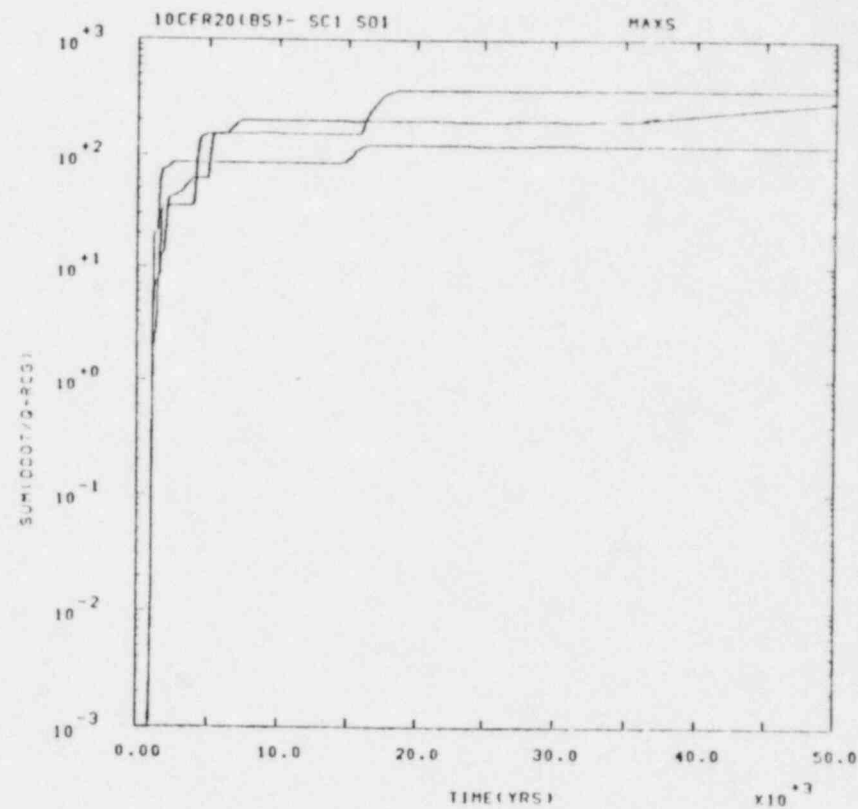
Figures 14 through 21 show the mean and maximum values of Equation 8 versus time. The predicted behavior above is followed reasonably well for the mean values plotted for Sources #1 and #2. The behavior of the maximums is somewhat less satisfactorily in agreement with prediction. Sampling error is acceptably small for the means and larger for the maximums, as may be expected. CCDF's have also been constructed for these scenarios and are shown in Figures 22 through 25. Sampling error is again small. The CCDF's are useful in assessing the likelihood of compliance with 10CFR20. The mean and maximum values versus time of Equation 8 are shown in Figures 26 through 29 for the four scenarios with Source #3. In examining results of analyses with the mixing cell source model (Source #3), the results of Source #2 are most relevant. Both Sources #2 and #3 are assumed to access the same fraction of waste for each input vector. The release rate for the mixing cell model asymptotically approaches that of the leach limited release rate with a time-dependence given by the mean residence time of the radionuclides in the mixing cell [1,2]. Thus, the value of Equation 8 for a given input vector is lower for Source #3 than for Source #2 even though the leach rate for Source #3 was sampled from a

higher range than for Source #2 as discussed previously. CCDF's for the four scenarios are shown in Figures 30 through 33. From these results it appears that the mixing cell assumption, if justifiable, could compensate for a less stable waste form.

Important radionuclides are shown in Table 4. For Sources #1 and #2, the rankings are identical since the source models are simply related. For Source #3 the release rate for several vectors is so low that no discharge occurs.

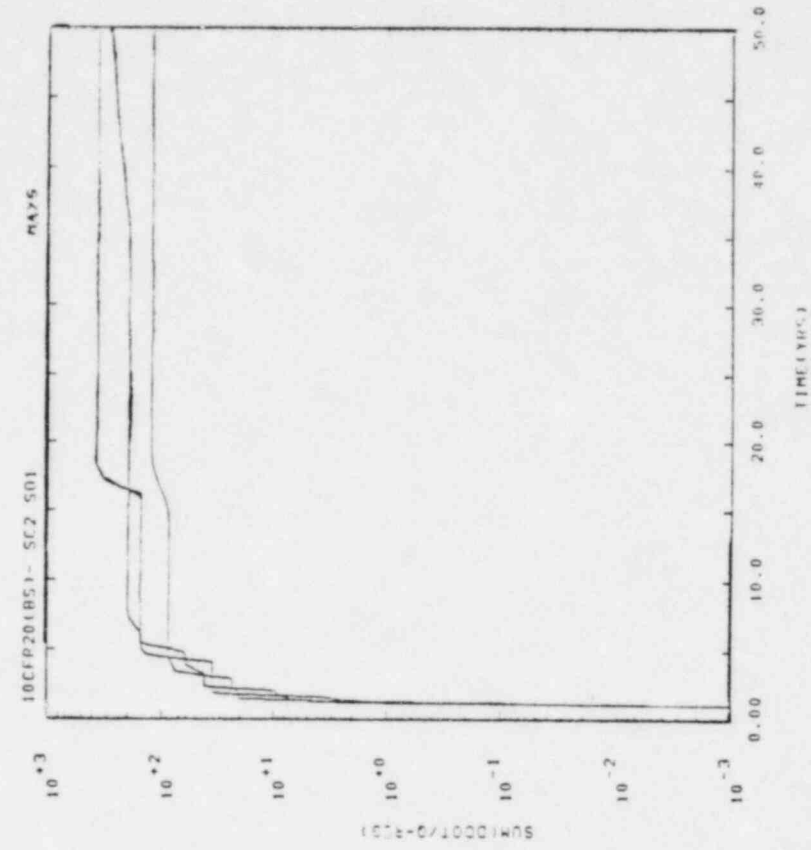


(a)

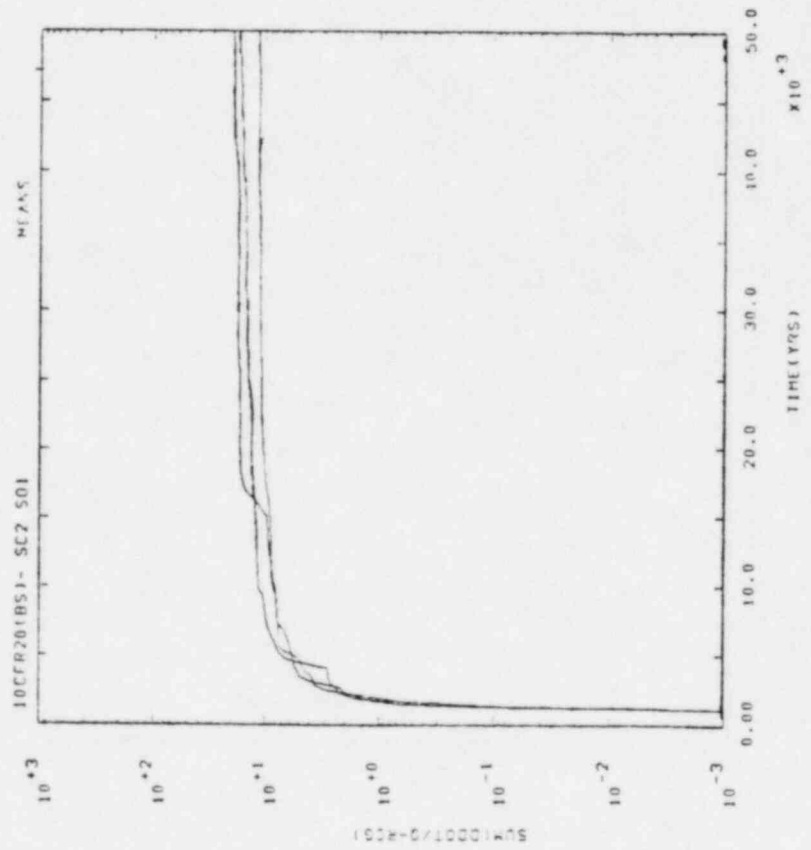


(b)

Figure 14. Bedded Salt Scenario 1, Source 1, mean and maximum versus time



(a)



(b)

Figure 15. Bedded Salt Scenario 2, Source 1, mean and maximum versus time

- 45 -

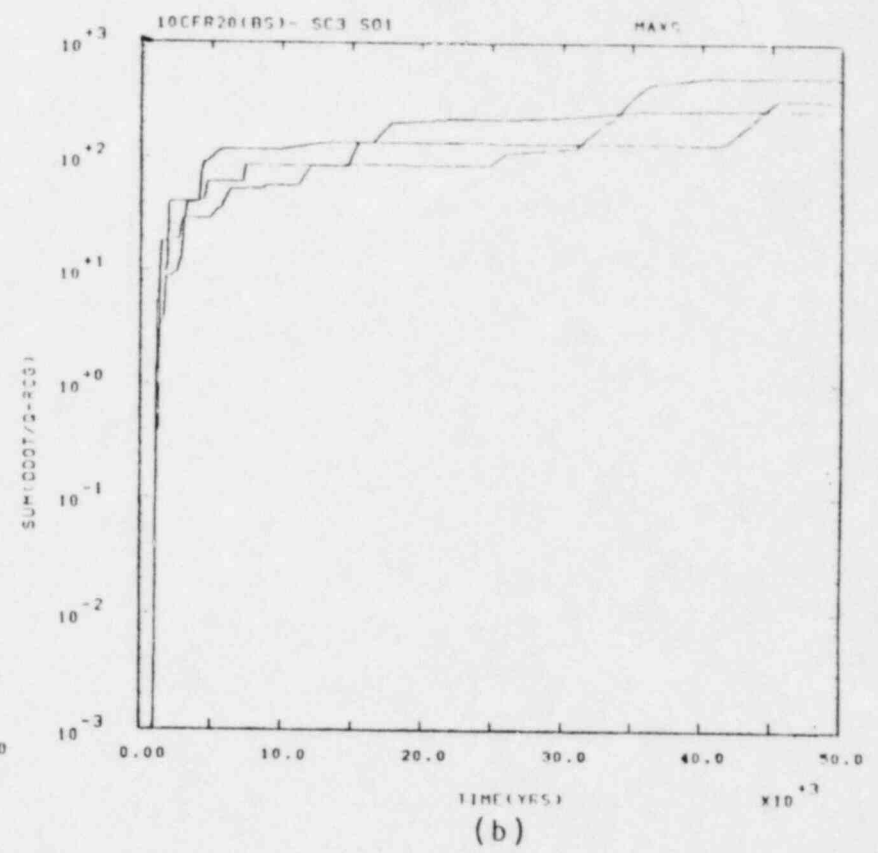
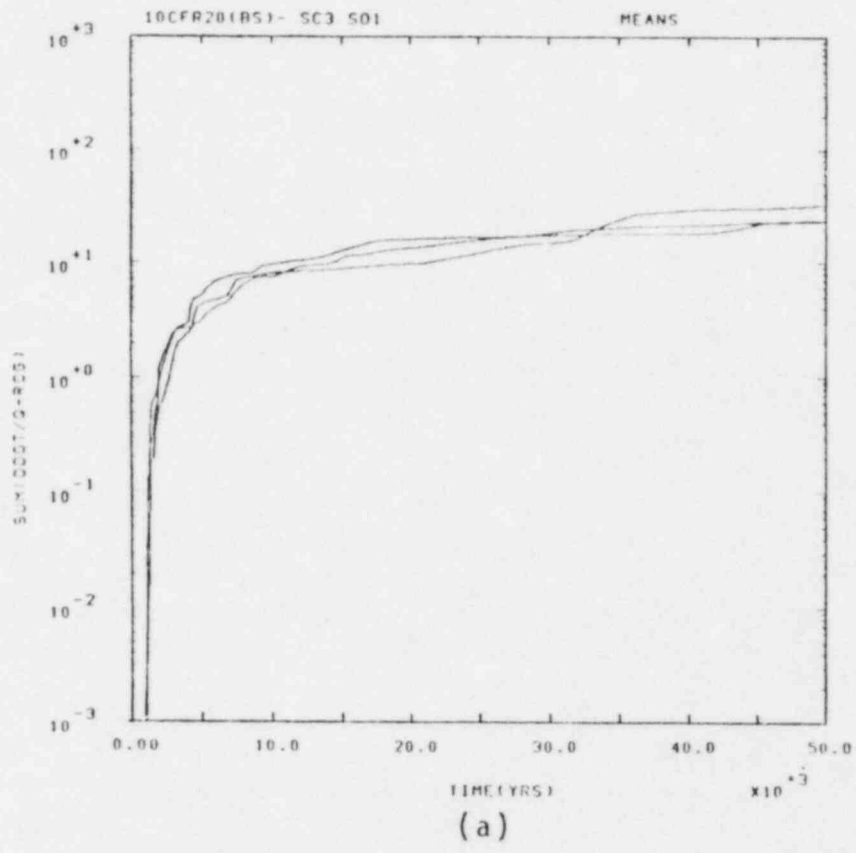
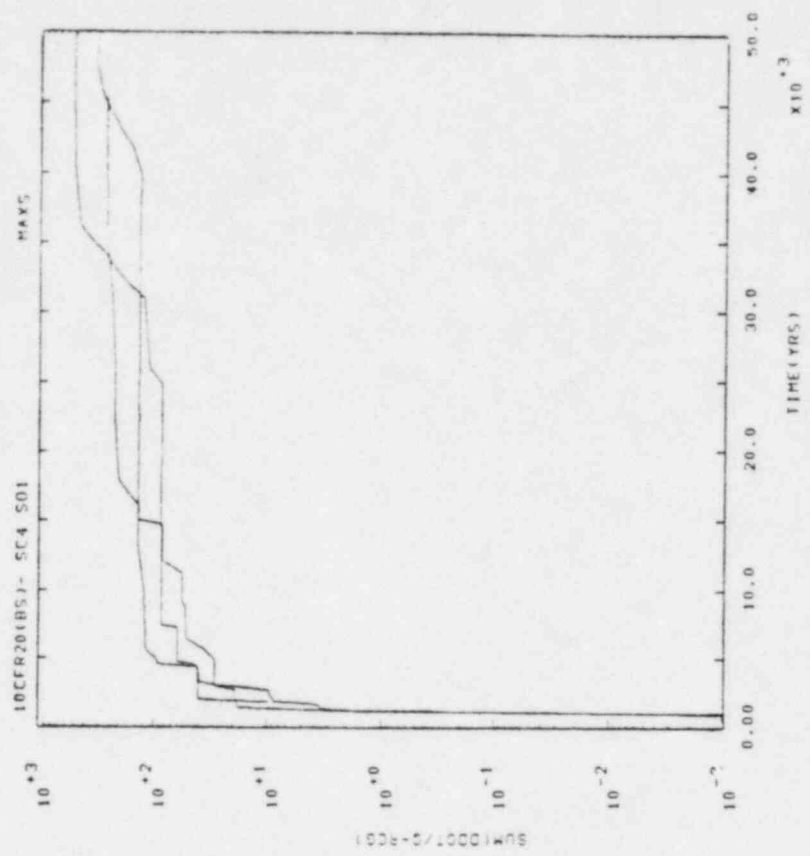
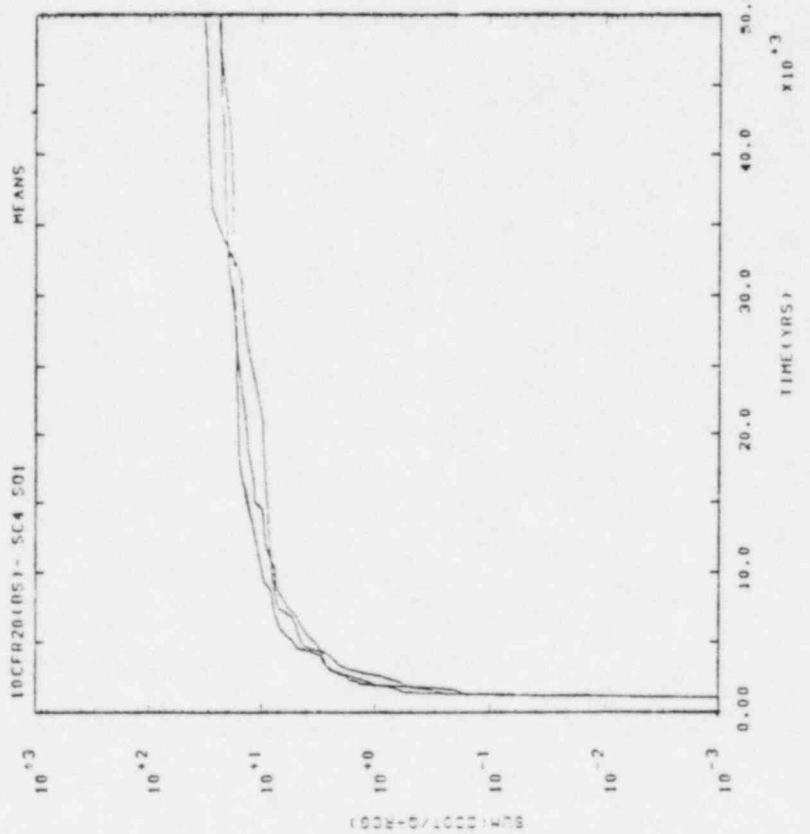


Figure 16. Bedded Salt Scenario 3, Source 1, mean and maximum versus time

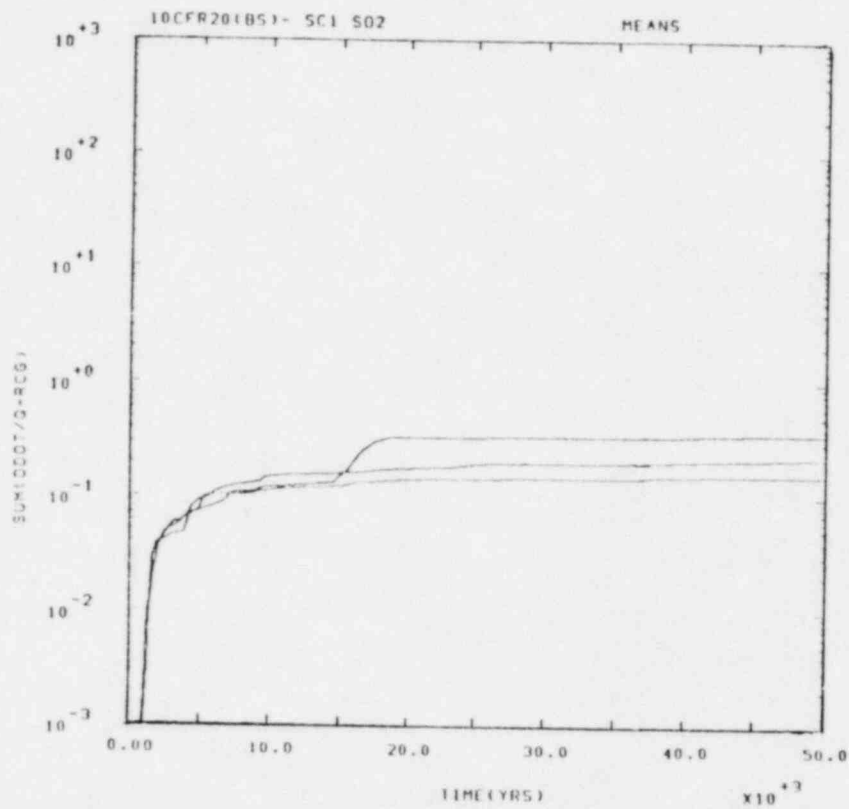


(a)

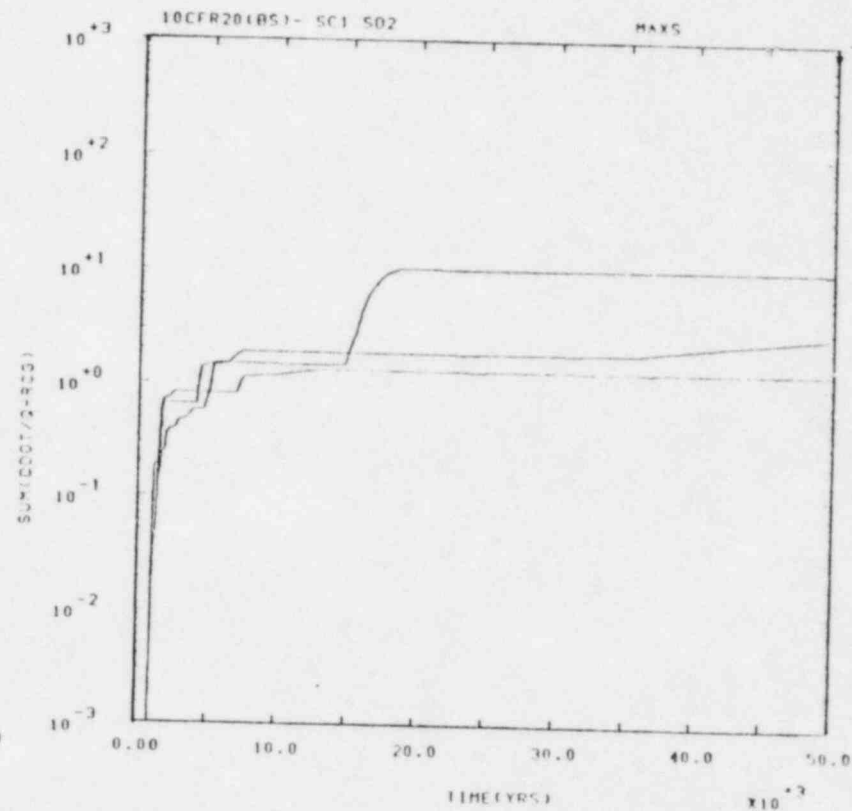


(b)

Figure 17. Bedded Salt Scenario 4, Source 1, mean and maximum versus time

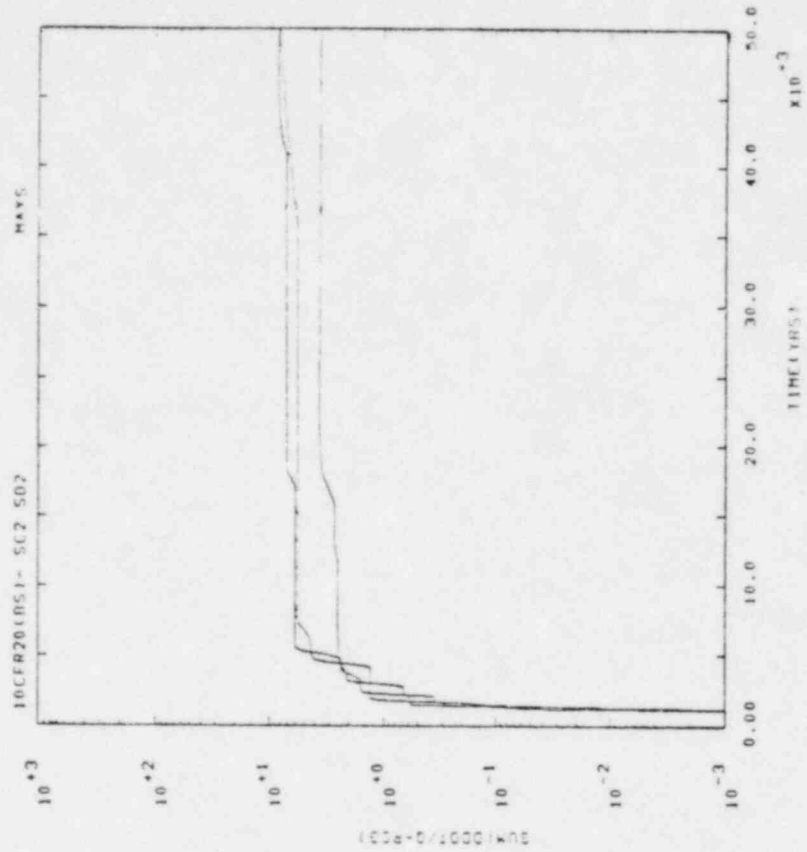


(a)

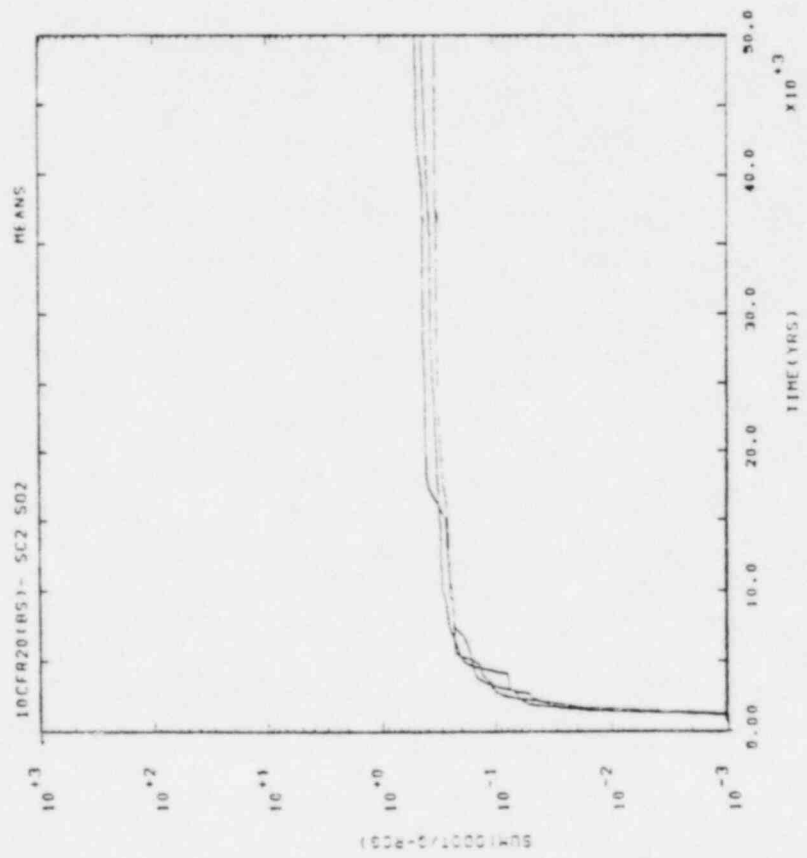


(b)

Figure 18. Bedded Salt Scenario 1, Source 2, mean and maximum versus time

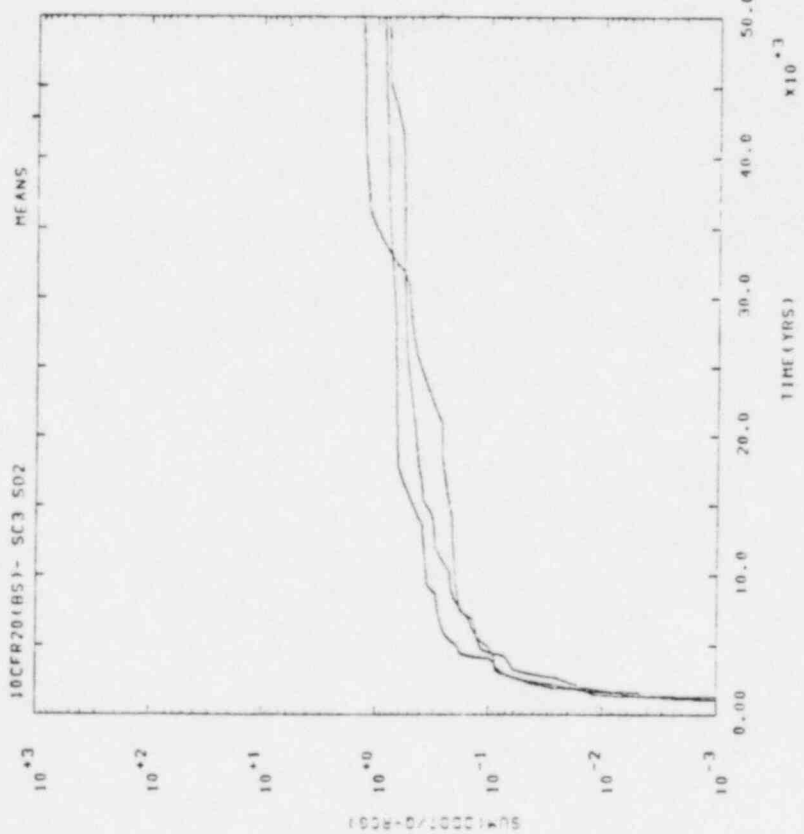


(a)

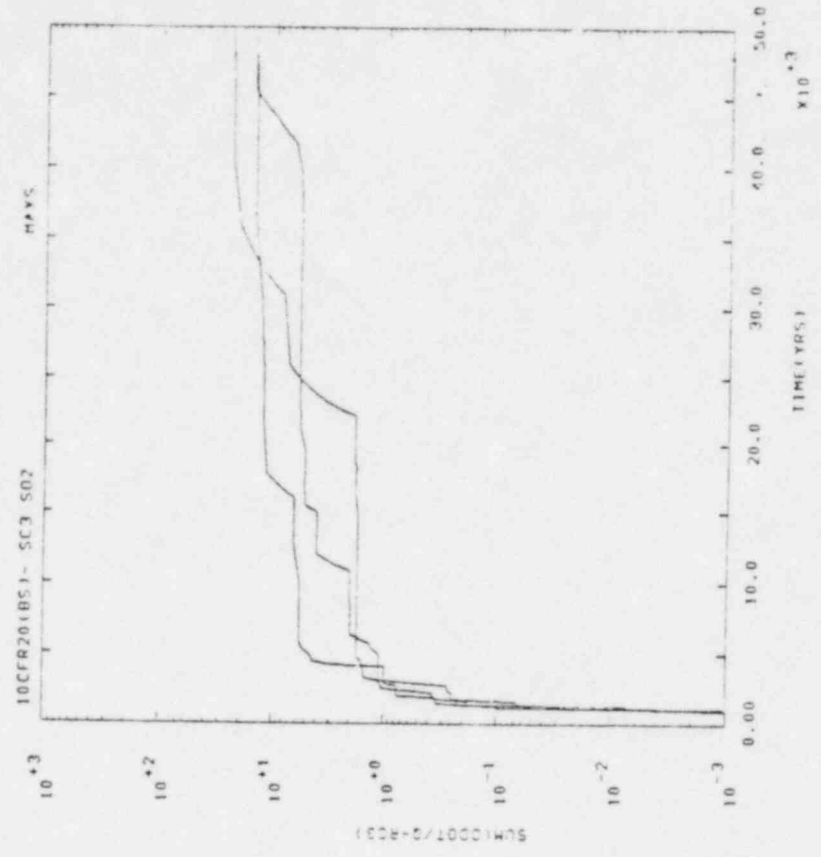


(b)

Figure 19. Bedded Salt Scenario 2, Source 2, mean and maximum versus time

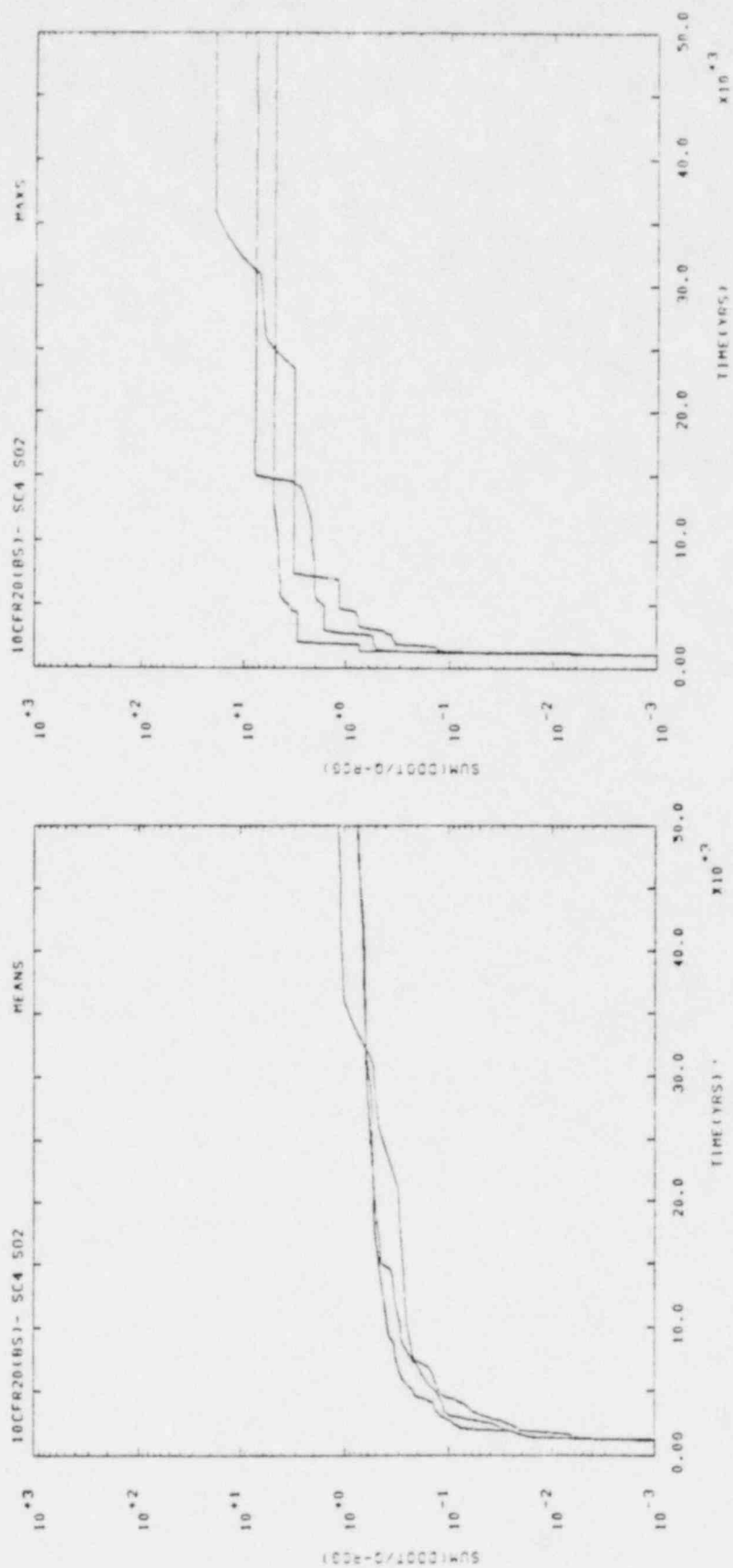


(a)



(b)

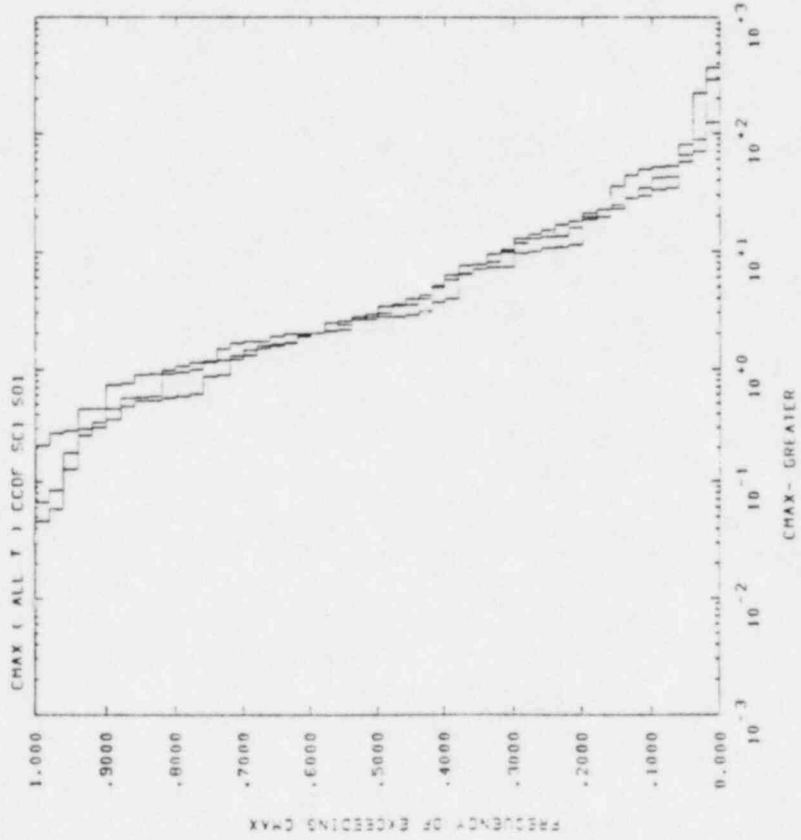
Figure 20. Bedded Salt Scenario 3, Source 2, mean and maximum versus time



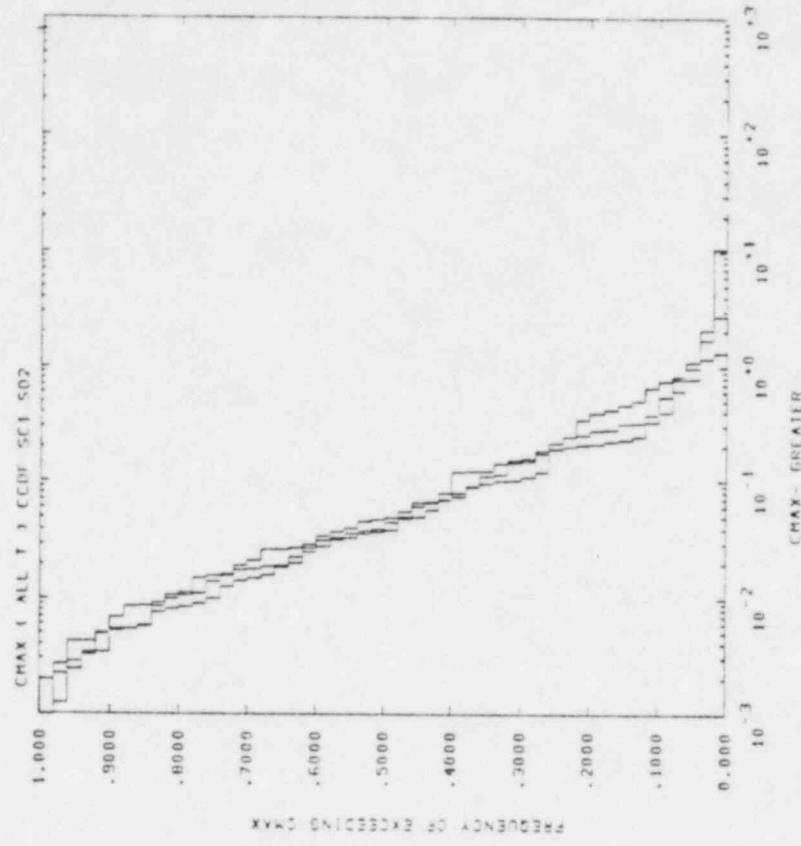
(a)

(b)

Figure 21. Bedded Salt Scenario 4, Source 2, mean and maximum versus time

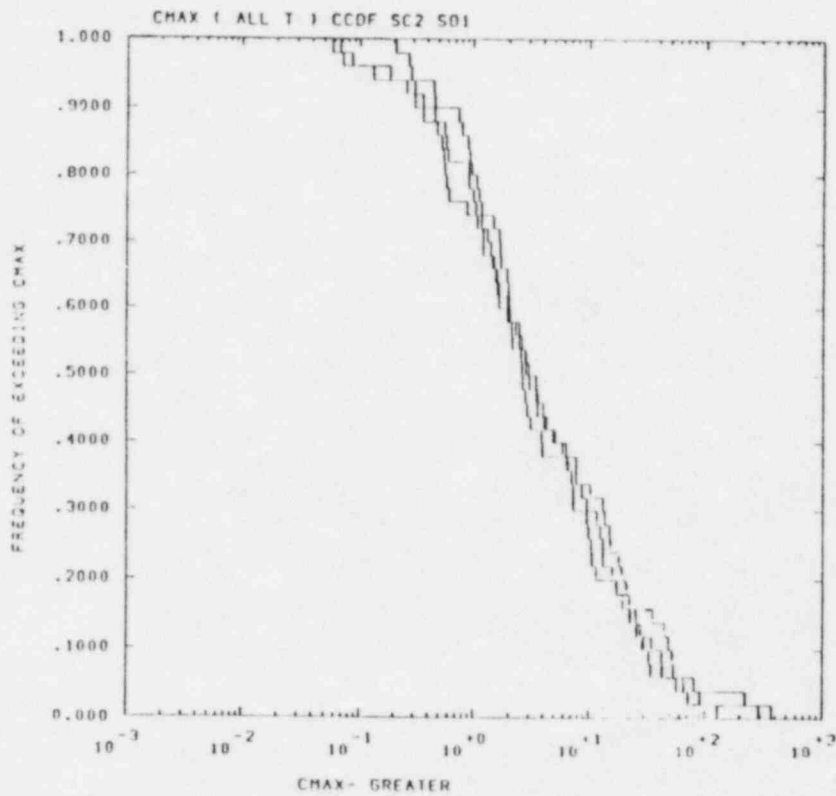


(a)

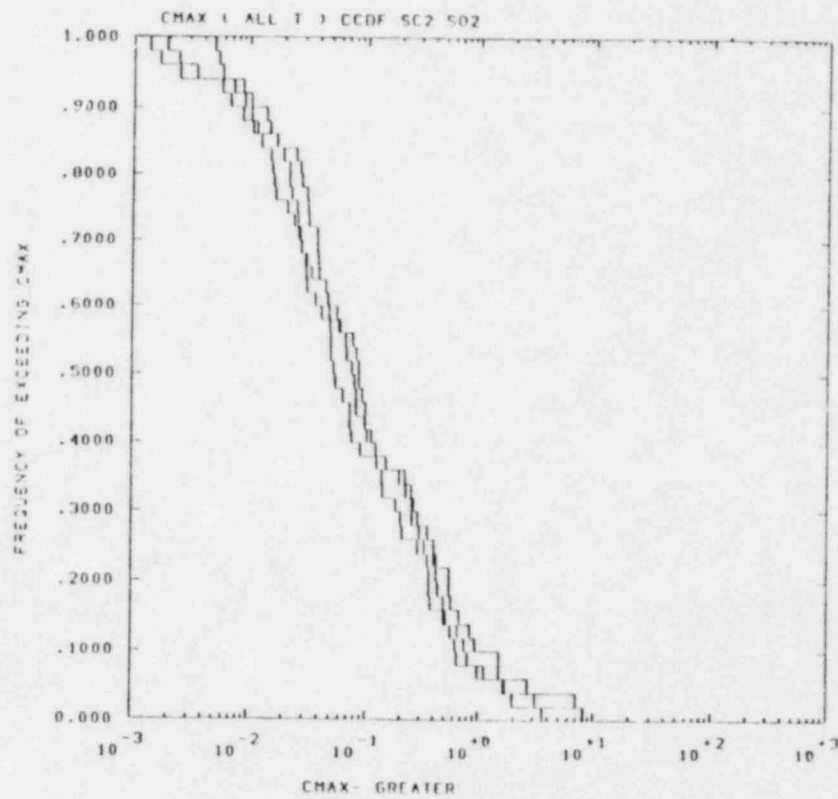


(b)

Figure 22. CCDF for Bedded Salt Scenario 1, Sources 1 and 2, maximum concentrations

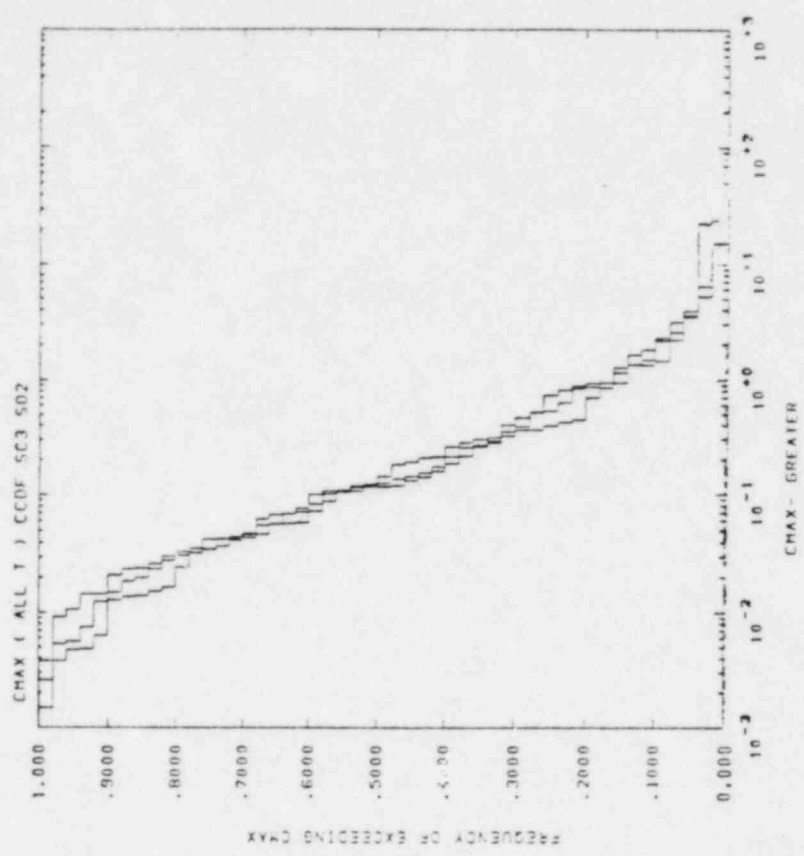


(a)

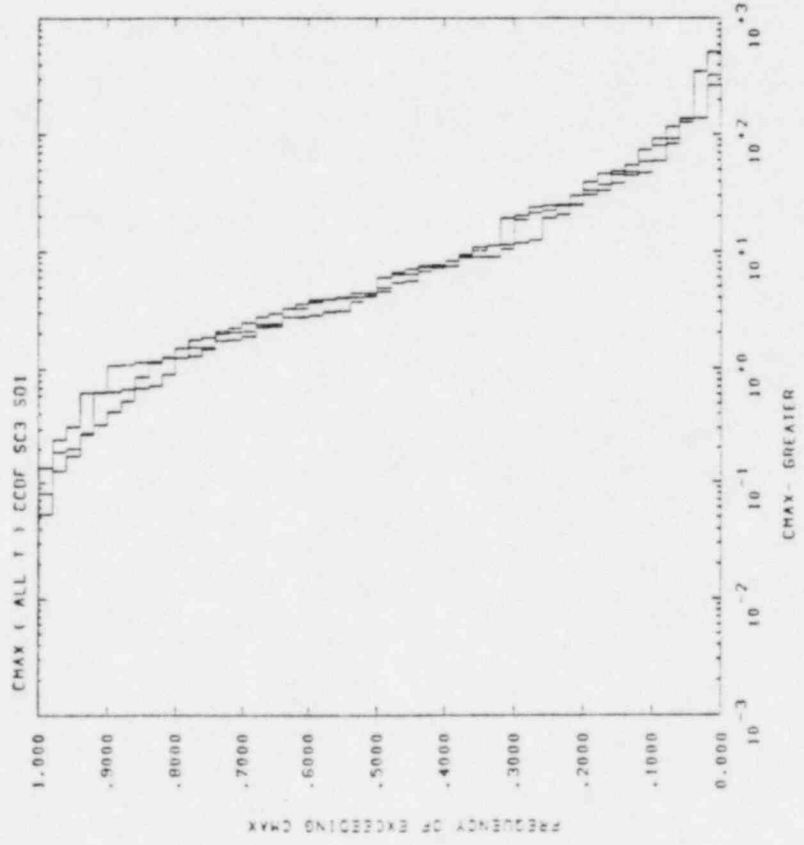


(b)

Figure 23. CCDF for Bedded Salt Scenario 2, Sources 1 and 2, maximum concentrations

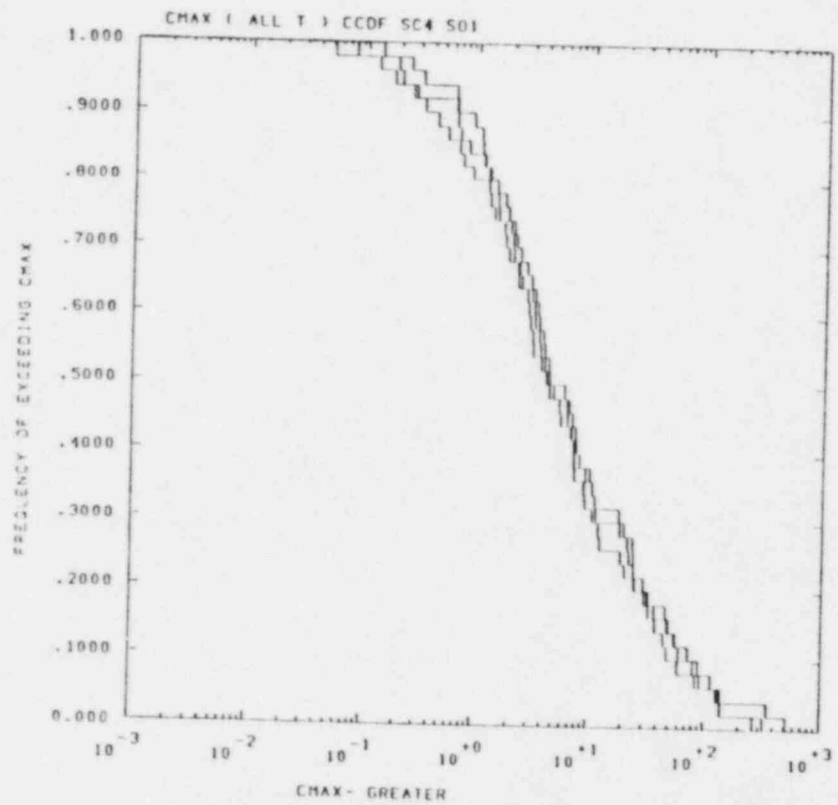


(a)

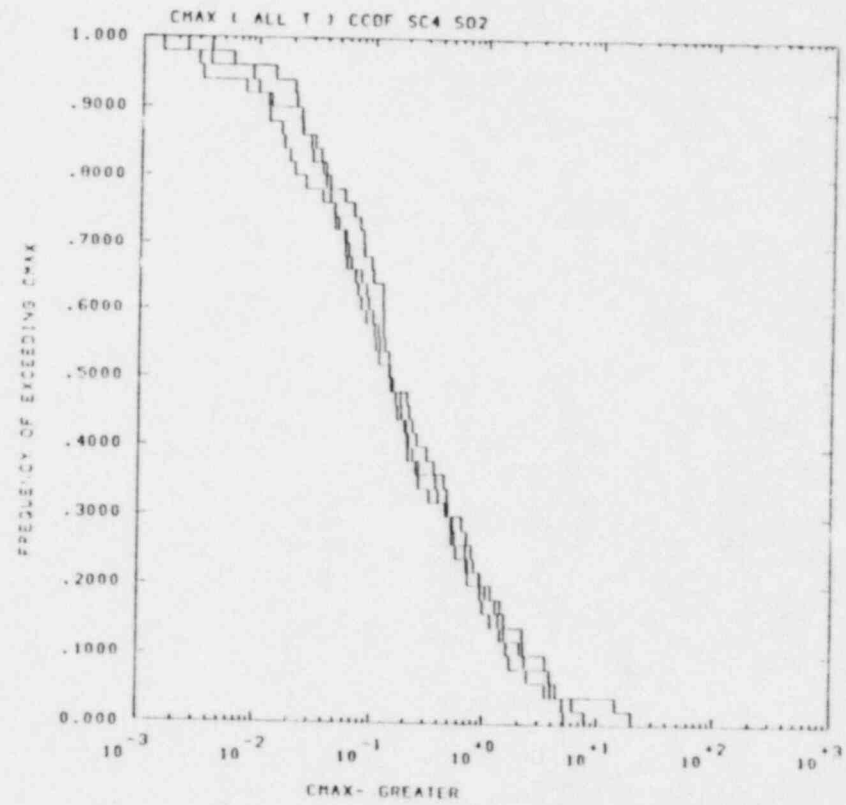


(b)

Figure 24. CCDF for Bedded Salt Scenario 3, Sources 1 and 2, maximum concentrations

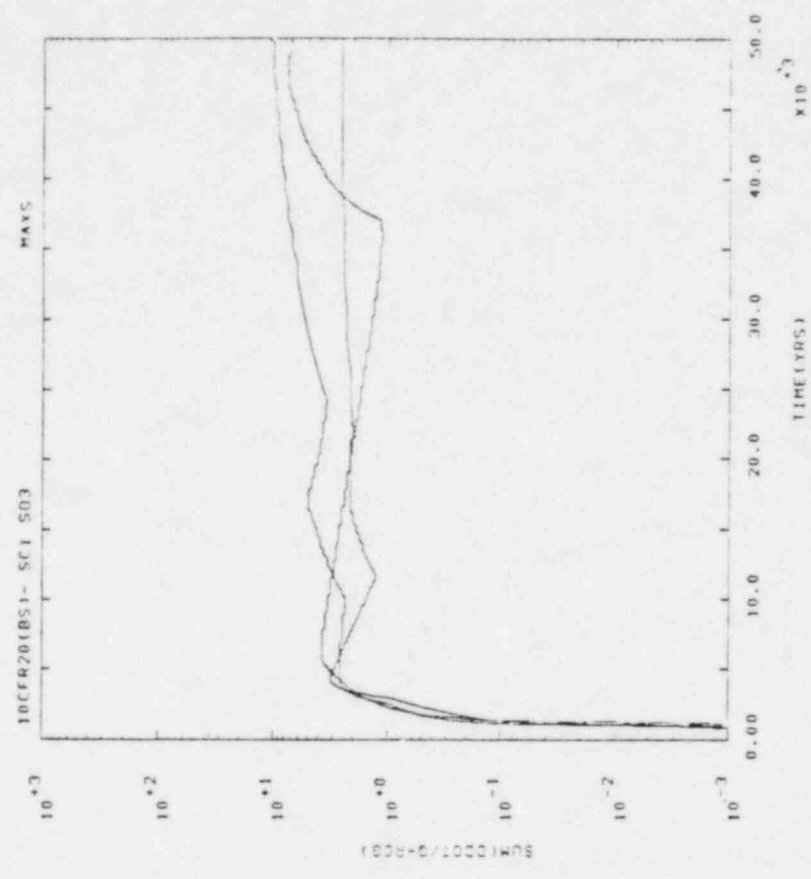


(a)

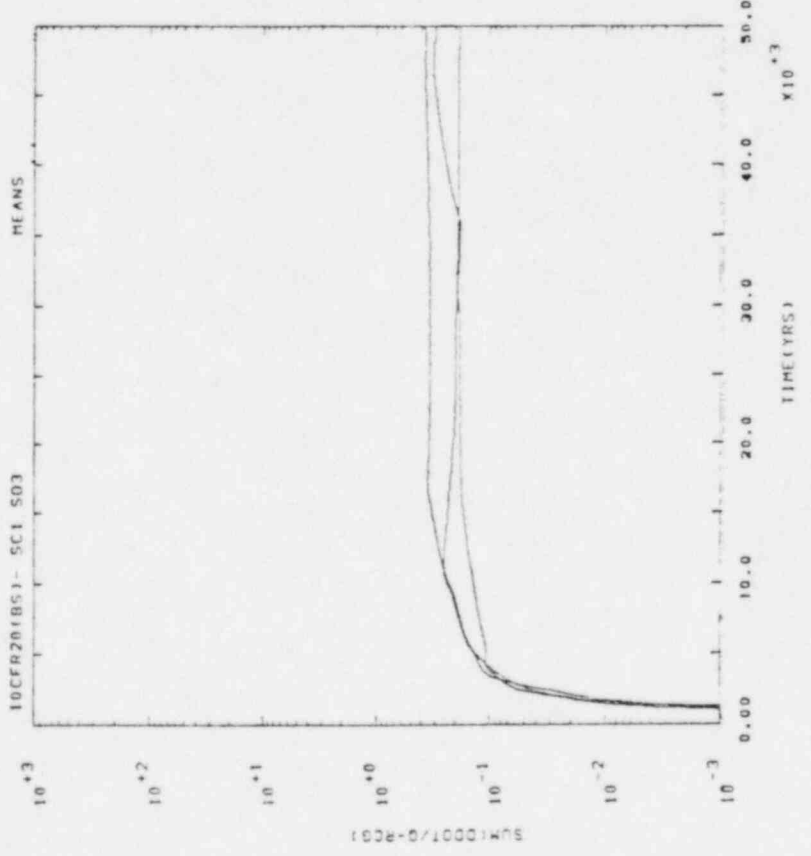


(b)

Figure 25. CCDF for Bedded Salt Scenario 4, Sources 1 and 2, maximum concentrations

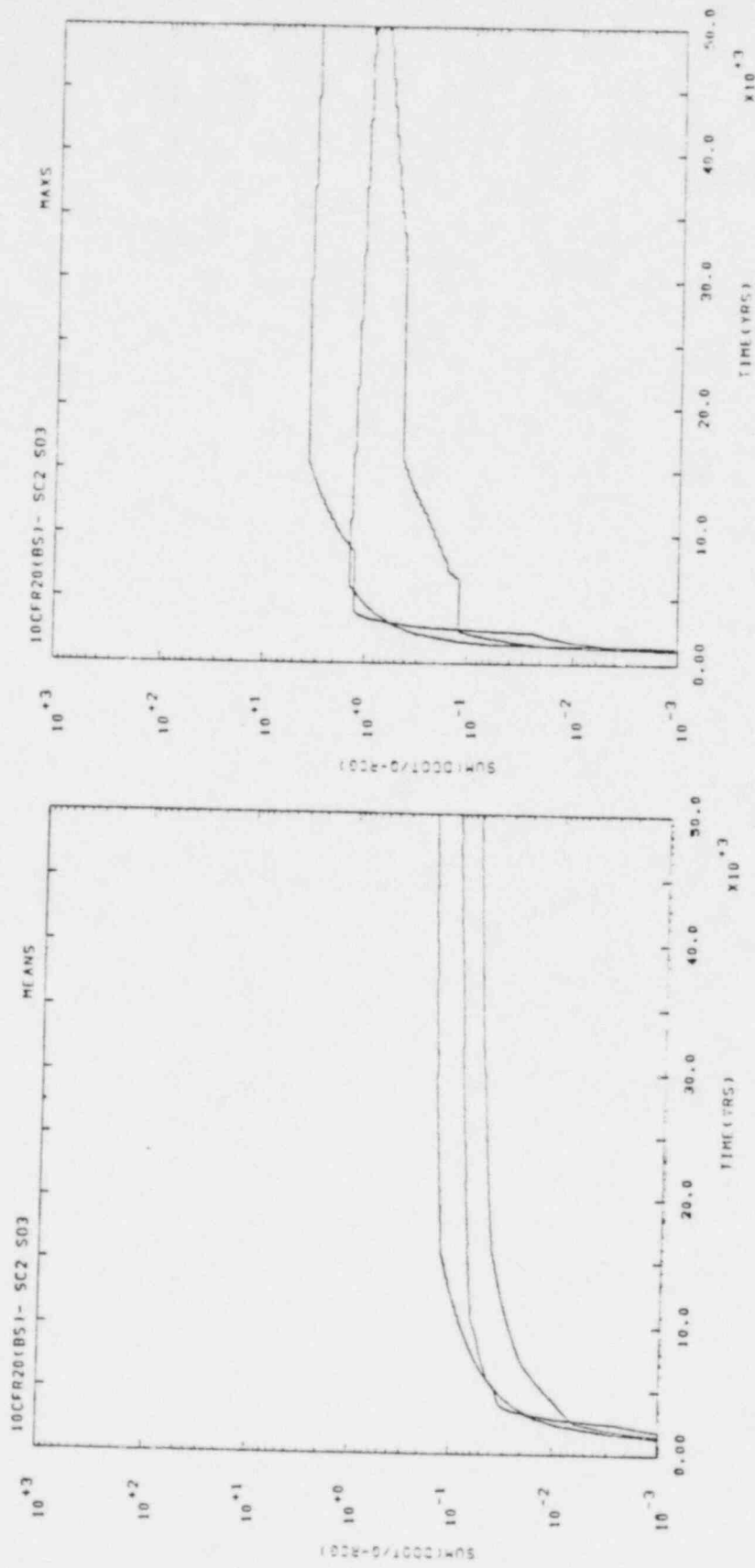


(a)



(b)

Figure 26. Bedded Salt Scenario 1, Source 3, mean and maximum versus time



(a)

(b)

Figure 27. Bedded Salt Scenario 2, Source 3, mean and maximum versus time

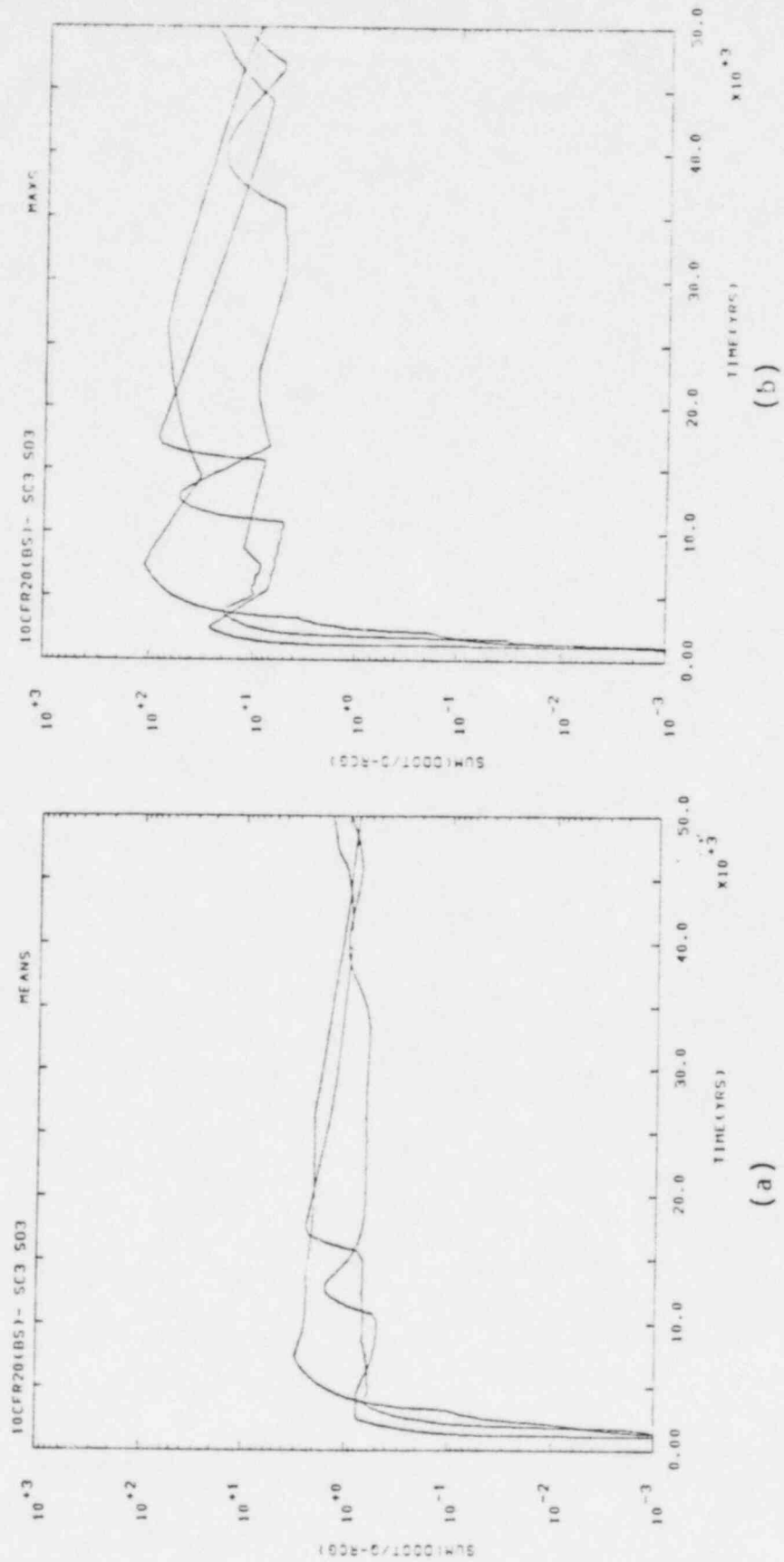
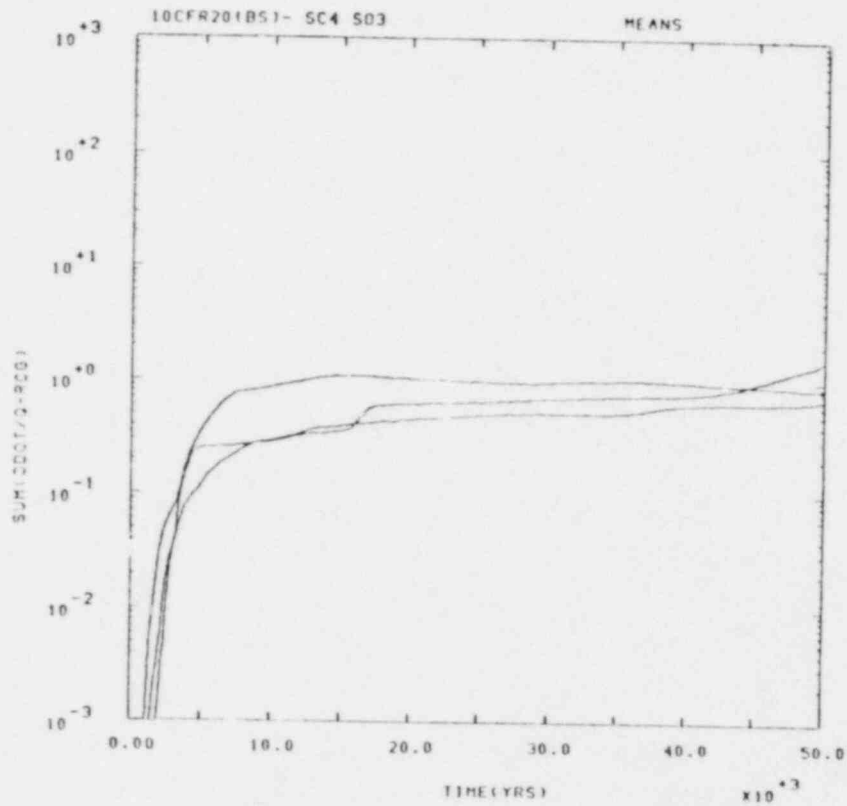
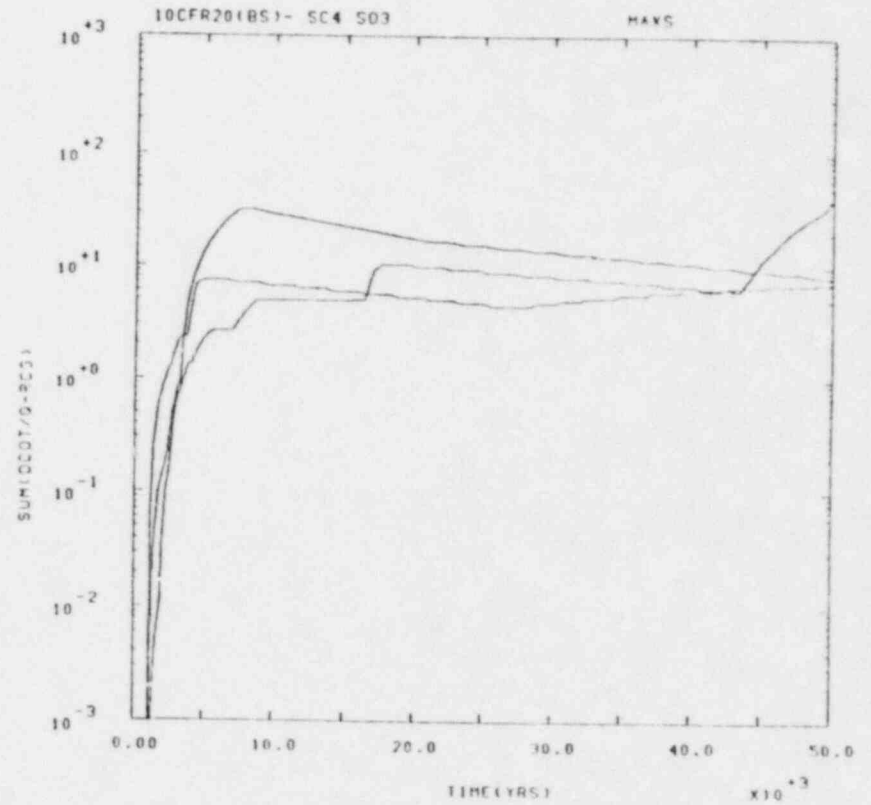


Figure 28. Bedded Salt Scenario 3, Source 3, mean and maximum versus time



(a)



(b)

Figure 29. Bedded Salt Scenario 4, Source 3, mean and maximum versus time

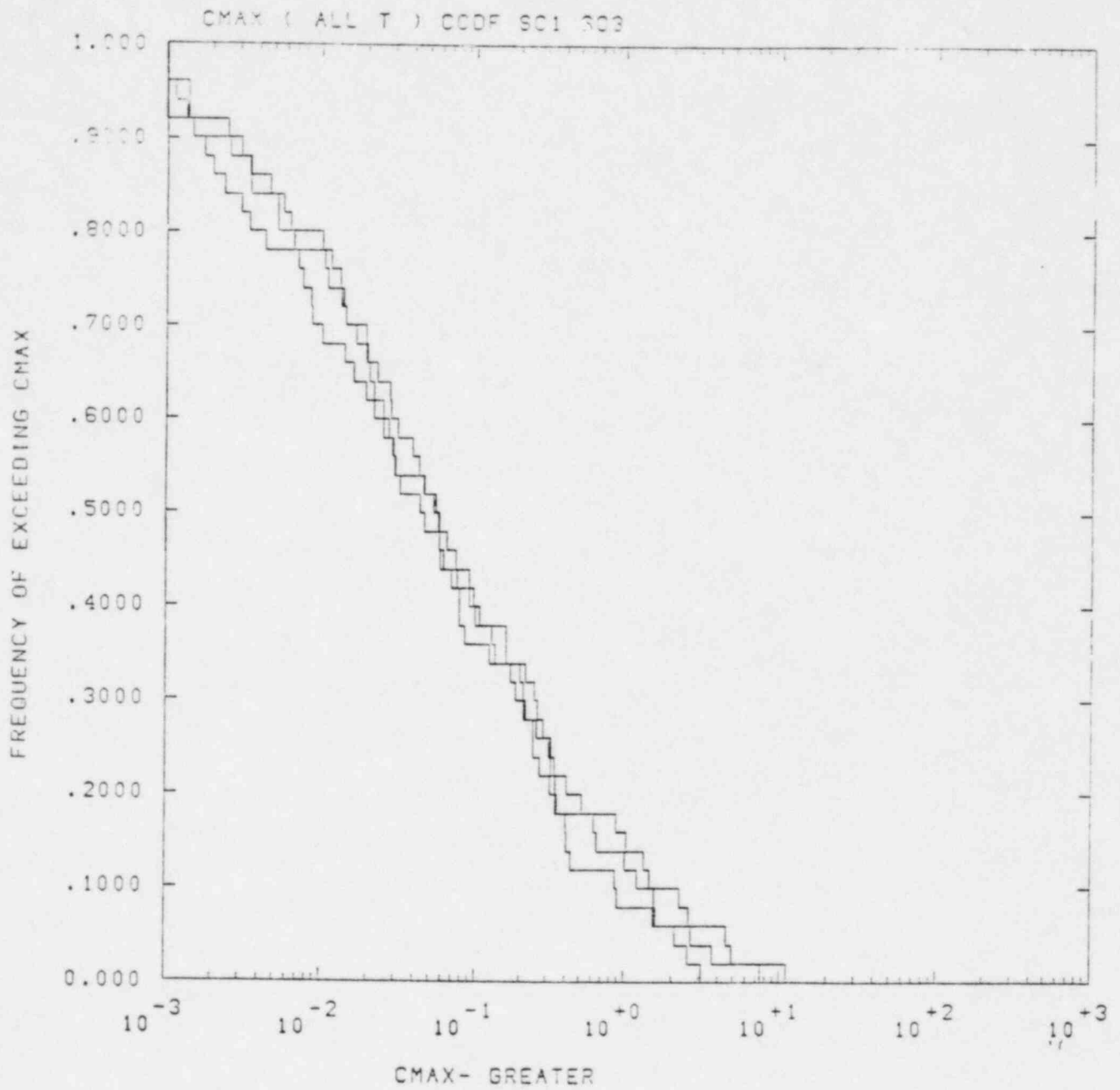


Figure 30. CCDF for Bedded Salt Scenario 1, Mixing Cell, maximum concentrations

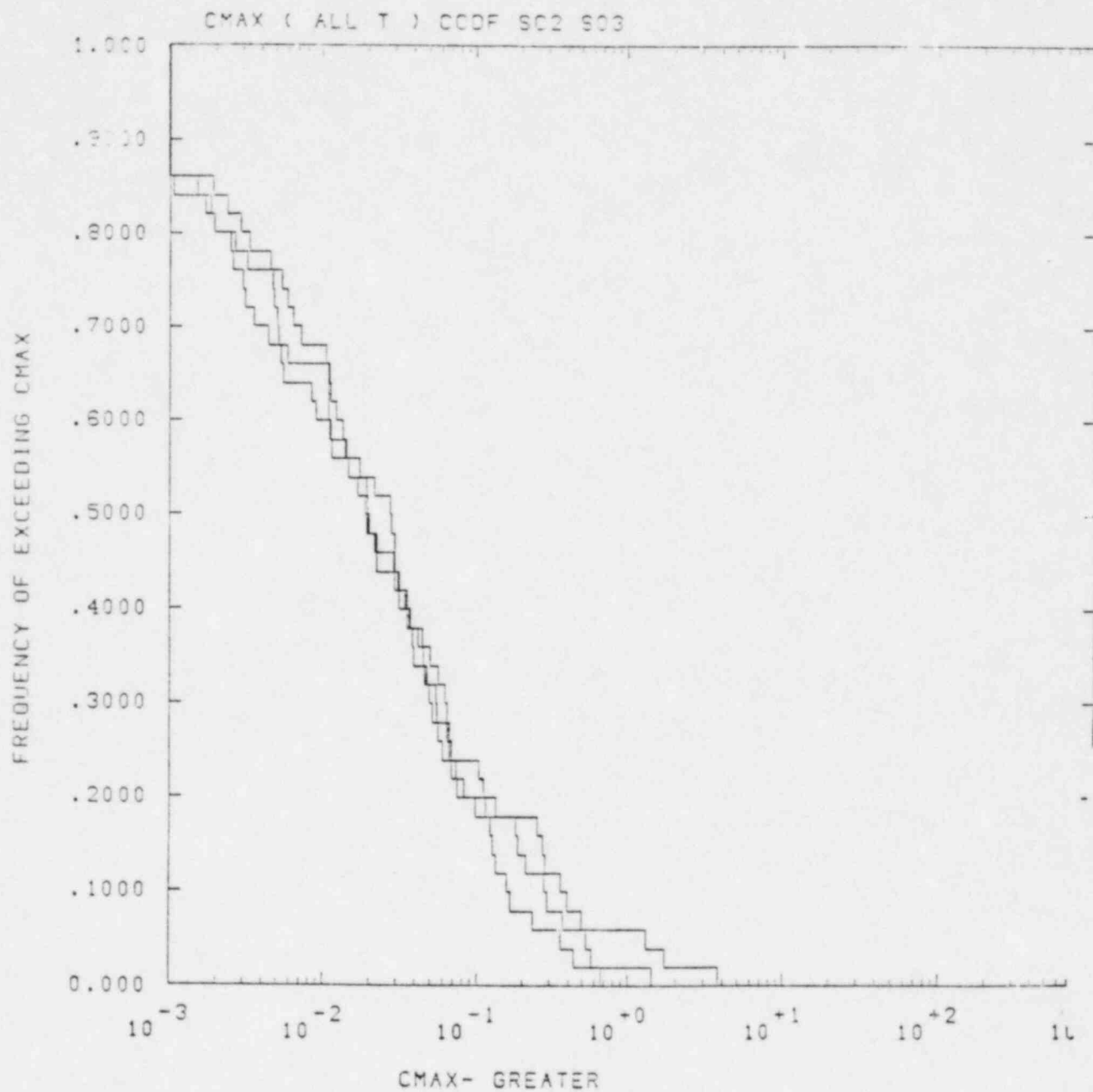


Figure 31. CCDF for Bedded Salt Scenario 2, Mixing Cell, maximum concentrations

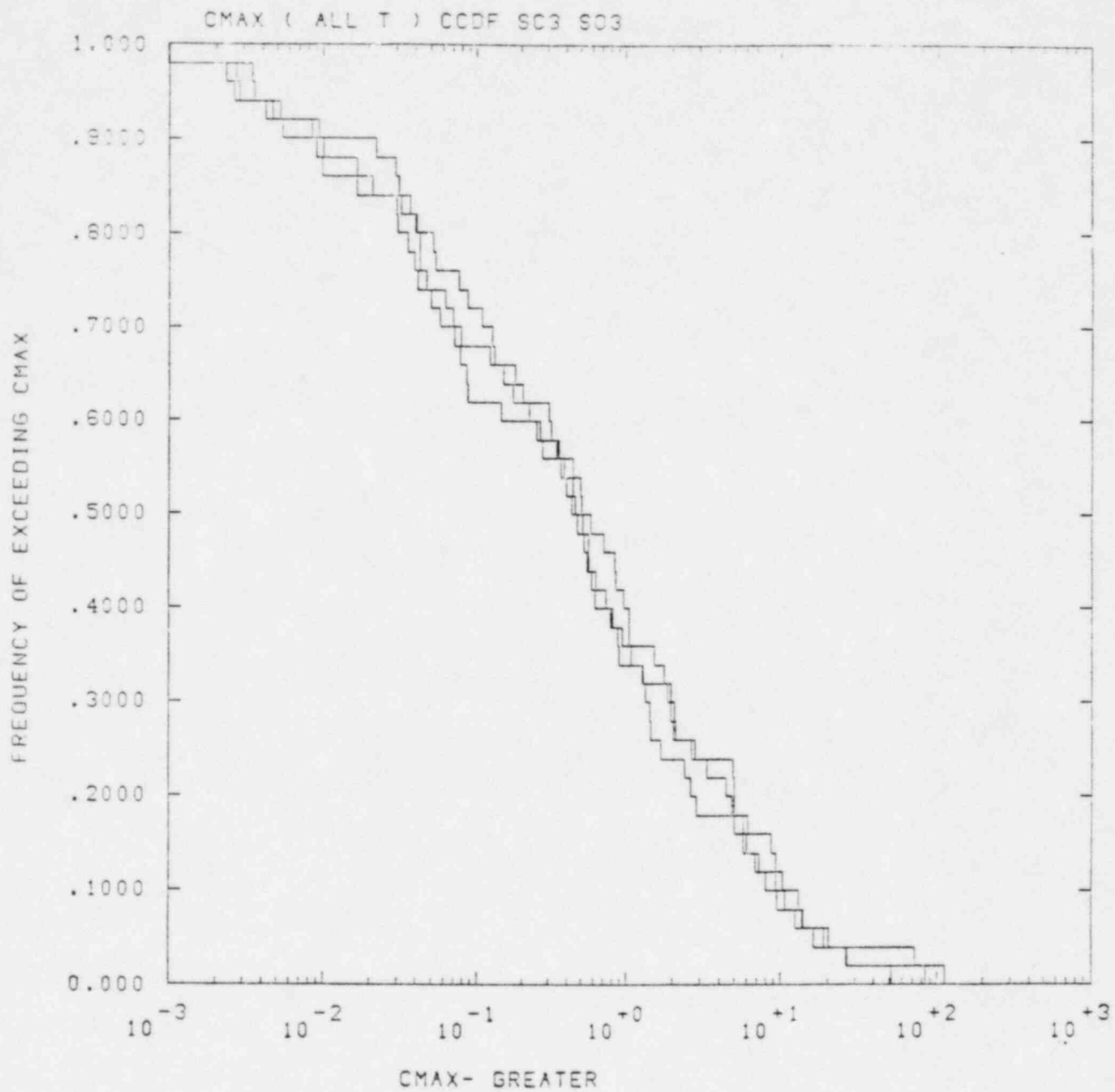


Figure 32. CCDF for Bedded Salt Scenario 3, Mixing Cell, maximum concentrations.

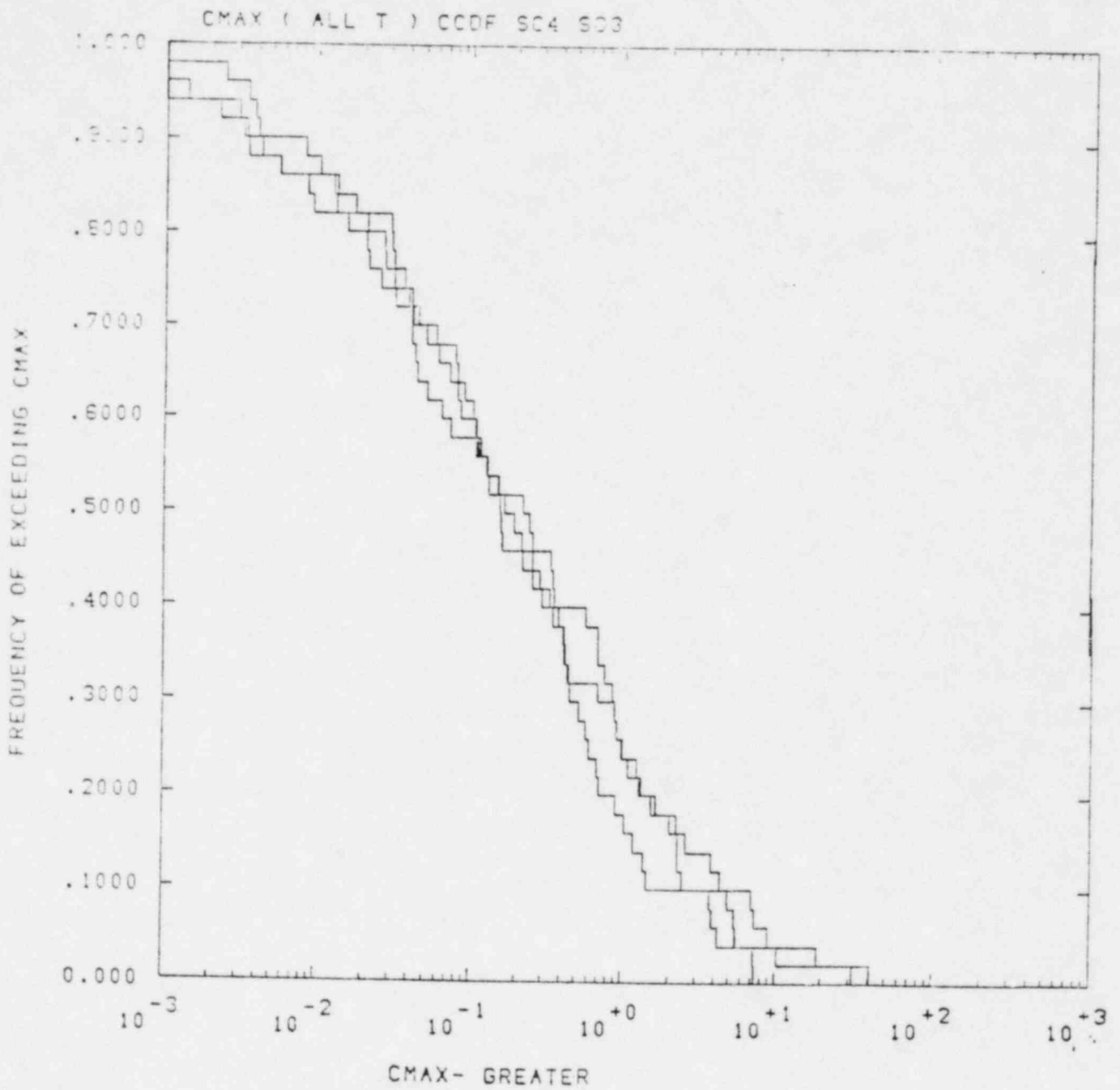


Figure 33. CCDF for Bedded Salt Scenario 4, Mixing Cell, maximum concentrations

Table 4

Important Radionuclides in Bedded Salt.
Scenarios (Based on First 50 Vectors)

Scenario:	<u>1</u>		<u>2</u>		<u>3</u>		<u>4</u>	
Source:	1 or 2	3	1 or 2	3	1 or 2	3	1 or 2	3
<u>Radionuclide</u>								
240Pu	6		6					
241Am								
237Np	38	6	39	6	13	1	11	1
233U			3	1	2	1		
238U	6	8	1	4	3	4	3	4
234U	24	21	21	18	25	17	24	20
226Ra	11	10	12	10	4	1	3	1
210Pb	2	4	2	2				
243Am	1	4	1	3				
239Pu	8	1	8	1				
235U						2		
231Pa	2	25	2	27	2	17	2	16
126Sn	43	20	43	21	38	24	38	24
135Cs	4	20	5	19	5	15	5	15
129I	50	50	50	30	43	44	43	44
99Tc	45	49	42	49	45	48	45	48
14C	31		43		47		47	

V. Conclusions

Using calculated results from a simple groundwater transport model, NWFT/DVM, and a simple Gaussian plume model to describe dispersion of radionuclides, we have estimated radionuclide concentrations in potential transporting aquifers and compared them to the standard for drinking water, 10CFR20. For many scenarios and source models analyzed, the probability of exceeding the 10CFR20 is non-zero. The value of the probability is given in Table 5. In particular, concentrations are high for many scenarios with a source model conceptually similar to but exceeding the minimum performance standards expressed in the draft 10CFR60 [8].

In performing these calculations a number of assumptions have been made which should be considered along with the results.

1. The calculated plume width is of a spatial extent comparable to that of the vertical extent of the aquifer. This may limit the vertical dispersion and dilution. However, we expect this effect to be relatively small and easily estimated.
2. The effects of large dilution volumes, as may be expected from a field of withdrawal wells rather than a single well, have been neglected.

Table 5
 Probabilities of Exceeding
 10CFR20 Requirements

Basalt

Scenario	1	2	3	4
	0	.3	.03	0

Bedded Salt

Scenario	1	2	3	4
Source				
1	.75	.75	.85	.85
2	.05	.10	.15	.15
3	.10	.05	.35	.20

Calculated results would be proportionately lower if dilution water was included.

3. Simple source terms have been assumed to describe the radionuclide release to the transporting aquifer. No detailed modelling of the source term has been performed. A potentially large reduction in concentrations may be achieved if the mixing cell assumption (Source #3) can be validated.

Further work in the description of radionuclide concentrations should address these areas.

VI. References

1. Pepping, R. E., Chu, M. S., and Siegel, M. D., "Technical Assistance for Regulatory Development - A Simplified Repository Analysis in a Reference Basalt Site," Sandia National Laboratories Report SAND82-0689, February 1982.
2. Pepping, R. E., Chu, M. S., and Siegel, M. D., "Technical Assistance for Regulatory Development : A Simplified Repository Analysis in a Hypothetical Bedded Salt Formation," Sandia National Laboratories Report SAND82-0996 (1982).
3. Campbell, J. E., Longsine, D. E., and Cranwell, R. M., "Risk Methodology for Geologic Disposal of Radioactive Waste - The NWFT/DVM Computer Code User's Manual," Sandia National Laboratories Report SAND81-0886, NUREG/CR-2081, November 1981.
4. U. S. Environmental Protection Agency, "Environmental Standards and Federal Radiation Protection Guidance for Management and Disposal of Spent Nuclear Fuel, High-Level and Transuranic Radioactive Wastes," 40CFR191, Draft 20, 1981.
5. Appendix B, Code of Federal Regulations, Title 10, Part 20.
6. Iman, R. L., Davenport, J. M., and Ziegler, D. K., Latin Hypercube Sampling (Program User's Guide), Sandia National Laboratories, SAND79-1473, January 1980.
7. Bennett, D. E., Sandia-ORIGEN User's Manual, NUREG/CR-0987, Sandia Laboratories, Albuquerque, NM, October 1979.
8. Nuclear Regulatory Commission, "Disposal of High Level Water in Geologic Repositories," 10CFR60, Federal Register, 48, July 8, 1981.